UNIVERSITAT DE BARCELONA

Fire Detectors Based on Chemical Sensor Arrays and Machine Learning Algorithms: Calibration and Test

Ana Maria Solorzano Soria

ADVERTIMENT. La consulta d'aquesta tesi queda condicionada a l'acceptació de les següents condicions d'ús: La difusió d'aquesta tesi per mitjà del servei TDX (**www.tdx.cat**) i a través del Dipòsit Digital de la UB (**diposit.ub.edu**) ha estat autoritzada pels titulars dels drets de propietat intel·lectual únicament per a usos privats emmarcats en activitats d'investigació i docència. No s'autoritza la seva reproducció amb finalitats de lucre ni la seva difusió i posada a disposició des d'un lloc aliè al servei TDX ni al Dipòsit Digital de la UB. No s'autoritza la presentació del seu contingut en una finestra o marc aliè a TDX o al Dipòsit Digital de la UB (framing). Aquesta reserva de drets afecta tant al resum de presentació de la tesi com als seus continguts. En la utilització o cita de parts de la tesi és obligat indicar el nom de la persona autora.

ADVERTENCIA. La consulta de esta tesis queda condicionada a la aceptación de las siguientes condiciones de uso: La difusión de esta tesis por medio del servicio TDR (**www.tdx.cat**) y a través del Repositorio Digital de la UB (**diposit.ub.edu**) ha sido autorizada por los titulares de los derechos de propiedad intelectual únicamente para usos privados enmarcados en actividades de investigación y docencia. No se autoriza su reproducción con finalidades de lucro ni su difusión y puesta a disposición desde un sitio ajeno al servicio TDR o al Repositorio Digital de la UB. No se autoriza la presentación de su contenido en una ventana o marco ajeno a TDR o al Repositorio Digital de la UB (framing). Esta reserva de derechos afecta tanto al resumen de presentación de la tesis como a sus contenidos. En la utilización o cita de partes de la tesis es obligado indicar el nombre de la persona autora.

WARNING. On having consulted this thesis you're accepting the following use conditions: Spreading this thesis by the TDX (**www.tdx.cat**) service and by the UB Digital Repository (**diposit.ub.edu**) has been authorized by the titular of the intellectual property rights only for private uses placed in investigation and teaching activities. Reproduction with lucrative aims is not authorized nor its spreading and availability from a site foreign to the TDX service or to the UB Digital Repository. Introducing its content in a window or frame foreign to the TDX service or to the UB Digital Repository is not authorized (framing). Those rights affect to the presentation summary of the thesis as well as to its contents. In the using or citation of parts of the thesis it's obliged to indicate the name of the author.

Fire Detectors Based on Chemical Sensor Arrays and Machine Learning Algorithms: Calibration and Test

Programa de doctorat:

Enginyeria i Ciències Aplicades

Enginyeria Biomèdica

Author: Ana Maria Solorzano Soria

Directors: Dr. Santiago Marco Colás and Dr. Jordi Fonollosa Magrinyà.

Tutor: Dr. Luis Fernández Romero.

Barcelona, Spain.

UNIVERSITAT DE BARCELONA

Para mis Titos: Jesús Soria y Martha Leaños

Acknowledgements

Comenzaré primero por agradecer al Dr. Santiago Marco quien me dio la oportunidad más bonita y enriquecedora de mi vida, sus grandes ideas y su manera de hacer ciencia siempre me acompañarán. Al Dr. Jordi Fonollosa que me enseñó a ver más allá de lo evidente, su disciplina de trabajo me ha convertido en una mejor científica. Al Dr. Luis Fernández, que desde mis primeros días se sentó a mi lado y de la manera más desinteresada me enseño todo lo que sabía. Siempre estuviste para darme una palabra de ánimo. Fui muy afortunada por estar bajo su dirección y tutela, gracias por todas las lecciones, jamás las olvidaré.

Gracias al Consejo Nacional de Ciencia y Tecnología de la República mexicana quien tuvo a bien becarme para realizar esta tesis doctoral.

A Sergio y a Raquel, quienes siempre tuvieron un oído crítico y un buen consejo científico para mi proyecto de tesis. Sergio, gracias por el gran "aventón" técnico que me diste al principio, sin tu paciencia y conocimiento no hubiera podido despegar. A todos mis compañeros de lab: Javi "el chido", Juanma (una pieza clave para que esta tesis se llevara a cabo), Marta Padilla, Silvia y Luciana. A nuestros seniors del grupo por sus consejos y buena onda, el Dr. Antonio Pardo y el Dr. Agustín Gutiérrez.

De manera más personal quiero agradecer a Sergio por todas las largas conversaciones en donde me quejaba, quería dejarlo todo y salir corriendo. Siempre estuviste ahí, siempre con una sonrisa, con un abrazo y con mucho amor. Eres mi mejor coincidencia de vida. A mi familia en México, mi fuerza y mi motivo: Tita, Mama, Paty, Agustín y mis grandes amores: Martha e Isabel. A mi familia en España: Jordi, Nanina and Morgen (You will be always in our hearts). A mis buenos amigos, los buenos ratos y las risas siempre me ayudaron a recargar pilas: los morrillos, els meus amics catalans, mis amigos de la secu, prepa y universidad. A Raquel por las cortaditas, los viajes, la bolera, los tacos, el fuet y todos los infinitos audios que me han acompañado.

Gracias a todos por formar parte de esta aventura!

Table of contents

Acknowledgements 5

Table of contents 7

List of figures 12

List of tables 19

Abstract 21

Chapter 1: Introduction 23

1.1 Fire Detectors Based on Smoke Detection 25

1.2 Gas Emission in Fires 26

1.3 Main Toxicants from Fire Emissions 28

1.3.1 Carbon Dioxide 28

1.3.2 Carbon Monoxide 28

1.3.3 Hydrogen Cyanide 29

1.3.4 Nitrogen Oxides 29

1.3.5 Sulphur Dioxide 29

1.3.6 Halogen Acids 29

1.3.7 Organic Irritants 30

1.4 Toxicity of Released Gases in Fire 30

1.4.1 Asphyxiant Gases 30

1.4.2 Irritant Emissions 32

1.5 Combined Toxic Effects 33

1.6 Toxicant Production Depending on Fire Scenarios and Burning Materials 34

1.7 Standards for Fire Detectors 39

1.8 Gas Sensors for Combustion Products 44

1.9 Fire Detectors Incorporating Chemical Sensors 48

1.9.1 Decision Tree and Hard Rules 48

1.9.2 Neural Networks 57

1.9.3 Probabilistic Neural Network 60

1.9.4 Hierarchical LDA 63

1.10 Fire Detectors Exclusively Based on Chemical Sensing 65

1.10.1 Single Sensor 65

1.10.2 Neural Networks 66

1.10.3 Hard Rules 67

1.10.4 Fuzzy Logic Rules 68

1.10.5 Principal Component Analysis and Nearest Neighbours Classifiers 70

1.10.6 Other Approaches 71

1.11 Summary 73

Chapter 2: Objectives 75

Chapter 3: Experimental Set-up 79

3.1 Standard Fire Room 80

3.2 Small Scale Chamber 84

Chapter 4: Experimental Protocols 87

4.1 Fire and non-Fire scenarios in the fire room 89

4.1.1 Experimental Protocol of Fire Experiments 89

4.1.2 Experimental Protocol of Nuisance Experiments 96

4.2 Fire and Nuisances scenarios in small-chamber 101

4.2.1 Experimental protocol 102

4.3 Summary of Measurement campaigns. 108

4.4 Datasets 109

Chapter 5: **Sensor Arrays 111**

5.1 Prototype 1: Sensor Array Using Off-The-Shelf Sensors 112

5.1.1 Sensor Selection 113

5.1.2 System Description 114

5.1.3 Sensor Description and Signal Conditioning Circuits 118

5.2 Prototype 2: SAFESENS Prototype 126

5.2.1 Sensor Selection 127

5.2.2 System Description 127

5.2.3 Sensor Description and Signal Conditioning 130

Chapter 6: **Machine Learning Algorithms for Fire Detection 135**

6.1 Methodology 136

6.1.1 Signal Pre-processing and Feature Extraction 137

6.1.2 Baseline Correction 138

6.1.3 Labelling 139

6.1.4 Labelling 140

6.1.5 Prediction Model 141

6.2 Results 143

6.2.1 Data Exploration 143

6.2.2 Fire Detector Algorithm Based On PLS-DA 144

6.2.3 Fire Detector Algorithm Based On SVM 154

6.3 Comparison 157

6.4 Conclusions 158

Chapter 7: **Reducing Experimental Costs by Using Small Scale Setups. 161**

7.1 Classification Models Methodology 161

7.2 Results 162

7.2.1 Sensor Signals 162

7.2.2 Classification Models Performance 165

7.3 Conclusions 173

Chapter 8: **Reduction of Calibration Cost Using Batches of the Same Sensor Array 175**

8.1 Dataset 177

8.2 Evaluation of calibration methods 179

8.3 Results and discussion 181

8.3.1 Individual calibration models 182

8.3.2 General calibration models 184

8.4 Conclusions 190

Chapter 9: **Conclusions 192**

Chapter 10: **References 195**

Appendix A: Confusion Matrices PLS-DA and SVM Algorithms for Fire Detection 205

Appendix B: Resumen en Castellano 207

OBJETIVOS 208

PROTOCOLO EXPERIMENTAL 208

Habitacion Estandar de Fuegos 208

Camara de Fuegos a Pequeña Escala. 209

Protocolo Experimental en la Habitacion de Fuegos. 210

Protocolo Experimental en la Camara de Fuegos. 211

Bases de Datos. 211

PROTOTIPOS PARA LA DETECCION DE INCENDIOS 213

Matriz de Sensores Usando Sensores Comerciales. 213

Prototipo Safesens. 213

ALGORITMOS PARA LA DETECCION DE INCENDIOS 214

Metodología. 214

Resultados. 217

REDUCCIÓN DE COSTOS DE CALIBRACIÓN USANDO ESCENARIOS EXPERIMENTALES A PEQUEÑA ESCALA 218

REDUCCIÓN DE COSTOS DE CALIBRACIÓN USANDO RÉPLICAS DE UNA MATRIZ DE SENSORES. 220

CONCLUSIONES 222

List of figures

Figure 1 Example of evolution of CO and HCN for a smoldering fire (NIST tests) [40]. 35

Figure 2 Example of the time evolution of O2 and CO2 during a smoldering fire [40]. 36

Figure 3 Time evolution of the toxic potency of the smoldering fire for the NIST test [40]. 36

Figure 4 Time to alarm in smoldering fires in the SP Fire Research Experiment. Comparison between photoelectric detectors and multisensory including CO Electrochemical Cell [42]. Photoelectric detector combined with CO sensor always produced faster alarm signals, and it was able to detect all the test fires. Standalone photoelectric detector did not trigger the alarm for three of the fires (not detected [N.D.]). Experiment #5 was not considered in the study as the fire developed to open fire. 37

Figure 5 Concentration and exposure time of the different interferent gases that appear in the standard ISO7240. Note the log scale. Specifically, the concentrations and exposure times are: 5 ppm of NO2 at 96 h and 50 ppm at 30 min, 5 ppm of SO2 at 96 h and 50 ppm at 30 min, 2 ppm of Cl2 at 96 h, 50 ppm of NH3 at 1 h, 100 ppm of Heptane at 1 h, 500 ppm of Ethanol at 1 h and 1500 ppm of Acetone at 1 h. 43

Figure 6 Nemoto NAP-505 three electrode CO sensing element. 47

Figure 7 Dimensions and distribution of the experimental area and control room of the standard fire room.....80

Figure 8 Internal distribution of the MIC camera. 82

Figure 9. Picture of the Measuring Ionization Chamber EC-912 from Delta. The MIC was using during the fire and nuisance experiments performed at the standard fire room 82

Figure 10 Picture of the Fourier Transform Infrared Spectrometer DX4000 from Gasmeter. The FTIR was using during the fire and nuisance experiments performed at the standard fire room. 83

Figure 11 Customized experimental chamber. On the left an actual picture of the small chamber, on the right a scheme with the chamber dimensions. 85

Figure 12 Experimental protocol of the Fire and Nuisance experiments performed at the Fire room. The methodology has 4 steps: Preparation, Start, End of Test and Ventilation. 90

Figure 13 Experimental protocol of the TF2 experiment performed in the fire room. The methodology has 5 steps: Start, Heating rate, End, Reduce fire and Ventilation. 91

Figure 14 Illustration of the TF2 fire experiment performed in the fire room. 92

Figure 15 Illustration of the TF3 fire experiment performed in the fire room. The draw shows how the cotton wicks are hanged to the structure. 93

Figure 16 Experimental protocol of the TF3 experiment performed in the fire room. The methodology has 5 steps: Start, Ignition, End, Reduce fire and Ventilation. 94

Figure 17 Illustration of the non-standard fire experiments performed in the fire room. The drawings show how the PVC, PET, Electronics, and Cables are distributed on the hot plate. All the materials are placed in an aluminum plate at the top of the hot plate. . 95

Figure 18 Experimental protocol of the non- standard fire experiments performed at the fire room. The non-standard fires performed at the fire room are: PVC, Electronics, Cables, and PET. The methodology has 5 steps: Start, Heating rate, End, Reduce fire and Ventilation 96

Figure 19 Illustration of the Gasoline, Vinegar, and Gasoline nuisance experiments performed at the fire room. 100ml of substance was placed into an aluminum box in the middle of the room. 97

Figure 20 Experimental protocol of the Gasoline, Vinegar, and Ethanol nuisances experiments performed at the fire room. The methodology has 5 steps: Start, Evaporation, End, and Ventilation 98

Figure 21 Illustration of the Air Freshener nuisance experiment performed in the fire room. The draw shows the 5 directions (north, south, east, west, and top) in which the air freshener was spread. 99

Figure 22 Experimental protocol of the Air Freshener nuisance experiment performed in the fire room. The methodology has 4 steps: Presentation, Exposure, End, and Ventilation. 99

Figure 23 Illustration of the Window Cleaning nuisance experiment performed in the fire room. The draw shows the distribution of the windows in the fire room. 100

Figure 24 Experimental protocol of the Window Cleaning nuisance experiment performed in the fire room. The methodology has 4 steps: Cleaning 1, Cleaning 2, End and Ventilation. 101

Figure 25 Experimental protocol of the Fire and Nuisance experiments performed at the customized chamber. The methodology has 4 steps for fire experiments: Start, Material,

Fire, and End. The methodology to induce the nuisances has 3 steps: Start, Material, and End. 103

Figure 26 *Picture of the TF2 and TF2 bis experiments performed at the chamber. TF2 used 4 sticks of beechwood and TF2 bis 1 stick of pinewood as fuel. The materials were heating using a hotplate. 104*

Figure 27 *Picture of the TF3 experiment performed at the chamber. TF3 consist of 4 cotton wicks of 10 cm and the fire is induced with the ignition of the wicks. 105*

Figure 28 *Picture of the Cable experiment performed at the chamber. Cable experiment consists of 10 pieces of flat cable of 10 cm and the fire is induced with the ignition of the wicks. 106*

Figure 29 *Picture of the plate using in the chamber to induce Vinegar, Ethanol and Floor Cleaning Product. One spray of each product was put in each vertex of the square..107*

Figure 30 *Picture of the Boiling water experiment. 100ml of water was heated in a hotplate.....107*

Figure 31 *Picture of the electronic air freshener using in the chamber to induce air freshener experiment. 108*

Figure 32 *Picture of the developed multi-sensor array for reliable fire detection.....115*

Figure 33 *Block diagram of the smart chemical system. The system includes 3 stages, the sensing stage formed by 12 different sensors, the signal acquisition stages which incorporated the circuit signal conditioning and an Arduino due that was used to acquire all the signals and finally the data processing and the prediction of fire stage implemented in a PC.....116*

Figure 34 *Distribution of the Arduino ports used to connect the gas sensors of the prototype 1. .....117*

Figure 35 *Graphical interface of the prototype 1.....117*

Figure 36 *Temperature Profile of the MOX heater sensor.....119*

Figure 37 *In the top MOX sensor control and conditioning circuit and in the bottom mox sensor filter analysis frequency analysis.....120*

Figure 38 *A bandpass filter was implemented as an amplified of the NDIR sensor outputs. In the top the complete sensor circuit and in the bottom the frequency analysis of the filter. 122*

Figure 39 *Montecarlo analysis of the NDIR filter. 123*

Figure 40 *EC-CO circuit acquisition using the AFE LMP91000.....124*

Figure 41 *PID sensor signal electronic circuit* 125
Figure 42 *Sensirion SH75 Humidity and Temperature Sensor connections. Sensirion sensor is connected directly to the Arduino DUE platform. Picture from www.sensirion.com.* 126
Figure 43 *Block diagram of the prototype 2 system.* 127
Figure 44 *Prototype 2 was implemented in a conventional Minimax Housing. The figure shows the final view.* 128
Figure 45 *View of the electronic boards that integer the prototype 2* 129
Figure 46 *View of the sensors integrated into the Prototype 2* 129
Figure 47 *Metal Oxide sensors in the prototype 2* 130
Figure 48 *Electrochemical Sensor for* $CH4$ 131
Figure 49 *FET-*$H2$ *sensor developed by BOSCH for the prototype 2* 132
Figure 50 *GSS Cozir LPTM NDIR* $CO2$ *sensor device* 133
Figure 51 *CO receiver from NEO.* 134
Figure 52 *Overall view of the methodology followed to build the fire predictors.* 137
Figure 53 *Raw signals (left) and filtered signals (right) of the* $CH4$, $H2$ *and* PID *sensors. The figure shows the sensor responses of one repetition of Cable fire.* 138
Figure 54 *Labels of one repetition of TF3 Fire (left) and one repetition of Window Cleaning experiment (right).* 139
Figure 55 *Performance of the post-processing time windows. The time windows are of 1s, 15s, the 30s, and 1 min* 141
Figure 56 *Overall construction and validation prediction model* 143
Figure 57 *PCA Scores of the large scale dataset 2 acquired with prototype 1 (left) and prototype 2 (right). In the top, the scores are colored by experiment type and in the bottom with the labels of fire and nuisances.* 144
Figure 58 *PLS-DA scores of the model trained with data acquired with prototype 1 (top) and with the dataset measured with prototype 2 (bottom). The training scores are colored by the actual labels and the scores of the test set are colored by the predicted labels.* 146
Figure 59 *Variable Importance of Projection of the model trained with data acquired with prototype 1 (top) and model built with the prototype 2 datasets (bottom).* 148
Figure 60 *Biplot of the PLS-DA models. In top the PLS-DA scores of the prototype 1 and in bottom scores of the measurements acquired with prototype 2* 150

Figure 61 True Positive Rate (Top) and True Negative Rate (False) of the prediction models based on PLS-DA in function of the pre- processing time window during Internal Validation. *152*

Figure 62 Experiment Response times of the fire alarms based on PLS-DA and commercial fire detector. *153*

Figure 63 True Positive Rate (Top) and True Negative Rate (False) of the prediction models based on SVM in the function of the pre-processing time window. *155*

Figure 64 Experiment Response times of the fire alarms based on SVM and commercial fire detector. *157*

Figure 65 Models and commercial detector performance in function of the true positives and false positives (ROC space). *158*

Figure 66 Description of the datasets using to train and to validate the models. *162*

Figure 67 Sensor signals of the TF2 wood fire, on the right the experiment was performed in the small scale setup and in the right the fire test was performed at the standard fire room. *163*

Figure 68 PCA scores of the large scale dataset 2 (validation set). On the left the scores are colored by type of experiment and on the right the experiments are colored by the actual labels of fire and non-fire. *164*

Figure 69 Biplot on the PLS-DA scores of the Fire Room Model *168*

Figure 70 Biplot on the PLS-DA scores of the Fire Room Model *170*

Figure 71 Biplot on the PLS-DA scores of the Data Fusion Model *172*

Figure 72 Figures of merit (classification rate, sensitivity, specificity and AUC) of the Fire Room, Small Scale and Data Fusion Model. *173*

Figure 73 Sensor responses to CO presentation under different humidity levels. Acquired signals for four MLK sensors (top panel), and CO and humidity set-points (bottom panel). Sensor conductivity changes according to the presented conditions. Blue (baseline) and green (measurement cycle) dots represent sampling points for the construction of the dataset. *178*

Figure 74 PCA scores of the different sensor array samples. Numbers correspond to the sensor array and color codes the gas (class). *182*

Figure 75 Confusion matrix obtained when the model is tested with data acquired with the same sensor array present in calibration (top, scenario 1) and when it is tested with data acquired with different copies of the array (bottom, scenario 2). The classification

accuracy decreases if the calibration model did not include data from the sensor array used for training. *184*

Figure 76 *Average of confusion matrices of the general calibration models. Models were trained with samples of four different arrays and evaluated with samples of a different array. The performance of the general model is similar to the performance of individual calibration models when were trained and tested with samples of the same array.* *185*

Figure 77 *PLS-DA score plots for the general calibration model. Color indicates the gas type and marker type indicates calibration/test point. (left) LV 1 vs LV 2, (right) LV 1 vs LV 3. Calibration and test points appear in the same regions, confirming thereby a generalization of the models.* *187*

Figure 78 *Performance of the models when evaluated with test samples from units not used in calibration, for different number of sensor arrays used in calibration. Keeping the number (56) of calibration samples constant (red), and using all the data available (56 per sensor array) for the units used in calibration (blue).* *188*

Figure 79 *Relative frequency of the area under the curve (AUC) computed for each model. General models are more accurate than individual models for the prediction of new samples from arrays not presented in training. The histograms present the relative frequency for all the possible combinations of arrays.* *189*

Figure 80 *Relative frequency of the number of latent variables and nearest neighbors used to build general and individual models. General models use fewer latent variables than individual models, providing an easier interpretation and a better generalization of the model.* *190*

Figure 81. *Distribucion de la sala de fuegos en donde fueron ejecutados los experimentos de fuegos e interferencias. La facilidad localizada en Minimax cuenta con un area experimental y un area de control.* *209*

Figure 82. *Dimensiones de la cámara de fuegos en donde los experimentos a pequeña escala fueron ejecutados.* *210*

Figure 83 *Señales y etiquetas del experimento TF3 y limpieza de ventanas.* *215*

Figure 84 *Metodologia para la construccion de los modelos de prediccion de incendios.* *216*

Figure 85 *Comparacion de los distintos modelos en funcion de los falsos positivos y falsos negativos presentados por cada uno.* *217*

Figure 86 *Area bajo la curva, especificidad, sensibilidad y ratio de clasificacion de los diferentes modelos. Modelo 1 esta construido con datos de la habitacion de incendios, modelo 2 esta construido con datos de la peque;a camara y modelo 3 esta construido usando la fusion entre ambos escenarios. 220*

Figure 87 *Matriz de confusion del modelo general construido usando diferentes lotes de una misma matriz de confusion.....221*

List of tables

Table 1 . Standard Test Fires described in the EN-54 standard. 40

Table 2 Concentration measurement ranges (in ppm) for fire emissions provided by different vendors..... 45

Table 3 Availability of electrochemical cells for the detection of toxics1. 46

Table 4 Target Gases of the instruments used at the customized chamber when the experiments of nuisances and fires were performed 86

Table 5 Date and duration of the measurement Campaigns performed in the fire room and in the small chamber. 109

Table 6 Fire and nuisance scenarios included in the different datasets. Large-scale dataset 1 and large-scale dataset 2 were acquired in the standard fire room and the small-scale dataset was acquired in the measurement chamber. 110

Table 7 Main gas emissions in smoldering fires 112

Table 8 Sensor Technologies Selection for the fire detection prototypes..... 114

Table 9 Advantages and disadvantages of the MOX sensors 118

Table 10 Temperatures and Power of the Heater AMS sensor..... 119

Table 11 Confusion matrix and figures of merit of the prediction model built with large scale dataset 1 (Fire Room Model) 167

Table 12 Confusion matrix and figures of merit of the prediction model built with small scale dataset (Small Scale Model)..... 169

Table 13 Confusion matrix and figures of merit of the prediction model built with the combination of the (Data Fusion Model)..... 171

Table 14 Percentage of the experiments correctly classified in function of the time window using a prediction model based on PLS-DA 205

Table 15 Percentage of the experiments correctly classified in function of the time window using a prediction model based on SVM..... 206

Table 16 Experimentos y sus repeticiones realizados en cada campaña de medidas 212

Abstract

Conventional fire alarms are based on smoke detection. However, in fire scenarios, a large variety of gases are emitted before smoke is released. In closed places or buildings, exposure to gas toxic emissions may lead to health consequences for the occupants. Gas sensor systems represent an alternative for the detection of gas emissions in fires . Fire detection systems based on gas sensors have been proposed since early 80s. Previous studies showed that gas sensors can provide a faster response, but are still prone to false alarms due to chemical interference or environmental conditions effects. Pattern recognition techniques can be useful to mitigate this limitation. In this thesis, two fire detectors based exclusively on gas sensors are developed. The detectors combine different technologies of gas sensors and provide a fire alarm based on machine algorithms. The detectors were exposed to standard EN54 fire tests and different nuisance tests. Two different approaches are presented: the first model is based on a Partial Least Squares Discriminant Analysis -PLS-DA-, and the second is based on Support Vector Machines –SVM-. The results confirm the ability to detect fires at an early stage of development and the rejection of most of the nuisances.

In addition, there are presented two methodologies for the reduction of calibration costs of gas sensors for fire detection. Standard Experiments are performed in a standard fire room are expensive due to the long duration and the limited availability of standard fire rooms. For this reason, the first proposed methodology combines data from a standard fire room and data from a small-scale setup (small scale setup experiments are faster and less expensive). Results show that prediction model performance can be improved using data fusion approaches. On the other hand, the need for individual calibration models for each sensor matrix (due to the variability of the sensor) increases the production costs. To reduce calibration cost, the second methodology rejects the variability of the sensor and provides general calibration models.

Chapter 1: Introduction

The most popular and widespread fire alarm systems are based on the detection of smoke and airborne particles. Two techniques for smoke detection emerge for fire detection: photoelectric detectors (light scattering) and ionization detectors. However, light scattering and ionization detectors are not sensitive to toxic emissions, so they may not offer enough protection in the case of slow fires, named smoldering fires. Such fires released a large variety of toxic emissions before smoke. In smoldering fires, conventional smoke detectors can trigger the alarm, when toxic gas concentrations may have already reached levels that threaten people's lives [1].

The importance of toxic emissions in fires has been recognized as a primary hazard for building's occupants since the 1970s, when surveys about fire deaths and non-fatal fire injuries were carried out in the UK. These surveys showed that a substantial proportion of casualties was due to fire emissions and not to actual burns. Additionally, the same studies demonstrated that the fraction of deaths due to toxic emissions was growing over time (a fourfold increase from the 50s to the 70s). This increasing trend continued during the 80s and 90s, although the overall number of fires remained approximately constant in that period. For example, during the 90s, only in the UK, the total number of injuries attributed to toxic fire emissions was about 6000 per year, and the total number of deaths was about 14/million inhabitants/year. The increase of injuries caused by toxic emissions in fires has been attributed to the increasing popularity of polymers in building materials, with the underlying idea that new building materials produce more toxic effluents than conventional materials. Other interpretations claim that the released toxic gases are the same ones for new and conventional materials, but volatiles are released at a much higher pace from new materials [2].

Additionally, smoke detectors are unable to discriminate between smoke particles from fires and particles from other events, leading to high rate of false positives. False alarms are always a concern for fire detection due to high associated costs and frequency. Only in the UK, for example, the Fire and Rescue Service Authorities claim that the associated cost of false alarms rises to 1 billion pounds per year [3]. The same source claims that in the period 2011–2012, 53% of the alarms were false positives. Moreover, even worse ratios of false alarms have been reported in studies performed in the 90s in Europe and the US. In some reports, the fraction of real alarms was as low as

11% [4]. Indeed, there are many daily activities that may lead to false alarms (nuisances), being burning toasts and cooking fumes in general, dust from building works, water steam from the shower, etc., examples of the most prevalent ones.

A promising alternative to counteract conventional fire detectors constrains may rely in fire detection using gas sensing. Since the 1990s gas sensors have been explored as indicator of open and smoldering fires. Fire detection based on chemical sensing could provide faster alarm signals when gases are released before smoke particles[5]. However, the current use of fire detection systems based on gas sensors has been limited to niche scenarios, such as fire detection in coal mines [6] or coal power plants [7].

However, it has been long found that it is difficult to discriminate nuisances from early fire by processing data from a single sensor [8]. In order to improve the reliability of fire detectors, multisensor systems had been explore [9]. Such multisensor systems can also benefit from algorithms built for single-sensor systems, as decision rules based on logic rules can be combined with the different sensors, but tailored algorithmic solutions to build calibration models for multisensor systems are more common than the extension of single sensor solutions to multiple sensor systems.

The reliability of fire predictions was successfully improved when heat and CO sensing was added to smoke detectors and they were combined with dedicated calibration models. Standardized tests for such kind of multisensor systems are available. However, different approaches based on non-specific gas sensors and other sensing devices have been proposed to reduce the costs and consider other combustion products beyond CO. These non-standardized systems have been subject of investigation by the community as they can detect more toxicants and combustion products and can provide faster detection, although they suffer from low specificity.

To build robust and reliable fire alarm systems, multisensor systems need to be exposed to many types of fires and nuisances. The quality of the classification model depends critically on the number and conditions of the considered fires and nuisances. However, the benchmark of the different systems is difficult due to the disparity of experimental setups and difficulties and cost of data generation. In this work, we will focus on the challenges and opportunities offered by fire detectors that include chemical sensors. In particular, we will focus on their ability to act as reliable fire detectors and

their potential to detect toxic emissions that may appear in the early phases of fire development.

1.1 Fire Detectors Based on Smoke Detection

Widespread fire alarm systems are based on the detection of smoke. Smoke is defined as “the airborne solid and liquid particulates and gases evolved when a material undergoes pyrolysis or combustion” [10]. However, in this context, smoke detectors refer exclusively to the detection of fire particulates, excluding gas detection. Two techniques for smoke detection emerge for fire detection: Photoelectric detectors (light scattering) and ionization detectors. Briefly, ionization smoke alarms use a radioactive source, usually Americium-241, that emits alpha particles to ionize air molecules. The generated ions close the path of an electric circuit. If smoke is present, the generated ions interact with smoke particles, reducing thereby the intensity that flows through the circuit. The need for a radioactive emitter to break the molecules into ions has decreased the popularity of ionization detectors. On the other hand, photoelectric detectors include a light emitter and a photodetector. If there is smoke in the chamber, smoke particles produce light scattering. Scattering or obscuration of light is measured with the detector. Typically, independently of the detection principle, the alarm signal is triggered when the signals reach some defined threshold.

The sensitivity, response time and reliability of the fire alarm usually depend on the sensing principle. In order to establish formal benchmarks between sensing principles, photoelectric and ionization fire alarms were compared extensively in controlled conditions [11]. Such studies suggest that usually, ionization alarms respond faster than photoelectric alarms to open flame fires. In contrast, photoelectric alarms tend to show faster response and higher sensitivity than ionization detectors in smoldering fires. For example, Underwriters Laboratories Inc. compared photoelectric and ionization detectors under different fire types inspired by the UL 217 standard (see Section 5) and other fires [12]. Flaming and smoldering fires produced combustion particles of different diameter, which conditioned the response of the different detectors. Smoldering fires produced larger particles, which were captured faster by photoelectric detectors. On the other hand, smaller particles, which are found in flaming fires, were detected faster by ionization detectors. Moreover, the results indicated that, given the same consumed mass, smoldering fires resulted in more smoke particles than flame fires. They also found that ionization alarms could not detect some smoldering fires that photoelectric alarms detected. This became more relevant for smaller burning

quantities that generated less smoke than the 10% obscuration/ft specified in the UL 217 standard.

Briefly, smoke detectors can be considered as particle detectors that are sensitive to a specific distribution of particle sizes. Usually, fire alarm is triggered when the sensor signal reaches an established threshold. As a result, these systems struggle in discriminating particles resulting from fires and non-combustion particles when the particles have similar size or refractive indices. For example, smoke detectors also show sensitivity to water vapor and dust [13]. Moreover, they cannot distinguish combustion products from a fire threat condition from combustion products produced under controlled conditions, such as cigarette smoke or some cooking activities [14].

In summary, both photoelectric and ionization fire alarm systems show cross-sensitivities that yield false alarms. The false alarm ratio sometimes becomes too high for the resident, who is then tempted to disable or ignore fire alarm signals.

In order to improve the specificity of the fire alarm, other sensors can be added to smoke detectors. For example, common nuisance scenarios such as cooking aerosols, water steam (from cooking or showers) and dust sources increase light obscuration but do not result in CO concentration increases. Hence, CO detection can be used to improve false alarm immunity and reject false alarms induced in scenarios that do not generate CO [15].

Unlike smoke-based fire alarms, systems based on single measurements from one gas sensor would not be suitable for fire detection, as the number of false alarms would be unacceptably high. For example, fire detection system based on single CO measurements would overlook flame fires and would be sensitive to exhaust gases from gas or oil furnaces. As a result, gas-based systems require multiple sensor or multi-criteria approaches, and, thereby, more complex data processing algorithm

1.2 Gas Emission in Fires

A wide variety of materials are found nowadays inside occupied buildings. The burning of these materials results in the release of different combustion products, namely aerosols and gases. Additionally, products not actually burning may reach temperatures high enough to suffer from thermal decomposition and pyrolysis, producing thereby additional emission of gases and volatiles [10]. All these products constitute health hazards for building occupants and emergency personnel.

Health hazards may be divided into several categories:

Irritants: Fire gases and particles producing irritation of the respiratory tract, that can impair the ability to escape and, at higher concentrations, can lead to incapacitation and death.

Asphyxiants: Inhalation of these gases can produce the depression of the central nervous system leading to disorientation, loss of coordination, loss of conscience and finally death.

Thermal effects: Thermal burns on the skin and the respiratory tract, as well as hyperthermia.

When exposed to the above-mentioned hazards, the impact on the building occupant's health depends on the previous health condition of the individual (age, morbidities, asthma, etc.) and on the nature of the exposure: exposure time, gas concentration, toxicity of the volatiles, etc. Moreover, the incapacity to find the escape path due to eye irritation and smoke obscuration produces longer exposures to these hazards. Fire survivors can also suffer from post-exposure and delayed health effects.

Emissions of gases and volatiles may occur during pyrolysis or during combustion. Pyrolysis is defined as "a process of simultaneous phase and chemical species change caused by heat", while combustion is "a chemical process of oxidation that occurs at a rate fast enough to produce temperature rise and usually light, either as glow or flame" [10].

Since the 1980s, the use of polymeric materials in commercial products has increased dramatically. This results in more volatile emissions during fires: when heated, polymeric materials may show phase change (melting in thermoplastics) followed by thermal decomposition. This leads to the emission of low weight volatile compounds, prior to actual combustion happens and before visible smoke appears.

Gas emissions are also particularly relevant during smoldering fires. This is a form of combustion that mostly occurs in porous or grained but densely packed materials. Air diffuses through the pores and produces combustion in the inner side of the material. The combustion products in smoldering fires are typically different from the ones generated in open flame fires.

In smoldering fires, the temperature is low (around 400 °C) and fire materials decompose due to a combination of pyrolysis and oxidation. In this type of fires, the CO/CO_2 ratio is close to 1, and CO may be the major toxicant to consider. Fire evolution is slow, temperatures are also low, and the smoke density is not dense. Under these conditions, the occupants may die from asphyxia, particularly if they are asleep. In fact, it is known that smoldering fires that have been running for 30 min or more before being detected produce more casualties than fires that produce rapid flame fires [5].

1.3 Main Toxicants from Fire Emissions

A review of the literature will easily show that fires may emit hundreds if not thousands of gases and volatile compounds, however few of these are particularly relevant due to either their volume or their toxicity. Current understanding of fire emissions concludes that carbon monoxide is still today the main toxic component in fires. However, the presence or addition of other toxics may lead to much faster death than when only the effect of CO is considered. As already mentioned, the presence of synthetic polymers in building materials and building contents (for instance, electronics, cables, electrical appliances, etc.) is more and more determinant for toxic emissions since many of these materials contain nitrogen or halogen compounds, leading to the presence of hydrogen cyanide (HCN) and inorganic acids. Stec remarked that CO is not the only toxic gas released in fires. She studied other toxicants, in particular, the significance of HCN from PVC fires. Her results confirmed the danger of HCN in under-ventilated conditions [16]. Finally, oxygen depletion to 10% or lower usually increases the effects of the toxicants.

1.3.1 Carbon Dioxide

$CO_2$is probably the most important combustion product. If there is enough ventilation, almost all carbon content is converted to CO_2. The toxicity of CO_2, individually is low, but as we will review in the next section, it can interact with other toxics exacerbating their effect.

1.3.2 Carbon Monoxide

Carbon monoxide is an asphyxiant gas. CO emissions are particularly relevant in smoldering fires. For example, in many fires, CO is emitted and then it is oxidized to CO_2. However, in the absence of sufficient ventilation, the second step is not efficient and larger concentrations of CO are found. In typical scenarios, lethal concentrations of CO may be reached close to the fire in less than 30 min. Moreover, after dilution, lethal concentrations may be reached in 1–2 h in the whole room.

The emission of CO is related to the air-fuel ratio (equivalence ratio) [17]:

$$\varphi = \frac{m_{fuel}/m_{air}}{(m_{fuel}/m_{air})_{stoich}} \quad (1)$$

Where m_{fuel} is the mass of fuel, m_{air} is the mass of air, and stoich refers to the stoichiometric conditions. When a fire happens in stoichiometric conditions (φ = 1), there is exactly enough air to burn all the fuel. For φ < 1, fire conditions are considered rich, while for φ > 1 conditions are considered lean. Lean conditions provide higher production of CO.

1.3.3 Hydrogen Cyanide

Hydrogen Cyanide is an asphyxiant gas. HCN originates from nitrogen-rich polymers such as wool, nylon, polyacrylonitrile, melamine, etc. The formation of this compound is not as well understood as the mechanism for CO formation, but in any case, its production is also enhanced in lean conditions. In the recent years, there has been an increasing concern on the relevance of this compound in mission intoxications of firefighters [18].

1.3.4 Nitrogen Oxides

Fire effluents analyzed by FTIR have shown that nitrogen oxides appear mostly in the form of nitric oxide (NO). This gas is stable at the low concentrations and low temperatures typical of actual inhalation by humans in fire incidents. Nitric oxide also appears in tobacco smoke and in exhaust gases from motor vehicles. Alternatively, we may also find nitrogen dioxide (NO_2). NO_2 is highly soluble in water and it is an acid irritant with highly toxic effects. It has a higher toxic potency than NO [19].

1.3.5 Sulphur Dioxide

Sulphur dioxide (SO_2) is an irritant gas. It may appear in the combustion of some textiles like wood or viscose [20], but also rubber materials. Mathematical models of lethal toxicity of fire smoke consider Sulphur dioxide a key component [21]. Sulphur dioxide has been detected in real overhaul operations in concentrations of around 2 ppm, with maximum values of 8.7 ppm.

1.3.6 Halogen Acids

Halogen acids appear from the combustion of polymers containing halogen elements (fluorine, chlorine, bromine). Examples are polyvinylchloride (PVC), neoprene, polyvinyl fluoride, polytetrafluoroethylene, and brominated flame retardants. The most relevant ones are consequently hydrogen fluoride (HF), hydrogen chloride (HCl) and hydrogen bromide (HBr). These compounds appear mostly in the pyrolysis

phase before actual combustion. Their concentration may be high since the efficiency of their production is very high. For instance, HCl is produced by PVC at temperatures between 225 to 275 °C [22].

1.3.7 Organic Irritants

Incomplete combustion and pyrolysis of organic materials can produce a large variety of Volatile Organic Compounds (VOCs). The most toxic ones are considered to be formaldehyde, unsaturated aldehydes like acrolein and isocyanates [23]. Acrolein can be emitted, among other materials, from polyethylene[24].

1.4 Toxicity of Released Gases in Fire

Toxic effects of fire gas emissions can be grouped in asphyxiants and respiratory irritants. Since, in the particular scenario of fires, the concentration of toxic gases is relatively high for a short period of time, the typical threshold limit values (TLV) used in occupational hygiene are not normally used.

1.4.1 Asphyxiant Gases

Carbon monoxide is the most important and studied toxic emission from fires. The toxic effects that produce incapacitation, first, and ultimately death is related to the combination of CO with hemoglobin to form carboxyhemoglobin ($COHb$). Hence, $COHb$ is a biomarker of smoke inhalation that can be used to investigate cause of death in fires. To determine if CO intoxication has been the main cause of death, $COHb$ in blood is measured during forensic investigations. Usually it is considered that if $COHb$ reaches 50% (normalized to the total hemoglobin content) death has been caused by CO inhalation during fire. An increase of $COHb$ diminishes the capacity of blood to transport oxygen. Additionally, at elevated levels of $COHb$, there is a shift in the equilibrium reaction of HbO_2 that hinders oxygen to be delivered to cells. Finally, when CO combines with myoglobin the transport of oxygen to muscle tissues (including cardiac) is reduced.

The Coburn-Forster-Kane (CFK) equation describes the dynamics of $COHb$ formation from CO inhalation [25]. This model has been thoroughly validated and information on the population distribution of its parameters has been largely studied [26,27]. Additionally, it has been refined to include the decrease in HbO_2 when $COHb$ increases. This effect can be neglected at low CO concentrations but it becomes relevant at high CO and O2 depletion, as it happens in fire scenarios [28]. The CFK model is recommended to simulate the

evolution of $COHb$ and compute the time to incapacitation (30% $COHb$) and the time to lethal conditions ($COHb$ > 50%). In this kind of simulation, a critical parameter in the CFK equation is the alveolar ventilation and the lung-diffusing capacity for CO, depending on the oxygen input flow. This input flow can change form 8 L/min at rest up to 100 L/min when escaping fast [29,30]. Under the academic hypothesis of a constant CO concentration, the Stewart-Peterson [31] equation provides the time required to reach a certain level of $COHb$:

where $COHb$ is in %, CO in ppmv, respiratory minute volume (RMV) in L/min and t in min. With these units B = 3.32 × 10−5. The CO concentration that is accumulated in the blood in the form of $COHb$ determines the effects on the subject. First symptoms in humans (headache) are reported when $COHb$ reaches values of about 10%, after the subjects were exposed to 15,000 ppm of CO for 2 min, or 30,000 ppm for one minute. Time to incapacitation depends on the accumulated CO and also on the physical activity of the subject. For example, at 10,000 ppm of CO, probable time to incapacitation for humans was estimated at 10 min, 4 min, or 1 min for resting state, light work, or slow running, respectively. Additionally, it is interesting to remark that the half recovery time for adults at rest is 320 min [31,32].

Carbon dioxide. CO_2 is not considered a toxic gas, but at high concentration levels, it increases the breath frequency and depth, leading to increased RMV. For instance, an atmosphere with 10% of CO_2concentration induces a 10-fold increased RMV on the exposed subject with respect to RMV in a not contaminated atmosphere. As a result, increased RMV produces faster intoxication by other gases and VOCs [33].

Oxygen depletion from 20.9% to 17% produces a degradation in motor coordination and, up to 10% of oxygen concentration, the exposed subject may still be conscious but will suffer incapacitation effects in terms of impaired judgment and fast fatigue conditions. From 10% to 7%, the person may lose consciousness. These conditions with very low oxygen concentration levels are only reached very close to flames, where heat is additionally the most important threat. Far from the fire flames, the most important effect of oxygen depletion is the combined effect with toxicants, for instance by augmenting the breath rate that leads to faster dynamics in the uptake of other toxics.

Hydrogen Cyanide (HCN) is lethal at doses much smaller than carbon monoxide and its toxic effects are very fast [34]. Like $COHb$, it can also be determined in blood to investigate its relevance in the event of death. In fact,

HCN in blood is routinely found in forensic investigations of fire. Levels around 3 mg/L have been suggested as lethal from animal experiments. The toxicity of HCN is due to the binding to cytochrome oxidase in the mitochondria, and this precludes oxygen consumption in cells, leading to cytotoxic hypoxia. Additionally, cyanide ions react with methemoglobin to produce cyanomethemoglobin. However, the dynamics of HCN uptake and its related toxic effects did not receive the same degree of attention as for CO uptake: currently, no mathematical for HCN uptake has been widely adopted by the community. While data on human exposure effects is scarce, it is assumed that 50 ppm of HCN may be tolerated for about 1 h, but 130 ppm may be lethal in 30 min, and 180 ppm of HCN can lead to death in only 10 min [31].

Nitric Oxide (NO) passes very fast into the blood where it reacts with hemoglobin. It can form methaemoglobin that is a form of hemoglobin unable to bind to oxygen. In low oxygen conditions, it also binds to hemoglobin to form nitrosyl-hemoglobin ($HbNO$). These mechanisms have asphyxiant character by decreasing the oxygen transport capacity of the blood. It has been claimed that NO has 1500 times more affinity for hemoglobin than carbon monoxide. However, the dynamics and the parameters of these reactions are not totally understood [19].

Nitrogen dioxide at high concentrations is known to cause lung edema. According to ISO 13571, the incapacitating volume fraction of NO_2 is 250 ppm [30]. This concentration is considered as the NO_2level that, if inhaled at any time, entirely limits the ability to escape from a hazard situation.

1.4.2 Irritant Emissions

Hydrochloric acid (HCl) is an irritant gas that is extremely irritant to the eyes and the pulmonary system at 100 ppm, and it threatens life for short exposures of 1000 ppm or more. HCl is mostly emitted from PVC (and other chlorine-containing polymers) and its incapacitating power can be bigger than that of CO, but smaller than that of HCN.

Hydrofluoric acid (HF) and hydrobromic acid (HBr): Limited data exist on the toxic effects of these gases when inhaled. However, we may take as reference the values contained in the ISO13571 standard [30]. This standard is used in the estimation of the toxic potency of mixtures (see the section below) and it considers different reference values to weight the effects of the different constituents of the fumes, namely LC50,HCl = 1000 ppm, LC50,HF =

500 ppm, LC50,HBr = 1000 ppm, where LC50 represents the gas concentration that is lethal for half of the exposed population during a time period (30 min).

Sulphur Dioxide (SO_2) is an irritant gas that produces an increase airway resistance depending on the inhaled concentration. It can lead to pulmonary edema [35]. The incapacitating concentration according to ISO13571 is 150 ppm.

Volatile Organic Compounds. It is well-known that fire emissions may contain hundreds, if not thousands, of VOCs, but only a few have been considered from the point of view of fire toxicity. To mention just a couple, ISO13571 cites 30 ppm of acrolein and 250 ppm of formaldehyde as incapacitating values.

1.5 Combined Toxic Effects

The toxic potency of fire emissions can be estimated using several standards such as ISO 13344 and ISO TS-13571. These standards base their toxic potency calculations on the concentration of asphyxiant and irritant gases. The key compounds considered by these standards are CO_2, CO_2, HCN, oxygen depletion, haloacids (HF_2,HBr, HCl), SO_2, nitrogen oxides, formaldehyde, and acrolein. Despite evidence that NO plays a significant role in fire emissions, current ISO standards only consider NO_2.

Different examples of models that take into account the combined effect of the toxic potency of mixtures with different toxicants have been presented. Fractional Effective Dose (FED) is obtained from the concentration of the components present in the mixture. Here, we present two examples of such models, (namely FED1 and FED2) [30,36]:

Equation (1)

$$\mathrm{FED1} = \frac{\mathrm{m[CO]}}{[\mathrm{CO_2}] - \mathrm{b}} + \frac{21 - [\mathrm{O_2}]}{21 - \mathrm{LC_{50,O_2}}} + \frac{[\mathrm{HCN}]}{\mathrm{LC_{50,HCN}}} + \frac{[\mathrm{HCl}]}{\mathrm{LC_{50,HCl}}} + \cdots$$

where FED is obtained from the concentration of the components and the parameters m and b. The parameters m and b model the increased ventilation caused by high concentrations of CO_2. If $[CO_2]$ < 5 %, m = −18 and b = 122000 ppm. If $[CO_2]$ > 5 %, m = 23 and b = −38600 ppm. FED values depend on LC50 values. A value of FED = 1 is, hence, supposed to be lethal for half of the population after 30 min.

The additivity of effects has been empirically found in studies with rodents [37,38] and this model was also validated by Pauluhn [21]. An alternative formulation is [39]:

Equation (2)

$$\mathrm{FED2} = \left\{\frac{[\mathrm{CO}]}{\mathrm{LC}_{50,\mathrm{CO}}} + \frac{[\mathrm{HCN}]}{\mathrm{LC}_{50,\mathrm{HCN}}} + \frac{[\mathrm{HCl}]}{\mathrm{LC}_{50,\mathrm{HCl}}} + \cdots\right\} \cdot \left(1 + \frac{\exp(0.14[\mathrm{CO}_2]) - 1}{2}\right) + 0.05[\mathrm{CO}_2] + \frac{21 - [\mathrm{O}_2]}{21 - \mathrm{LC}_{50,\mathrm{O}_2}}$$

It is important to remark that the values of LC50 are not the same for both models. This discrepancy is due to the diverse animal studies that were used to build the respective models. The FED values calculated with both equations may differ by approx. 30% [5].

When interpreting FED values, it is important to consider the large variability in the resistance of people to the toxicological effects of fire fumes. In particular, children, the elderly, and people suffering from respiratory problems are more sensitive to toxicants. For this reason, the goal is maintaining fire conditions, when possible, in FED values substantially lower than 1. The literature mentions that at FED = 0.3, 11% of the population may suffer lethal consequences [5].

1.6 Toxicant Production Depending on Fire Scenarios and Burning Materials

The emission of fire effluents depends on the combustion conditions. In turn, combustion conditions depend on many factors such as ventilation, burning materials, room geometry, and overall fluid dynamics. We have already exposed that fire types can be divided according to their behavior and burning conditions: smoldering fires and open fires. Smoldering fires have been traditionally characterized by CO emissions, although many other volatiles appear, especially since the use of new building materials. Open fires do not pose a major threat in terms of intoxication danger in well-ventilated scenarios (φ < 1). However, in scenarios with limited ventilation, an open fire rapidly consumes available oxygen and it transits to under-ventilation (lean)

conditions (φ > 1) that typically lead to the emission of toxic gases at high concentration levels. In this section, we focus the study on smoldering fires and open fires that already transited to lean conditions.

Since smoldering fires are cold fires (compared to flaming fires), the smoke is colder, and the buoyancy is also smaller. In consequence, the smoke disperses slowly in the full volume of the room, instead of rising straight to the ceiling, where smoke detectors are located. As a result, time to alarm can be longer for smoldering fires with respect to open fires.

As example of smoldering fire and the release of volatiles, we can refer to a series of NIST tests fires performed with armchairs made of polyurethane foam with cotton fabrics [40,41]. The total mass was 5.7 kg, and the total volume of the room was 12 m3. The fire was initiated with two cigarettes placed over the chair. In this particular test, the fire run in smoldering conditions for 1 h before developing a flame. Figures 1–3 show the progress of combustion products. We can observe how CO concentration builds up slowly in the room while the HCN presence only starts when flame conditions occur (Figure 1). On the other hand, O2 concentration also remains constant at 21% and lowers drastically only with the presence of open fire. Finally, the CO_2 concentration increases slowly and finally it grows fast also in the case of open fire (Figure 2). We should remark that lethal conditions are attained due to the build-up of toxicants in the smoldering phase before flames appear. The Fractional Effective Dose reaches FED = 1 before the flame appears and before CO, HCN and CO_2 concentration rise (Figure 3).

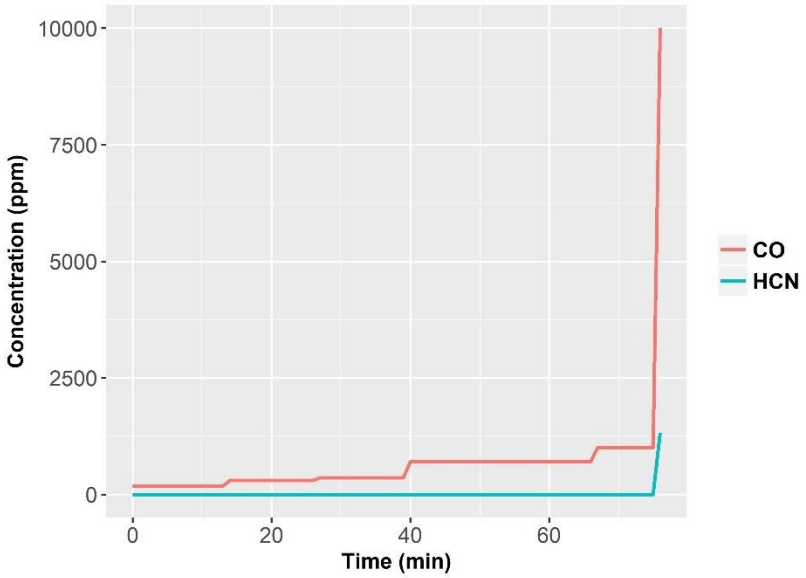

Figure 1 Example of evolution of CO and HCN for a smoldering fire (NIST tests) [16].

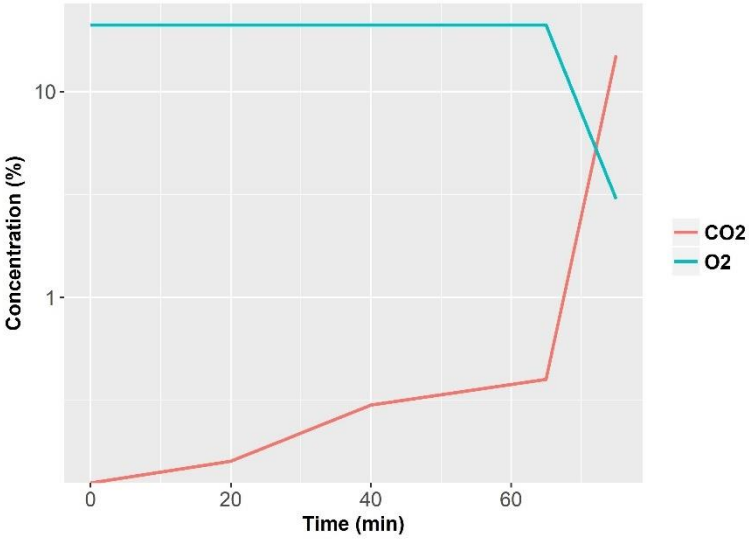

Figure 2 Example of the time evolution of O2 and CO2 during a smoldering fire [16].

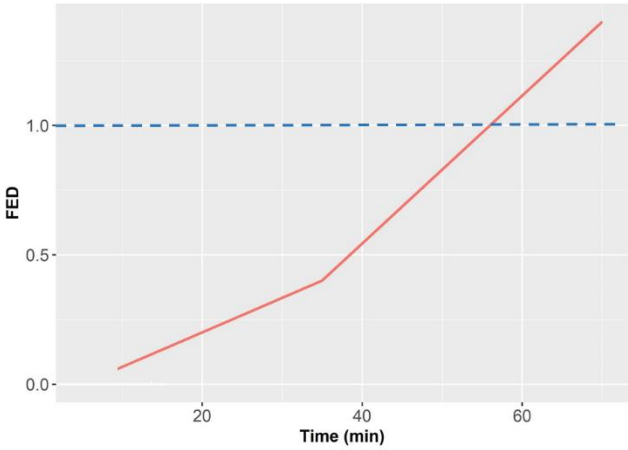

Figure 3 Time evolution of the toxic potency of the smoldering fire for the NIST test [40].

In a second recent example, SP Fire Research in Norway described a number of experiments based on smoldering fires [42]. The main goal of the report was to investigate if smoke detectors including CO sensors can alert occupants earlier than photoelectric smoke detectors. A secondary goal is to measure the concentration of toxic gases, mostly CO, during the development of the fire and determine if incapacity conditions are achieved before the photoelectric alarm triggers. The scenario they reproduce is a bedroom with a polyether foam mattress and cotton bed sheets. The room had a surface of

8.6 m2 and a total volume of 20.7 m3. The fire conditions were set to induce a smoldering fire on the mattress. Ten experiments were carried out, although one of the experiments was excluded because the fire developed into a flaming fire.

The main conclusions of the study were that the smoke detectors combined with CO sensors activated much faster than photoelectric detectors. The incapacitation limits due to CO intoxication were in some experiments achieved much before the alarm was triggered. This can, of course, have lethal consequences. In fact, in three of the experiments, the photoelectric detectors never triggered an alarm (three distinct brands and three different units for each brand were used). The time to alarm ranged typically from 2 to 3 h. Figure 4 compares the activation time between photoelectric detectors and detectors combined with CO sensors. Results show that detectors equipped with CO cells triggered the alarm signal for all the considered fires (whereas standalone photoelectric detector missed 3 of the performed fires) and produced alarm signals faster than photoelectric detectors.

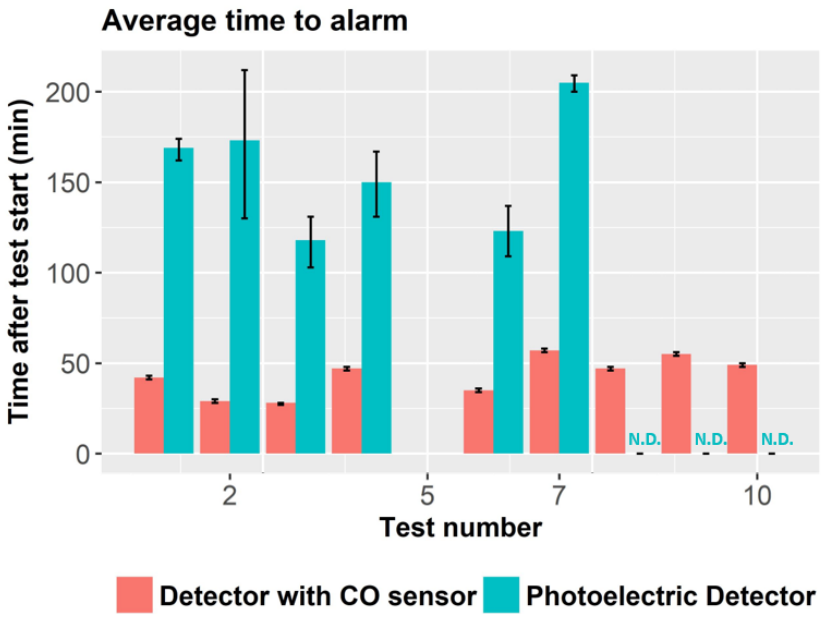

Figure 4 Comparison between photoelectric detectors and multisensory including CO Electrochemical Cell [42]. Photoelectric detector combined with CO sensor always produced faster alarm signals, and it was able to detect all the test fires. Standalone photoelectric detector did not trigger the alarm for three of the fires .

The concentration of CO when the photoelectric triggered the alarm (evaluated at the mean time of the different units) ranged from 600 to 1500 ppm. The photoelectric detector triggered the alarm in six of the performed fires. In four of them, the integrated dose of CO had already reached incapacitation limits (calculated in windows of 30 min) when looking the CO levels at the mean time to alarm. Instead, the CO concentration ranged between 30 and 60 ppm when the combined detector triggered the alarm and, in no case the CO incapacitation limit was achieved thanks to the faster alarm response and the moderate concentration levels at the time of activated alarm (Table 2).

In summary, there are very clear evidences than in some fire scenarios (smoldering fires) the inclusion of chemical sensors (EC CO cells in this case) is the path to provide enough safety to building occupants. However, we would like to remark that commercial and standardized fire detectors do only consider the detection of CO as toxic gas. At this point, it is well established that many other toxicants may lead to lethal consequences (particularly but not only HCN). Since most of these toxic gases are not detected properly by CO electrochemical cells, current detectors cannot provide proper protection to building occupants. The widespread presence of polymers in building materials and also in consumer appliances and electronic products leads today to the appearance of new families of toxicants that need dedicated detection.

The use of polymers is widespread in furniture, but also in electrical appliances and consumer electronics that may overheat and be at the origin of fires. These materials start the emission of volatiles when overheated. This process is also known as thermal degradation or pyrolysis. Finally, the flammable gases emitted by the materials may burn themselves if sufficient heat is available. In fact, once initiated positive feedback, the process may be self-sustained. Additional terms that appear in the description of this process are polymer melting and charring. The gasification of polymer materials is a complicated process. When overheated, the non-volatile polymer breaks down into smaller molecules of many chemical species, each one characterized by a certain vapor pressure. In this way, the smaller and more volatile fragments will evaporate first, followed by bigger fragments. Eventually, bigger fragments may stay at the surface and suffer a posterior break down to smaller molecules. Typically, several residues appear that are mostly char and inorganic materials.

Polymers can be categorized according to many criteria. Chemical composition is the most suitable classification criteria when thermal

degradation is under study. First, carbonaceous polymers only contain carbon and hydrogen atoms, being polyethylene and polypropylene two examples of carbonaceous polymers. There are also aromatic hydrocarbon polymers such as polystyrene. Some of these polymers appear blended with other polymers in commercial formulations. A second family of polymers is characterized by the presence of oxygen atoms. Among them, we encounter cellulosics, polyacrylics (like PMMA) and polyesters. Examples of polyesters are polyethylene terephthalate (PET), polycarbonates. Additional polymers with (H, C, O) are polyethers and polyacetals. The thermal decomposition of these polymers produces a large variety of alkanes and alkenes.

The third family of polymers is characterized by the addition of nitrogen (H, C, O, N). Examples are nylons, polyurethanes, polyacrylonitrile, and polyamides. For instance, thermal degradation of polyacrylonitrile starts between 250 and 350 °C and, among other products, it emits HCN and $NH3$ long before actual oxidation takes place.

Finally, polymers can contain other elements. Polymers containing chlorine are, for instance, polyvinyl chloride (PVC), polychloroprene or poly(vinylidene chloride). It has been reported that the emission of HCl from PVC starts at temperatures between 225 °C and 275 °C. Polymers like polytetrafluorethylene (PTFE), polyvinylidene fluoride (PVDF) or fluorinated ethylene polymers may also contain fluorine atoms [40]. Thermal decomposition of PTFE starts at temperatures around 475 °C and the main products emitted are CF_4, HF, and hexafluoropropene.

Hence, a diversity of polymers that are nowadays used and found in home settings, and the different composition of these polymers results in a large variety of released volatiles at higher temperatures, when material degradation takes place.

1.7 Standards for Fire Detectors

Prese Over the years several standards have been established worldwide to test the sensitivity and reliability of smoke fire detectors. One of the best well-known is EN54: “Fire Detection and Fire Alarm Systems” that specifies the conditions to be fulfilled by components and systems devoted to fire detection. This standard is mandatory in the European Union. It was created by the European Committee for Standardization (Comité Européen de Normalization—CEN) and it was also adopted by Latin American and Asian countries. For this paper, the most relevant section is EN-54: part 9: “Components of automatic fire detection systems. Methods to test the

sensitivity to fire". The EN-54 standard covers the requirements, test methods and performance criteria for point smoke detectors working under the principles of ionization, transmitted or scattered light. The same document states that for other types of fire detectors (e.g., fire detectors based on chemical sensors) the document must be considered only as guidance or inspiration. The standard covers the dimensions of the fire room, the position of the detectors in the room, and the required instrumentation that must be available for the tests. The document also details the procedure to perform the standard test fires. Table 3 lists the standard test fires described in the mentioned standard. The EN54 fires aim to prove that alarms have enough sensitivity to fire. The range of standard fires covers a diversity of aerosol types. It is important to note that not all fire detectors are suited to detect all fires. For instance, optical smoke detectors have poor sensitivity to liquid fires modeled by TF6, where smoke production is very limited. On the other extreme, flame detectors based on infrared or ultraviolet emissions are not suited for smoldering fire detection [43]. The principle of operation of the fire alarm selects the subset of standard fires to be used when testing the sensitivity of the detector. For more details on the technicalities and recommended procedure to implement those fires, the reader is referred to the EN-54 standard.

Table 1 . Standard Test Fires described in the EN-54 standard.

Experiment	Material
TF1	Open wood fire
TF2	Rapid smoldering pyrolysis wood
TF2a	Slow smoldering pyrolysis wood
TF2b	Smoldering pyrolysis wood
TF3	Rapid smoldering cotton
TF3a	Glowing slow smoldering cotton
TF3b	Glowing smoldering cotton
TF4	Open plastics fire (Polyurethane)
TF5	Liquid fire (n-heptane)
TF5a	Small n-heptane fire
TF5b	Medium liquid n-heptane fire
TF6	Liquid fire (ethyl alcohol)
TF7	Slow smoldering wood
TF8	Low temp. liquid fire (decalin)
TF9	Deep-seated smoldering cotton

It is important to mention that there is a dedicated standard for smoke detectors aimed at residential use, namely EN 14604: "Smoke Alarm Devices". In fact, EN54-7 and EN14604 share the methodology to select the most

challenging conditions for smoke detectors, being test fires TF2 to TF5 the most relevant ones to be considered in dwellings.

It is also worth noting that, although the standard is described for smoke detectors, TF6 does not produce smoke or aerosols. Hence, the detection of this fire type requires different operation principles than those in conventional smoke detectors. In fact, the detection of TF6 fires requires multicriteria detectors [44] that usually include additional temperature sensors.

Additionally, the ISO-7240 standard "Fire detection and alarm systems" [45] is the international version of EN-54, and many parts are identical. There are, however, some differences because the working groups preparing the standards both are different. The definitions of the standard test fires are the same in both. Australia also adopted the ISO-7240 standard with only minor differences under the name AS-7240.

Other standards exist in the US, in particular, the NFPA-72: National Fire Alarm and Signaling Code [46]. This is a standard published by the National Fire Protection Association (NFPA) and recognized by the American National Standards Institute (ANSI). NFPA-72 focuses on the entire alarm system and on the electrical signals between fire alarm components. It does not cover the description of standard fires for fire sensitivity analysis. Hence, we will refer to the activity of Underwriters Laboratories (UL). UL is a global company headquartered in the US dedicated to safety. They have published more than 1500 standards in the area of safety [47], including standards relevant to the area of fire detection:

- **UL217**: Standard for single and multiple station smoke alarms
- **UL268**: Smoke detectors for fire alarm systems
- **UL2034**: Standard for single and multiple station carbon monoxide alarms

UL217[48] and UL268[49] standards are described for different fire scenarios, although they share a lot of similarities. UL217 has the focus on residential smoke alarms, and UL268 focuses on smoke detectors connected to a central control unit. On the other hand, UL2034[50] is a standard for CO alarms to prevent intoxication due to inhalation. While the integration of CO and smoke alarms is very relevant, these products are not the focus of the UL2034 standard. The European equivalent of the UL2034 standard is EN50291 [51]. UL217/268 initially considered four flaming tests: namely paper fire (Test A), gasoline fire (Test C), polystyrene fire (test D), and wood fire (Test B) plus a smoldering test consisting of ponderosa pine on a hotplate. Lately,

the test set has been extended with flaming and smoldering versions of polyurethane foam [52].

The standard ISO7240-part 6: “Carbon Monoxide Fire Detectors using Electrochemical Cells” [45] is also very relevant for the consideration of fire detectors based on gas detection. Indeed, the mentioned standard acknowledges the importance of CO as a fire indicator. It also regulates the use of this type of systems for fire detection since this kind of products have been available since the late 90s. We have already mentioned the importance of CO as a toxic agent, mostly in slow, smoldering fires of carbon-based materials (wood, paper, etc.). The standard states that these detectors are important in scenarios where conventional smoke detectors are plagued with false alarms due to the large presence of dust, steam or other aerosols. The standard also warns users that detectors based solely on CO are not suitable for clean-burning liquids, PVC insulated cables, combustible metals, some self-oxidizing chemicals and non-carbonaceous materials. Additionally, since there are sources of CO that are not fire-related, some caution is necessary to take CO as an indicator of fire. This may happen particularly in scenarios that host CO sources like car parks. The standard sets the desired alarm level at 60 ppm of CO, and the standard also requires that no alarm should be given when CO concentration is lower than 25 ppm.

Alarms based on the ISO7240 standard are based on the definition of a single threshold value, whereas systems based on the UL2034 or EN50291 standards consider the accumulated dose of CO (interpreted in terms of $COHb$ production). This results in the fact that alarms based on ISO7240 are even more sensitive to CO concentration than standalone CO detectors standardized under UL2034, or EN50291. For instance, at 60 ppm of CO (the alarm level for ISO7240), the UL2034 standard only mentions that the alarm should never be triggered before 28 min, and even not firing at this concentration is consistent with the standard.

A relevant feature of the ISO7240 standard, common to other standards in the area of chemical sensing, is the selection of a number of interfering chemicals that should not trigger the alarm (see Figure 5). The exposure of the detector to the presence of the interfering volatiles should not alter the compliance of the detector to the sensitivity tests. In this case, the standard selects nitrogen dioxide, sulfur dioxide, chlorine, ammonia, heptane, ethanol, and acetone. Additionally, the alarm should not be triggered in the presence of 5000 ppm of CO_2. The robustness of detectors against interfering chemicals and nuisances is a must in detectors based on chemical sensors. The selection

of the interfering chemicals and their concentration levels is always a matter of controversy and, obviously, it becomes dictated by the scenario where the alarm is to be installed.

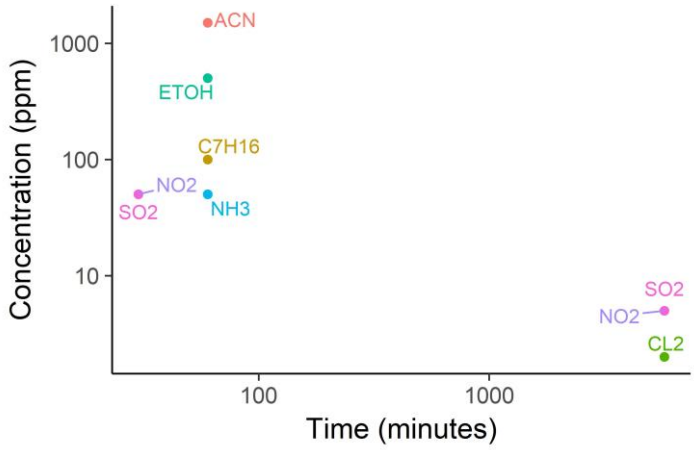

Figure 5 Concentration and exposure time of the different interferent gases that appear in the standard ISO7240. Note the log scale. Specifically, the concentrations and exposure times are: 5 ppm of NO2 at 96 h and 50 ppm at 30 min, 5 ppm of SO2 at 96 h and 50 ppm at 30 min, 2 ppm of Cl2 at 96 h, 50 ppm of NH3 at 1 h, 100 ppm of Heptane at 1 h, 500 ppm of Ethanol at 1 h and 1500 ppm of Acetone at 1 h.

The combination of smoke detectors, heat sensors and CO electrochemical cells to form a multicriteria fire alarm achieved higher commercial success than the use of standalone CO detectors for fire detection. Actually, this combination is standardized under ISO 7240-part 27: “Point-type fire detectors using scattered light, transmitted light or ionization smoke sensor, an electrochemical cell carbon monoxide sensor and a heat sensor”. In this case, the alarms are tested against standard test fires TF2, TF3, TF4, TF5, and TF8. The same chemical interfering volatiles considered in part 6 are also used for this embodiment of the fire alarm.

There are also country-specific standards covering electrochemical cells for fire detection. For instance, the Loss Prevention Standard LPS1274 covers “Testing procedures for the LPCB approval and listing of carbon monoxide/heat multisensory fire detectors using electrochemical cells”. This standard proposes to test the devices against TF2, TF3, TF4, and TF5, defined as in the EN-54 standard [53]. Similarly, we can encounter LPS1279: “Testing

procedures for the LPCB approval and listing of point multisensor fire detectors using optical or ionization smoke sensors and electrochemical cell CO sensors and, optionally, heat sensors" [54]. In this case, TF8 is added as in the ISO standard [53].

As far as the authors know, there is no published standard regarding fire detection based exclusively on chemical sensor arrays. Obviously, ISO7240-part 6, can be taken as guidance. However, this document is tailored to CO electrochemical cells. The standardization of the fire sensitivity tests for fire detectors based on chemical sensor arrays could push forward the development of this type of detectors. In such a case, beyond standard test fires, attention should be paid to nuisances (causes of false alarms) as well. In the opinion of the authors, in addition to the selection of a number of interfering volatiles and their concentrations, nuisance scenarios have to be selected such that they ensure robust operation of these detectors in the selected scenario of use (domestic premises, buildings, commercial, etc.). This selection is not an easy task since the number of potential of sources of false alarms is large, especially when the sensor array includes sensor technologies with low selectivity, such as metal oxide sensors (MOX) or photo-ionization detectors (PID). As we will review in Sections 6 and 7, while proposals already appeared in the literature, the community still needs to reach a consensus.

1.8 Gas Sensors for Combustion Products

The list of the most significant gas fire emissions contains CO, HCN, HCl, HF, HBr, NO, NO_2, $SO2$ as inorganic asphyxiants and irritants, but one also needs to consider O_2 depletion and CO_2 levels, for their synergy with toxics: mostly because it results in an increased breathing rate. Additionally, it is well established that many VOC can also be emitted from fires, being acrolein and formaldehyde two of the most relevant examples. However, this only constitutes a short list and it is clear that the number of chemicals is enormous, it is practically impossible to have a chemical sensor dedicated to every single compound present in fire emissions. In this section, we will not refer to the possibility of using Fourier Transform Infrared (FTIR) analyzers for the simultaneous analysis of many emission compounds through the analysis of the absorption signature. We will refer only to the use of sensor components.

The technology of choice for the analysis of most of the toxicants that appear in fire emissions is electrochemical cells. In fact, electrochemical cells are the standardized option when coupling carbon monoxide sensing to smoke detectors. Current standards do only refer to this technology and CO

detection, disregarding other popular options such as metal oxide sensors with a larger number of target volatiles and cross-sensitivities [55–57]. Electrochemical sensors are based on REDOX reactions that produce an external current that is then measured. Typically, a potentiostat circuitry in a three-electrode configuration is used. Figure 1 shows working principle for CO detection using electrochemical cells. There is a large variety of worldwide vendors offering sensors based on electrochemical cells for toxic gas detection. Some examples of commercially available sensors relevant for fire detection are given in Table 2, and additional vendors for these sensors follow in Table 3 [58]. We refer interested readers in the principle of operation of electrochemical cells to already published reviews [58,59].

Table 2 Concentration measurement ranges (in ppm) for fire emissions provided by different vendors

Gas	IST	Alphasense	GfG
NH_3	√ 10 ppm	√ 100 ppm	√ 200 ppm
CO	√ 300 ppm	√ 500 ppm	√ 300 ppm
H_2	√ 2000 ppm	√ 2000 ppm	√ 2000 ppm
HCl	√ 30 ppm	√ 100 ppm	√ 30 ppm
HCN	√ 30 ppm	√ 100 ppm	√ 50 ppm
HF	√ 10 ppm		√ 10 ppm
HBr			√ 30 ppm
H_2S	√ 30 ppm	√ 100 ppm	√ 100 ppm
NO	√ 100 ppm	√ 100 ppm	√ 100 ppm
NO_2	√ 50 ppm	√ 20 ppm	√ 30 ppm
SO_2	√ 100 ppm	√ 20 ppm	√ 10 ppm
O_2			25%

Table 3 Availability of electrochemical cells for the detection of toxics1.

Gas	Honeywell	Casella	Draeger	Geotech	IS	Ion Science	MSA
NH_3	√	√	√	√	√		√
CO	√	√	√	√	√	√	√
H_2	√	√	√	√	√		
HCl	√	√	√	√	√		√
HCN	√	√	√	√	√		√
HF	√	√					√
HBr	√	√					√
H_2S	√	√	√	√	√	√	√
NO	√		√				
NO_2	√	√	√	√	√		
SO_2	√	√	√	√	√		√
O_2	√	√	√	√	√	√	√

[1] IST: International Sensor Technology (http://www.intlsensor.com/); GfG: Innovative Gas Detection Technology (http://www.gfg-inc.com/); Alphasense: (http://www.alphasense.com/); Honeywell: (http://www.honeywellanalytics.com); Casella: (http://www.casellasolutions.com); Draeger. (http://www.draeger.com); Geotech (http://www.geotechuk.com); IS: Industrial Scientific (http://www.indsci.com); MSA: (http://www.MSAsafety.com).

Finally, we remark that some vendors offer different ranges of concentration for their products (the higher limits of the corresponding sensor ranges in Table 4 are only given for illustration purposes) and HCl, HBr and HF are sometimes detected with the same sensors designed for halogen acid detection.

As already mentioned in Section 4, CO_2 is a relevant gas in fire emissions. While it is not a direct toxicant, it increases the effects of others as we have seen in the models of toxic potency. The detection of CO_2 at relevant concentrations in fire emissions is easily accomplished by miniature Non-Dispersive Infrared Cells (NDIR) provided by different vendors. The principle of operation relies on energy absorption in the infrared. CO_2 absorbs at 2.7, 4.3 and 15 µm. NDIR sensors use infrared lamps, absorption chambers, wavelength filters and infrared detectors, although nowadays all the elements are integrated into a single system. Typically, an absorption band and a reference band are used for compensation purposes. Additionally, temperature sensors are included to compensate for the influence of the operating temperature.

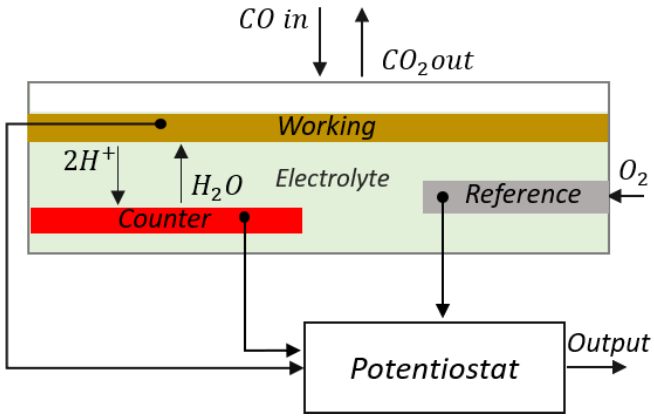

Figure 6 Nemoto NAP-505 three electrode $\boldsymbol{CO}$ sensing element.

Finally, there are several VOCs that are also of interest but their selective detection at ppm level with simple sensors is not feasible today. Consequently, the detection of acrolein or formaldehyde, for example, should be targeted with non-selective sensors. Two main technologies are available nowadays. On the one hand, we can find photo-ionization detectors (PIDs) that are based on the ionization of target molecules by a UV lamp. Different volatile compounds have different efficiency regarding the ionization process but, if the molecules can be ionized by the energy of the lamp (typically from 8.4 eV to 11.8 eV), the detector will give a response. Thus, PIDs are considered as non-selective sensors since a weighted overall VOC reading is obtained. The advantage of PID sensors is that they achieve very low detection limits (in the order of ppb) but at the expense of being also sensitive to harmless chemicals that may appear as nuisance during normal daily activities (cleaning products, perfumes, etc.). Metal oxide gas sensors (MOX) are a more robust alternative, but this choice is also plagued with problems of very poor selectivity. On the one hand, the broad response of MOX is beneficial to detect a large number of combustion products and provide additional safety to a building's occupants, but, on the other hand, the non-selectivity makes this technology more prone to false alarms. To gain some selectivity for fire signatures, arrays of MOX sensors or temperature modulation strategies must be used. Consequently, the use of these devices for fire detection should necessarily include some computational intelligence that is able to differentiate fire signatures from nuisances. Therefore, only after a data processing step one can obtain reliable fire detection.

1.9 Fire Detectors Incorporating Chemical Sensors

1.9.1 Decision Tree and Hard Rules

Traditionally, fire alarm systems based on smoke detection make use of a single threshold value to define the fire region. This region can be defined more accurately by considering readings from other sensors and building a set of thresholds (or rules) that incorporates the multiple sensor signals.

In the early nineties, Ishii et al. presented an approach based on hard rules and a smoke sensor coupled with a thermocouple and a semiconductor CO sensor [8]. The multi-sensor system was placed in a 6.7 × 4.3 × 2.5 m3 room in which smoldering fire (wood), flaming fire (n-heptane) and cooking activities (grilled fish) were performed. Based on the instantaneous reading of the three sensors, the authors defined specific regions in the sensor space to limit the fire region. Figure 8 shows the defined regions and their complexity. Based on the set of rules, fire alarm is only triggered when the acquired point falls outside the volume enclosed by the different planes. As a result, cooking activity did not trigger fire alarm, although smoke density showed response to this activity, which may have reached obscuration threshold limit defined for smoke detectors.

The proposed set of rules, though, is very specific to the experimental setup and tested fire/nuisance scenarios. In order to provide a more general model, the authors proposed a method that uses dynamic features and relies on sensor correlation. Using a similar experimental setup, they found out that heat release and volatile release come together in the performed fire test (metal chair with polyurethane cushion and polyolefin fabric). This sensor correlation was significantly smaller in the tested nuisance scenario (cooking). They proposed, thereby, to use the correlation between heat release and volatile release (and its rate of change) to detect fires. However, unfortunately, authors did not validate this approach with unseen measurements. Moreover, smoldering fires with very slow combustion process may initiate heat release significantly after volatile release and, therefore, the proposed signal correlation may not be a good indicator to predict slow smoldering fires.

In the mid-nineties, research teams from the Department of Fire Protection Engineering and the Department of Chemical Engineering at the University of Maryland (College Park, MD, USA) joined efforts to detect fire situations using a variety of sensors. Initially, researchers performed experiments in a small-scale setup (see Section 7), in which only chemical sensors were used and samples were introduced using an atomizer. In this section, we will focus their efforts on a continuation work where the sensor system was placed in a larger experimental setup (3.6 × 3.6 × 2.4 m3), and it included gas sensors and light obscuration sensing.

Specifically, the system integrated TGS880 and TGS822 MOX gas sensors (Figaro, Japan), CO (PIR 2000, range 0–1% Horiba, Irvine, CA, USA), CO_2 (Horiba PIR 2000, range 0–5%), O2 (540A, range 0–20.95%, Servomex, Belgium) sensors, a temperature sensor (thermocouple) and light obscuration detector (OSD-100-5T-BNC, Centronic, UK). Moreover, for comparison purposes, the setup was equipped with two commercial smoke detectors (one photoelectric and one ionization) [60,61]. They performed 87 tests, including 34 flame fires, 16 smoldering fires and 37 nuisances.

The dimension of signals captured with the two MOX sensors, CO and CO_2 sensors and temperature and light sensors was reduced to three dimensions by means of Principal Component Analysis (PCA). Therefore, the dimension of the space was shrunk from six to three, while the three principal components captured 76% of the variance of the original data. They built hard rules on this new space to classify flame fires, smoldering fires or nuisances. The scores were used to define the boundaries of each region as follows:

- ***If:*** *PC3 > 5: Flaming fire.*
- ***If*** *−8 < PC2 < 0: Smoldering fire.*
- ***Else:*** *Nuisance.*

They compared the performance of the chemical system with a commercially available smoke detector. While commercial detector did not trigger the alarm for 16 of the 50 tested fire conditions, this number was reduced to only two for the multisensory system based on

dimension reduction and hard rules. Proposed method also outperformed commercial system in response time, as, by average, flaming fires were detected 45 s faster and smoldering fires were detected 245 s faster, which represented a time reduction of 57% and 30% respectively. However, the system with gas sensors was very sensitive to nuisances as it produced false alarms for 10 out of 37 conditions (10 nuisances were wrongly identified as smoldering fire), while the smoke detector only showed 4 false alarms [62].

False alarm ratio was improved, at the cost of reducing sensitivity to smoldering fires, when the authors revisited the dataset and considered a new set of sensors. In particular, the system included two MOX sensors, CO and CO_2 sensors and the temperature sensor [62]. In other words, the photocell was removed from the array of sensors. Using hard rules based on the sensor signals the authors could classify smoldering fires, flame fires, nuisance cases, and background. The rules were defined as follows:

- ***If***: $CO_2 > 210$ ppm **or** $T > 105$ F: ***Flaming fire***.
- ***Elseif***: $V_{TGS822} > 0.9$ V **and** $V_{TGS880} > 0.15$ V: ***Nuisance***.
- ***Elseif***: $CO > 17$ ppm **and** $CO_2 > 22$ ppm **and** $V_{TGS822} > 0.27$ V: ***Smoldering fire***.
- ***Else***: ***Background***.

where V_{TGS8xx} denotes acquired voltage from the corresponding MOX sensor conditioning circuit.

The systems that included chemical sensing outperformed smoke detector in terms of sensitivity to fires. Similarly, the system with the light obscuration sensor showed higher sensitivity to smoldering fires than when the light sensor was removed. However, whether this is due to the information provided by the light sensor or due to the employed decision algorithm remained unexplored. On the other hand, chemical systems showed a higher rate of false alarms than the smoke detector. Actually, as all considered methods rely ultimately on the definition of thresholds, sensitivity and specificity could be adjusted by tuning the corresponding thresholds.

In another work, the same research group explored fire sensitivity and nuisance immunity using another multi-sensor system and different hard rules [64]. Specifically, they exposed a photoelectric smoke detector, ionization smoke detector, CO sensor and thermocouple to 32 fire tests (smoldering and flaming) and 11 nuisance (cooking tests, smoking and candle) scenarios. Captured signals were filtered to reduce noise and get rid of data spikes. Instantaneous values and rate of rise for each of the sensors were considered.

Authors proposed nine different hard rules using different combinations of sensors and features. Resulting sensitivity and specificity were evaluated individually for each set of rules, and they were compared to thresholded smoke detectors. Results indicated that the rule involving the rate of temperature rise, CO concentration, and smoke detection (using ionization detector) provided the best immunity to false alarms and fire sensitivity. In particular, the selected rule was as follows:

- ***If:*** *(Rate of T > 0.2 °C/s)* ***or*** *(CO > 17 ppm)* ***or*** *(Ion > 0.15% Obs/m): Fire.*
- ***Else****: Background.*

The authors concluded that rules that included CO measurements resulted in faster detection of smoldering fires than smoke detectors. Similarly, the rate of temperature rise resulted in faster fire detection, or at least, similar, than smoke detectors. Authors also proposed several rules to define fire/non-fire regions after PCA was applied to data. However, authors did not find any significant improvement after defining ellipses in the lower-dimension space. Authors attributed the similar performance of the rules defined directly in the sensor space with the rules defined after the PCA to the limited number of sensors which is not large enough to flourish the benefits of dimensionality reduction.

In summary, the research efforts carried out by the Department of Fire Protection Engineering and the University of Maryland showed that simple hard rules could be defined such that fire and nuisance situations can be discriminated. They also showed that dimensionality

reduction could be performed before the definition of the decision rules. When compared to smoke detectors, chemical-based fire detectors showed improved sensitivity, although it came at expenses of higher false positive rate. The remaining challenge is keeping high sensitivity while specificity remains at acceptable levels.

Chen et al. proposed a system that combined smoke detector with carbon monoxide and carbon dioxide measurements [65]. They compared the performance of the multi-sensor system with the performance of only the smoke detector. The smoke detector was based on light scattering and, when operating alone, it triggered a fire alarm when the threshold of 15% obs/m was reached. CO and CO_2 detection were performed by means of a diode laser-based absorption spectrometer, which was composed of a laser, InGaAs diodes and reference and measurement cells.

The proposed algorithm for the multi-sensor system was based on dynamic features, specifically, the rate of change of the smoke, CO, and CO_2 signals. Then, a decision tree was built to output, continuously, fire/non-fire prediction. Briefly, fire was only predicted when smoke rate of rise was higher than a threshold and the rate of rise of CO or (non-exclusive) the rate of rise of CO_2 were higher than the corresponding thresholds. The authors explored two methods to estimate the signals' rate of increase. First, the rate of rise was estimated fitting a linear function to the captured data points using 10-s time windows. The second method included a moving average filter before the linear fit was computed. The thresholds were adjusted for each volatile and method, resulting in the following rules for the first and the second methods respectively:

- ***If**: (Rate of Vsmoke > 1 mV/s) **and** [(Rate of CO > 0.15 ppm/s) **or** (Rate of CO_2 > 25 ppms/s)]: Fire.*
- ***Else**: Non-fire.*
- ***If**: (Rate of Vsmoke > 1 mV/s) **and** [(Rate of CO > 0.05 ppm/s) **or** (Rate of CO_2 > 8 ppms/s)]: Fire.*
- ***Else**: Non-fire.*

where Vsmoke represents the voltage captured from the output of the smoke detector. The mentioned algorithm was patented by the authors [66].

The authors tested their approach using a collected dataset that included a total of 30 fires (smoldering and flame) performed in a 2.2 × 1.4 × 4 m3 unventilated room. Smoldering fires included HDPE beads, PVC clad wire, mixed fabrics (with different ignition methods) and green canvas. Flame fires included heptane, toluene, methanol and mixed plastics. Two or three repetitions were carried out for each fire type. Authors also tested immunity to false alarms. In particular, they tested nuisances that may be present in aircrafts. Specifically, tested nuisances included dry ice, insecticide bomb (aerosol), halon, water, methanol, ethanol, acetone, and ammonia.

Results indicated that there is no significant difference between the two methods proposed to compute the signal derivatives, and no false alarms were detected throughout the tests. However, the multi-sensor system showed better sensitivity to fire than the smoke detector. Due to the small amount of smoke released by heptane, methanol, PVC wire and mixed fabrics, smoke detector did not trigger fire alarm for these four types of fire. The multi-sensor system only missed methanol fire. However, the authors adapted the rules such that fire is predicted when two of the three rate of rise features exceeded the corresponding threshold. With the new formulation, the multi-sensor system was able to detect methanol fire as well. Moreover, multi-sensor system also showed improved detection time, reducing, for example, detection time of HDPE bead fire from 616 s to 320 s.

The authors showed that defining rules based on the rate of change of the signals may be beneficial, as these dynamic features overcome issues with baseline shifts and may detect changes faster. Finally, the outstanding sensitivity and robustness to false alarms of the multi-sensor system may be due to the specificity of the employed chemical gas sensors. The immunity to false alarms may not be found when using less-costly, broad-response gas sensors.

Gottuk et al. presented a system that combined smoke detectors with CO detection using an electrochemical gas cell [67]. The authors

performed fires and nuisances in a 49 m3 room. Large variety of flame and smoldering fires (heptane, alcohol, gasoline, flaming polyurethane, smoldering polyurethane, cardboard, cotton fabric, flaming cotton wick, smoldering cotton wick, cotton batting, upholstery fabric, PVC cable, smoldering wood at different temperatures) and nuisances (Wesson oil, toast, melting cheese, bacon, propane burner, kerosene heater, cigarette smoke, people smoking, water steam) were induced in the room, with different number of repetitions each scenario. Two smoke detector systems (ionization and photoelectric), along with gas sensors were installed in the test room.

The authors set the detection threshold of smoke detectors to 4.52% obs/m for the ionization detector and 6.72% obs/m for the photoelectric smoke detector. Results confirmed that ionization detectors show better sensitivity to flaming fires, whereas photoelectric detectors show better performance for smoldering fire detection.

The proposed multi-sensor algorithm for fire detection was based on the readings from the ionization fire detector and the CO sensor. The authors developed a simple rule that takes into account the readings from both sensors such that high concentrations of CO also triggered fire alarm. In particular, the criteria was as follows: the alarm was triggered when the product of the ionization detector output (% obs/m) times the CO sensor reading (in ppm) was greater than 10 (% obs/m)(ppm). By coupling the CO sensor to the ionization smoke detector, boundaries of fire/non-fire regions could be defined.

The multi-sensor system was compared to traditional smoke detectors. Despite the simplicity of the proposed rule, the multi-sensor system detected 42 out of 53 fire tests, while ionization and photoelectric detectors detected 25 and 29 of the tested fires, respectively. Briefly, the multi-sensor system detects the union of the set of fires that are detected by the ionization and the photoelectric detectors, except for some smoldering wood (at lower temperature) and PVC cable, which can be detected by photoelectric detector and did not trigger alarm for the ionization smoke + CO detector.

Immunity to false alarms was also improved with CO measurement. For example, water steam increased obscuration measure and triggered smoke detector alarms, but it did not increase CO sensor readings, which prevented triggering fire alarm for the multi-sensor system. Photoelectric and ionization showed false alarm to 17 and nine of the 27 tested nuisances. Multi-sensor system only triggered false alarm in six of the nuisance scenarios. Moreover, time response was also improved. Ionization detector coupled to CO sensor showed faster response time than ionization detector alone, except for heptane and polyurethane fires.

The authors showed that adding CO measurements to light obscuration sensor can improve both fire sensitivity and false alarm immunity. Simple hard rules can successfully process sensor signals. However, the authors already discussed a limitation of the proposed rule as its asymptotic nature makes it necessary very high levels of CO concentration (or smoke) if smoke (or CO concentration) levels are very low. This rule will delay the detection of fires that, for instance, generate small CO concentration. The authors proposed adding additional rules to cut the asymptotic behavior in its limits.

All in all, hard decision rules have been explored recurrently over the years. The popularity of this choice is probably due to the classic operation of smoke-detectors that rely on signal thresholds. The natural path is, hence, reshaping fire regions defined with light obscuration thresholds to obtain more accurate fire regions that incorporate additional information from chemical gas sensors. On the bright side, hard rules are considered as “white boxes” as they are easy to interpret [68]. Acquired knowledge of the system behavior is translated to a readable set of rules.

On the downside, decision rules may become too complex when many different nuisances are considered, as each scenario may require its own set of conditions to be excluded from the fire region. Also, and most significantly, hard rules depend heavily on the presented dataset. This is usually not-desired as one aims at building models robust to noise and able to generalize to new data or new experimental conditions (room size and geometry, fire types, nuisances, etc.). One

limitation that we found in the literature is the fact that generalization to other experimental conditions is not explored. To what extent defined rules are valid when the system is placed in a different room, under different ventilation conditions or when the sensors are at different distances from the fire source remained, mostly, unexplored.

Dynamic features were also proposed to improve the accuracy and the generalization ability of the models. For example, it was found that rate of rise of CO and CO_2 concentration levels can improve the ability of the system to discriminate between fire and nuisance scenarios. In reference [69], only one nuisance showed CO_2 increase rate higher than 0.1 ppm/s, and only two nuisances induced CO increase rate higher than 0.025 ppm/s. Although CO_2 was found to increase at high rates during fire, it also does so when the room is occupied by individuals (the presence of people in a non-ventilated room can induce CO_2 increase rates as high as 0.5 ppm/s). Therefore, CO rate of rise was suggested over CO_2 rate of rise to discriminate fire from nuisances.

Also, using dynamic features, such as rate of rise, becomes beneficial as these features are insensitive to baseline shifts and may provide faster responses. For example, derivative features were shown to change faster than the mean of the signal computed in the same time window [65].

Similar to static features, thresholds for dynamic features may be also specific to room size or geometry. However, experiments in two test rooms suggested that room effects can be incorporated to the model by including (and adjusting) rate of rise thresholds in the algorithms [63].

Finally, approaches based on linear data transformation (PCA) have been proposed to define hard rules in the transformed sensor space. These rules may be intricate and complex in the original space, but they may become simple in the new space. Moreover, if enough repetitions are included in the original data matrix, the new data projection can find the mean direction for each fire/nuisance type and reject inherent variability for each scenario [64].

Hard decision rules have been proved to provide good prediction ability when tested under the same conditions than the calibration conditions. However, other classification algorithms that usually show lower generalization error [68] have also been explored for reliable fire detection.

1.9.2 Neural Networks

In the early 1990's, Okayama studied the use of neural networks to assess the risk of fire using a variety of sensors [70]. He adapted the configuration of the neural network to address three different tasks, using different sensor ensembles and sensor features for each task.

First, a three-layer neural network with three input neurons, five hidden neurons and three output neurons was used to output three fire indicators. Three sensors (temperature, carbon monoxide sensor, photoelectric smoke sensor) were considered to feed the input layer of the network. Static features for CO and smoke sensors were extracted, whereas dynamic feature (rate of rise) was extracted from the temperature sensor. Additionally, to extract the corresponding features sensor readings were normalized such that the ranges 0–20% obs/m, 1–100 ppm of CO, and 0–10 °C/min were mapped to the interval 0–1. The output of the network was associated with three indicators (fire probability, fire risk and smoldering fire probability), which were also set in the range of 0–1. The neural network was trained using 12 fire patterns.

In the second task, only the photoelectric smoke sensor was used. Two features were extracted from the sensor signal: instant value and rate of rise. The features were also normalized to the range 0–1, corresponding to 0–20% obs/m and 0–20% obs/m per minute, respectively. The architecture of the network consisted of two input, four hidden, and two output neurons. The relevant output neuron was associated with fire probability and 18 fire patterns were presented to train the network weights.

Similar to the second task, the third task considered only the photoelectric sensor, but the dynamic feature was changed. In particular, the two extracted features were the instantaneous sensor

reading and the time duration (normalized to 0–1) since the sensor signal exceeded a defined threshold. The network consisted of two input neurons, four hidden neurons, and one output neuron (that accounted for fire probability). The network was trained with 10 patterns. Finally, task 3 was extended to consider ventilation conditions. Ventilation was incorporated to the neural network as a third digital input that took 0/1 for ventilation on/off.

After the mentioned neural networks were trained, output values provided by the model showed acceptable correlations with the defined values, also when chemical sensors were combined with smoke detectors. Unfortunately, different measurements were used to train the different models, making not possible the comparison between the considered tasks. Moreover, very few details on the experimental protocol are presented in the original work, the time at which the vector of features was extracted to feed the neural network was not specified, or details on the criteria to quantify the output indicators were omitted, which represent the alarm signals. Nevertheless, results presented by Okayama were encouraging as, although the simplicity of the neural network, the model could assign a probability to the presented measurements. He also considered dynamic features, showing that there is relevant information in the temporal response of the signals. Actually, he envisioned that further work should consider models that are able to process time-series directly.

In a following work, Okayama and Sasaki considered nuisance scenarios, which were omitted in Okayama's previous work. They coupled a MOX gas sensor to a smoke detector to discriminate fire from nuisances using a neural network (four input neurons, four hidden neurons, one output neuron) [71]. The sensors were exposed to sixteen measurements that included fire repetitions (beechwood smoldering fire at 2 m or 3 m from the sensors) and non-fire situations (smoking, cooking, coffee aroma, background). Four features were considered to feed the three-layer neural network: normalized sensor level and normalized rate of change per minute, for each sensor. The output neuron was associated to fire probability. For training the network, fire

probability was manually assigned in the range 0–1 according to the distance of the sensors to the fire source or the type of nuisance.

Unlike their initial work, the neural network processed all the captured signals continuously. As a result, fire probability was provided as a function of time. Results showed that the system was able to output fire probability continuously, providing reasonable values as smoldering fires were being developed. However, the model showed difficulties to reject nuisances (mainly cooking activities). This shortcoming was attributed to air turbulence that took place in the test room (270 m3) that limited the accuracy of the classifier [71,72].

In a similar work also using neural network, Okayama studied the feasibility of fire detection using only chemical sensors (see Section 7, reference [73]).

In order to reduce fire detection time and increase the reliability of fire detectors, Derbel integrated three metal-oxide gas sensors with a commercially available optical (light-scattering) fire detector and a temperature sensor [4]. Specifically, the gas sensors were selected for carbon monoxide, hydrogen, and ammonia detection.

The system was exposed to flaming fires (TF1, TF4, TF5) and smoldering fires (TF2, TF3) inspired by the EN54 standard, a non-standard fire (cable fire) and two nuisance scenarios (disco-fog generated with a commercial fog machine, and cigarette-smoke using a force pump that regulated the burning process).

In order to build a model to detect fires, different dynamic features were tested. First, a moving window and FFT transformation provided features from the sensors' signals. Second, feature extraction was performed by means of scaling the quadratic mean value of the signals, and then a back-propagation neural network was used to output the prediction. In both cases, results indicated that incorporating chemical and temperature sensors to the optical fire detector provided faster alarm signals in a more reliable manner (unlike the optical fire detector, the multisensory system did not show false alarms for cigarette smoke and disco-fog).

However, since no repetitions were acquired, models were trained and tested using features of the same measurements. Features of sensor signals corresponding to the same measurement were distributed in train and test. TF1, TF2, TF3, TF5, cable fire and cigarette smoke appear both in training and test, and only disco-fog and TF4 were left completely for test. Hence, training and test vectors are not completely independent. This questionable dataset partitioning yielded, most likely, to overfitting and overoptimistic results.

Finally, to what extent the performance increase of the system is due to the integration of the temperature sensor or the chemical sensors was not explored. This would provide very meaningful insights for the design of chemical-based fire detection systems.

Neural networks have shown good performance for fire prediction. However, more elaborate networks have been presented to account for the prior probability distribution function, such as Probabilistic Neural networks. Taking into account prior probability seems critical in fire prediction, as one expects the system in rest state for most of the time.

1.9.3 Probabilistic Neural Network

A remarkable work in fire detection was published by Rose-Pehrsson et al. (Naval Research Laboratory) in 2000 [74]. They studied the response of different sensor technologies to 24 different types of fire and 12 nuisances (see Table 7 for the complete set of fire/nuisance scenarios considered in the study). Several repetitions of the scenarios were performed in a 96 m3 test compartment, for a total of 240 events (120 background recordings, 82 fires and 38 nuisance sources). To the best of our knowledge, the considered dataset represents the largest dataset, with the largest variety of fire types and nuisance scenarios, collected for fire detection with chemical gas sensors. The large variety of fire and nuisance sources enabled a thorough study on fire detection sensitivity and system reliability. Moreover, the authors also placed a large number of sensors in the measuring compartment. The variety of sensing technologies and the benchmark measurements performed with commercial smoke detectors allowed to achieve another relevant

goal of their work: the study of sensor similarities and the selection of an optimal subset of sensors for reliable fire detection.

In particular, the authors placed 20 sensors of different types in the measuring compartment. A variety of chemical gas sensors was installed to target various combustion products. Chemical sensors included carbon monoxide (at two concentration ranges), oxygen, hydrogen, hydrogen chloride, hydrogen cyanide, hydrogen sulfide, sulfur dioxide, nitric oxide and nitrogen dioxide electrochemical cells, a NDIR for CO_2 and a MOX for hydrocarbon detection. Commercially available smoke detection systems (ionization and photoelectric) and an optical density meter system were also included to obtain reference measurements, and temperature and humidity were monitored during the measurements as well.

The sensitivity to fire detection and the immunity to nuisance sources of photoelectric and ionization fire detectors were used to benchmark the system that incorporated gas sensors. Conventional alarms were triggered when signals reached different obscuration thresholds. In particular, three thresholds were tested for each smoke detector. First, alarm thresholds were set to 4.2% obs/m for ionization and 11.0% obs/m for photoelectric detectors, which correspond to typical alarm thresholds. Minimum alarm level allowed by the UL 268 Standard (1.63% obs/m) and half of it (0.82% obs/m) were also tested as alarm thresholds. Using a total of 120 events (82 fires and 38 nuisances), confusion matrices for each detector type and threshold values were computed.

Results with smoke detectors showed that, at lower alarm levels, systems showed high sensitivity to fires, but low immunity to nuisances. At lower alarm levels, 73% of the fires were correctly detected by the photoelectric detector, but false alarm ratio was as high as 47%. Oppositely, at the higher alarm level, the system could detect only 38% of the fires, while 82% of the nuisances were rejected. Similar behavior was observed with the ionization detector. When background measurements were also included, best overall classification ratio were obtained at lower threshold alarm levels (83% and 88% for photoelectric and ionization detectors respectively).

The obtained classification ratio values served as a benchmark to compare the performance of gas sensor-based fire detection systems. The authors developed a pattern recognition algorithm for fire detection based on probabilistic neural networks (PNN). All gas sensor signals were filtered with Savitzky-Golay routine to reduce noise. Only steady-state features were considered, which were extracted at discrete times defined by reference photoelectric detector. Finally, before training PNN, matrices were scaled to zero-mean and unit-variance. The authors followed a leave-one-out cross-validation strategy, i.e., they sequentially trained all but one observation and predicted the class of the sample that was left out. This procedure was repeated until all the measurements were set aside for test.

Best results were obtained with a subset of five sensors: O2 (model 6C, City Technology, Portsmouth, UK), H_2S (model TC4A-1A, City Technology), RH (model HX93, Omega, Stamford, CT, USA) ionization smoke detector (model 4098-9716, Simplex, Westminster, MA, USA) and photoelectric smoke detector (model 4098-9701, Simplex). With this array, 98% of correct classification was achieved.

The authors concluded that smoke detectors are important for the detection of fires. Results showed that systems including at least one smoke detector had higher sensitivity to fire. However, results indicated that gas sensors provide additional useful information for the discrimination of nuisances and early fire detection. Actually, nuisance rejection could be improved up to 25% when CO_2, O2, CO, hydrocarbons, temperature and NO sensors were combined with smoke detectors at the lower threshold level.

In a continuation of their work, the authors demonstrated the flexibility of the PNN algorithm [75]. Using a subset of sensors (photoelectric smoke detector, ionization smoke detector, CO and CO_2 sensors), they adjusted probability density function for each class. As a result, they could define the boundaries for each class. When the threshold was set to 100%, no false alarms were found, but only 60% of fires were successfully detected. As the threshold was lowered, fire detection ratio increased, at the cost of increasing false alarm ratio as well. By plotting the sensitivity and false alarm rate in a Receiver

Operator Curve (ROC), the authors could select the threshold (85%) that provided similar detection rates than reference smoke detectors. However, false alarm rate was greatly reduced. At the selected threshold, the system detected 78% of the fires and less than 20% of the nuisances produced false alarm. This result clearly improved performance of reference smoke detection systems, as they showed 66.7% and 74.1% of sensitivity and 66.3% and 41.7% of false alarm ratios for ionization and photoelectric systems, respectively. Results, therefore, confirmed their previous findings that suggested that combining gas sensors with smoke detectors helps to reduce false alarm rates.

All in all, work from Rose-Pehrsson et al. confirmed the feasibility of chemical gas sensors for fire detection and that gas sensors can improve false alarm immunity. The work is particularly valuable as it relies on an extensive dataset that included 24 fire types and 12 nuisances. By collecting such dataset, the authors ensured the generalization of their approach, which sometimes is overlooked by other works due to the cost of the experimental setups and data acquisition. They also explored different sensors targeting various combustion products and proposed a reduced set of sensors for fire detection. A final decision on the sensing technologies should be taken according to target specifications and other considerations such as system cost, time stability, calibration cost, power requirements, size, and others.

Finally, the authors also remarked that future developments need to consider temporal sensor responses. Since fires are dynamic events, authors expected that considering dynamic features would help in the detection of fires capturing the dynamic change of oxygen and carbon monoxide [32].

1.9.4 Hierarchical LDA

In another very interesting work performed at Saarland University, researchers developed a system based on a single MOX sensor to reduce false alarms in underground fires, specifically, in coal mines [76]. Although their approach relies on a single MOX sensor, the

authors benefit from the fact that MOX sensors exhibit different sensitivity and selectivity when operating at different temperatures, behaving therefore like different virtual sensors. Sensor's operating temperature can be controlled by applying certain power on a built-in heater placed next to the sensing layer. Briefly, the authors modulated the sensor's operating temperature and extracted multiple features using a single sensor.

The gas sensor operated in temperature modulation cycle (65-s period function) to increase the sensitivity and selectivity to the target compounds. The temperature profile included temperature ramps and high temperature operation steps. The authors considered several features from the acquired sensor signal. They extracted sensor values at defined temperatures (at discrete times) and slopes of the signal when transitioning between operating temperatures. Extracted features were selected such that, according to previous studies, they are suitable for the discrimination of relevant compounds.

The authors studied thoroughly the scenario of underground fires and identified the volatiles that result from fire (CO and ethane), its ratio (100/1), and the interfering gases (relative humidity, methane, CO, NOX or hydrogen). Based on previous investigations, the researchers designed a measurement profile that simulated, in a laboratory setting, fire and non-fire situations in underground atmosphere. Different concentration levels of CO, C_2H_4, NO_2, H_2 were presented to the sensor at different humidity (30%, 50%, 70%) background levels.

Next, they performed a 4-step hierarchical strategy based on Linear Discriminant Analysis (LDA). At each step, the captured data was sequentially classified according to the three levels of humidity (first layer), three levels of methane (second layer), presence of H_2 or presence of CO or NO_2 (third classifier), fire/non-fire condition (final classifier). This methodology is equivalent to a decision tree that leads to different final classifiers, the output of which predicts fire, non-fire, or warning situation. The proposed method may be overfitted to the used empirical data since it considers only discrete values of interferences, while in real scenarios, those values will take a continuous distribution.

In a more recent study [2], data acquired in laboratory conditions was compared to field test data. Authors showed that field test data resemble data generated in lab conditions, validating their approach. However, all data was classified as normal operational situation since data only represented "non-fire situations", i.e., CH_4, CO and NOx were found at standard concentration levels. The system was operating over several months, which revealed sensor drift. Changing sensor sensitivity in time may make system predictions unreliable as system calibration becomes obsolete. To counteract drift effects, however, authors proposed self-monitoring and self-diagnosis strategies [77].

In our view, the above-discussed work provides a very valuable example of using a temperature-modulated sensor to extract various informative features from a single sensor. Using a single sensor, rather than an array of sensors, results in smaller and cost-efficient systems. All in all, the authors performed a very detailed analysis of the scenario and exposed the monitoring system to the relevant volatiles at different humidity levels. The authors developed a 4-step hierarchical classification algorithm that, according to the atmosphere composition, selects the final classifier to predict the presence of fire. This approach seems unpractical when the number of conditions of the environment (the number of interfering gases and concentration levels) increases, for example beyond the restricted scenario of underground mines. The proposed model is not defined when, for instance, the sensors are exposed to 60% RH (which path should the decision model follow? 50% or 70% RH?). In more complex environments, with a larger number of interfering volatiles, it seems more reasonable to build an integral model that considers all the conditions simultaneously and is defined for continuous variables.

1.10 Fire Detectors Exclusively Based on Chemical Sensing

1.10.1 Single Sensor

Already in 1974, Bukowski and Bright, at the National Bureau of Standards (currently known as National Institute of Standards and Technology, NIST, US) explored the feasibility of semiconductor gas sensors to detect fires [78]. They compared a Taguchi gas sensor with photoelectric and ionization fire detectors in small-scale and large-scale setups. They used the

same algorithmic approach for smoke detectors and the MOX sensor. Specifically, a signal threshold was defined such that fire condition was signaled when the sensor signal reached the established value. Smoldering fires in the small-scale chamber were carried out for sensitivity comparison at different air flows. Ionization, photoelectric and gas sensor systems triggered the alarm under similar light obscuration conditions. However, when tested on a large room with flaming (shredded paper, wood cribs, gasoline, polystyrene, polyurethane) and smoldering (cotton) fires, gas sensor showed poor sensitivity as it only detected one fire (shredded paper), while ionization and photoelectric detectors detected most of the 26 fires. Authors attributed the inferior performance of MOX sensors to the ventilation of the room that resulted in higher oxygen supply that enabled complete combustion, reducing thereby MOX sensitivity to fire (CO_2 cannot be detected with MOX sensors).

Obtained results led the authors to draw discouraging conclusions, and they already remarked shortcomings of chemical gas systems, such as long-term drift, and a high number of potential false alarms. Nevertheless, the inferior performance of the chemical system in large-scale setup can be attributed to flame fire tests that induced small quantities of combustion products detectable with MOX sensors. Moreover, more sophisticated data processing algorithms than signal thresholds, adding a variety of gas sensors to the system, and considering other features that capture sensor dynamics could improve the performance of chemical-based detectors.

Some years later, Pfister explored again the feasibility to detect fire with chemical sensors [79]. In particular, he studied the sensitivity of metal oxide gas sensors to the gas concentration levels usually found at early stages of fire. He concluded that combustion products such as CO and hydrocarbons could be sensed for fire detection, although he already pointed at reliability limitations due to cross-sensitivity to humidity.

1.10.2 Neural Networks

Okayama [73] pioneered fire detection using multiple gas sensors and neural networks. Okayama developed two SnO_2conductometric gas sensors with different film thickness, and therefore, different sensitivity. The sensors were exposed to volatiles generated from smoldering fires using diverse types of paper, cardboard, cotton, rubber, wood, and polystyrene among others. Volatiles that appear in inhabited environments, such as alcohol-based perfumes, coffee powder, and cigarette butts were also included to test false alarm immunity. The experimental setup was based on a small chamber and a sampling system that brought the volatiles to the sensors.

After confirming the feasibility of fire detection by measuring the sensitivity to the different combustion products, Okayama built a neural network to classify the origin of the detected volatiles. The neural network was composed of two input neurons, five hidden neurons, and two output neurons that represented fire and nuisance probabilities. The instantaneous readings of the two sensors were fed to the input neurons. A definition table with 26 conditions was presented to the neural network. The signals of the same set of experiments were plotted in the sensor space along with model outputs. Such figures enabled sensor signals visualization in a 2-dimension space. Signal trajectories indicated that measurements start in a well-defined area and they spread out in the space according to their nature.

In summary, Okayama confirmed the feasibility to detect combustion products using chemical sensing and therefore detect fire exclusively with gas sensors. Although the pioneering work, he had the vision to explore cross-sensitivities to other volatiles that are present in inhabited environments and he proposed a classifier to discriminate the origin of the detected volatiles. No quantification for fire sensitivity and false alarm immunity could be extracted from the work as the neural network was not evaluated with test experiments.

1.10.3 Hard Rules

Milke et al. studied the chemical composition of combustion products to build models for the discrimination of fire situations and nuisances. Initially, the authors built a 30 × 30 × 150 cm3 tunnel in which combustion products or volatiles present in relevant nuisances were introduced through a small aperture. A variety of sensors were integrated into the center of the tunnel: temperature sensor (type K thermocouple), light obscuration sensor (Centronic OSD-100-5T-BNC), CO (Horiba PIR 2000, range 0–1%), CO_2 (Horiba PIR 2000, range 0–5%) and O2 (Servomex 540A, range 0–20.95%) sensors, and a metal oxide gas sensor (TGS822 Figaro) [69,72].

The authors generated a dataset with 31 experiments that included open flame fires, smoldering fires, heated samples and samples at ambient temperature that were introduced using an atomizer. After signal visualization for each type of measurement, the authors extracted some conclusions: unlike smoldering fires, flaming fires showed CO_2 concentration peaks higher than 1500 ppm; and smoldering fires exhibited CO concentration levels higher than 28 ppm, which, in turn, was not present in any of the tested nuisances. Based on the extracted conclusions, a set of three rules relying exclusively on chemical sensing was defined to classify the origin of the samples:

- ***If*** *CO_2 > 1500 ppm: Flaming fire.*
- ***If*** *CO > 28 ppm* ***and*** *VTGS822 < 6 V: Smoldering fire.*
- ***Else****: Nuisance.*

As it can be noted from the set of rules, temperature and smoke sensors were not used by the classification model. This simple set of rules achieved to correctly classify 28 out of 31 experiments.

With the same dataset, the authors built a three-layer neural network that incorporated temperature and light obscuration inputs to the considered chemical sensor array (CO, CO_2 and MOX sensors). The network was composed of six input neurons, six hidden neurons, and three output neurons that indicated flame fire, smoldering fire, or nuisance. After training the network with two-thirds of the data, and testing its prediction with the remaining third, authors improved the classification to 30 out of 31 experiments, being only one smoldering fire misclassified as flaming fire.

Both classification models, the set of rules and the neural network, relied on CO_2 concentration for the identification of flaming fires, and non-flaming fires were mainly detected from higher CO concentration levels. However, the authors already expressed some concern regarding the performance of MOX sensors, as they had exhibited lack of response when previously tested in larger setups [78]. This brought the researchers to confirm their promising results at a larger scale setup, although the sensor system was extended to include light obscuration sensors as well (see Section 6).

1.10.4 Fuzzy Logic Rules

In the early nineties, Obayu [80] explored fuzzy logic rules applied to fire detection relying exclusively on chemical sensing. In particular, a multi-sensor system for the detection of catastrophic events in home settings was implemented and integrated with a Z-80 microprocessor. Specifically, the target events included combustible gas leak, carbon monoxide generation, and smoldering fire. The implemented system was composed of a combustible gas sensor (TGS # 109 Figaro), a pair of carbon monoxide gas sensors (# 203, TGS, Japan), and temperature and humidity sensors (HT-150, SOAR). However, the temperature sensor was not considered for the detection of the mentioned events.

The three fire events were simulated in a 44.5-L chamber, while the sensor signals were captured. The combustible gas leak was simulated by

introducing liquefied petroleum gas, carbon monoxide was introduced into the chamber to reach a concentration of 180 ppm to simulate carbon monoxide generation, and smoldering fire was simulated by setting fire on a piece of a cotton cloth. Moreover, cigarette smoke was also introduced in the measurement chamber to include nuisance scenario in the dataset.

Based on the observation of the signals when the sensors were exposed to the different target scenarios, a fuzzy set of rules was built to identify the type of event:

- ***IF*** *Combustible Gas Sensor is very high* ***AND*** *Carbon Monoxide Gas Sensor is high* ***AND*** *Humidity Sensor is slightly high,* ***THEN*** *Smoldering Fire occurs.*
- ***IF*** *Combustible Gas Sensor is very high* ***AND*** *Carbon Monoxide Gas Sensor is rather high,* ***THEN*** *Combustible gas leak occurs.*
- ***IF*** *Combustible Gas Sensor is high* ***AND*** *Carbon Monoxide Gas Sensor is very high,* ***THEN*** *Carbon Monoxide Generation occurs.*
-

The model showed some limitations to identify the type of event, in particular, it showed poor ability in differentiating between smoldering fire and smoke from cigarettes, which would yield to a large number of false alarms. Only one repetition of each event was considered to build the set of fuzzy rules. Therefore, the reproducibility of the sensor responses could not be evaluated.

Moreover, the rules were built after the system was placed in the measurement chamber and the sensor responses acquired. To what extent the intensity of the sensor responses (low, normal, high, etc.) depends on the volume of the chamber or the induced concentration levels in the chamber remained unexplored. This is particularly needed as rooms in home settings are orders of magnitude larger than the employed test chamber, and a wide range of concentration levels can be induced by gas leaks, fires or carbon monoxide sources. Müller and Fisher proposed the use of fuzzy logic to process signals acquired with smoke and temperature sensors. They stated the need for large datasets to properly set the fuzzy rules. They simulated 8 years of data, which allowed the optimization of their model [81]. This points out the difficulties of extending a set of fuzzy rules to account for different environments, fire types and backgrounds.

Nevertheless, it is remarkable the fact that in this work, Obayu went beyond a mere study on sensor sensitivity and proposed a classification algorithm for fire identification.

In a very recent work, Mobin et al. proposed an intelligent system for fire detection that combines a multi-sensor system and fuzzy logic rules.[82]. The system includes two flame sensors, two gas sensors and one temperature and humidity sensor. The sensor data were acquired using an Arduino UNO (Italy). Basically, when the signals of the sensors are high, the algorithm processes the sensor data and decides if there is a fire situation. If a fire situation is in progress, the system activates the control circuit of the extinguisher and mitigates the fire. The experiments were done using a cigarette lighter to emulate a fire situation. The algorithm is capable to detect 95% of the flames presented to the system. Even when the work is useful to study the feasibility of intelligent systems to detect and mitigate fire, further work is required to explore the reliability and robustness of the system in more complex fire scenarios.

1.10.5 Principal Component Analysis and Nearest Neighbors Classifiers

Ni et al. proposed a methodology based on a k-nearest neighbor after dimensionality reduction [83]. They focused the interest on the scenario of electrical fires, which is particularly favorable for gas-based fire detectors. High intensity flowing through electrical cables may be a sign of early fire condition. However, high-temperature excursion may be required until insulation materials (typically thermal resistant materials) release quantities of smoke that smoke detectors can detect. On the other hand, during pre-combustion, vapor generation happens before smoke formation, and therefore, gas sensors can detect released volatiles before a significant amount of smoke is produced. As a result, chemical-based detection systems are especially well suited to provide early detection of electrical fires.

In their work, Ni et al. tested several materials that are used as wire insulation (PVC, Teflon®, Kapton®, and silicone rubber). Electrical failure was simulated by inducing thermal excursions on the materials. 15-cm length pieces of wire were used for each measurement, and the minimum power (between 6.1 W and 13 W) that released volatiles was applied to each sample type. The baseline was acquired for 3 min, after which thermal excursion was carried out for 5 min. Four replicates of each sample type were heated up, and the released volatiles were presented to the sensors, for a total of 16 measurements.

Different sensing technologies were studied, including electrochemical sensors, quartz microbalance sensors with different polymer coatings, and metal oxide sensors. After sensitivity tests, eight MOX and three

electrochemical sensors were selected to build the classification model. Specifically, sensor signals at specified time points were selected to build the classification model. Authors used acquired baseline at the beginning of each experiment to compensate baseline shifts. After feature normalization, a classification algorithm was performed based on Principal Component Analysis coupled to K-nearest neighbor. PCA reduced the dimension of the data to two dimensions, and K-NN was used to predict the type of sample (wire insulation) under thermal stress. The performance of the model was evaluated with leave-one-out methodology. Although the simplicity of the classification methodology, the authors achieved 100% classification accuracy. It is important to note, although, that if the normalization step was omitted, only 82% of the samples were classified correctly.

The authors proposed a methodology to classify wires by the insulation type. This scenario does not correspond exactly to fire detection, as other important considerations such as false alarm immunity and change of environmental conditions were not included in the analysis. However, they provided an example of the importance of feature selection and data pre-processing, as feature normalization was necessary to obtain higher classification accuracy. Nevertheless, electrical fire is definitely a scenario in which chemical-based systems can show their superior performance with respect to smoke detectors and, therefore, it needs further research, including the study of false alarm immunity and other fire conditions.

1.10.6 Other Approaches

Sawada et al. studied fire detection using exclusively MOX gas sensors [84]. Specifically, they placed 8 MOX gas sensors of the same type (TGS#800, Figaro) in a 55 m3 test room. The eight sensors were distributed in the measuring room at different distances from a source of volatiles. Four scenarios were tested in the room, with three repetitions each: person smoking, cigarette smoke, burning cigarette end on a cotton cloth, and burning cigarette end on a curtain.

The authors explored the feasibility to group the data by measurement type. After sensors' signals were filtered to reduce noise, two features were considered using only the two sensors closer to the source. The first feature was the sensor reading (amplitude of the signal) one minute after the measurement started. The second feature was the slope of the linear fit between the signals acquired with the two sensors. Using the repetitions for each case, they built scatter plots: the amplitude of the signal versus the slope

of the fitted function. They found that data points that correspond to a person smoking appeared in a different region than the rest of the scenarios.

Authors did not build a classifier for the detection of fire or identification of fire types. However, several conclusions can be drawn from their work. Gas plume dynamics may help to differentiate fire from nuisances. Interestingly, the authors found different dynamics of the sensor signals at various locations: sensors placed close to the fire source showed faster fluctuations as they are more sensitive to gas plume movements. As volatiles tend to travel in patches, shifted-temporal signal correlations between sensors placed at various locations may be expected. These correlations may help to corroborate (or distrust) sensor predictions and thereby improve false alarm immunity.

The authors also did not implement any temporal correction on the signals captured from the differently located sensors. However, in the presented figure, one can observe a delay in the response of the sensor placed further from the source. This delay can be used as well to provide additional information on the position of the fire source.

In a recent work, Krüger et al. presented a MEIS hydrogen sensor for fire detection applications and performed several fire experiments [85]. The experiments were performed in two different scenarios; in a smoke chamber inspired by the ISO 5659-2 and in a 2-room apartment with similar proportions than the ratios specified in the EN 54. The experiments performed in the chamber correspond to polymeric materials: Polyethylene, polyurethane and wood. To test the sensors under real-working conditions, they burned different materials in the apartment such as carpet, kitchen roll, kitchen sponge, cheese and armchair. In both scenarios, they observed that H_2 was released in the early stages of the fire experiments (before smoke). Also, the sensor responses were different depending on the materials and scenarios.

Recently, Adib et al. [86] presented an interesting work for fire detection using a chip that integrates 16 SnO_2 nanowires gas sensors and classification algorithms based on Linear Discriminant Analysis (LDA). To test their system, they performed tests of smoldering PBC, Bench and cotton using a hot plate. The experiments were performed in a chamber and in a big container. They obtained a classification rate of 88% in experiments performed in the chamber and 86% in the experiments performed in the container. Further work is required to explore the robustness and the generalization of the model using an extensive dataset.

Lee et al. developed NiO, SnO_2, WO3 and In2O3 NCs nanocolumns gas sensors using the glacing angle deposition technique (GLAF) [87]. The sensors were designed for fire detection. To study the behavior of their sensors under fire conditions, they performed smoldering PVC fire experiment. Their methodology consists of heating 5 g of PVC plastic and increasing the temperature from 5 °C to 350 °C. They observed that different gases were emitted depending on the temperature of the hotplate. Additionally, the response time of sensors was much faster than the smoke sensor. They concluded that their developed sensors are able to detect PVC fire and identify different stages of PVC combustions.

Finally, Courbat et al. developed a colorimetric CO sensor based on a rhodium complex [88]. The sensor relied on the chemochromic properties of the reagent when exposed to CO: its color changed from purple to yellow when CO concentration level increases. The colorimetric film was integrated with LED and photodetectors. The sensitivity of the device was explored with test fires inspired by EN-54 standard (TF2, TF3, TF5) downscaled in a 1 m3 volume chamber. The system showed sensitivity to the tested scenarios, and sensor showed baseline recover after some minutes. However, cross-sensitivity to other volatiles and scenarios was not evaluated, and, therefore, the viability of the device remained uncertain.

1.11 Summary

The use of gas sensors for fire detection has both strengths and weaknesses. The possibility to detect toxic emissions from fires before actual smoke reaches the detector is a remarkable strength with respect to conventional fire detectors. Earlier warning to building occupants may lead to better protection against intoxication, incapacity and, ultimately, death. This path has been already explored with the integration of carbon monoxide electrochemical cells in multisensor systems for fire detection. However, the range of toxicant emissions from fire, plastic overheating or new building materials covers many other volatiles beyond carbon monoxide. Consequently, the inclusion of chemical sensor arrays to detect other hazardous compounds deems necessary. While this is possible, and it can lead to higher fire sensitivity and earlier fire detection, it can come at the expense of less reliable predictions. Actually, high rate of false alarms constitutes a downside for gas-based fire detectors. This is a direct consequence of the poor selectivity of low-cost solid-state sensors, which are also sensitive to volatiles generated during normal daily activities, such as cleaning or cooking, for

example. For this reason, the only path to improve false alarm immunity is the use of pattern recognition algorithms that could differentiate between sensor signatures induced from fire or nuisance scenarios. While this can be accomplished by a large variety of soft-computing and machine learning methods, it requires extensive and time-consuming testing since fire conditions and nuisance scenarios can be extremely diverse. The reviewed literature shows that the number and type of nuisances proposed by authors are also large. Standardization specifically tailored for fire detectors based on chemical sensors lags, and efforts are required to find a consistent set of testing conditions that ensures the robustness of detectors against nuisances. Additional problems may appear due to sensors drift or sensor to sensor tolerances.

Chapter 2: Objectives

The early emission of gases and volatiles in smoldering fires opens the possibility to build fire alarm systems based on chemical sensors with shorter response times than widespread smoke detectors. However, gas sensor arrays for fire detection are also sensitive to other non-fire volatiles that appear in closed scenarios, such as offices or houses. For that reason, fire detectors based on chemical sensors should include the signal processing and pattern recognition algorithms to discriminate between fire and nuisance signatures. The presented PhD thesis is framed in the FP-7 European Project SAFESENS. The project has as objective the co-integration of gas sensor and presence technologies that enable an enhanced safety and security in fires.

The main aim of this PhD project is ***THE DEVELOPMENT OF A SMART ROBUST ALARM FOR AN EARLY AND RELIABLE DETECTION OF FIRE BASED EXCLUSIVELY ON LOW COST CHEMICAL SENSORS***. The fire detector should be capable to reject non-fire stimulus and detect toxic emissions in a very early stage of the fire situation. The proposed fire detector is focused on the detection of smoldering fires. Smoldering fires are described in Chapter 1 and refer to those fires that do not produce flame and have a slow combustion and a small temperature increase.

Despite fire detection using gas sensors has been explored for many years, the development of *robust* systems is still an open problem. To develop robust fire detectors based on chemical sensors the usual challenges of chemical sensor arrays must be faced, such as cross sensitivities, environmental stability and calibration costs. Also, to train fire prediction algorithms capable to reject all the non-fire stimulus, the models should be trained using a large number of fire and non-fire data. However, in fire detection the limited and expensive use of standard fire rooms to perform experiments constrain the number of fire/ non-fire conditions to which the system can be trained and calibrated. Several research projects have been developed with the objective to find a reliable based gas sensor system to detect fire.

The presented PhD thesis has two specific objectives. Those objectives are detailed below.

Objective 1: *Smart fire detector*: The development of a smart fire detector depends on the accomplishment of a series of specific objectives in three different fields; *hardware design, training and test sets generation* and *development and validation of fire detection algorithms.*

Hardware design: The electronic design of the smart detector is crucial to the acquisition of high-quality data. The first objective of the thesis is the selection of an optimal set of sensors of diverse technologies, the design and construction of their signal conditioning circuits and the visualization of the signals on real time for visual inspection of the measurements.

Training and Test sets generation: The generation of the training and test sets for calibration and performance evaluation constitutes another goal and it requires a careful design of experiments and measurement process protocol under a large variety of fire and nuisance conditions. The series of measurements must be executed in compliance with the test conditions established in the EN-54 standard. The standard provides the dimensions of the standard fire room, quantity of material used in the fire experiments, time and temperature of heating and others. These datasets should include additional test conditions in order to ensure the reliability of the alarm against potential nuisances.

Fire detection algorithms: A key part of a fire detector based on chemical sensors is the embedded algorithms that provide intelligence to correctly detect the fire signatures while counteracting the instabilities, cross sensitivities to other gases, volatiles and environmental perturbations. In this thesis, we will use proper signal processing and machine learning techniques to obtain reliable fire prediction. The algorithms will be tested in external validation conditions.

Objective 2: ***Reduction of experimental costs.***

In order to build robust prediction algorithms, it is key to devise solutions to acquire a large number of fire and non-fire data to train the predictive models. This requirement often makes the calibration of sensor systems costly and even unpractical for real applications. For this reason, in this PhD thesis we will develop methodologies to reduce costs.

Methodology 1: The methodology is based on the use of data fusion of measurements acquired in a standard fire room and a small-scale cabin. All the small-scale experiments were inspired by the fire test standard and properly scaled down.

Methodology 2: In the same spirit, in this PhD dissertation, we aim to propose a novel methodology to build detector independent calibration models to reduce calibration costs (and in consequence, mass production costs).

Chapter 3: Experimental Set-up

Due to the environmental conditions and the exposure to other non-fire volatiles, the stability and reliability of gas sensors systems for fire detection is a challenge. To counteract the sources that can reduce the efficiency of the detector, the detector has to be exposed to several fire and non-fire conditions to train the fire detection algorithms.

However, to perform fire tests it is necessary to comply with different security norms. The challenge relies on the necessity to perform fire tests under safe conditions. In the '80s, the assessment of fire alarms to detect fire was empirical. However, the need to have similar conditions around the world to test the detectors promoted the design and development of standards for the fire tests. In *Chapter 1* and *Chapter 3* standard fire norms are described.

The proposed gas-based fire detector was trained under these standard conditions. The database used to train and assess the performance of the detector includes experiments performed in a standard fire room.

However, performing experiments in a standard fire room could be complicated due to the lack of availability of rooms. This results in a limited quantity of tests that can be performed under standard conditions, as a consequence, the number of experiments to train the detector algorithms is limited.

This dissertation presents an alternative to performing more experiments. Doing experiments in a reduced scenario could reduce costs and save time. In consequence, the number of experiments to train the system can be increased. A small chamber inspired in a standard fire room was built on the intelligent signal processing laboratory at the University of Barcelona.

Summarizing, we performed experiments in two different setups: a standard fire room and in a small chamber. The acquired datasets contain experiments from two different scenarios in order to get a large number of experiments to train the fire algorithms. In this chapter, the different fire scenarios (setups) are described.

3.1 Standard Fire Room

In Europe, the norm EN-54 establishes the minimal requirements to perform fire experiments to test-fire detectors. In addition, the norm describes the features that should be included and regulates the performance during a fire situation. The standard contains 30 different parts and regulates the performance of most of the current instruments for fire detection, fire extinguisher, and fire protection. The norm describes the expected behavior of instruments based on smoke detection, heat detection, the combination of smoke and CO detection and others. As mentioned in *Chapter 1*, there is not a norm that establishes the expected behavior of gas-based fire detectors.

The fire detector systems presented in this dissertation were tested in an EN-54 standard fire room. The fire room is located at the facilities of Minimax Company (Bad Oldesloe, Germany) [152]. The facility includes an experimental area (fire room) and a control room.

The room has an inner volume of 240,000 liters, with dimensions of 10m x 6m x 4m (LxWxH). All the fire test should be performed in the center of the room floor. Two circular brackets of 6 and 5.5 meters of diameter are installed in the center of the ceiling that point the area in which the systems to be tested should be placed and also enable the installation of sensing platforms. Figure 7 shows the scheme of the standard fire room.

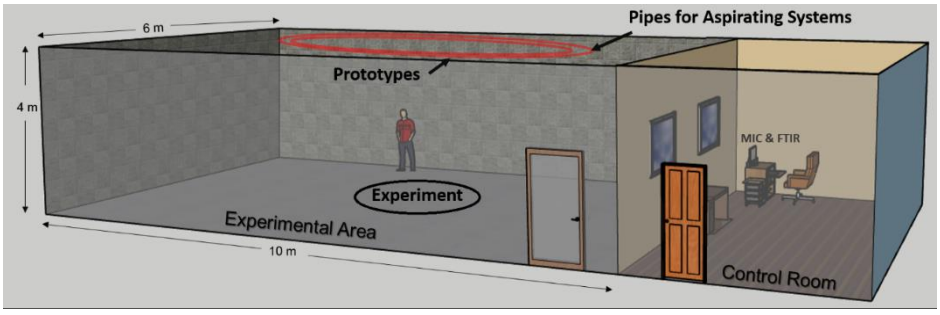

Figure 7 Dimensions and distribution of the experimental area and control room of the standard fire room

The standard fire rooms allow the control of the different environmental conditions and ensure the correct performance of the tests. According to the standards, the rooms should be rectangular, with a flat horizontal ceiling with dimensions of 9 to 10 m of length, 6 to 8 m of width

and 3.8 to 4 m of height. The fire room includes a window for visual inspection of the test. The experimental area has a ventilation system to reduce the number of gases and heat during fire tests. Additionally, behind the experiment space there is room to monitor the test.

The fire room includes sensors and reference instruments to monitor environmental conditions. Specifically, the room should be equipped with a Measuring Ionization Chamber (MIC), an obscuration meter and a temperature and pressure sensor and a probe placed in the hotplate to measure the temperature (for smoldering fire tests) [153].

The MIC instrument has an internal chamber in which the ambient air is constantly aspirated. Inside the chamber there is a radioactive source (americium-241) that emits alpha particles and ionizes air molecules and a pair of electrodes. The electrodes are connected to a voltage source. The ionized air molecules come into contact with the electrodes and generate a current between the electrodes. When smoke particles enter the chamber, some ions attach to the particles and do not contribute to the current between the plates. Then, the generated current between the two electrons will be decreased. MIC instrument requires a constant calibration using clean air. During the calibration, the instrument saves the Reference current generated in clean air. The Equation (3) describes the current generated inside the MIC chamber. Figure 8 shows the internal distribution of the MIC camera.

Equation (3)

$$X = \frac{I_{t0} - I_t}{I_{t0}}$$

$$I_{t0} = Reference\ Current$$

$$I_t = Actual\ Current.$$

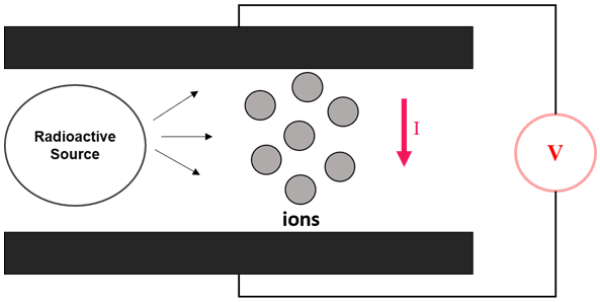

Figure 8 Internal distribution of the MIC camera.

The MIC instrument used in the Fire room is EC-912 from Delta [154]. The MIC EC-912 fulfills the specifications of the EN-54 norm. Figure 9 shows a picture of the MIC model used in the fire room experiments.

Figure 9. Picture of the Measuring Ionization Chamber EC-912 from Delta. The MIC was using during the fire and nuisance experiments performed at the standard fire room

The obscuration meter selected by Minimax to be used during the fire test is the MIREX EC-911 from Delta. The MIREX is based on light scattering using infrared light (880nm). In the presence of smoke, the path of the light is attenuated and the current provided changes [155]. The principle of operation of the instruments MIREX and MIC are light scattering and ionization respectively. MIREX and MIC are a good reference for fires because most of the commercial detectors have the same principle of operation. According to the standard fires, MIC and MIREX instruments are used to indicate the end of a fire test depending if there is or not a fire condition (smoke production). Usually, the instruments aspirate the smoke using a probe located in the ceiling, above the fire experiment.

To measure gas concentration, the best reference instrument is a Fourier Transform Infrared Spectrometer (FTIR) [155]. The FTIR meter is used to measure the gas concentrations of the fire test experiments. The fire room is equipped with the FTIR DX400 from Gasmeter. The FTIR has a resolution of 4 cm^{-1} with a range of 900 – 4200 cm^{-1} . The system is capable of analyze 30

different volatile compounds using an internal library of infrared absorption spectra and chemometric prediction models. Specifically the gases are: *acrolein, acrylonitrile, ammonia, arsine, benzene, boron trichloride, carbon dioxide, carbon monoxide, carbon disulfide, dichloromethane, ethylene oxide, formaldehyde, hydrogen chloride, hydrogen cyanide, hydrogen, methane, methyl methanethiol, nitrogen dioxide, sulfuric fluoride, toluene, water vapor, acetic acid, acetone, acetaldehyde, isopropanol, and isopropyl.*

The FTIR uses an aspirated system to measure the gases released during the tests. The inlet probe was at the ceiling of the fire room. The flow used is 4 l/min. There might be a possible delay in the FTIR signals due to the sampling frequency (1 sample per minute) and the aspiration. The limit of detection of the FTIR placed in the fire room is 1 ppm. However, the measurements are used to analyze the possible gas emissions and their relation with the material used in the fire experiment. Figure 10 shows a picture of the FTIR used in the fire room.

Figure 10 Picture of the Fourier Transform Infrared Spectrometer DX4000 from Gasmeter. The FTIR was using during the fire and nuisance experiments performed at the standard fire room.

A pipe system is located in the ceiling of the fire room. The pipe is used for aspirated smoke systems and FTIR measurements. Aspirated smoke systems are usually installed in rooms that need a fast detection of smoke (clean rooms, food industry, etc.) Aspirated systems include a pipe system that aspirates samples of air continuously and sends them into a small chamber in which a smoke detector is placed. The fire room also has 31 supports for fire detectors and three mounting brackets for general applications. The mounting brackets are installed in the ceiling of the fire room.

To monitor the environmental conditions of the fire room (temperature, pressure, air quality) an automated measuring system is

incorporated in a control area. The environmental signals were collected using a dedicated software developed by Minimax. The Minimax software takes one sample per minute of each environmental condition and allows the visualization of the signals in real time. The fire room includes a time synchronization output for external systems.

3.2 Small Scale Chamber

The second scenario corresponds to a customized test chamber. The dimensions of the chamber are 55 x 55 x 90 cm (LxWxH), for a total inner volume of 272 liters. The bottom, top and upper part of the walls (50 x 35 cm) were made of aluminum. Only the lower part of the lateral walls (50 x 50 cm) was built with glass panels to allow visual inspection of the experiments. Airflow from the outside of the chamber was favored to maintain oxygen concentration and avoid fire suffocation. Hence, 25-mm apertures were opened along the chamber, between the top and bottom lids and the lateral walls. Finally, one of the glass panels was enabled as a door for easy access to the inner volume of the chamber.

For safe operation, the measurement chamber was placed inside of a fume hood smoke, which is equipped with an extraction system to facilitate the evacuation of the smoke generated inside the chamber. Airflow was measured in the chamber using a flow meter while the extraction system was switched on. Induced airspeed was 1.5m/s at the lower region of the chamber and 0.2 m/s at the position of the sensors. Figure 11 shows the dimensions of the customized test chamber (right) and an actual picture of the small chamber located on the laboratory of the intelligent signal processing group at the University of Barcelona.

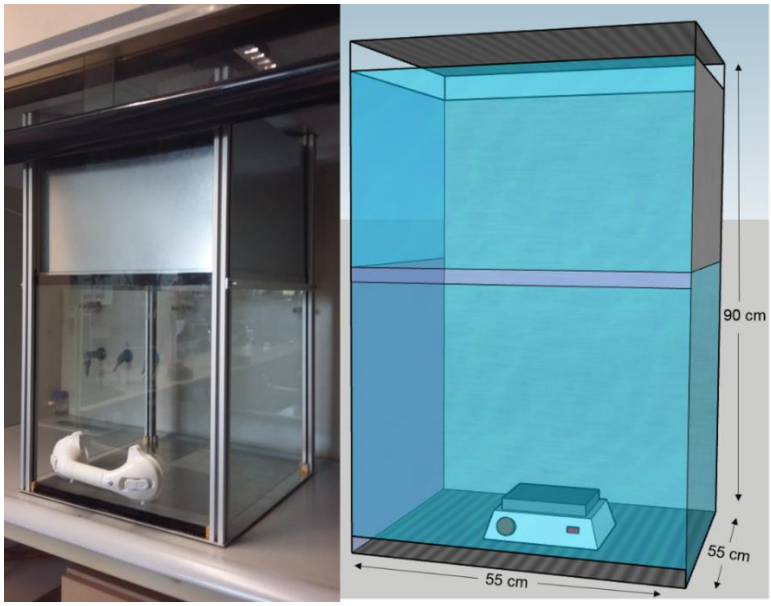

Figure 11 Customized experimental chamber. On the left an actual picture of the small chamber, on the right a scheme with the chamber dimensions.

For further reference, additional commercially available gas sensors and fire alarms systems (smoke detectors) were also integrated into the measurement chamber. As reference systems we selected the multisensor Dräger x7000, which includes one electrochemical sensor of CO, one of H_2 and one of NO_2 and a PID sensor. In addition, a PID sensor ppbRAE 3000 from RAE Systems and NDIR CO_2 GasCheck from Edinburgh Sensors were also placed as reference. They were integrated in the chamber, along with the smoke detectors Hochiki SLR-24H (Photoelectric/heat) and NOVA-500 S250 (Ionization) [157]. Unfortunately, the smoke detectors only provided a binary signal indicating the alarm status. Table 4 summarizes the detectors and sensors used as references during the small-scale experiments. Table 1 also shows ranges of detection of the gas sensors references.

Table 4 Target Gases of the instruments used at the customized chamber when the experiments of nuisances and fires were performed

Instrument	H_2	NO_2	CO_2	CO	VOCs	Smoke
Dräger	0-2000 ppm	0-50 ppm	0-5 Vol. %	0-2000 ppm	0–2,000 ppm Isobutylene	-
ppbRAE	-	-	-	-	0 -10,000 ppm	-
Edinburgh	-	-	0– 3000 ppm	-	-	-
Srl-24h	-	-	-	-	-	✓
500 S250	-	-	-	-	-	✓

The complete instrumentation included the necessary hardware for signal acquisition, which was synchronized and stored. Reference instruments sent data directly to the CPU (host PC) by means of the proprietary software provided by the respective manufacturers, or by means of a data logger (Data Taker DT800) that interfaced with the sensor with the CPU with a frequency of 1 sample per second.

In summary, the gas sensor array for fire detection was tested under EN-54 test conditions in a standard fire room. The standard fire room is equipped with instruments that allow the monitoring of environmental conditions such as temperature, pressure and air quality. In addition, the room provides the measurement of gas emissions using an FTIR. The quantity of smoke density was measured using a MIC and the synchronization of plugged-in instruments allows the integration of the prototype.

However, to counteract the small number of samples to calibrate the sensors due to the limited fire room availability we built a small chamber. The experiments were scaled-down saving time and costs. In this way, the number of experiments can increase, and we can develop more robust and reliable algorithms.

Chapter 4: Experimental Protocols

There are effective solutions for the detection of those fires that produce a large amount of smoke or heat. The most used technologies are ionization and light scattering. While this type of detector produces fire alarms in the presence of smoke, it is well known that prior to the emission of smoke particles we have toxic gas emissions. Moreover, conventional detectors could not produce fire alarms in fire situations that do not produce smoke.

The challenging fires for conventional detectors are the smoldering fires. These types of fires produce smoke in a very slow way resulting in a late response of the fire detectors. This situation can be mortal for the building occupants.

As explained in chapter 1, all the systems developed for fire detection must be tested as established in standard EN-54. This standard establishes the experimental protocols and experimental setups used to test the fire detectors. The standard establishes the requirements to test smoke detectors, heat detectors, flame detectors and there is a special standard to test-fire detectors which include electrochemical sensors of Carbon Monoxide (EC-CO). However, there is not a standard that regulates the test requirements for fire detectors based on chemical sensors.

As mentioned in Chapter 3, the norm establishes the conditions, fire conditions, under the detector has to emit an alarm. There are several types of fire experiments. In this dissertation, we focus on the smoldering fire experiments establish on the norm. From the standard smoldering fires, we selected those that emit a low quantity of smoke, Smoldering Wood (TF2) and Smoldering cotton (TF3). TF2 and TF3 are one of the most challenging for conventional smoke detectors. In TF2 and TF3 fires, the production of smoke is very slow and the increase in temperature is too low. In consequence, the fire alarm of a conventional detector triggers in a very late stage of the fire. Moreover, these two experiments are included in the standard EN-54-26 to test CO-based fire detectors due to the high emission of Carbon Monoxide.

Additionally, some fire scenarios outside the norm are added. Specifically, we include PVC, PET, Cables, and Electrical Fires. These are some of the most common sources of fire in buildings due to the widespread use of plastic in construction, furniture and toys, and others. Additionally, fires

produced due to an electric failure are one of the most common in buildings [158-161]. This type of fires are smoldering fires and in some cases are produced in walls and are not easy to detect. Additionally, plastic fires produce an enormous quantity of toxic emissions (as explained in *Chapter1*) resulting in a hazardous scenario for the occupants. Unfortunately, plastic fires are not considered in the EN54, for that reason we decided to include as part of the experimental protocol.

On the other hand, to counteract the responses to emissions from non- fire sources, the dataset must include different nuisances' experiments that could produce false alarms [162]. Here, we have to consider that the number of potential interferents for chemical based fire detectors is vast, while the number of nuisance tests should be finite. In this respect, the cross sensitivities produced by alcohol and some types of fuels can be a problematic issue for fire detection indoors. Scenarios that can be easily found at offices, houses or industries were selected. The nuisances set include cleaning products and solvents. In offices, cleaning products are commonly used and most of the cleaning products contain alcohol and may produce false alarms in gas-sensor-based fire detectors. On the other hand, solvents are widely used in industry or parking. For that reason, is important to include this type of nuisance scenario as part of the experiments set.

Since machine learning based solutions are based on examples, and taking into account the large variety of fires and nuisances, ensuring a minimum coverage of the input space forces to perform a huge amount of calibration experiments. As mentioned in chapter 3, the availability of standard fire rooms to perform experiments is limited and expensive. However, the main disadvantage is the duration of a fire experiment. A fire experiment performed in a fire room has an average duration of 45 to 60 minutes. Also, the production of smoke is high and requires around 2 hours of ventilation to clean the room of smoke and particles. For that reason, a way to carry on shorter experiments was devised. Those experiments have a duration of 15 or 20 minutes and need only 30 minutes of ventilation. The path towards shorter experiments is to perform the fire/nuisance experiments in a Small-scale chamber.

All the experiments performed on the small scale were inspired by the experiments performed in the standard fire room. The materials were scale-down to adapt the experiments to the small-scale scenario.

4.1 Fire and non-Fire scenarios in the fire room

We centered the focus of interest on smoldering fires. Smoldering fires do not produce flame and release small quantities of volatiles and airborne particles. Smoldering fires produce a late response in commercial detectors. We considered smoldering fires present in international standards. The considered fires are used to test CO-based fire detectors. Specifically, we considered two smoldering fire types selected from the EN-54 standard: ***TF2 [wood fire]*** and ***TF3 [cotton fire]***. Since there is not a standard norm that establishes the requirements to test gas-sensor-based fire detectors, we included smoldering fires that are beyond current standards. As mentioned in *chapter 1*, the most common sources of smoldering fires indoors include electrical failures. In this respect, we also include ***electronics*** and ***cable*** fires. Fire emissions released in plastic fires are one of the most dangerous in closed scenarios (offices, houses, and industries). Newer building materials include plastic materials and bottles and plastic tubes are common sources of plastic fires. For that reason, we also performed non-standard smoldering fires that include plastic materials, such as ***PET*** and ***PVC.***

In buildings, several non-fire scenarios can produce a stimulus in a fire detector based on gas sensors; however, the more challenging ones are those that contain substances with a high level of volatility. For that, we selected common non-fire scenarios easy to find in offices or closed places. The selected materials produce a high chemical response in gas sensor arrays. The selected nuisance scenarios are ***Gasoline***, **e*thanol, air freshener, turpentine, vinegar,*** and ***window cleaner.***

4.1.1 Experimental Protocol of Fire Experiments

The selected set of fire experiments to perform at the standard fire room includes two standard fires; ***TF2*** (4 beechwood sticks of 75 x 20 x 20 mm) and ***TF3*** (40 cotton wicks of 80 cm length), two plastic fires; ***PET*** (50g) and ***PVC*** (100g) and two types of electrical fires; ***electronics*** (FR-4 of 10 cm) and ***cables*** (10 pieces of 10cm length and 1 cm of diameter).

Figure 12 shows a general overview of the fire and nuisance experiments performed in the fire room. The first step corresponds to the preparation of the experiment, the second step is the beginning of the experiment and starts when the door is closed and finally the experiment

ends, and the ventilation starts. In nuisance experiments, the end of the experiment is after 15 minutes of exposure. In case of the fire experiments, the experiment ends when the fire conditions are achieved (smoke density or light obscuration), one of the fire room alarms is activated or a flame is produced.

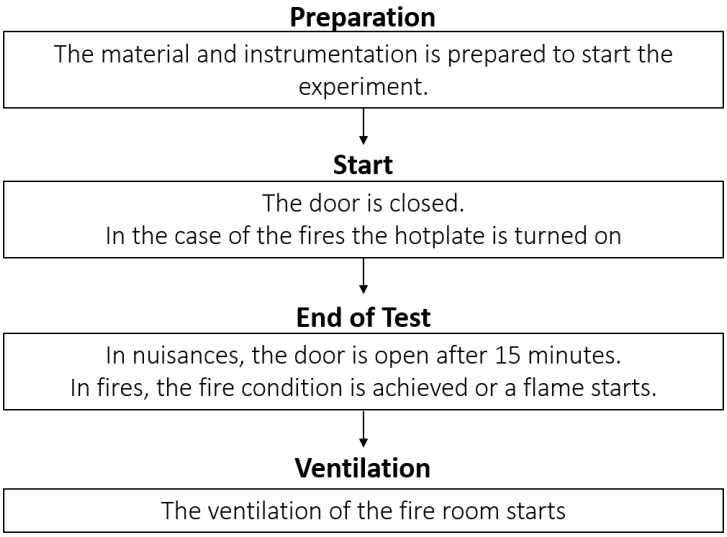

Figure 12 Experimental protocol of the Fire and Nuisance experiments performed at the Fire room. The methodology has 4 steps: Preparation, Start, End of Test and Ventilation.

4.1.1.1 TF2 Beechwood Smoldering Fire

During this experiment, 4 sticks of beechwood are placed on a hotplate and heated. The sticks are dried (moisture content ~5%) and each stick has a size of 75 x 20 x 20 mm. This type of test produces white smoke and the increase in temperature is undetectable. According to the standard, the hotplate should have a diameter of 22 cm and the temperature of the hotplate should be measured by a sensor (thermocouple type K) attached in an extreme of the circumference. The hotplate has to be capable to reach 600 ºC after 10 minutes.

The experimental protocol has five steps: Start, Heating rate, End of Test, Reduce of fire and Ventilation. The detailed steps are described in Figure 13.

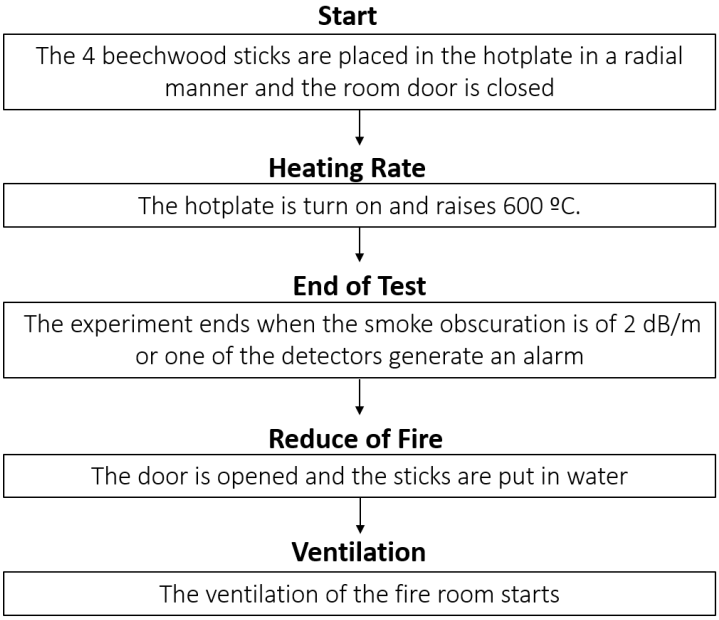

Figure 13 Experimental protocol of the TF2 experiment performed in the fire room. The methodology has 5 steps: Start, Heating rate, End, Reduce fire and Ventilation.

The duration of the experiment is around 45 minutes. This experiment is one of the most used to test fire detectors due to the light-colored smoke and the low temperature. During a TF2, CO_2, hydrogen, CH_4 and a high concentration of CO_2 are released. Figure 14 shows the distribution of the sticks at the hotplate. TF2 is described in detail in the Norm EN-54.

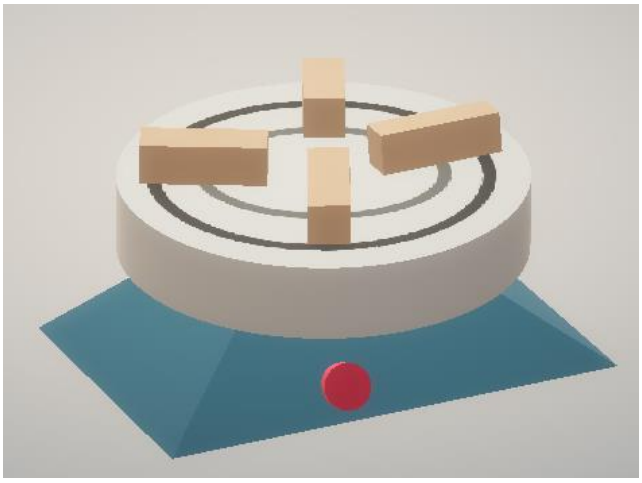

Figure 14 Illustration of the TF2 fire experiment performed in the fire room. The draw shows the distribution and quantities of wood on the hot plate.

4.1.1.2 TF3 Cotton Smoldering Fire

A reduced TF3 experiment was performed in the fire room. 30 pieces of braided cotton wick of 80 cm long were used to produce the smoldering fire. The cotton wicks are hanged in a 10 cm diameter ring suspended at 1 meter to the floor. The ring is above a non-combustible plate Figure 15 shows the way in which the wicks have to be hanged. It is worth to note that the EN54 standard requires the TF3 fire to be initiated by means of a flame, although TF3 is a smoldering fire.

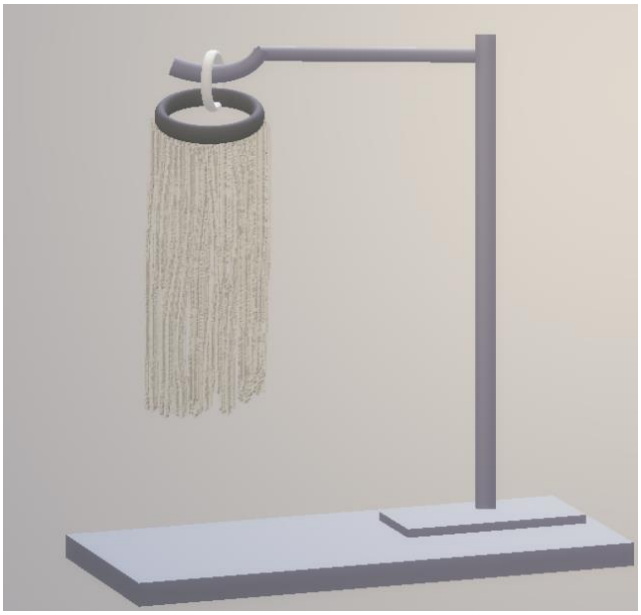

Figure 15 Illustration of the TF3 fire experiment performed in the fire room. The draw shows how the cotton wicks are hanged to the structure.

As for TF2, wood smoldering fire, TF3 experiment has 5 steps to be performed, start, ignition, end of test, reduction of the fire and ventilation. Figure 16 shows the complete methodology of the test. The methodology establishes the ignition of the end of each cotton wick and blow out any flame, the beginning of the test is when the wicks are glowing. In the fire room, ignition was made using a torch of methylated spirit.

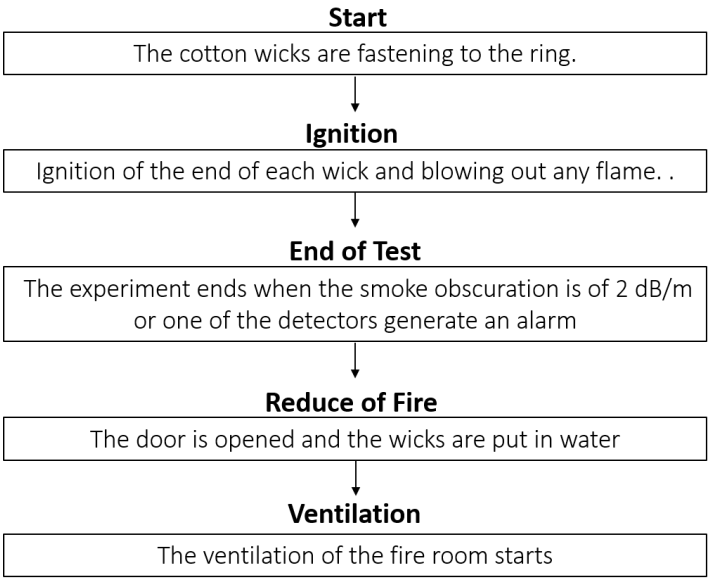

Figure 16 Experimental protocol of the TF3 experiment performed in the fire room. The methodology has 5 steps: Start, Ignition, End, Reduce fire and Ventilation.

4.1.1.3 PET, PVC, Cables, and Electronics Smoldering Fire

Four different non-standard smoldering fires were induced. The selected experiments are two plastic experiments: PVC and PET fire and Cables and Electronics experiments. PVC experiment consists of 10 pieces of a PVC tube. The pieces have 4 cm of diameter and 5 cm of length. PET experiment consists of approx. 10g of PET plastic. The plastic comes from a bottle of plastic. Cables experiment includes 15 pieces of cables of 10cm of length. In addition, Electronics fire consists of burn populated electronics PCB.

All these materials were placed on a hotplate. The hotplate used is the same for the TF2 fire. In non-standard fire experiments, a flat aluminum plate of 200 x 200 x 50 mm was placed on top of the hotplate. Burning materials were placed on top of the aluminum plate to allow the easy cleaning of the surface between measurements. Figure 17 shows the way to place the materials over the hotplate.

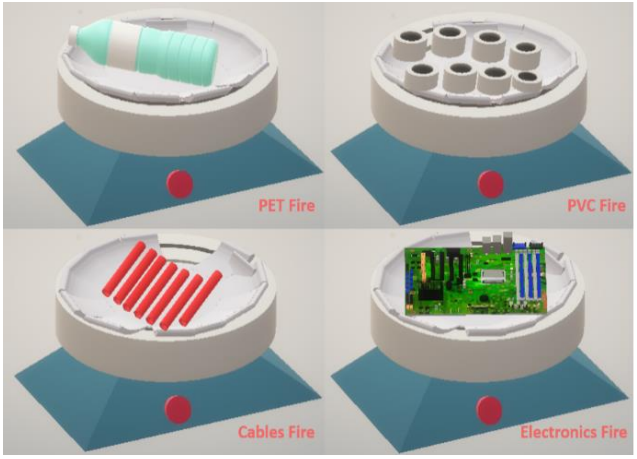

Figure 17 Illustration of the non-standard fire experiments performed in the fire room. The drawings show how the PVC, PET, Electronics, and Cables are distributed on the hot plate. All the materials are placed in an aluminum plate at the top of the hot plate.

In the standard fire room, the beginning of the experiments corresponded to the moment in which the door of the room is closed. As a second step, the hot plate is turned on and the temperature starts to increase. The measurements were extended for 15 - 30 additional minutes after fire conditions were reached (smoke density, explained in chapter 3), or the fire was extinguished. The detailed methodology is shown in Figure 18.

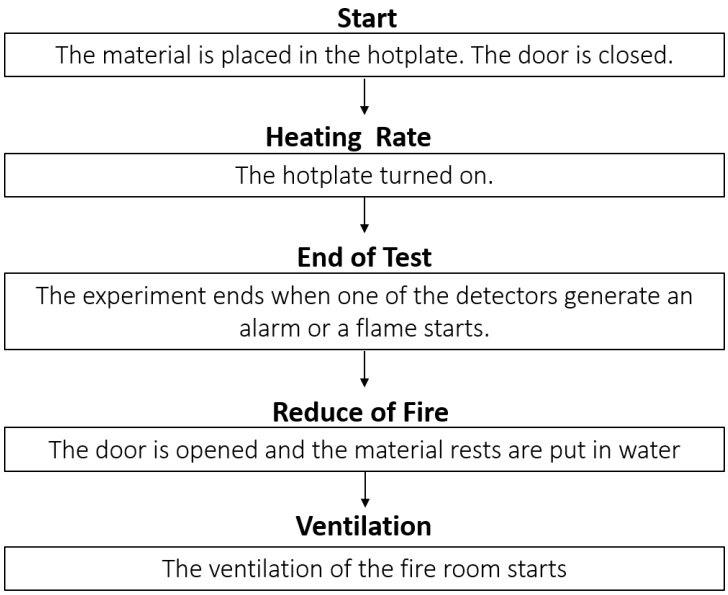

Figure 18 Experimental protocol of the non- standard fire experiments performed at the fire room. The non-standard fires performed at the fire room are: PVC, Electronics, Cables, and PET. The methodology has 5 steps: Start, Heating rate, End, Reduce fire and Ventilation

4.1.2 Experimental Protocol of Nuisance Experiments

In order to build a fire algorithm robust to nuisances, the gas-sensor-based detector was exposed to nuisance experiments. The selected nuisances were those interferences that could be easy to find indoors. Specifically, we selected, ***Gasoline*** (100ml), e***thanol*** (100ml), ***air freshener*** (4 sprays), ***turpentine*** (100ml), ***vinegar*** (100ml) and ***window cleaner***

4.1.1.1 Gasoline, Ethanol, Turpentine, and Vinegar.

There are several chemical sources that could provide false alarms indoors. Those that contain alcohol could be more challenging to discriminate from real fire. Turpentine and Vinegar are products commonly used for cleaning. Also, turpentine is used as painting solvent. Ethanol is presented in

most of the cleaning and aromatizing products. In addition, gasoline is the most used fuel and could be found in industries or garages.

Nuisance scenarios that rely on the evaporation from a liquid form (gasoline, turpentine, vinegar, and ethanol) were presented to the sensors inside of a container of 200 x 200 x 50 cm.

The container was placed in the experiment area of the room, in the same position in which fire is originated. Approximately 100ml of substance (gasoline, ethanol, turpentine, and vinegar) were placed into the container. After place the container in the center of the room the doors are closed and the exposure to the nuisance has a duration of 15 minutes. Then, the doors are open, and the ventilation starts. Figure 19 shows a scheme of how the container was placed.

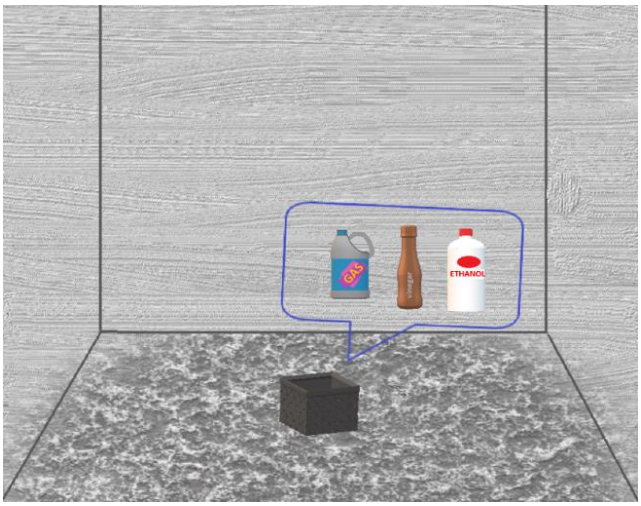

Figure 19 Illustration of the Gasoline, Vinegar, and Gasoline nuisance experiments performed at the fire room. 100ml of substance was placed into an aluminum box in the middle of the room.

The methodology of the experiment has 4 steps. Preparation, Exposure, End of the experiment and Ventilation. The complete methodology is presented in Figure 20.

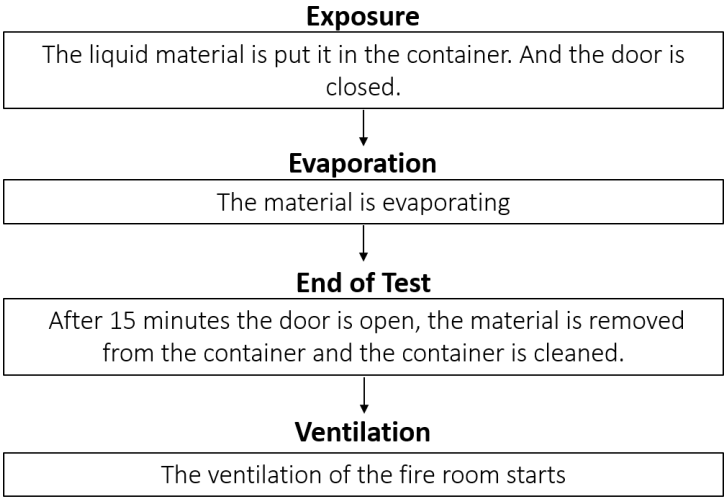

Figure 20 Experimental protocol of the Gasoline, Vinegar, and Ethanol nuisances experiments performed at the fire room. The methodology has 5 steps: Start, Evaporation, End, and Ventilation

4.1.2.1 4.1.2.2 Air Freshener.

Air freshener is commonly used to emit fragrance. Nowadays, there are several branches that offer air fresheners in different presentations. Commercial air fresheners contain several VOCs. Air fresheners produce more than 100 different VOCs. Among them we can find formaldehyde, ethanol, BTX and phthalates but also terpenoids such as and alpha-terpinol and linalool, terpenes as limonene, α-pinene and β-pinene. In consequence, air fresheners can be nuisances for fire detectors based on gas sensors.

An air freshener experiment was executed used a common spray bottle (*Airwick spray 6-1*). The air freshener was introduced at the fire room by spraying a bottle 10 times inside the room (10 sprays, 0.025 oz). One person gets inside at the fire room and stands up in the middle of the room (at the same place that the hot plate or container). Then, the person sprays 2 times to the north, 2 times to the south, 2 times to the east, 2 times to the west and 2 to the top of the fire room. Figure 21 illustrates the direction of the sprays. The experimental protocol of air freshener has four steps and is described in Figure 22.

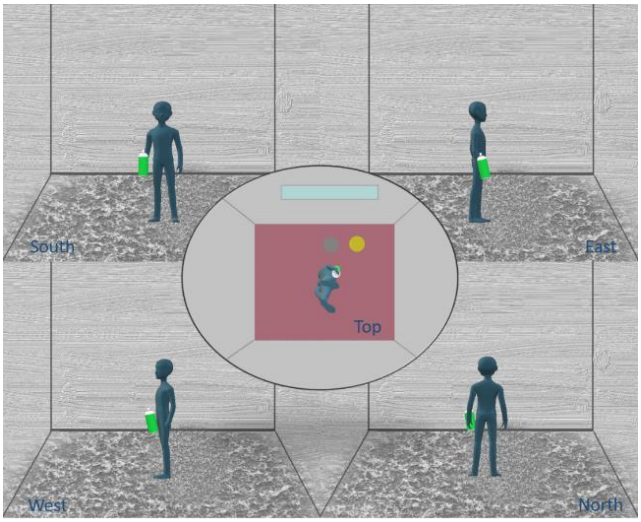

Figure 21 Illustration of the Air Freshener nuisance experiment performed in the fire room. The draw shows the 5 directions (north, south, east, west, and top) in which the air freshener was spread.

Presentation

A person enter into the room, stand up in the middle of the fire room, sprays 2 times in each cardinal points and to the top of the fire room.

↓

Exposure

The person outs of the room and closes the door

↓

End of Test

After 15 minutes the door is opened.

↓

Ventilation

The ventilation of the fire room starts

Figure 22 Experimental protocol of the Air Freshener nuisance experiment performed in the fire room. The methodology has 4 steps: Presentation, Exposure, End, and Ventilation.

4.1.2.2 Window Cleaning.

Equally, to the Air freshener, most of the commercial products used to clean the windows and glass contain alcohol. The use of window cleaners indoors could produce nuisances. In order to mimic a more real situation a window was cleaned inside the fire room. The fire room contains 2 windows for monitoring. Booth glasses are on the same wall.

To execute the experiments a person enters into the room sprays 6 times (6ml) of window cleaner Putz-Meister brand in one window (first glass) and uses a towel to clean the window. When finish to clean the first window, repeat the same process into the second window (sprays 6 times and clean with a towel). Once the windows are cleaned, the person gets out to the room and closes the door. After 15 minutes the experiment ends, the door is opened, and the ventilation starts. The Figure 23 illustrates the experiment and figures the complete methodology.

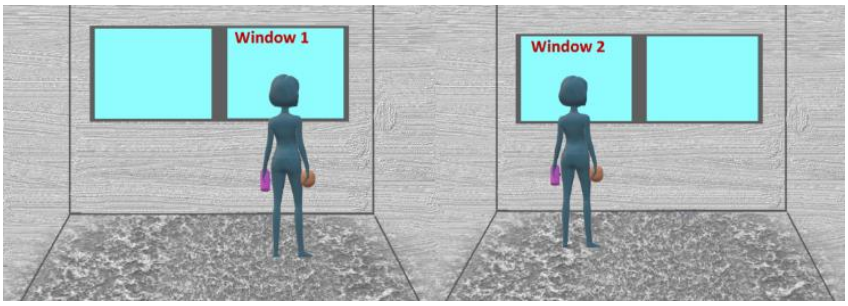

Figure 23 Illustration of the Window Cleaning nuisance experiment performed in the fire room. The draw shows the distribution of the windows in the fire room.

The detailed experimental protocol is presented in the following Figure 24. There are four steps, the first two correspond to the cleaning of the window, third is the end of the experiment and finally the ventilation.

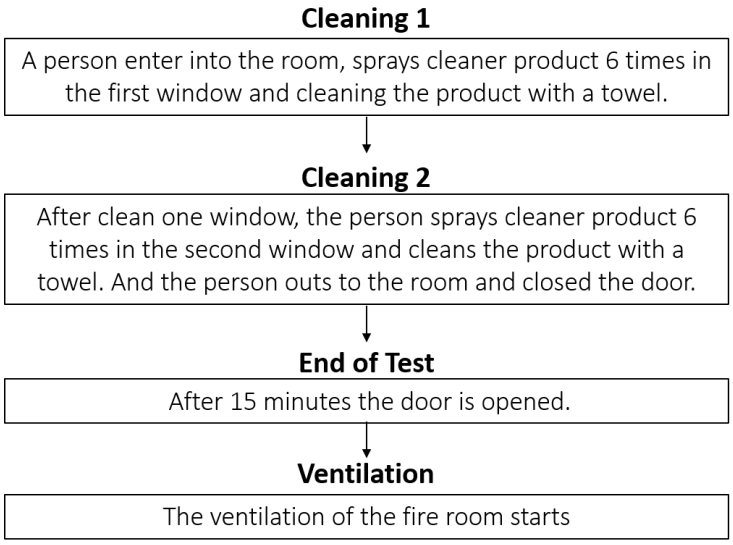

Figure 24 Experimental protocol of the Window Cleaning nuisance experiment performed in the fire room. The methodology has 4 steps: Cleaning 1, Cleaning 2, End and Ventilation.

4.2 Fire and Nuisances scenarios in small-chamber

In the case of the small chamber, we scaled-down all the quantities of the fires and nuisance experiments in order to reproduce as much as possible the fire and nuisance tests conditions of the fire room. Additionally, to the standard fires performed at the standard fire room (**TF2 and TF3**), we included a variation of the TF2 experiment using pinewood, we named **TF2 bis**. As in the fire experiments performed at the standard fire room, we performed a non-standard fire experiment. Specifically, we selected ***cable fire***. Similarly, as in the fire room, different nuisances were induced inside the measuring chamber. For nuisance scenarios, we employed ***distilled boiling water***, ***air freshener***, ***ethanol***, and two commercial cleaning products, ***vinegar*** and ***floor cleaner***.

4.2.1 Experimental protocol

The Fires performed in the chamber includes; ***TF2*** (1 beechwood stick 75 x 20 x 20 mm) and ***TF3*** (4 cotton wick 10cm length), **TF2 bis** (4 pinewood sticks 100 x 20 x 9 mm) and ***cable fire*** (flat cable 100 x 12 x 0.5 mm). For the nuisances set we selected: ***distilled boiling water*** (100ml), ***air freshener***, ***ethanol*** (96% purity, 1.2ml), and two commercial cleaning products, ***vinegar*** (1.2ml) and ***floor cleaner*** (1.2ml).

The measurements in the small chamber were performed in three phases. During the first phase (2 minutes) no test material was introduced into the chamber, which was completely empty. This stage constitutes a baseline for the signals. In the second phase (2 minutes) the material under test was introduced into the chamber. This stage constituted the start of volatile release for the non-fire scenarios (air freshener, ethanol, floor cleaner, and vinegar cleaner). For the experiments that required temperature increase (all fires, hotplate blank and boiling water), the material to be tested was introduced into the measuring chamber, without it being previously burnt or heated. Finally, in the third phase, the heating/ignition of the material was performed. Materials placed on the hotplate were heated up to 280 ºC by switching the hotplate to full power until the commercial detectors triggered (or 15 min if smoke-based detectors did not trigger any alarm before 8 min after the fire was set). Nuisances that were started in phase 2 remained in the chamber for 10 additional minutes. The experimental protocol is shown in Figure 25.

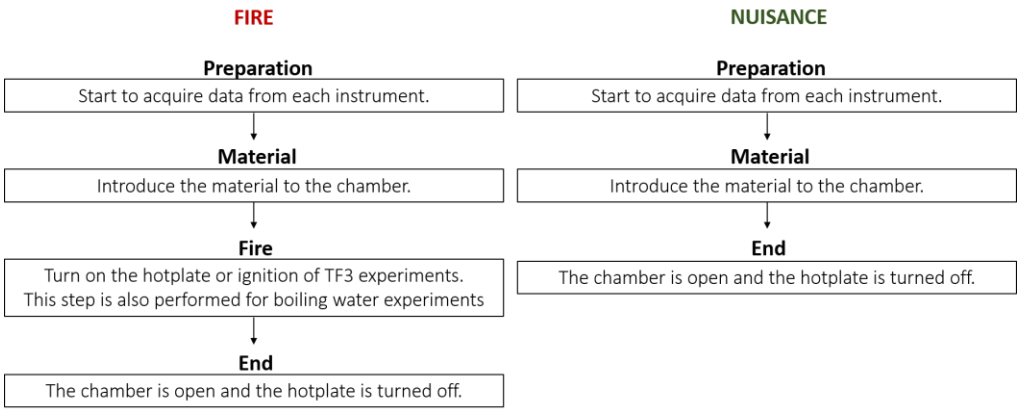

Figure 25 Experimental protocol of the Fire and Nuisance experiments performed at the customized chamber. The methodology has 4 steps for fire experiments: Start, Material, Fire, and End. The methodology to induce the nuisances has 3 steps: Start, Material, and End.

4.2.1.1 TF2 and TF2bis

TF2 and TF2bis are inspired in the standard fire room TF2. We used 4 sticks of beechwood (TF2) and 1 of pinewood (TF2 bis) to perform the experiment. As mentioned in 4.1.1, wood samples were conditioned to reduce the moisture content. For this purpose, the sticks were heated in an oven at 85 °C for 24 h before being used in the experimental tests. The used hotplate raises 280 ºC.

During the first 2 minutes, the sensors are recovering the baseline. Then, the wood and the hotplate are introduced to the chamber and the sensors signals are acquired for two 2 more minutes. The third step corresponds to the beginning of the experiments and the hotplate is turned on. After 15 minutes the chamber is opened, the hotplate is turned off and the material is removed. The fire experiment ends. A picture of the experiment is shown in the next figure (Figure 26).

Figure 26 Picture of the TF2 and TF2 bis experiments performed at the chamber. TF2 used 4 sticks of beechwood and TF2 bis 1 stick of pinewood as fuel. The materials were heating using a hotplate.

4.2.1.2 TF3

A scaled TF3 was performed at the small chamber. The experiment uses 4 cotton wicks of 10 cm. Similarly, as in standard TF3, the fire is induced with the ignition of the end of each cotton wick and blow out any flame, the beginning of the test is when the wicks are glowing.

After recover 2 minutes of ambient air and 2 minutes of ambient air when the material is introduced, the wicks are ignited. The duration of the experiment is 15 minutes. Figure 27 shows a picture of the TF3 performed in the small chamber.

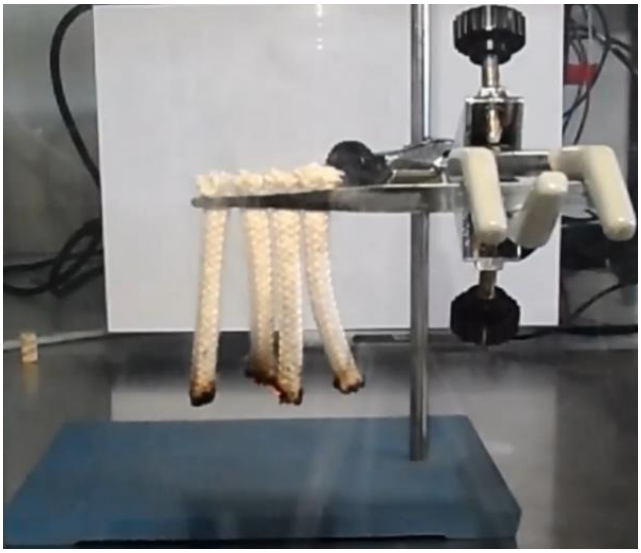

Figure 27 Picture of the TF3 experiment performed at the chamber. TF3 consist of 4 cotton wicks of 10 cm and the fire is induced with the ignition of the wicks.

4.2.1.3 Cables

As mentioned in 4.1 one of the most common fire sources in buildings is caused by electric failures. The hazard of the electric fires originates from all the toxic emissions released due to the plastic thermal decomposition, pyrolysis and eventually combustion. In the small chamber, we perform a cables fire. For this experiment, we heated in the hotplate 10 pieces of flat cable (PVC plastic covered), which is commonly used in PC or other electronic systems. The flat cable pieces have a length of 10 cm. The pieces are heated for 15 minutes. Figure 28 shows the distribution of the cables in the hotplate.

Figure 28 Picture of the Cable experiment performed at the chamber. Cable experiment consists of 10 pieces of flat cable of 10 cm and the fire is induced with the ignition of the wicks.

4.2.1.4 Vinegar, Ethanol, Floor Cleaning Product

In the chamber, apple vinegar (5% of acetic acid), ethanol, and floor cleaning (lagarto brand) product were presented to the sensors using a plastic plate. During the first stage of the experiment, the sensors' readings correspond to the ambient air of the chamber.

In the second step a plastic plate is introduced and the product (vinegar, ethanol or floor cleaning) is sprayed four times. The plate has a square form (Figure 29), and each spray was carried out in each corner of the square. Then, the chamber is closed, and the sensors are exposed to the product for 10 minutes more before the end of the experiment.

Figure 29 Picture of the plate using in the chamber to induce Vinegar, Ethanol and Floor Cleaning Product. One spray of each product was put in each vertex of the square.

4.2.1.5 Boiling Water

As in a fire test, the boiling water experiment has 4 steps to be performed. The first one corresponds to record the ambient air of the chamber, then the boiling water is introduced to the chamber and after 2 minutes the hotplate is turned on and the water starts to boil. After 15 minutes the hotplate is turned off and the experiment is over. Figure 30 shows a picture of the boiling water experiment.

Figure 30 Picture of the Boiling water experiment. 100ml of water was heated in a hotplate.

4.2.1.6 *Air freshener*

All the chamber experiments measure for 2 minutes the ambient air in the chamber. After this first step, an electronic air freshener was introduced into the chamber. Two minutes after the electronic air freshener (Airwick essential oils) is turned on. The experiment ends 15 minutes after. Figure 31 shows the electronic air freshener in the chamber.

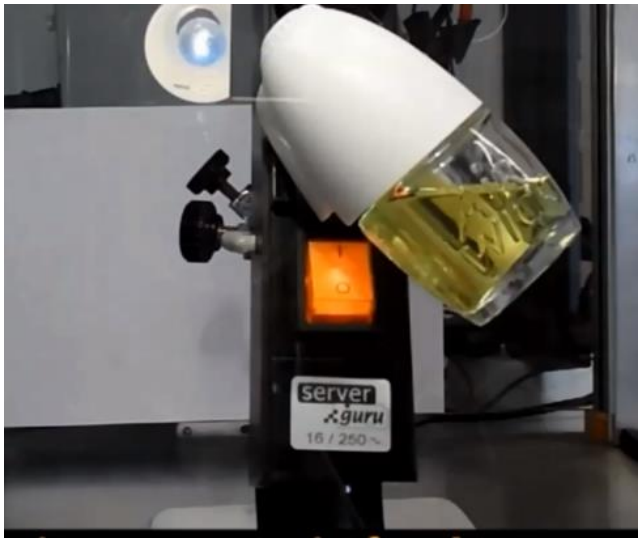

Figure 31 Picture of the electronic air freshener using in the chamber to induce air freshener experiment.

4.3 Summary of Measurement campaigns.

Four measurement campaigns were performed for over two years. One measurement campaign was performed in the small-scale setup and three in the standard fire room.

The first measurement campaign was performed in the customized chamber. The measurement campaign had a duration of 4 days, from 03-07-2016 to 03-10-2016.

In November of 2016, the first measurement campaign in the standard fire room was performed. The campaign has a duration of 4 days. The first

measurement campaign started on 11-26-2016 and ended 11-30-2016. The second and the third fire room measurement campaigns were performed in February and June of 2017 respectively (02-06-2017 to 02-10-2017 and 06-26-2017 to 06-30-2017). Both measurement campaigns were performed along 5 days.

The Table 4 summarizes the measurement campaigns, the scenario in which were performed, the duration and the dates.

Table 5 Date and duration of the measurement Campaigns performed in the fire room and in the small chamber.

MEAS CAMPAIGN	SCENARIO	DURATION	DATE
Small-scale	Chamber	4 days	03-07-2016 *to* 03-10-2016
Large-scale 1	Fire Room	4 days	11-26-2016 *to* 11-30-2016
Large-scale 2	Fire Room	5 days	02-06-2017 *to* 02-10-2017
Large-scale 3	Fire Room	5 days	06-26-2017 *to* 06-30-2017

4.4 Datasets

In total, four different datasets were acquired, three of them were acquired in the standard fire room, and the other one was generated using the small-scale setup. Each dataset was acquired in a different measurement campaign. Namely, the first: **i)** *Large-scale dataset 1, LD1*, **ii)** *Large-scale dataset 2*, *LD2*, **iii)** *Large-scale dataset 3*, *LD3* and **iv)** *Small-scale dataset*. The large-scale dataset 1 (i) was acquired at the standard fire room in November of 2016 and contains 18 experiments; 6 types of smoldering fires, and 5 types of nuisances. The second Large-scale dataset 2 (ii), LD2 was acquired in February of 2017 and includes 6 types of smoldering fires and 5 types of nuisances, in for a total of, 28 experiments. The third dataset acquired at the standard fire room, *Large-scale dataset 3*, *LD3 (iii)* contains 33 experiments, 16 fires, and 17 nuisances; this dataset was acquired in June of 2017. Finally, the dataset acquired in the small-scale setup, the small-scale dataset, SD1, (iii) was performed in March of 2016 and includes 40 experiments, 4 types of fires and 6 nuisances. Each measurement campaign has a duration of 4 days and the

experiments, in both, at the fire room and in the chamber were performed in a random order such that no fire or nuisance scenario of the same type was performed the same day. Table 6 details all the fire and nuisance scenarios included in the different datasets, with the corresponding number of repetitions.

Table 6 Fire and nuisance scenarios included in the different datasets. Large-scale dataset 1 and large-scale dataset 2 were acquired in the standard fire room and the small-scale dataset was acquired in the measurement chamber.

Experiment	Material	Large scale 1 (repetitions)	Large scale 2 (repetitions)	Large scale 3 (repetitions)	Small Scale (repetitions)
Nuisance N1	Hotplate blank	0	0	0	2
Nuisance N2	Air freshener	2	4	3	4
Nuisance N3	Ethanol	2	3	3	4
Nuisance N4	Boiling water	0	0	1	4
Nuisance N5	Floor cleaner	0	0	0	3
Nuisance N6	Vinegar	1	3	1	4
Nuisance N7	Turpentine	1	3	3	0
Nuisance N8	Gasoline	1	3	3	0
Nuisance N9	Window Cleaner	1	3	3	0
TF2	Pinewood	0	0	0	4
TF2 bis	Beechwood	2	2	3	4
TF3	Braided cotton wick	1	1	3	4
Electrical fire	Electronic components	1	2	3	0
Cable fire	Cables	2	2	3	4
Plastic Fire	PVC	2	2	3	0
Plastic Fire	PET	2	0	0	0

In summary, the complete dataset includes 3 different measurement campaigns acquired in a standard fire room and one measurement campaign performed in a small scale scenario. The datasets were acquired through one and a half years. The acquired dataset is used to train fire detection algorithms.

Chapter 5: Sensor Arrays

The greatest danger to human beings in smoldering fire situations is released toxic emissions [163]. During a smoldering fire, a wide variety of toxic emissions are released. According to the literature [164-166] different gases are produced depending on the material in combustion. Actually, in *Chapter 1* it is described that some materials, especially plastics, produced toxic emissions during pyrolysis. Also, in chapter 1, it is discussed the hazardous gases for human health in fires.

Fire detectors based on gas sensors should be include sensor technologies capable to detect toxic emissions. In the presented chapter, we describe the sensor technologies their conditioning circuits included in the developed fire detectors.

Fire alarms based on gas sensors allow the detection of the toxic emissions produced in a fire. Fire detection with gas sensors should be able to detect toxic emissions at low concentrations and at the early stages of the fire.

The variety of gases released during a fire prevents the construction of a fire detector that combines sensors sensitive to all dangerous toxic emissions. An alternative is the construction of a fire detector which includes sensors for those gases that appear most frequently in fire situations. Additionally, fire detectors based on chemical sensors should include sensors capable to detect the most dangerous toxic emissions. As mentioned in chapter 1 the most dangerous gases released in a fire are *Carbon Monoxide* CO, *Carbon Dioxide* CO_2, *Methane* CH_4, *Nitrogen Dioxide* NO_2, *Hydrogen* H_2, *Sulphur Dioxide* SO_2, *Carbon Tetrachloride* Cl_4 and *Cyanide*.

All these gases are mortal. The consequences of exposure depend on the time of exposure and the concentrations to which the victim is exposed. The table shows the most dangerous gases released during a fire situation. Table 7 describes the main symptoms of each gas, the maximum concentration of exposure and the materials which release that gas in a fire situation.

Table 7 Main gas emissions in smoldering fires

GAS	Symptoms	Max Exposure	Material
Carbon Dioxide	**Low exposure:** Headaches, loss of attention. **High exposure:** Oxygen deprivation.	0 ppm	All organic materials
Carbon Monoxide	**Low exposure:** Dizziness, Fatigue, Mental confusion, Nausea. **High Levels:** Coma, Death.	Depends on the exposure time	All organic materials
Sulfur Dioxide	Burning sensation in the nose and throat.	5 ppm	Sulfur containing plastics
Nitrogen Dioxide	Cough, Fatigue, and Nauseous.	Depends on the exposure time	Wool, silk, plastics.
Carbon Tetrachloride	Liver or kidney problems, Blurred vision, Dizziness, Blood pressure.	100 ppm	Wool, silk, plastics.
Cyanide	Headaches, Dizziness, Nausea, Death.	90 ppm	Cellulosic Wool, Silk, plastics.
Methane	Fatigue, Dizziness, and headaches	5% in Air	All organic materials
Hydrogen Chloride	**Low exposure:** Irritation of the eyes, and respiratory tract. **High exposure:** corrosive damage to the eyes and pulmonary edema and death.	20 ppm	Polyvinyl Chloride (PVC)

In the present dissertation we use 2 different prototypes to develop the fire alarm. Prototype 1 is designed with off-the-shelf sensors and prototype 2 was developed during the European SAFESENS Project. Prototype 2 includes sensors developed by partners of the SAFESENS as IMEC, BOSCH, AMS, and NEO.

5.1 Prototype 1: Sensor Array Using Off-The-Shelf Sensors

The general objectives of the SAFESENS project include: *i)* The development of chemical sensors for the detection of toxic emissions in fires, *ii)* The construction of a multi-sensor array, *iii)* The elaboration of a database and *iv)* The development of intelligent algorithms for the early and reliable fire detection.

The device should have a better performance than any commercial device. Currently, there are not fire detectors based only on chemical sensors. However, there is a wide range of commercial sensors that allow the detection of toxic emissions produced in a fire. For this

reason, it was important to develop a system based on commercial sensors. In this way, the performance of commercial sensors could be compared with the sensors developed during the project.

Moreover, developing a multi-sensor array with commercial sensors, allows the availability of a prototype to perform experiments since the first stage of the project. Prototype 1 presented in this thesis was build using only commercial sensors and is described in more detail below.

5.1.1 Sensor Selection

Sensors were selected aiming to target main combustion products and to capture other volatiles that may help to discriminate fire and nuisances. In smoldering fires, the main gas emissions released (target gases) are Carbon Monoxide (CO), Carbon Dioxide ($\mathrm{CO_2}$), Hydrogen ($\mathrm{H_2}$), Methane ($\mathrm{CH_4}$), Nitrogen Oxides (Nitrogen Dioxide ($\mathrm{NO_2}$), Nitrogen Oxide (NO)) and large variety of VOCs [167,168].

Once the targeted gases were selected, we made the analysis of the sensor type. A large variety of sensor technologies are able on the market. The selection of the sensors was based on the state of the art [169-172]. Table 8 summarizes the main sensor technologies used to detect the main hazardous gases emitted in a fire situation. MOX sensors are able to detect a large variety of toxic emissions. The main two advantages of gas sensors are their miniaturization and price. However, MOX sensors are especially sensitive to changes in environmental conditions. During a fire situation, temperature, humidity, and pressure suffer big changes, resulting in changes in the sensor response. NDIR technologies are one of the most robust to interferences and present a large lifetime. However, they are more expensive and usually the electronics needed to acquire the sensor response and to activate the infrared lamp are complex, resulting in high costs. Electrochemical cells (EC) are also a good option to detect oxide gases. However, like MOX sensors, EC sensors are largely influenced by environmental conditions. As mentioned in previous chapters all the problems related to gas sensors could be alleviated using pattern recognition techniques and good experimental design.

Table 8 Sensor Technologies Selection for the fire detection prototypes

	Sensor Technology			
Gas	**Electrochemical Cell**	**Photoionization Detector**	**Non-Dispersive Infrared**	**Metal Oxide**
Carbon Dioxide	✓		✓	
Carbon Monoxide	✓		✓	✓
Sulfur Dioxide	✓			✓
Nitrogen Dioxide	✓	✓		✓
Carbon Tetrachloride				
Cyanide				
Methane			✓	✓
VOCs				✓

Sensor selection is based mostly in the state of the art. However, as mentioned in 5.1, one of the objectives is to compare the prototype developed using commercial gases and the developed prototype during the SAFESENS project. Hence, *prototype 1* includes most of the sensor technologies used in *prototype 2*. Specifically, we selected MOX sensor, NDIR sensor for $\boldsymbol{CO_2}$, Electrochemical Sensor for $\boldsymbol{CO}$ and PID for VOCs.

5.1.2 System Description

A smart system (with the integration of signal processing and prediction algorithms) was built integrating different off-the-shelf gas sensors and fire prediction algorithms. All the sensors were selected according to those who are especially sensitive to fire combustion products. The prototype integrated the necessary signal conditioning circuits and provided the electrical conditions to operate all the sensors. Specifically, the customized sensor array includes an electrochemical gas sensor for CO detection, a photoionization detector (PID) for volatile organic compound detection, and a non-dispersive

IR (NDIR) sensor for CO_2detection, all manufactured by Alphasense company. Additionally, the prototype integrates eight metal oxide (MOX) sensors from AMS and we also included temperature and humidity sensors from Sensirion. Figure 32 shows the developed multi-sensor array.

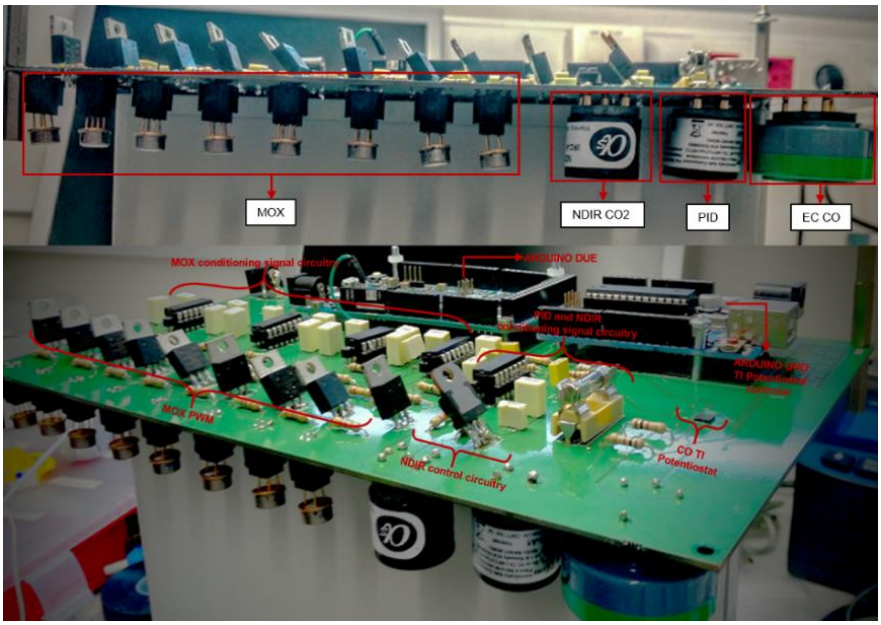

Figure 32 Picture of the developed multi-sensor array for reliable fire detection

The developed system combines three different blocks; i) the sensing block which includes the 12 gas sensors, ii) the acquisition of the signal block and iii) the data processing and the fire prediction stage.

Currently, one of the most used microcontrollers is from the ARM family. There is a large variety of ARM microcontrollers and are easily implemented in different applications. We selected an Arduino DUE board for the acquisition of the sensor responses. Arduino Due is based on a 32-bit ARM core. The main advantage of the board is the ease of programming through its USB port and the IDE (Arduino software). The signals are sampled at 10Hz. We selected the sampling frequency based on the principle that in intervals of 0.1 seconds the fire conditions would no change significantly. The ADC resolution of the Arduino DUE is 12 bit. The Arduino DUE ADC pins have an impedance of 100 MΩ. Finally, the data processing and the fire prediction stage was implemented in a CPU (host PC) that receives all the data directly from the

Arduino DUE. The combination of the three different blocks resulting in a smart fire detection system. The resulting block diagram of the complete system is shown below (Figure 33).

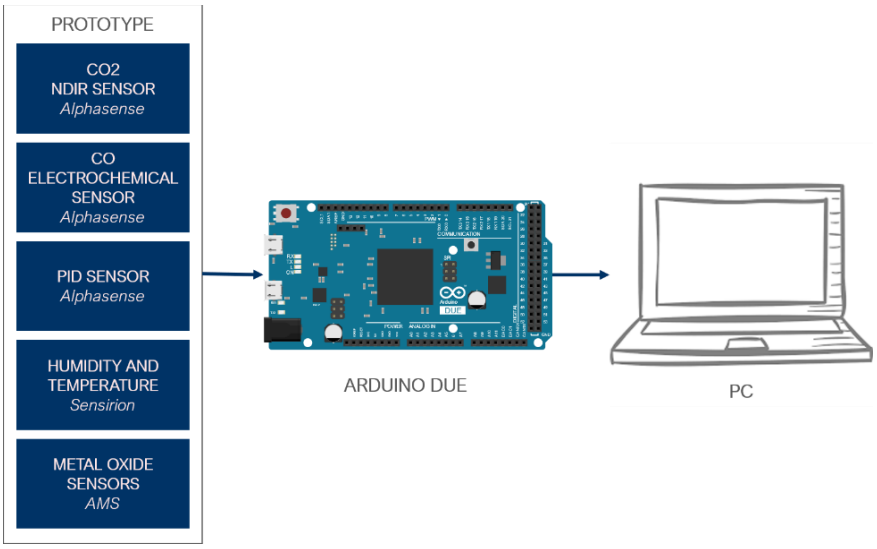

Figure 33 Block diagram of the smart chemical system. The system includes 3 stages, the sensing stage formed by 12 different sensors, the signal acquisition stages which incorporated the circuit signal conditioning and an Arduino due that was used to acquire all the signals and finally the data processing and the prediction of fire stage implemented in a PC.

In the following figure (Figure 34), the used Arduino pins for the readings of the sensors and those used to exiting their respective inputs. We use the 11 analog inputs to read the sensor responses; from A0 to A7 for the Sensor outputs of the Mox sensors, A8 is used for the PID sensor and A9 for the EC sensor and A10 to A11 for the Active and Reference output of the NDIR sensor respectively. Additionally, MOX sensors heater temperature was controlled with a PWM. The PWM was implemented using the Arduino platform. . On the other hand, all the sensors outputs were adapted from 5V to 3.3V range using a regulator voltage for that purpose. The selected regulator is from Texas instrument number LM117. The regulator allows the regulation of 5 volts to volts from 1.2 to 37V[173].

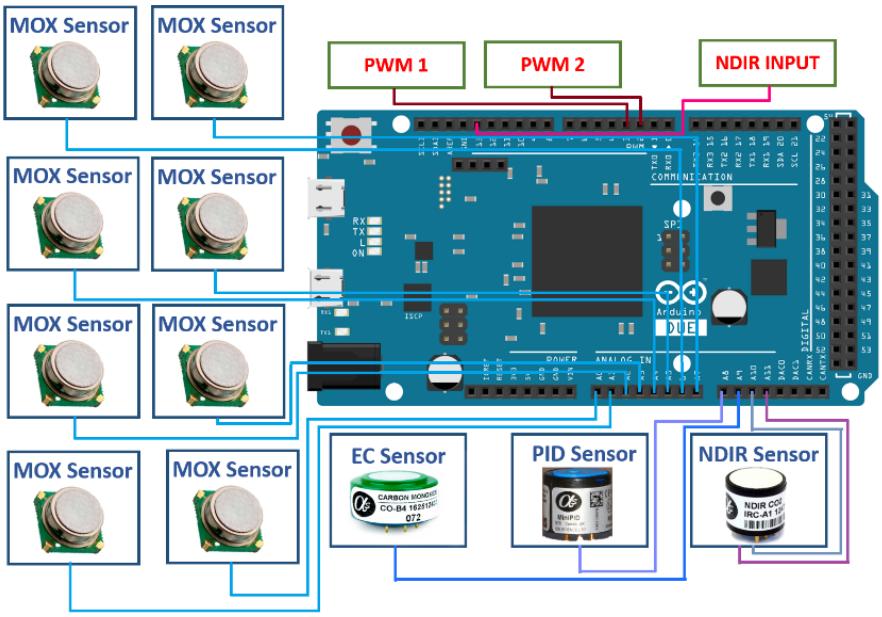

Figure 34 Distribution of the Arduino ports used to connect the gas sensors of the prototype 1.

Additionally, the system integrated a Graphical User Interface for the sensor signals visualization in real-time. The GUI is based on the aves python package [174]. The figure below shows the interface.

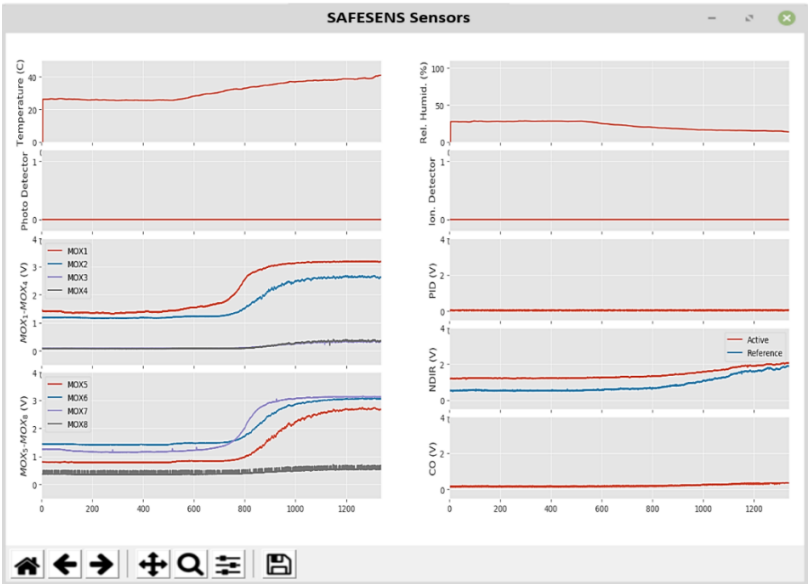

Figure 35 Graphical interface of the prototype 1

5.1.3 Sensor Description and Signal Conditioning Circuits

5.1.3.1 Metal oxide gas sensors

The prototypes developed in this dissertation have as one of their objectives the early detection of fires. For that it is important to include a sensor capable to react fast as possible and with enough sensitivity to low gas concentrations. Among the advantages offered by Metal Oxide sensors (MOX sensors) are their rapid response and rapid recovery time. These two features are of particular interest for fire detection.

However, MOX sensors have certain disadvantages. This type of sensor has a high cross-sensitivity with environmental conditions (as temperatures and humidity). Likewise, these sensors have poor selectivity. The use of pattern recognition techniques are required to counteract such drawbacks. MOX sensors technology is selected to be included in the prototypes. Table 9 summarizes the main advantages and disadvantages of MOX sensors [175].

Table 9 Advantages and disadvantages of the MOX sensors

Advantages	Disadvantages
✓ Low Cost ✓ Long Life Time ✓ Fast Response ✓ High Sensitivity ✓ Fast Recovery Time	- Cross sensitivity with environmental conditions - Poor precision - Sulphur Poisoning - High Power Consumption

The system included four types of MOX sensors: *AS-MLK* (targeted to volatile organic compounds), *AS-MLC* (targeted to Carbon Monoxide), *AS-MLX* (targeted to Methane), *AS-MLN* (targeted to Nitrogen Dioxide), all of them provided by AMS[143]. To add diversity to the system two copies of the same sensor were included operating at two different temperatures. The relations between the temperature and the applied voltage and current are shown in Table 10 and Figure 36. The colour indicates the grade of stress applied to the heater.

Table 10 Temperatures and Power of the Heater AMS sensor

P [*mW*]	T [°*C*]	R [*Ohm*]	P [*V*]	P [*mA*]
20	182	120	1.55	12.9
40	303	139	2.35	17.0
60	404	154	3.04	19.2
80	486	167	3.66	21.9
100	547	177	4.20	23.8

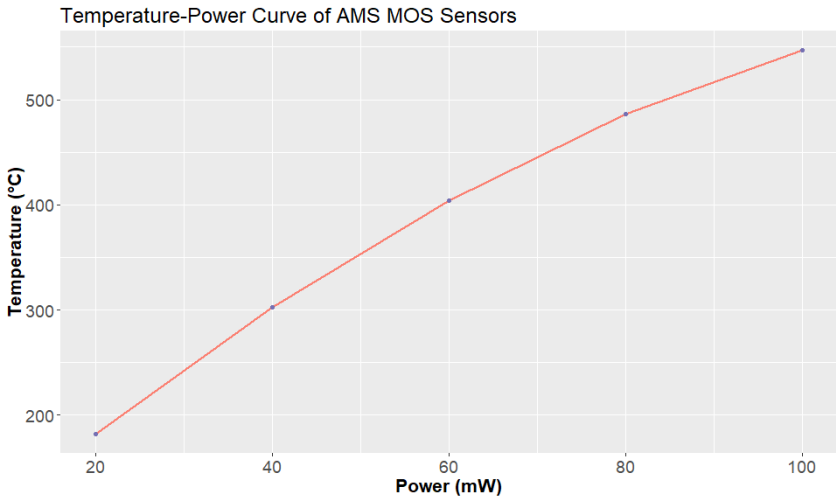

Figure 36 Temperature Profile of the MOX heater sensor

The sensor heater temperatures were controlled by means of a Pulse-Width Modulation (PWM) provided by the Arduino DUE platform. Arduino DUE platform was programmed to provide PWM of 1kHz of frequency. The induced temperatures are of 259ºC and 446°C which corresponds to a PWM duty cycle of 37% and 73% respectively. Hence, the MOX sensor array is composed of 8 sensing elements with different sensitivities in each channel.

The PWM controller circuit includes a current amplifier based on N-MOSFET (*BUK954- NXP Semiconductors*) transistor. In addition, to avoid the presence of the PWM in the output due to capacitive coupling in the sensor dielectric membrane, a low-pass filter was implemented at the output of the

MOX sensors. The filter was designed at 5Hz cut-off frequency at - 3dB. To couple the impedance between the filter and the sensor we used a voltage follower. The selected OpAmp is MCP6004 from Microchip. Both, BUK-NXP MOSFET and OpAmp MCP6004 are approved for the European Union to be used in fire detection instruments. MULTISIM software was used to design and simulate the circuit. The complete circuit design and the frequency analysis of the MOX filter sensors are shown in Figure 37.

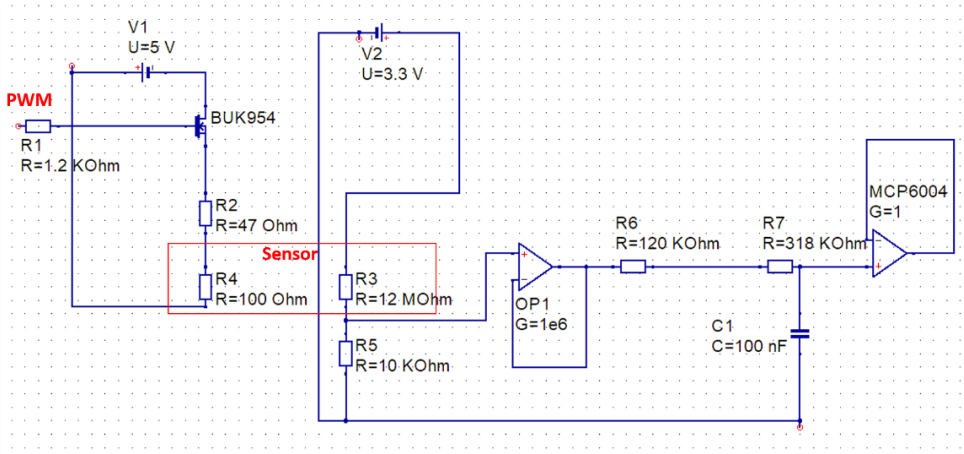

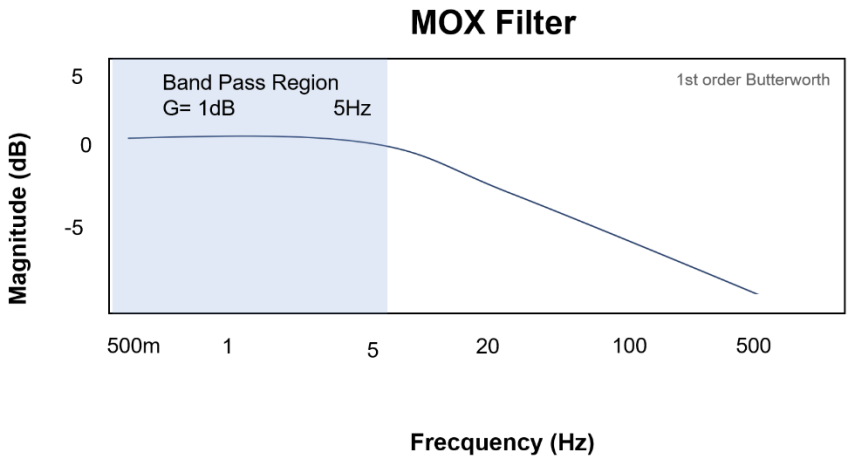

Figure 37 In the top MOX sensor control and conditioning circuit and in the bottom mox sensor filter analysis frequency analysis.

5.1.3.2 NDIR, Alphasense IRC-A1 Carbon Dioxide.

Carbon Dioxide (CO_2) is produced in most of the organic combustions. It is well known that long exposure to high concentrations of CO_2 is harmful to human health. Also, in buildings, a high concentration of CO_2 could be produced due to the high occupancy [176,177]. In fire detection with chemical sensors, it is important to record the behaviour of CO_2 across fire and non-fire scenarios, to capture the sensor signature and to classify it correctly.

For CO_2 detection, the most widely used technology is the Non-Dispersive Infrared Sensors (NDIR). This type of sensor is based on the detection (absorption) of a gas sensor in a specific wavelength [*principles of infrared technologies, Miller*]. This principle results in a highly selective and sensitive sensor. Moreover, NDIR sensors provide long-term stability in their measurements.

For the presented Ph.D. project, we chose a CO_2 NDIR sensor from Alphasense company. Specifically, we selected the NDIR – A1 [*178*]. The sensor is based on an infrared thermopile detector and it provides two outputs: the *active output* and the *reference output*. The reference output is used to correct changes in the intensity of the infrared light (e.g. due to lamp aging).

The changes of the IR source can produce cross-sensitivities and non-selectivity in the NDIR sensor. In order to improve the selectivity of the IR lamp, the IR source should be modulated. The alphasense NDIR sensor requires modulation of the infrared (IR) lamp at 3 Hz. Modulation of the source allows the modulation of the infrared radiation. The NDIR filter allows the passage of the desired wavelength only. In this way, the sensor will be selective only to the gas target, CO_2. The Arduino platform is used to provide the stimulus to the sensor. As in the MOX sensor circuit, an N-MOSFET (*BUK954*) transistor was used to amplify the current. Alphasense NDIR requires a minimal operation current of 300mA.

On the other hand, the amplitude of the NDIR output signals is in the range of several millivolts (from 40 - 100mV). Hence, it was necessary to add an amplification stage to take advantage of all the input voltage range of the Arduino inputs (from 0 to 3.3V). A bandpass resonator filter was used for that propose. The same filter design has been implemented on both output signals. In order to suppress the different frequencies from the central one, the selected topology of the filter is a Butterworth of second order. The central

frequency of the designed filter is 3Hz (which are the operating frequency of the sensor) and a gain of 36dB. The gain corresponds to amplify the signal from 100mV to 3.3V. The filter must operate with a unipolar voltage supply (from 0 to 5V). For that reason, a voltage reference of 1.2v was implemented. The reference voltage is obtained using a voltage regulator, specifically we use the LM117 regulator from Texas instruments. MULTISIM software was used for the design and implementation of the filters. The final design and the frequency analysis of the NDIR filters is shown in Figure 38.

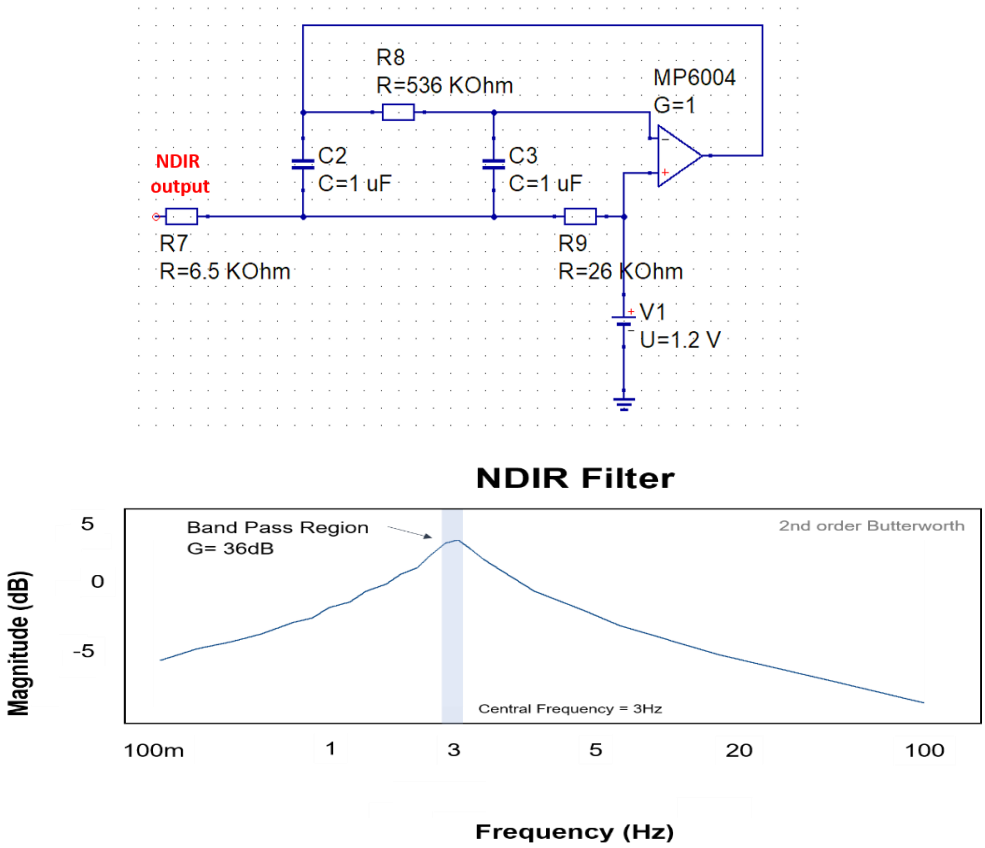

Figure 38 A bandpass filter was implemented as an amplified of the NDIR sensor outputs. In the top the complete sensor circuit and in the bottom the frequency analysis of the filter.

The design of the filter was made considering common commercially available components. However, commercial components with tolerances above 5 or 10% produced a shift in the centre frequency of the filter, causing an attenuation of the NDIR output. For this reason, we required precision components (tolerances below 1%).

However, even when the selected commercial devices have some low tolerances (around 0.005%), the deviation of the values may affect the correct behaviour of the filter (shift the central frequency and change filter gain). In order to study the impact of the tolerance devices a Monte Carlo analysis was performed. The MC analysis confirms that using resistors and capacitors with 0.1% and 10% tolerance respectively, the central frequency and the gain of the filter remains in the desired specifications for the considered signals. Figure 39 shows the MC analysis of the FTIR filter.

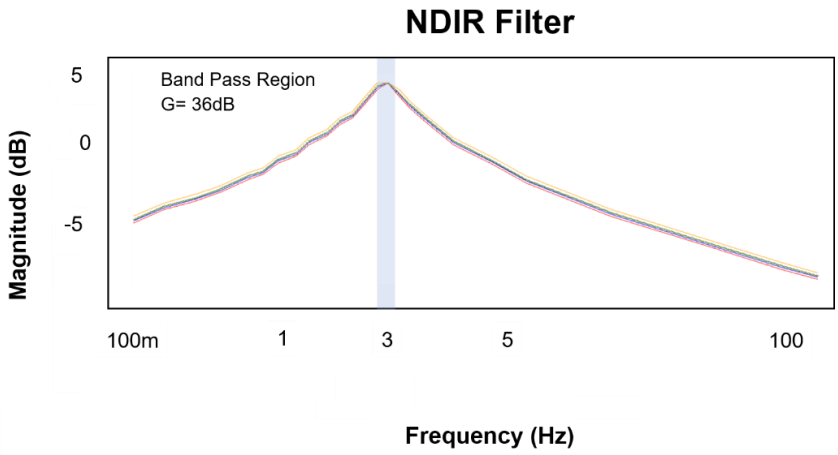

Figure 39 Montecarlo analysis of the NDIR filter.

5.1.3.3 CO-BF Electrochemical sensor.

The selected sensor of CO is an electrochemical sensor from Alphasense sensors. The Alphasense COB-F4 is an electrochemical sensor of 4 pins. 1 working electrode, 1 counter, and 2 reference pins. However, for this purpose, we use only 1 electrode of reference. The electrochemical sensor has a resolution of 500 nA/2 ppm of CO. Also, the sensor is capable to measure up

to 2000ppm of concentration. The electrochemical sensors require a potentiostat circuit to stabilize the potential between the counter and reference electrodes. The potentiostat is a control circuit that controls the potential, using the detection of the current of the counter electrode.

The potentiostat used for the EC-CO sensor was implemented using a Texas Instrument the LMP91000 Programmable Analog Front-End (AFE) potentiostat for Low-Power Chemical Sensing Applications [179] The Texas Instruments AFE can be used in electrochemical cells from 0.5 nA/ppm to 9500 nA/ppm ranges. The AFE uses a trans-impedance amplifier (TIA) configuration to convert the current generated by the EC-CO sensor into a voltage. This AFE can work in voltages from 2.1 to 5.25V. The gain of the TIA, and the variable bias is programmable using an I2C communication protocol. The TIA gain can be programmed from 2.75kΩ to 350kΩ. The I2C interface is controlled by the Arduino platform. The recommended parameters from alphasense were used in the EC-CO- BF4 sensor. Alphasense recommends 22K of TIA gain resistance and a max. bias voltage of 300mV. The complete connection scheme is shown in Figure 40.

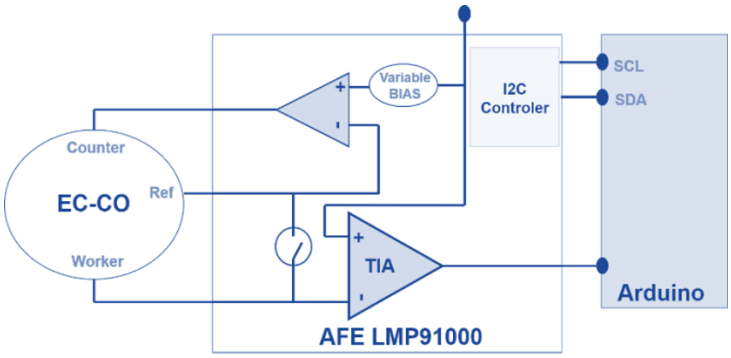

Figure 40 EC-CO circuit acquisition using the AFE LMP91000.

5.1.3.4 Photo Ionization Detector

A photoionization detector (PID) is an ion detector that uses ultraviolet (UV) light to excite the molecules, resulting in the temporary loss of electrons from the molecules and the formation of positively charged ions. The gas acquires the electric charge and produces an electric current.

The selected PID sensor is the Alphasense PID-A1 sensor. PID sensor includes a 10.6eV lamp. The sensor has a resolution <50 ppm with a 200ppm range and is sensitive to all VOCs ionizable at 10.6eV. The sensor can work with a voltage between 3 and 3.6 volts. The power consumption of the sensor is 85mW. The output of the sensor goes from a minimum of 50mV to the maximum voltage supply. For that reason, a barrier/segregation resistor was added at the output of the sensor and directly connected to the Arduino platform. According to the manufacturer [180] the input must include a fuse of 120mA to limit the input current. Figure 41 shows the schematic for the signal conditioning of the photo-ionization sensor.

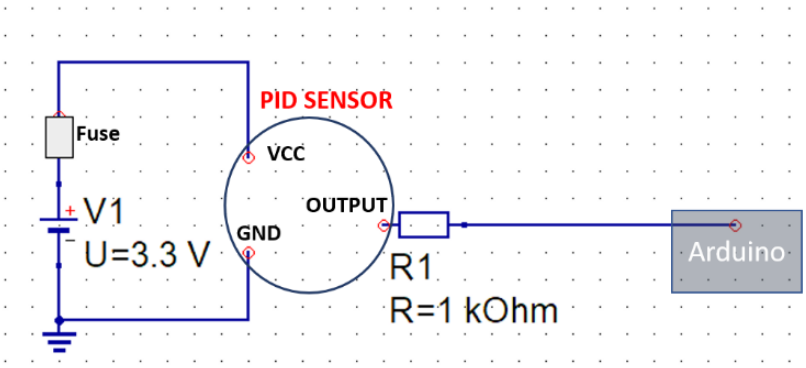

Figure 41 PID sensor signal electronic circuit

5.1.3.5 Temperature and Humidity sensor

Prototype 1 also includes a temperature and humidity sensor. The selected sensor is from Sensirion, number SH75. Sensor SH75 uses a I2C protocol to acquired the sensor readings. The communication of the sensor was made using the Arduino platform. The sensor requires a voltage supply of 3.3 V. Figure 42 Shows the connections of the sensor to the Arduino due platform.

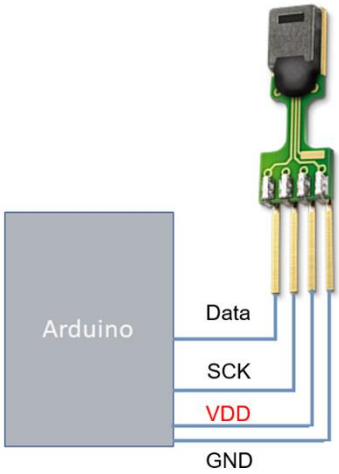

Figure 42 Sensirion SH75 Humidity and Temperature Sensor connections. Sensirion sensor is connected directly to the Arduino DUE platform. Picture from www.sensirion.com.

5.2 Prototype 2: SAFESENS Prototype

The SAFESENS project integrated sensor technologies in combination with intelligence sensor fusion algorithms which should address the disadvantages of state-of-the-art detection systems. Current fire detection systems could produce false alarms in the presence of dust and oils. Also current detectors are not able to produce a fire alarm in the first stage of a fire (before smoke). In summary, the SAFESENS fire detector should provide detection of fire before the visible smoke appears and should distinguish between the start of the fire and a nuisance situation.

The developed SAFESENS fire detector should enable early and accurate fire detection by measuring multiple gases (VOCs, CO, CO_2, and others). The target gases are mentioned in the introduction of this chapter.

BOSCH, IMEC, AMS sensors and NEO technologies contributed to the development of gas sensors that were included in the SAFESENS prototype. The SAFESENS prototype will be named ***prototype 2*** from now. The sensors included in this prototype are described in the following sections.

5.2.1 Sensor Selection

During the SAFESENS project, different gas sensors for the detection of the target gases were developed. The developed sensor technologies are a metal oxide, FET-based structures, optical and impedance-based on polymer layers and electrochemical. Specifically, the sensors and their developer are:

- Metal Oxide Sensors were designed for the low-temperature detection (low power consumption) of target gases: H_2, CH_4 and NH_3. MOX sensors were developed by AMS company.
- BOSCH company developed a Nobel metal layer for FET gas sensors. The FET sensor was developed for the detection of H_2
- IMEC developed low cost and robust electrochemical cells for the detection of CH_4. Electrochemical cells using an ionic liquid as electrolyte.
- Additionally, two standalone sensors were placed. A CO_2 sensor developed by Gas Sensing and a laser detector of CO from NEO monitors.

5.2.2 System Description

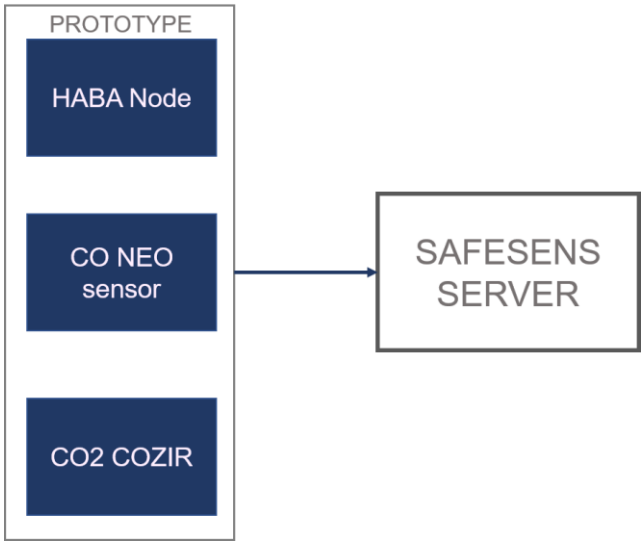

Figure 43 Block diagram of the prototype 2 system.

Prototype 2 integrates then, 4 MOX sensors from AMS, 1 CH_4 Electrochemical cell from IMEC, 1 H_2 FET sensor from BOSCH, CO_2 COZIR and 1 CO optical monitor from NEO. MOX sensors, IMEC cell, and BOSCH FET sensor are integrated into one system, called HABA node.

Figure 43 shows a diagram of the system. HABA node, NEO monitor and COZIR sensor send their measurements to the SAFESENS server using an ethernet connection.

The prototype 2 node was designed to fit into a standard MINIMAX fire detector housing (Figure 44). The prototype consists of two separated PCBs which can be stacked together to match the dimensions of the housing. On the lower PCB, there is microcontroller and electronics for converting the 12V input voltage to 9V used by the MOX sensors. The selected microcontroller is the ARM cortex m3. Microcontroller collects and sends trough Ethernet connection the measurements of the gas sensors. H_2-FET BOSCH sensor and 3.3V used by the rest of the sensors. The upper PCB is for hosting the sensors (Figure 45).

Figure 44 Prototype 2 was implemented in a conventional Minimax Housing. The figure shows the final view.

Figure 45 View of the electronic boards that integer the prototype 2

The *prototype 2* configuration includes four AMS-DE MOX sensors and an AMS-NL humidity/temperature sensor, a methane electrochemical cell provided by IMEC and also a Bosch H_2-FET sensor (Figure 46).

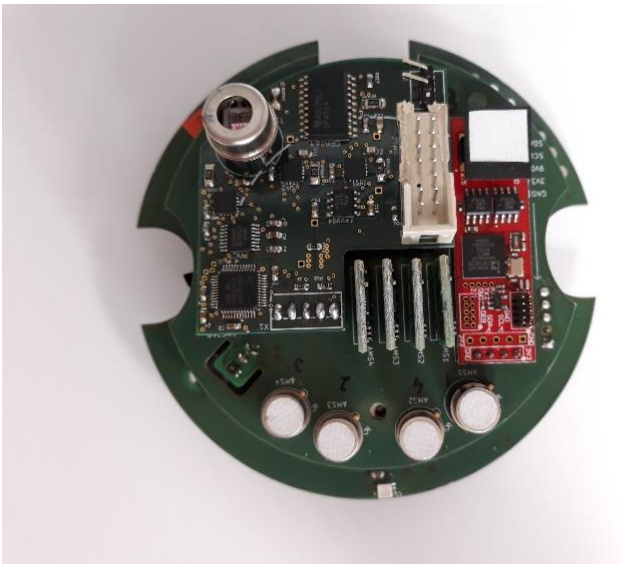

Figure 46 View of the sensors integrated into the Prototype 2

Additionally, to *prototype 2* and as a part of the same system, 2 stand-alone systems were connected and acquired measurements during all the measurement campaigns at the standard fire room. The stand-alone systems correspond to a CO_2 NDIR sensor from BOSCH and a CO detector based on diode laser spectroscopy. All the sensor readings from the *prototype 2* are collected by the microcontroller, that converts them into JSON format and sends the JSON encoded data to the SAFESENS server through an Ethernet connection. The stand-alone systems are connected via Ethernet to the server. The SAFESENS server collects the signals every second (1 Hz). The SAFESENS server also includes a GUI for the real-time visualization of the sensor signals from the *prototype 2* and the stand-alone systems, the interface shows the prediction of the fire detection algorithms.

5.2.3 Sensor Description and Signal Conditioning

5.2.3.1 Metal Oxide sensors

The *prototype 2* (SAFESENS prototype) used three types of the AMS MOX sensors used in the *prototype 1* (off-the-shelf sensors prototype), the sensors were operating at 375°C: MLK, MLN, and MLC. Also, during the SAFESENS project, AMS developed new sensors based on Nickel Oxide (NiO) active films. Recent works explore the sensitivity of layers based on NiO in fires. Studies show that NiO layers present more sensitivity at fire emissions, especially plastic emissions than layers based in SnO_2 [190]. The active films of NiO (with an optimized thickness of 20 / 30 nm) were deposited along with a shadow mask by reactive magnetron sputtering from a Ni target in a mixture of Ar and O_2(Figure 47). The heater current was applied directly from the microcontroller.

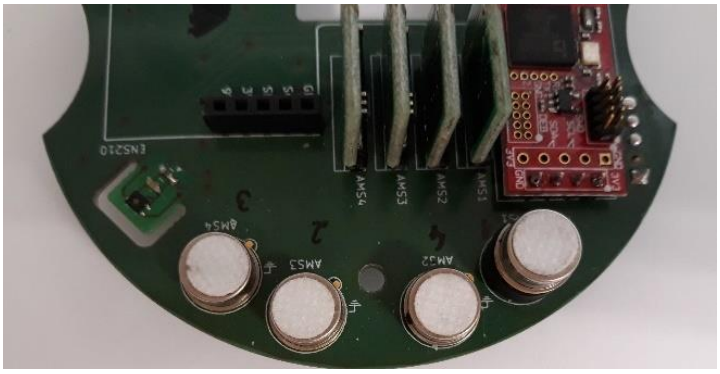

Figure 47 Metal Oxide sensors in the prototype 2

5.2.3.2 *Methane Electrochemical sensor*

A methane electrochemical sensor (EC-CH_4) developed by imec [191] was also included in the *prototype 2*. The electrochemical sensor consists of platinum electrodes on a silicon substrate. This substrate is over-molded at using an Advanced Packaging Modul (APC) from NXP to protect the areas of the sensor that should not be in contact with the measured gas and to provide solder pads onto which a connector is soldered. After packaging, the ionic liquid drops cast onto the electrodes, and finally, a polyester + PTFE laminate membrane is glued on top of the sensor to protect the sensor against particles [192]. The sensor has dimensions of 4cm x 2cm. The sensitivity of the sensor is 2nA/ppm with a 5% range.

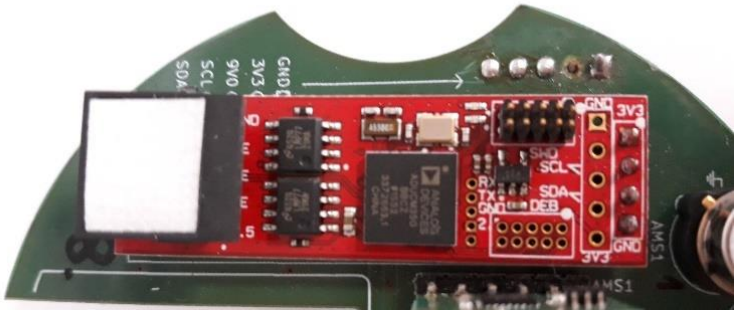

Figure 48 Electrochemical Sensor for $\boldsymbol{CH_4}$

The methane sensor includes a miniaturized potentiostat (50 x15 mm). The potentiostat current output is directly proportional to the concentration of the reactive gas in the air surrounding the sensor. The output of the EC-CH_4 imec sensor was stored by the SAFESENS server (Figure 48).

5.2.3.3 *Hydrogen Field Effect Transistor*

The hydrogen field-effect transistor (H_2-FET), included in the *prototype 2* comprises the electronics readout and control of the heater temperature (100°C). The sensing element is 2mm x 3mm large silicon chip, comprising two

FET structures and a Pt-meander for measuring the chip temperature. The FET is operated at a constant gate and source-drain voltage of 4V each. The source-drain current changes when $H_2$is present (Figure 49).

Figure 49 FET-$\boldsymbol{H_2}$ sensor developed by BOSCH for the prototype 2

5.2.3.4 Description of standalone sensors

Apart from prototype 2, two more instruments were placed during the measurement campaigns. The signals collected from those instruments were also used in the development of the fire detection algorithms.

$\mathrm{CO_2}$ *sensor:*

A $\mathrm{CO_2}$ node sensor used in the measurement campaigns is the smallest NDIR $\mathrm{CO_2}$ off the shelf sensor from Gas Sensing Sensors, $\mathrm{CO_2}$-COZIR sensor (Figure 50). At the beginning of 2017, the company GSS introduced its highly miniaturized CO_2sensor Cozir LPTM to the market which was chosen as a sensor component of the standalone SAFESENS CO_2node. CO_2– COZIR sensor was selected since is a low power consumption sensor and provides a

calibrated signal in ppm and their measurement is accurate [193]. COZIR sensor has a power consumption of only 3.5 mW with a range of detection from 0-5000 ppm and a working temperature of 70°C.

A Raspberry Pi 3B was used for the acquisition of the signals and the voltage input signals for the correct performance of the sensor. The LAN interface of the Raspberry Pi was used to transmit sensor data to the SAFESENS server using JSON messages. Configuration of the sensor node before and during measurements was done by WiFi communication.

Figure 50 GSS Cozir LPTM NDIR CO_2 sensor device

CO sensor:

A commercial sensor from partner NEO Monitors was used during the fire room tests. The sensor is based on traditional tuneable diode laser spectroscopy (TDLS). The setup consists of two separate units: a transmitter with a laser source and a receiver with a detector. The sensor was mounted in the ceiling of the fire room (Figure 51). The CO sensor sent via Modbus communication protocol (Ethernet cable). The CO concentration is computed directly in the sensor so that no post-processing is necessary. The CO sensor has a resolution of 10 ppb.

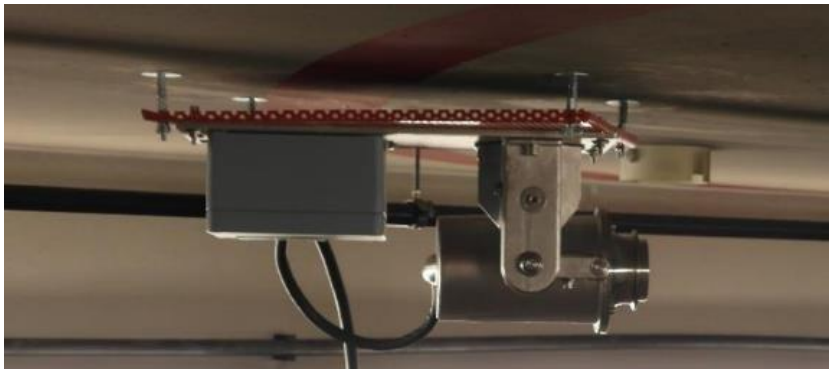

Figure 51 CO receiver from NEO

In summary, two fire detection prototypes were developed. Prototype 1 was built using commercial sensors and prototype 2 includes gas sensors developed during the European project SAFESENS. Specifically, prototype 1 includes: 1 PID, 1 NDIR CO_2 sensor, 1 EC-CO sensor, all from Alphasense and 4 MOX sensors from AMS. Prototype 2 includes FET- H_2 from BOSCH, an EC-CH_4 from IMEC, and 4 AMS sensors from AMS. Additionally, prototype *2* includes 2 stand-alone sensors, an NDIR- CO_2 sensor from gas sensing [x] and Laser detector of CO from NEO monitors. Both prototypes were used to develop fire algorithms. The developed algorithms are detailed in Chapter 6.

Chapter 6: Machine Learning Algorithms for Fire Detection

In chapter 1 of this thesis, some of the widest prediction algorithms for fire using gas sensors have been explored. However, one of the main drawbacks is the lack of experiments. There are not many databases that include gas sensor arrays measurements acquired over several months. The acquisition of datasets over time allows the assessment of prediction power algorithms.

On the other hand, as mentioned in Chapters 1 and 2, to build robust algorithms against nuisances the training set has to include nuisance measurements. Likewise, previous works were developed using databases that do not include nuisances or include a few cases.

In the presented dissertation we built a dataset that includes measurements for 3 different measurement campaigns along 5 months. During all the measurement campaigns several nuisance experiments were included. The datasets are described in Chapter 4.

In the presented Chapter 6, we present different methodologies that allow the construction of robust prediction algorithms. These algorithms can reject a large number of interferences. In addition, the predictive power of the algorithms has been tested using a database acquired along several months.

Early fire detection is one of the most important features in fire alarms. However, common technologies are based on the detection of smoke, heat or sparkles. In smoldering fires, fire or smoke appear in the latest stages of fire. The different methodologies developed in the presented Ph.D. project were built to predict fires when the fire emission is starting to emit.

Two different methodologies were developed to build fire algorithms. The first methodology is based on Partial Least Discriminant Analysis PLS-DA and the second one is based on Support Vector Machines SVM. The detailed description of the methodologies is presented in the following sections.

6.1 Methodology

In order to provide a reliable and early fire alarm we trained two sets of different fire prediction algorithms, one set used the sensor signals of *prototype 1* and the other set of algorithms was built using the signals acquired with the *prototype 2*. These prototypes are described in detail in Chapter 5.

Both prototypes were exposed during two different measurement campaigns performed in the Fire Room of Minimax Company [152]. The first one was performed in February 2017 and the second one in June 2017. The detailed description of the dataset is in chapter 3. There is an additional campaign performed in November 2016 in the fire room, however, only prototype 1 participated in that campaign. It is important to explore and compare different algorithms trained with both prototypes (prototype 1 and prototype 2), for that reason algorithms than appear in this chapter use only large-scale dataset 2 and large scale dataset 3.

The overall methodology to train and validates the fire alarm follows 5 different steps.

1. **Pre-processing:** Sensor signals were filtered in order to remove noise and in some cases compensate possible environmental influences.
2. **Baseline Correction:** The baseline of the signals was corrected in order to compensate for possible changes related to the remaining emissions from previous experiments.
3. **Labeling:** Fire/non-fire labels were set for each experiment.
4. **Model:** Fire prediction algorithms were built and assessed.
5. **Post-processing:** A simple post-processing step was applied in order to increase the reliability of the fire alarm.

Figure 52 shows the overall methodology to build the fire alarm algorithm.

Figure 52 Overall view of the methodology followed to build the fire predictors.

6.1.1 Signal Pre-processing and Feature Extraction

Before building the fire detection models the signals were pre-processed to compensate the environmental influence and correct for instrumental noise. *Prototype 1* acquired 10 samples per second. After signal visualization of *prototype 1,* we confirmed the need to filter the CO sensor (Electrochemical sensor from Alphasense) and the PID sensor signals (Alphasense) due to a significant level of noise. To do so, a median filter with a window size of 0.7 second and 0.5 seconds respectively was employed.

Optical NDIR-CO_2sensor (Alphasense) provides a reference signal that may help to compensate variations in the active signal due to changes in environmental conditions, (Temperature, Humidity…) lamp aging or dust accumulation. NDIR active signal was corrected as in Equation (3). The starting time of the day of measurements corresponds to $t0$ and the actual measurement time to t.

Equation 4

$$NDIR(t) = \frac{(Active(t) - Active(t0))}{Reference(t)}$$

In the case of the *prototype 2* only the sensor signals of CH_4 (IMEC), H_2(Bosch) sensors were filtered. Equally, a median filter of 3 seconds and 5 seconds were used respectively. Figure 53 shows in the left the raw signals (without preprocessing) of the CH_4, PID and H_2 sensors of one repetition of cable fire. In the right Figure 53, illustrate the signals after the application of a median filter.

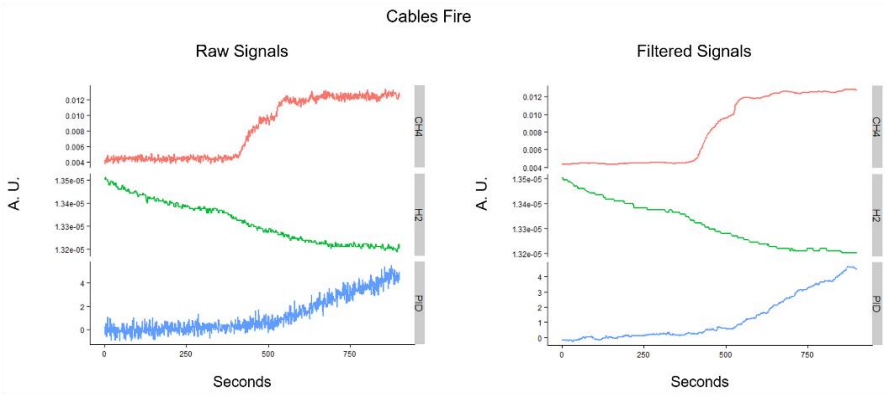

Figure 53 Raw signals (left) and filtered signals (right) of the $\boldsymbol{CH_4}$, $\boldsymbol{H_2}$ and $\boldsymbol{PID}$ sensors. The figure shows the sensor responses of one repetition of Cable fire.

After the preprocessing step a feature extraction step was also performed. All the captured voltage and resistance values from the MOX sensors of both prototypes were transformed into sensor conductance (*S*). Finally, for each signal of the *prototype 1*, the signals were cut into 1-second segments. The selected feature was the mean of the 10 data points included in each segment.

6.1.2 Baseline Correction

The fire room was ventilated after each fire or nuisance experiment. However, in some cases, volatiles from previous experiments remain in the fire room. Due to air contamination, the sensors changed the baseline during a day of experiments performed at the fire room. Also, environmental conditions such as temperature, could change the baseline of the sensors. In consequence, the discrimination power of the algorithms decreases. In this way a baseline correction step is a mandatory process prior to building the fire alarm algorithms. We captured the initial value of the sensors and we computed the rest of the baseline value and the actual value during an experiment.

6.1.3 Labelling

The experiment labels were set for every measurement (that corresponds to 1 second in the original raw signal) . It sets the label to *zero* "0" when there is a non-fire situation and turns to one "1" when the non-fire situation changes to a fire situation. The labels were set from visual inspection, the labels are "0" in nuisances experiments and during the first stage of fire experiments. Hence, the label only turned "1" when at least one of the sensors start to react due to the release of volatiles during the heating/ignition of the material. **Error! Reference source not found. Error! Reference source not found.** illustrates, in the left, the sensor responses of one repetition of TF3 fire experiment (cotton fire) and its label. The label during the TF3 experiment started in "0" for non-fire situations and turns to "1" once that at least one of the sensors starts to respond. On the right side of the Figure 54 **Error! Reference source not found.**sensor responses and the label of one repetition of window cleaning experiments are showed. During all the window cleaning experiment the label continues in "0" because is a non-fire situation (nuisance experiment).

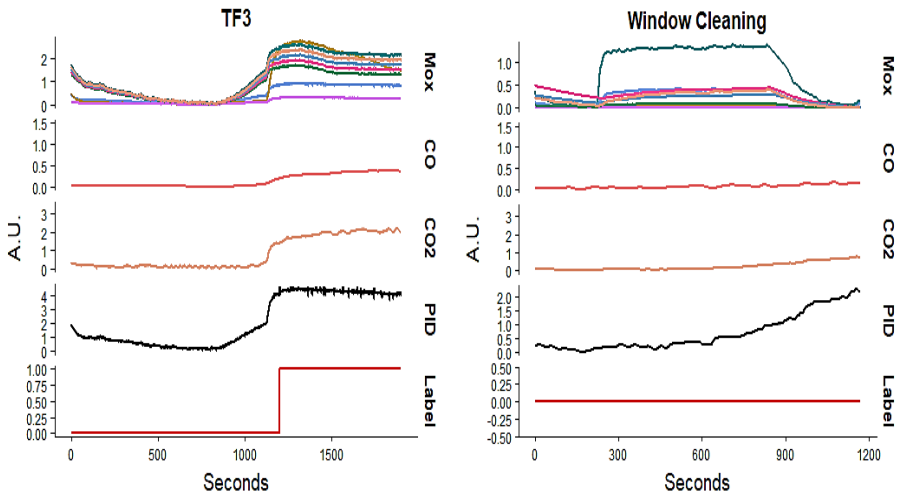

Figure 54 Labels of one repetition of TF3 Fire (left) and one repetition of Window Cleaning experiment (right).

6.1.4 Labelling

Prediction models may produce false alarms due to the sensitivity of the sensors to other non-fire volatiles (cross sensitivities). If the combined response of the sensors is too high, then the classifier could misclassify a nuisance experiment (set the fire alarm to 1).

In order to prevent a high number of false alarms we implemented three different post-processing time windows; 15, 30, 60 seconds. The classification model needs to output "fire alarm" for at least ***t*** seconds, where ***t*** is the length of the post-processing window. With this constraint, incidental and brief fire alarm predictions are not considered as such.

Figure 55 shows the prediction accuracy of the Boiling water and Electrical fire to conditional classifiers for the four tested durations of the windows, 1s, 15s, 30s, and 60s. The prediction without post-processing window is called "Actual". In boiling water experiment, the classification model set the alarm for 16 consecutive seconds. Hence, after post-processing step, the experiment is classified as fire for shorter time windows. However, for larger time windows (30s and 60s) the experiments are classified correctly as nuisance. Intuitively, the longer one waits to trigger the alarm, the less number of false-positives one obtains.

However, for some types of fires, at the end of the experiments, the concentration of the gases decreases or the released volatiles at this stage are different from the volatiles released at the first stage of the combustion. For that reason, some sensors start to recover during a fire event, this causes fire alarms change from 1 to 0 at the end of the experiment. In the case of the Electrical fire experiment shown in Figure 55, the classification model sets the output for 58 seconds. As a result, for time windows under 1 minute the experiment is classifier correctly but in time windows of more than 1 minute the experiment is classified as not fire, a false negative. In this example, the fire was too short to be identified as fire after post-processing step using a time window of 60s. Intuitively, the shorter the window is, the less number of false-negatives one obtains.

The optimal time window duration is one that presented the maximal True positives Rates (Fire experiments correctly predicted), at the expense of some false alarms, since the fire alarm should always trigger in case of fire. The time window length is selected in internal validation.

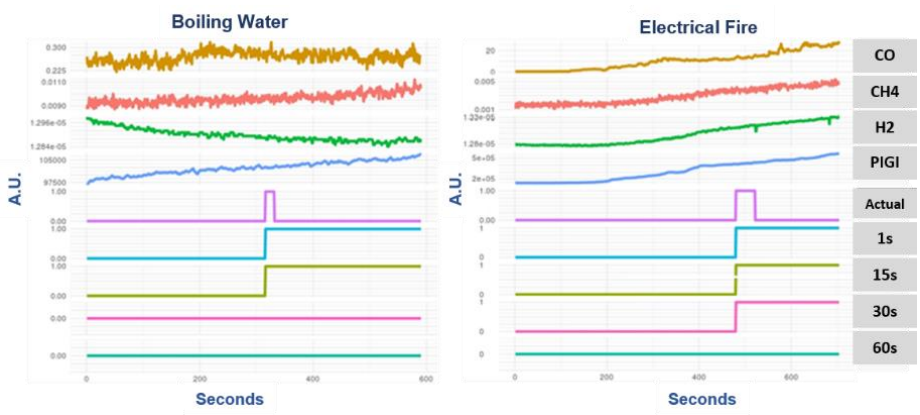

Figure 55 Performance of the post-processing time windows. The time windows are of 1s, 15s, the 30s, and 1 min

6.1.5 Prediction Model

In chapter 1, we described the performance of different algorithms for fire detection. In past works Neural Networks, Fuzzy Rules and the combination of PCA and kNN were applied to predict fire situations using gas sensor readings. However, these algorithms present some limitations for the early prediction of fires.

Use fuzzy logic can be a good option for several processes [194], however, their application in a process that required short response times is not recommended. Usually fuzzy logic requires an extensive number of rules to be accurate and this results in a retarded prediction [195]. In consequence, fuzzy rules may not provide a fast prediction of fire. On the other hand, Neural networks require a large number of data to provide a good prediction [196], increasing experimental costs. As mentioned in chapter 3 and 4, one of the main constraints for the developed fire algorithms is the small number of experiments. In consequence, neural networks are not a good solution for real-time fire detection. In previous works, PCA + kNN algorithms could provide a good classification between some fire scenarios. However, when the fire scenarios are too similar, the classification of the algorithm decreases [197].

In this dissertation, we explored the performance of two different supervised algorithms. Specifically, the models were based on *Partial Least Squares Discriminant Analysis (PLS-DA) and Support Vector Machines (SVM)*. PLS-DA can provide a good prediction of fire since it is an algorithm recommended to be used when the number of samples is low. PLS-DA provides a good and easy understanding of the behaviour of the different gas sensors for fire detection. PLS-DA is a good option for linear discrimination problems [197]. On the other hand, SVM provides a non-linear classification, also, the transformation to a high dimensional space allows a fast and accurate classification of new samples [198].

Two sets of models were built using *large scale dataset 2 (described in Chapter 3 Section 4.2)* as a training set. The first set of models were built using the signals acquired with the *prototype 1 (off-the-shelf-sensors)* and the second set of models were built using the experiments acquired with the *prototype 2 (SAFESENS project)*.

The dataset used as a training set, *large scale dataset 2* (acquired in February), includes 28 experiments (19 fires and 9 nuisances). The hyper-parameters of the prediction models (number of Latent Variables -LV- for PLS_DA and Cost and Gamma for SVM) were selected by means of internal cross-validation.

To perform internal validation, the training set was divided into 2 sets; Training and Test. 80% of the data was used to train the models and 20% to assess their performance to optimize the model. Specifically, we use 15 fires and 7 nuisance experiments for training and for test, 4 fire, and 2 nuisance experiments. Once the experiments were split, we built a model using the training data and assessed the model with the test data. Applying a random subsampling methodology, the procedure was repeated 28 times, such all the experiments were once in validation set. The metaparameters of the models (LV, gamma and costs) were selected as a function of the maximum accuracy of the classification rates sweeping the space. In order to improve the performance of the model, after the selection of the metaparameters different post-processing time windows were applied. The selected window corresponds to the one that predicts a high number of fires with a less number of false positives.

For External Validation we used the *large scale dataset 3* (June) that was acquired 6 months later than the *large scale dataset 2* (February) used to train the models. Using datasets acquired with 6 months of distance, it is possible to assess the prediction power of the models through time. Figure 56 shows the complete methodology to build and evaluate the models.

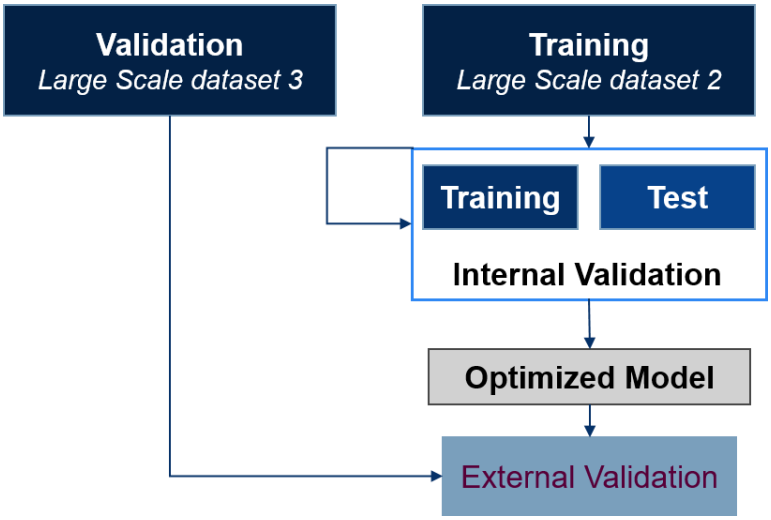

Figure 56 Overall construction and validation prediction model

6.2 Results

6.2.1 Data Exploration

To gain some insights on the variance distribution of the dataset and visualize the separability of fire and nuisance scenarios, we plotted all the experiments and repetitions in a reduced subspace using Principal Component Analysis (PCA). Figure 57 shows how all the scenarios are entangled. From Figure 57, one can confirm the complexity of the dataset. Fire and nuisance scenarios start in the same area (background-position) of the feature space, each scenario (nuisance or fire experiment) follows different trajectories reaching an area of the feature space depending on the gases and volatiles released during the fire or nuisance event. However, some experiments of nuisance and fires are close to each other in feature space. In addition, there

are experiments of fires (or nuisances) of the same type (repetitions) that presented different trajectories. However, the dynamics of fire is different from nuisance experiments. Usually nuisance volatiles are evaporated faster than fire emissions during a fire experiment. In consequence, we expected that the difference between nuisance and fire scenarios would be higher than the differences between repetitions.

For example, PVC and TF2 fires in both *prototype2* presented similar excursions but reach different regions of the sensor space. On the other hand, **Error! Reference source not found.** shows that fire and not fire samples appear entangled. However, scenario trajectories start from the same initial point and some of the fires travel to areas far away from the experiments' origin. This particular behavior is a good indicator of the possibility to discriminate fire situation from no fire situations.

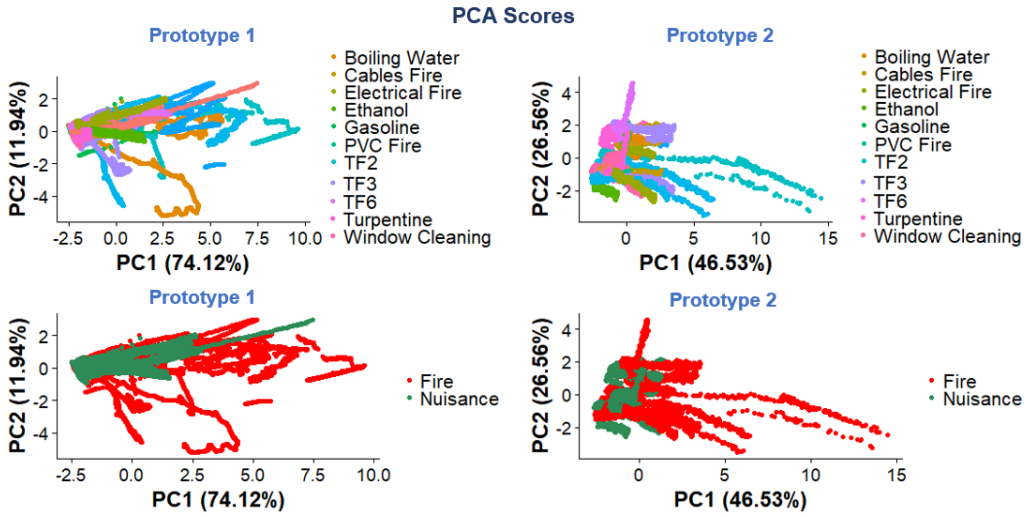

Figure 57 PCA Scores of the large scale dataset 2 acquired with prototype 1 (left) and prototype 2 (right). In the top, the scores are colored by experiment type and in the bottom with the labels of fire and nuisances.

6.2.2 Fire Detector Algorithm Based On PLS-DA

Partial Least Squares Discriminant Analysis (PLS-DA) is a statistical classifier that finds a linear regression by the projection of the labels and the variables in a new space. PLS-DA is used when the labels are binary and when there is multicollinearity between the values of X.

One of the main advantages of PLS-DA is that the relevant sources of data variability are modelled by the so-called Latent Variables (LVs), which are linear combinations of the original variables, and, consequently, it allows graphical visualization and easy understanding of the different data patterns and relations by LV scores and loadings. Loadings are the coefficients of variables in the linear combinations which determine the LVs and therefore they can be interpreted as the influence of each variable on each LV.

Two classifiers to discriminate fire from non-fire scenarios were built using PLS-DA. The **PLS-DA model 1** was trained with the acquired data from *prototype 1* which included: 8 MOX (AMS) sensors, CO_2-NDIR (Alphasense) sensor, EC-CO (Alphasense) sensor, and PID (Alphasense) sensor. The PLS-**DA model 2** used data acquired with the *prototype 2* that includes: PIGI, MLC, MLN and MLK MOX sensors, H_2 FET sensor (Bosch), EC-CH_4 sensor, CO (neo) and CO_2 NDIR sensor (Bosch).

After internal validation, the optimized resulting models are of 4 LV's with a post-processing time window of the 60s for the **PLS-DA model 1** and 6 LV's and time window of 30s for the **PLS-DA model 2**. After assessing the models using external validation, the models are able to discriminate most of the fires and reject nuisances. However, some of the nuisance experiments were predicted as fires at advanced stages of the experiment in both prototypes.

Figure 58 shows the PLS-DA scores of the resulting prediction models. All the experiments (both, fires and nuisances) start almost at the same point (origin or background) and travel from there to other regions of the feature space according to the evolution of the fire or the nuisance experiment. In **PLS-DA model 1**, most of the fires induce a big excursion in the space, and they travel far from the nuisance scenarios. However, there are fire experiments in which their trajectory is too close to the nuisance scenarios. This results in misclassification of the samples. In **PLS-DA model 2**, nuisances seem to have a shorter trajectory in the PLS-DA space than fires. However, the prediction of fire is much slower than the predictions of **PLS-DA model 1**.

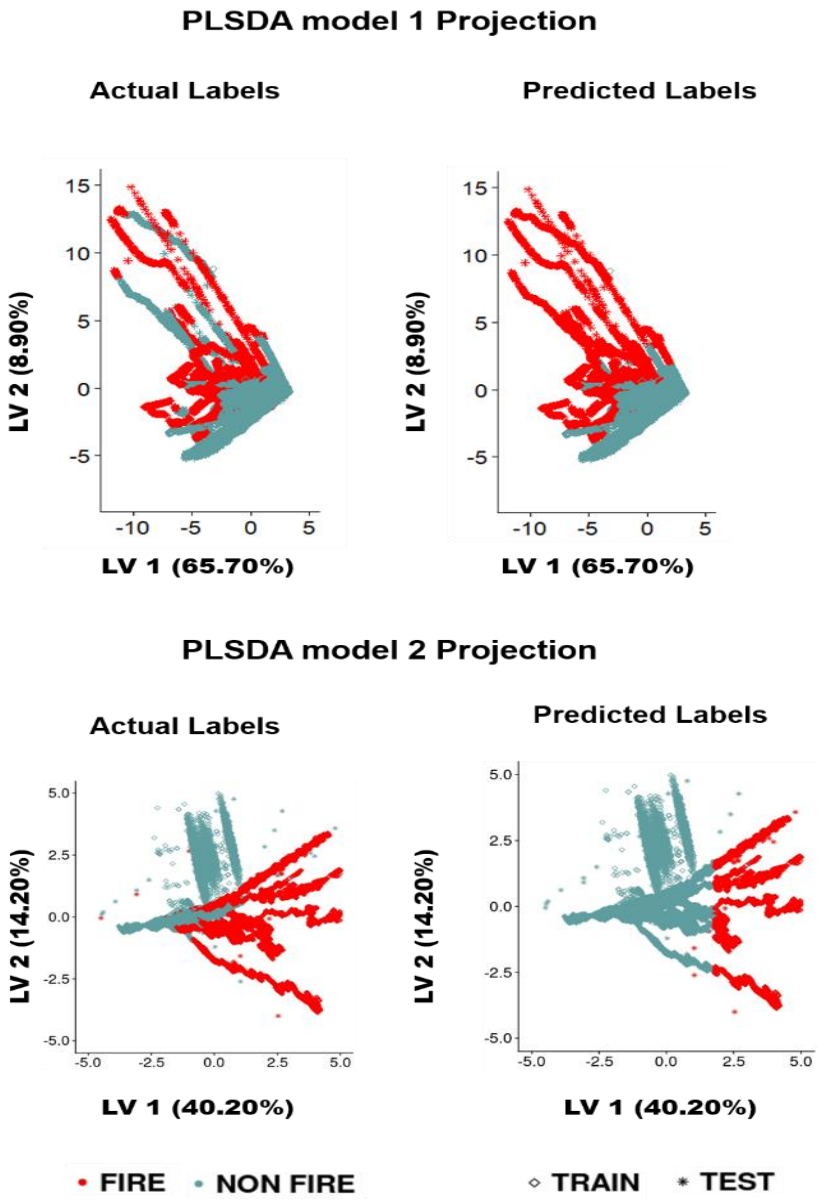

Figure 58 PLS-DA scores of the model trained with data acquired with prototype 1 (top) and with the dataset measured with prototype 2 (bottom). The training scores are colored by the actual labels and the scores of the test set are colored by the predicted labels.

6.2.2.1 Sensor importance in the PLS-DA algorithm

Variable Importance in the PLS projection (VIP) is the accumulated importance of each feature in each component. VIP accounts for the contribution of each feature according to the variance explained in each latent variable [198].

A Variable Importance of Projection (VIP) algorithm was applied in order to explore the contribution of each sensor to discriminate fires from nuisances. Figure 59 shows that in **PLS-DA model 1** the importance of the projection is spread among all the sensors, meaning that each sensor has a discriminant power and a contribution to the algorithm. However, there is a smooth hierarchy between the sensors. In the top of the **PLS-DA model 1** VIP, CO and CO_2 sensors are the most important for the classification followed by the MOX sensors and the PID . We expected that specific sensors would be the most important for discrimination since this type of sensors are targeted to combustion gases. Fire experiments need air (constant ventilation) to be performed and in consequence, produce huge quantities of CO and CO_2. In the case of MOX sensors, this type of sensors are faster than other sensors in the sensor array and also are sensitive to several volatiles released during the fire and non-fire events.

On **PLS-DA model 2** VIP, the principal contributors for the classification are also the specific sensors, CO, CH_4 and CO_2 sensor. Even if the H_2 sensor is a specific sensor, only TF3 and TF2 produce a huge quantity of H_2. In this projection, the CO_2 sensor has less importance than CO_2 sensor of prototype 1, this is because CO_2 COZIR sensor are much slower than CO_2 alphasense sensor (3s vs 40s) resulting in some experiments in a lack of response. Also, the accuracy of the sensors is different, *Prototype 2* CO_2 COZIR has an measurement error of 3% of the readings against 0.5% of error of the NDIR-CO_2. Here we can also observe that the PIGI sensor is one of the most important MOX sensors. After visual inspection this sensor is fast and with a clean signal, resulting in a very informative signal. The models from both prototypes show that the CO sensor and MOX sensors played an important role for fire and nuisance classification.

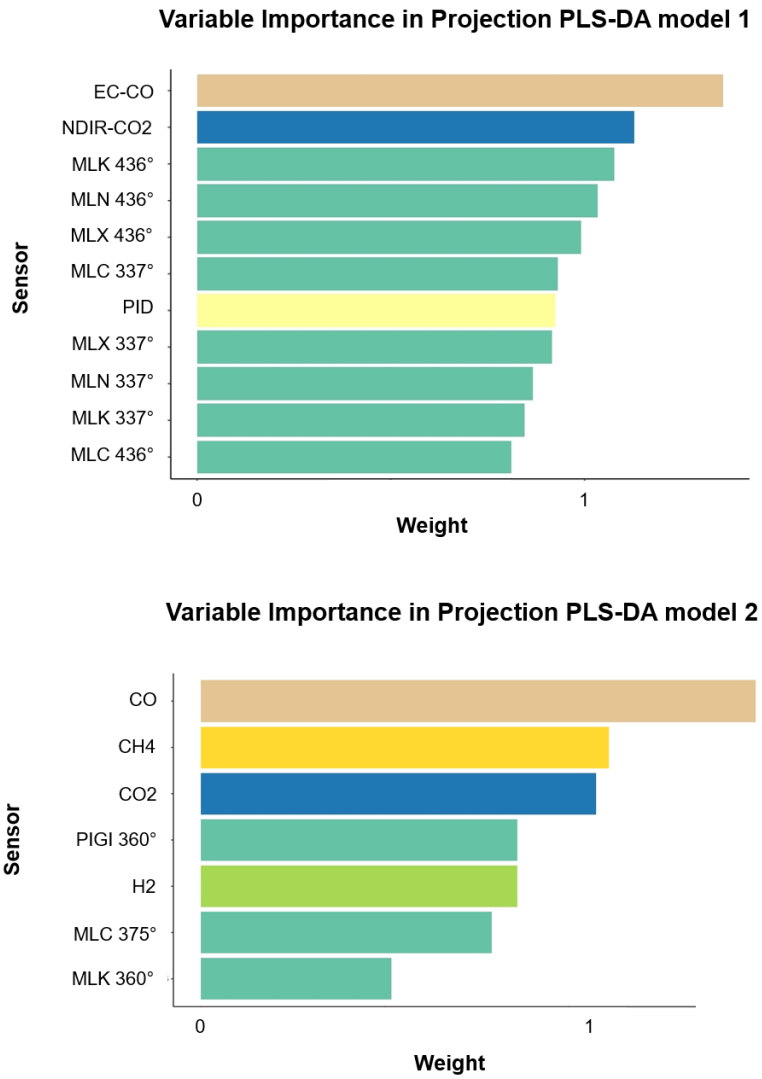

Figure 59 Variable Importance of Projection of the model trained with data acquired with prototype 1 (top) and model built with the prototype 2 datasets (bottom).

The biplot of the PLS-DA spaces is shown in Figure 60. Several conclusions can be drawn from the biplot visualization. In both, *prototype 1* and *prototype 2*, the initial part of electrical fires seems to be characterized by large emissions of VOCs and few combustion emissions like CO or CH_4. As mentioned in Chapter 1, acrolein and formaldehyde are two of the main VOCs emitted during a plastic fire. This is a major challenge to current hybrid alarms based on the combination of smoke detectors and CO sensors. Nevertheless,

this opens the opportunity to use MOX sensors for those sensors that produce VOCs or other combustion gases at early stage of fire.

In prototype 1, (Figure 60 top) one can conclude that CO_2 and CO have almost the same direction and contribute to the separation of fires with a large time of execution like TF2 and TF3. TF2 and TF3 produced huge amounts of CO an CO_2. In electrical fires, MOX sensors respond before CO or CO_2 sensors. MLC and MLN seem to be the principal contributors to the separation of this type of fire from the nuisances. On the other hand, MLX and MLK MOX sensors establish the direction of the nuisance scenarios.

Similarly, to *prototype 1*, in the biplot of the *prototype 2* specific sensors are in the direction of fire experiments. CO , CH_4, PIGI and MLC MOX sensor mark the direction of the fire experiments and seems to have a very different direction from the rest of the sensors, resulting, in the separation of fires from nuisances. This is expected since carbon monoxide and methane are combustion gases and do not appear in nuisance experiments. MLK MOX, H_2 and CO_2 sensors point to the direction of the nuisance experiments, meaning that those gases appear mainly in non-fire situations. PIGI sensor is orthogonal to CO_2 and MLC sensors. CO and CO_2 sensors have opposite directions. This means that in fires experiments the production of CO is anticorrelated with the production of CO_2. Usually, in fires, CO appears at the beginning of the experiment and, when the fire scenario is ventilated, the concentration of oxygen increases allowing for the transformation of CO into CO_2. Moreover, CO_2 sensor is crucial to discriminate nuisance experiments. Specifically, those performed with a person inside of the room, window cleaning, and air freshener.

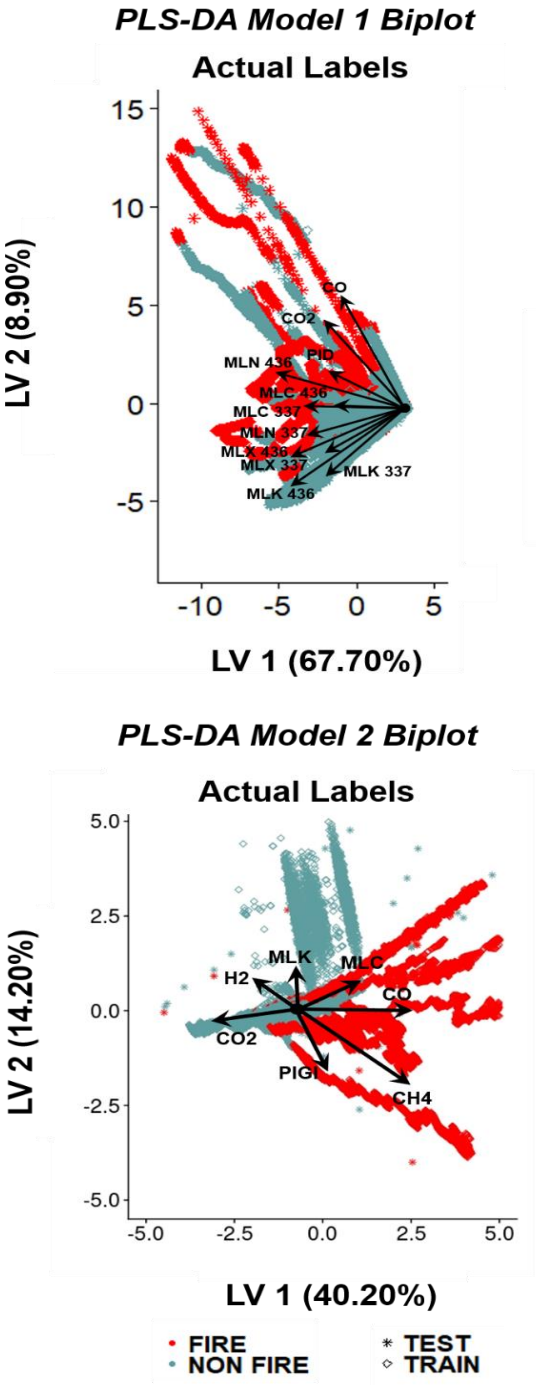

Figure 60 Biplot of the PLS-DA models. In top the PLS-DA scores of the prototype 1 and in bottom scores of the measurements acquired with prototype 2

6.2.2.2 Reliable and Early prediction of fire

To prevent false alarms and build robust prediction models a post-processing step based on time windows of 1s, 15s, the 30s and 60s was implemented. The size of the post-processing windows is selected during internal validation. Figure 61 shows the True Positives Rate (top) and the False Positives Rate (bottom) during internal validation, of both models when different time windows were applied. In this way, we can conclude that the longer one waits to trigger the alarm, the smaller number of false-positive one obtains. Nevertheless, large time windows increment the number of False Negatives. Due to the importance of triggering a fire alarm always that a fire has been produced, we chose time windows that provide a 100% of TPR and the least amount of false positives. Specifically, for **PLS-DA model 1** the optimal time window is of 60s and 30s for **PLS-DA model 2.**

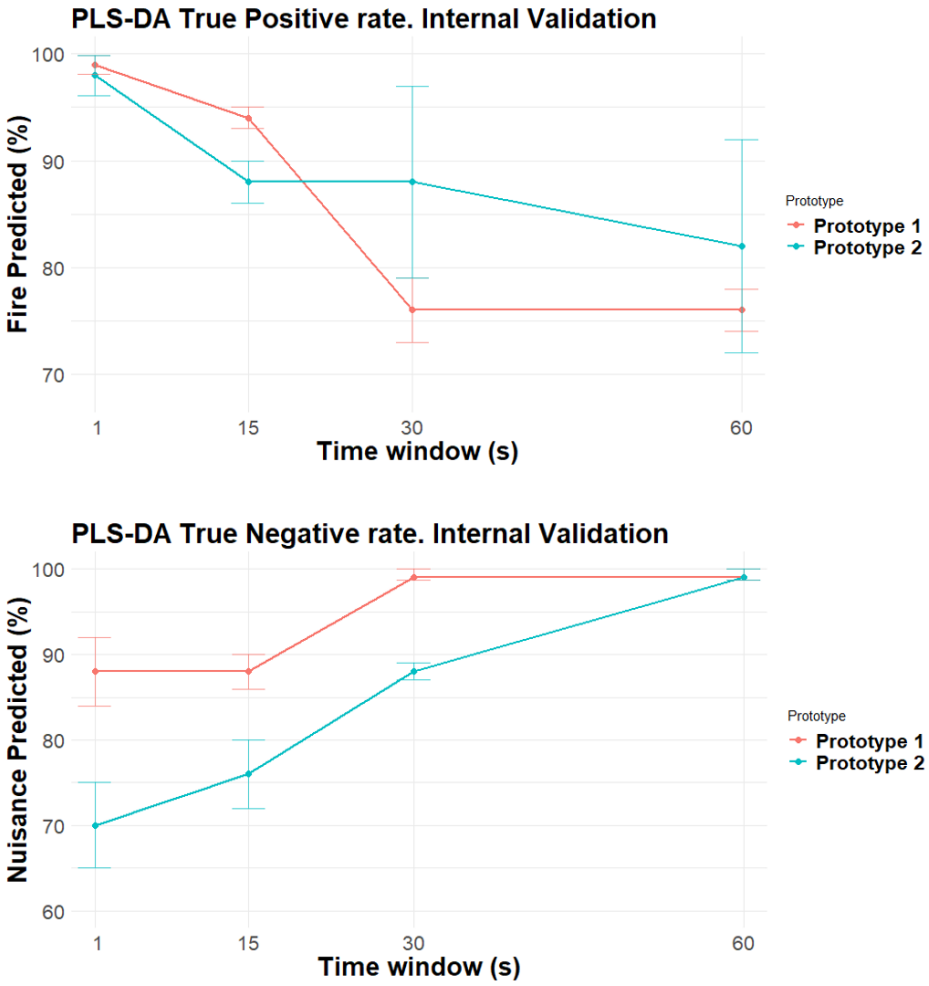

Figure 61 True Positive Rate (Top) and True Negative Rate (False) of the prediction models based on PLS-DA in function of the pre- processing time window during Internal Validation.

PLS-DA model 1 triggers the fire alarm for one repetition of Gasoline (for 28 seconds) and one repetition of Ethanol (for 17 seconds). Using the time window selected in the internal validation of 60s the repetitions of ethanol and gasoline were rejected (classified as non-fire scenarios). However, for some fire experiments **PLS-DA model 1** provides a fire alarm for a few seconds and then the alarms return to non-fire stage. This is the case of TF6 (after 28s) and one repetition of Electrical Fire (after 17s). Using the post-processing time window, **PLS-DA model 1** the true negatives rate goes from 82 to 100%. However, the true positives rate decreases from 100% to 86%.

PLS-DA model 2 gives a fire alarm for one repetition of Ethanol, for 50 seconds and for one repetition of Boling water for 8 seconds. In consequence, Ethanol is classified as fire for the selected time window of 30s. The rest of the nuisances were rejected. However, using a time window of 30s one repetition of TF3 (10s) and TF6 fire (18s) are classified as non-fire. As a result, with time windows of 30s the True Positive Rate is 80% and the True Negative Rate is 93%.

Time windows help to provide a reliable fire alarm. However, the use of time windows could increase the time response of the alarm. Figure 62 summarizes the fire alarm times of the prototype, Prototype 2 and the Minimax commercial smoke detector placed in the fire room during the experiments. The commercial detector of minimax provides three fire alarms, each with a different sensitivity. A medium level of sensitivity of the smoke detector was selected to be compared with our system. Also, the commercial smoke detector of minimax did not present any false alarm. However, the TF6 fire did not trigger the fire alarm.

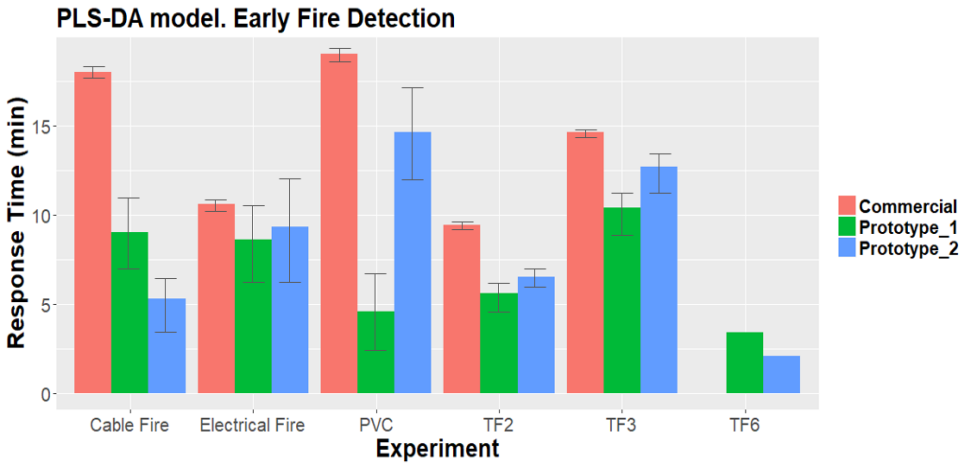

Figure 62 Experiment Response times of the fire alarms based on PLS-DA and commercial fire detector.

From Figure 62 we can conclude that PLS-DA models are faster than the commercial fire detector. Nevertheless, the time responses of PLS-DA models have more variability than time responses of the commercial detector. PLS-DA models time response variance is small in standard fires. In electrical fire, TF3, PVC, and TF3, prototype 1 is faster than prototype 2. However, in Cables fire and TF6 experiment *prototype 1* responds after *prototype 2*. Since commercial fire detectors are based on smoke and particle detection, present less false alarms than fire detectors based on gas sensors using PLS-DA algorithms. however, the PLS-DA algorithm provides faster fire detection than conventional fire detectors. Also, fire detectors based on gas sensors and PLS-DA algorithms are capable to detect all the fires instead of on commercial detectors which are unable to predict those fires that not produce smoke or particles.

6.2.3 Fire Detector Algorithm Based On SVM

Support Vector Machine (SVM) is a supervised classifier. The SVM projects input data in a higher-dimensional space and provides the maximum separation between classes using a hyperplane which is defined with a subset of training samples ("support vectors"). SVM is a non-probabilistic binary linear classifier but can be extended using the so-called kernel trick to also perform nonlinear classifications[199]. The selected kernel for this fire predictor is a radial basis, a nonlinear SVM.

The hyperparameters of the SVM are optimized during internal validation. We explore a grid of combinations of gamma and Cost. Gama values go from 0.01 to 0.1 and we tested Cost values from 1000 to 10000. After internal validation the resulted optimized **SVM model 1** has a cost of 100 and a gamma of 0.5 and a time window of 30s. In the case of **SVM model 2** the optimized model is a cost of 7000 and gamma of 0.02 and the time window is of 30s. Large scale dataset 3 is used as external validation to assess the performance of the model to predict fires and reject nuisances.

6.2.3.1 *Reliable and Early prediction of fire*

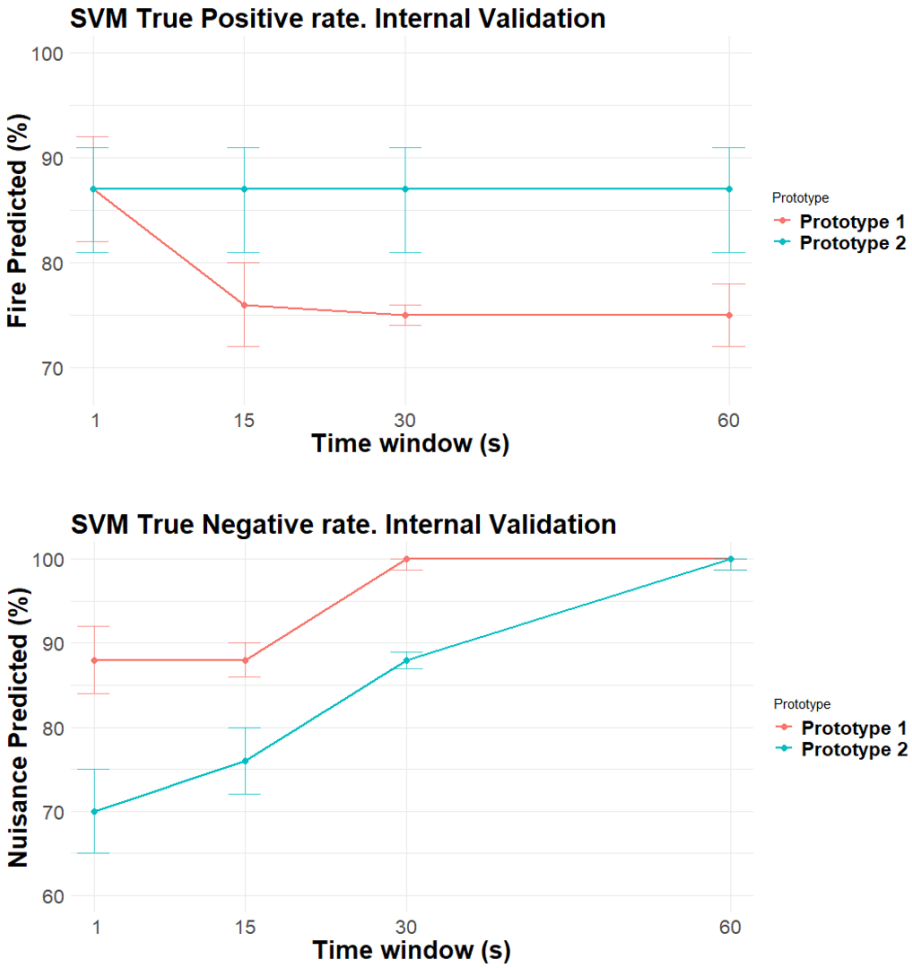

Figure 63 True Positive Rate (Top) and True Negative Rate (False) of the prediction models based on SVM in the function of the pre-processing time window.

The optimized post-processing time window for the SVM Model was selected during internal validation. Figure 63 summarized the percentage of false positives rates and true positives rates for both prototypes during internal validation.

For **SVM model 1,** The size of time windows does not influence the number of fires correctly classified. For large time windows, the number of nuisance situations correctly predicted increases. The selection of a large time

window increases the time response. For SVM-model 1 the optimal time window is of 30 seconds with 73% of true positives and 94% of True Negatives.

The optimal time window for **SVM model 1** is 1 second. Even when larger time windows increase the number of false-positive rejected, the number of fires correctly predicted decreases in time windows higher than 1 second. In fire detection it is preferable to have a high number of fire correctly predicted in order to protect the building occupants.

Using the post-processing time windows of 30 seconds for **SVM model 1, two** nuisances were misclassified. Specifically, the model set the fire alarm in one repetition of ethanol for 18 seconds and one repetition of turpentine for 140 seconds. Using a time window of 30 seconds ethanol experiment can be rejected. However, for a time window of 30s one repetition of turpentine experiment is classified as fire. On the other hand, the fire alarm did not detect one repetition of electrical fire and one repetition of TF2. Also, **SVM model 1** triggers the alarm for a few seconds for some fire experiments. This is the case of one repetition of TF2 in 26 seconds and one repetition of TF3 in 8 seconds. In consequence, for a time windows 30 seconds the True Positive Rate of the alarm decreases from 86% to 73%.

For the model trained with data from the *prototype 2*, **SVM model 2**, triggers the fire alarm for two repetitions of Ethanol in 51 and 53 seconds and two of Air freshener during 17 and 26 seconds. Using a time window of 1 second, **SVM model 2** misclassify these two nuisances' experiments. Also, one repetition of TF6 as non-fire during all the experiment. In consequence, the maximum True Positives Rate is 88% and the True Negative Rate is 76 %.

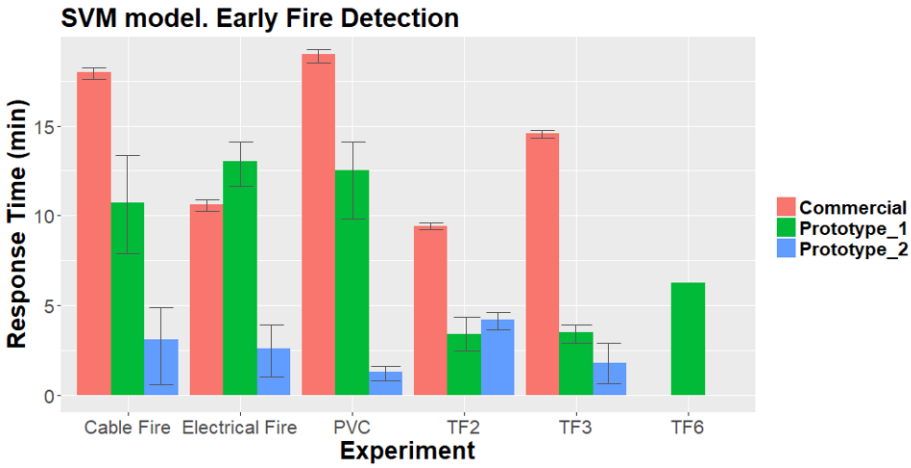

Figure 64 Experiment Response times of the fire alarms based on SVM and commercial fire detector.

The time responses of the experiments are shown in Figure 64. Equally with models based on PLS-DA, models based on SVM are faster than the commercial detector but with a higher variance of the time responses. However, in this case *prototype 2* is much faster than *prototype 1*. However, TF6 is only detected with the SVM model trained with signals from prototype 1. ***SVM model 1*** predicts only 76% of the fires, using a time window of 30 seconds. Even when the number of True negatives correctly predicted is high, the number of fires not predicted can risk building occupants' life. On the other hand, ***SVM model 2*** is faster but with a high number of false positives. However, ***SVM model 2*** performance is preferable over the SVM model 1 performance.

6.3 Comparison

Prediction models based on SVM and PLS-DA were built to classify different fire scenarios and discriminate non-fire scenarios (nuisance experiments) that may produce deceptive alarms. To increase the reliability of the prediction, post-processing time windows were implemented.

After internal cross-validation for PLS-DA model 1 the optimized time window is 60s and for PLS-DA model 2 we selected a time window of 30s. In the case of models based on SVM, SVM model 1 and SVM model 2, the selected time windows are 30s for both.

Figure 64 shows the performance of the four different models and commercial detector in a ROC space. Based on the figure fire detectors based on PLS-DA are the best option, for the detection of these types of fires and the rejection of those particular nuisances. Moreover, the algorithm provides a simpler interpretation of the results.

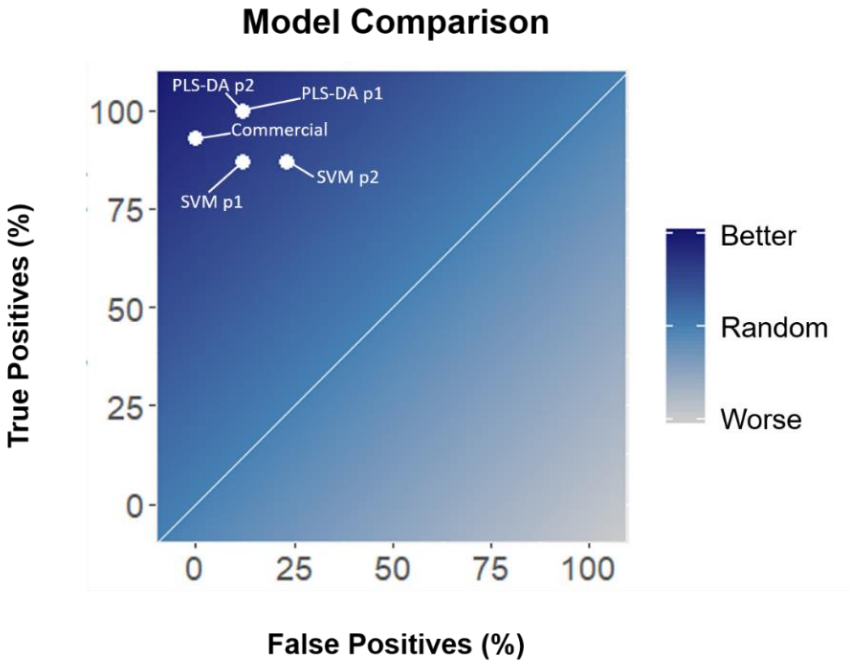

Figure 65 Models and commercial detector performance in function of the true positives and false positives (ROC space).

6.4 Conclusions

The results obtained from the fire detectors algorithms might be considered satisfactory, showing better performance than the state-of-the-art and with a large margin for improvements.

Fire detection in the first early stage of a fire is possible even without smoke released by a smoldering material. For this purpose, a heterogeneous gas sensor array was developed and tested in a fire room that matched the standards in the field of fire prevention. Two different sensor arrays integrated fire detection algorithms based on PLS-DA and SVM.

Due to the limited available data set to train the models several false alarms were produced. However, the implementation of post-processing time windows dealt with that problem and provided a more reliable fire prediction.

From the two different algorithms: PLS-DA based-models are more robust with no false negatives in prototype 1 and small number of false alarms. PLS-DA model achieves 88% and 100% of nuisance rejects in prototype 1 and prototype 2 respectively. On the other hand, SVM models show a very fast fire detection in the performed experiments but with more complex interpretation of the results and computational costs during development. Also, SVM misclassifies some fires in both prototypes. This could result in an unreliable fire alarm. However, the performance of both algorithms is still to be explored under a larger dataset to reduce the false alarm rate and to lower the fire alarm times.

The presented fire detectors were evaluated and tested with fire and nuisance tests that are derived from real demo cases. The fire risk in these cases is a slow starting smoldering fire, for example by overheating cables or faulty electronics. In these situations, the early fire stage can remain several hours with comparable low fire damage.

Chapter 7: Reducing Experimental Costs by Using Small Scale Setups

7.1 Classification Models Methodology

Fire detectors used to detect fires in buildings or industries should be tested according to the fire standards EN54. As mentioned in Chapter 1 and Chapter 3, fire standards establish that all the tests to assess the performance of fire detectors should be performed in dedicated rooms- Fire rooms-. The availability of fire rooms is limited and expensive. Moreover, a standard fire room test can take around 1 hour.

In chapter 3, we mentioned that robust calibration models include a high amount of fire and nuisance experiments. The gas sensor systems trained with a limited amount of samples result in less general and less robust algorithms. To build useful fire detection algorithms it is needed to perform measurement campaigns with a duration of several months and hours. This resulting in expensive experiment campaigns.

In this way, our hypothesis is that those classification models could be improved using datasets acquired in a small scale setup. It is well known that combining data from different sources can improve the performance of the algorithms since the information provided by the new fused dataset is improved. Data improvement means less expensive dataset and with more relevant information [199].

In order to prove this hypothesis, we built three different models. The first model, ***fire room model***, was trained using data from the *large-scale dataset 1*, the second model, ***small-scale model***, used as training set data from the *small-scale dataset* and finally the model three, ***data fusion model***, used the combination of the *large-scale dataset 1* and the *small-scale dataset* as a training set. All the datasets were acquired using *prototype 1.* Prototype 1 includes off the shelf sensors and is described in chapter 5. In all the models, the validation set is the large-scale dataset 2. Figure 66 shows the dataset used as training and validation in every model.

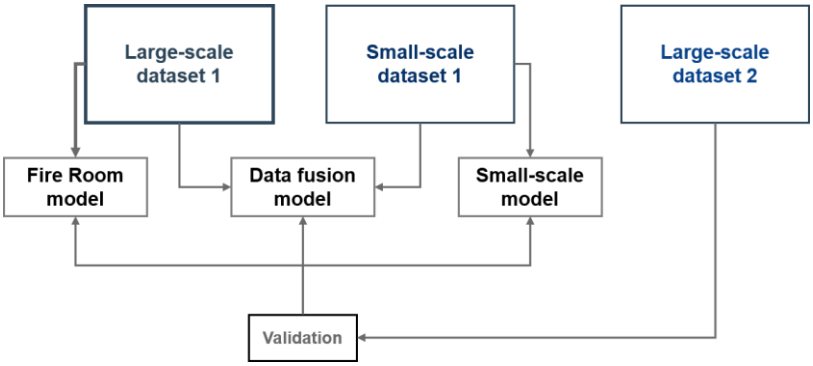

Figure 66 Description of the datasets using to train and to validate the models.

The prediction models are based on Partial Least Squares Discriminant Analysis (PLS-DA). Internal validation was used to optimize the complexity of the PLS-DA model (number of Latent Variables). The dataset used to train the model is split into two sets; Internal Training and Internal Validation. For Internal Validation we used the "leave one experiment out" technique, where each complete experiment of fire and nuisance is used as validation once, while the rest of the samples are used to train the predictive models with different number of LV. An external validation was used to assess the performance of the classifier. To test the statistical significance of the results, we used a permutation test where the models were trained with permuted labels 2000 times. We tested that the accuracy does not belong to the null hypothesis, with a 95% confidence.

7.2 Results

7.2.1 Sensor Signals

Sensor signals were continuously acquired for fire and nuisance scenarios, both in the large-scale setup and in the small-scale setup. Visual inspection of the sensor signals confirms that gas sensors respond to released volatiles during combustion and to volatiles present in many nuisances in both scenarios, small and large. However, classification models trained with data acquired in small-scale setups are not easily transferred to data acquired in large scale setups due to the differences in amplitude and dynamics of the sensor signals. Figure 67 shows a wood fire experiment (TF2) in the different setups, in the right side the sensor array signals acquired in the small-scale setup and in the left the signals acquired in the large-scale setup.

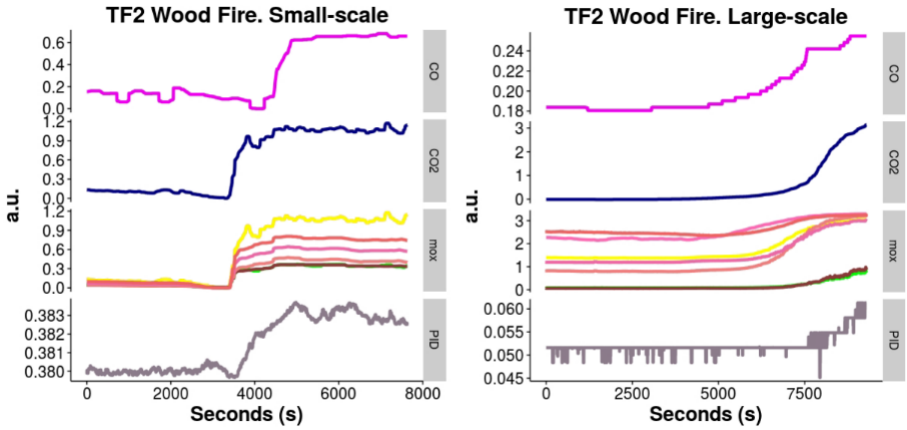

Figure 67 Sensor signals of the TF2 wood fire, on the right the experiment was performed in the small scale setup and in the right the fire test was performed at the standard fire room.

To gain some insights on the variance of the dataset and visualize the reparability of fire and nuisance scenarios, we plotted all the experiments of the large-scale dataset 2 (validation set) and repetitions in a reduced space using Principal Component Analysis (PCA). The Figure 68 shows the PCA of the three different datasets: *large scale dataset 1*, *small scale dataset* and *large scale dataset 2*. In the top, the PCA is colored according to the type of situation, fire or nuisance. On the bottom of the figure, the data is colored according to the dataset. From Figure 68 one can confirm the complexity of the dataset as data (fire and nuisances) appears entangled. However, all the datasets' executions start at the same background and go to different spaces of the PCA projection according to the emitted gases.

Fire prediction algorithms should be trained with informative datasets in order to provide a robust classification algorithm. Fire prediction algorithms should provide good discrimination between fire and no fire experiments. Moreover, the data fusion algorithms may provide a good prediction for different fire scenarios and along different months.

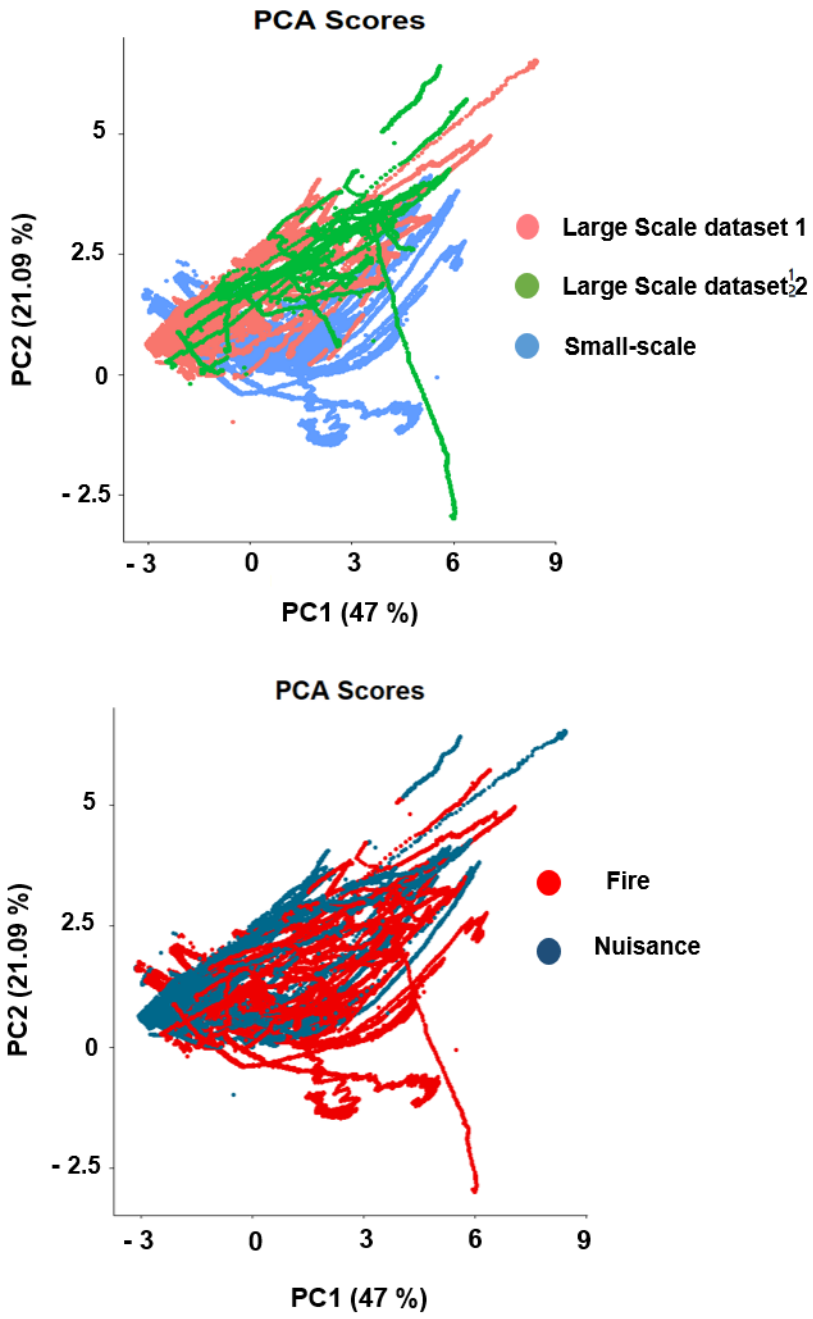

Figure 68 PCA scores of the large scale dataset 2 (validation set). On the left the scores are colored by type of experiment and on the right the experiments are colored by the actual labels of fire and non-fire.

7.2.2 Classification Models Performance

Sensor signals were used to train the different classification models based on PLS-DA that outputs continuously fire or non-fire situations. In order to compare the performance of the different prediction models (Fire Room Model, Small Scale Model, and Data Fusion Model) the validation set corresponds in all the cases to the *large-scale dataset 2* acquired at the standard fire room in February of 2017. There are several months between the acquisitions of the different data sets. Fire Room models were trained with data acquired in the fire room in February of 2017 and the small-scale model was trained using data from the small chamber in March of 2016. On the other hand, the data fusion model used data from the Fire room in February 2017 and small-scale data acquired in 2016. In consequence, data fusion algorithms not only combined data from different scenarios also includes information on different dates.

7.2.2.1 Pre-processing data.

As it is mentioned in Chapter 6, the data from the different prototypes was processed. Some of the signals were filtered. Specifically, from prototype 1; PID and MOX sensor signals and from prototype 2; H_2 sensor and CH_4 sensor. Moreover, a baseline correction was implemented.

7.2.2.2 Fire Room Model

The Fire Room model was built using as training set the large-scale dataset 1 acquired at the standard fire room in November 2016. The methodology used to build the models is described in Chapter 6. Internal validation was used to optimize the number of Latent Variables of the model. The large-scale dataset 1 was acquired during one week of experiments. The dataset contains 19 experiments (11 fire experiments and 8 nuisances experiments) and was partitioned for internal validation as follows: *i)* Training: 7 fire and 5 nuisances experiments. *ii)* Test: 4 fires and 3 nuisances experiments. The validation experiments were selected randomly (random subsampling methodology). Internal validation splits are performed 20 times

and each iteration has a different test set. The optimal number of LVs is selected according to the maximum classification rate criterion. In internal validation, models achieved 75% of experiments classified correctly. 97% of the fires were predicted correctly but model misclassified 60% of the nuisance experiments. The nuisance experiments correctly classified were vinegar and turpentine. The selected order of the model corresponds to 8 Latent Variables.

After the internal validation, the resulting model is able to correctly predict 82% of the fires experiments of the *large-scale data set 2*. The mistakes correspond to one repetition of Electrical Fire and one repetition of PVC fire. However, the Fire Room model (trained with large scale dataset 1) misclassifies 69% of the nuisance experiments. The final model classified correctly only one repetition of Air Freshener and two repetitions of Turpentine, Window Cleaning respectively. Table 11 shows the Confusion Matrix, classification rate, sensitivity, specificity, AUC and p-value of the model.

Figure 69 shows the PLS-DA scores and the biplot of the model. The scores are colored by the labels of Fire and Non-Fire predicted. The biplot shows that CO, CO_2, PID, MLC 337° are the important variables in the distribution of the fire. In the opposite side, MOX sensors are the most sensitives to nuisance experiments.

The permutation test confirms the low prediction power of the model. After 1000 iterations the p-value obtained is 0.7. The area under the ROC curve of this model is 0.6.

Table 11 Confusion matrix and figures of merit of the prediction model built with large scale dataset 1 (Fire Room Model)

	PREDICTED	
ACTUAL	Fire	Non Fire
Fire	9	2
Non Fire	11	5
Classification Rate		52% [32 , 72]
Sensitivity		82% [48 , 98]
Specificity		32% [11 , 58]
AUC		0.6
p-value		0.7

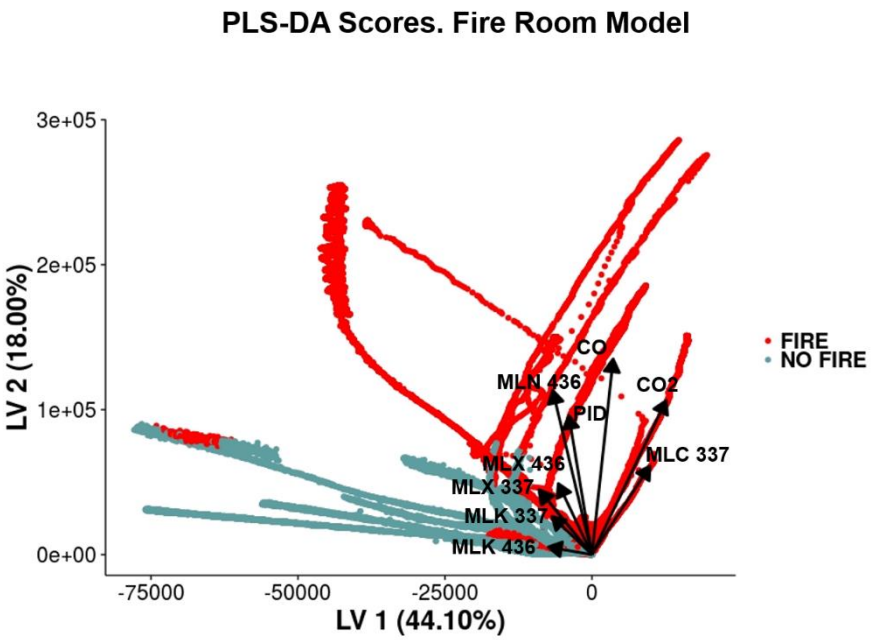

Figure 69 Biplot on the PLS-DA scores of the Fire Room Model

7.2.2.3 Small Scale Model

Small Scale model used exclusively as training set data from the small-scale setup acquired at the small fire cabinet in March 2016.

As in the fire room model, internal validation was used to optimize the order of the model. During internal validation, the Small-scale dataset was split in training and test set. For training 15 experiments of fires and 15 experiments of nuisances were used. The rest of the experiments were used to assess the model (6 nuisances and 5 Fires). Internal validation methodology was repeated 35 times until each experiment was part of the test set at least once. The order of the model was selected according to the maximal Classification Rate. The highest classification rate achieved during internal validation is 93% which corresponds to the 100% of fire and 86% of the nuisance experiments correctly predicted. Model misclassified 2 experiments of ethanol. The order of the model is 5 Latent Variables.

The Small Scale Model presented a low positive rate with only 63% of the fire scenarios correctly classified (one repetitions of PVC fire, one

repetition of TF3, one repetition of Cables Fire and one repetition of Electrical Fire). The performance of the model to discriminate nuisances from fires is also low. In this case, 68 % of the nuisances are classified correctly. The model confused with fire: Two repetitions of Ethanol, one repetition of Air Freshener, one repetition of Gasoline and one repetition of Window Cleaning. The Confusion Matrix of the model is shown in Table 12. The area under the ROC curve for this model is 0.7 and after the permutation test the p-value is 0.04.

The biplot of the model [Figure 70] shows that CO, CO_2, and MLC 337° are variables with a high weight of variable importance in the PLS-DA and contribute with the direction of the fire experiments evolution. On the other hand, MLX MOX sensors are important contributors to the discriminant direction of the nuisance experiments.

Table 12 Confusion matrix and figures of merit of the prediction model built with small scale dataset (Small Scale Model)

	PREDICTED	
ACTUAL	Fire	Non Fire
Fire	7	4
Non Fire	5	11
Classification Rate		70% [49 , 86]
Sensitivity		63% [32 , 83]
Specificity		68% [54 , 93]
AUC		0.7
p-value		0.04

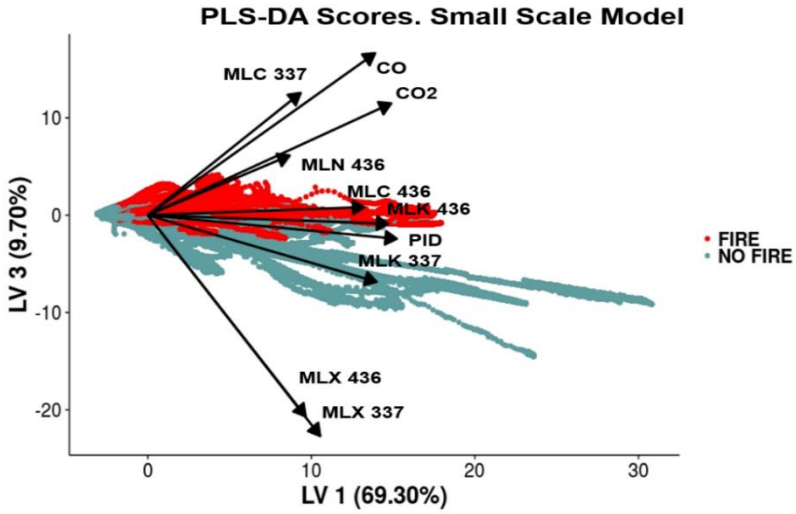

Figure 70 Biplot on the PLS-DA scores of the Fire Room Model

7.2.2.4 Data Fusion Model

Finally, the Data Fusion Model was trained with the combination of *Small Scale dataset* and *Large Scale dataset 1*. The ability of the model to predict fires is of high quality since only one repetition of PVC fire was classified as nuisance, resulting in a 90% sensitivity. In terms of true negative rates (Specificity) the model achieves 81% [

Table 13]. Data Fusion model confused two repetitions of Air Freshener and one of Ethanol as fire. The Area Under the Curve is 0.89 and the permutation test shows the statistical significance of the results (p-value < 0.01).

The biplot of the model is presented in Figure 71. The PLS-DA scores are colored according to the resulting label predicted. Again, CO and CO_2sensors are the main responsible for the classification of Fires and MLX MOX sensors determine the direction of the nuisance scores.

Table 13 Confusion matrix and figures of merit of the prediction model built with the combination of the (Data Fusion Model)

	PREDICTED	
ACTUAL	Fire	Non Fire
Fire	11	1
Non Fire	3	12
Classification Rate		88% [71 , 98]
Sensitivity		90% [60 , 99]
Specificity		81% [54 , 96]
AUC		0.89
p-value		0.01

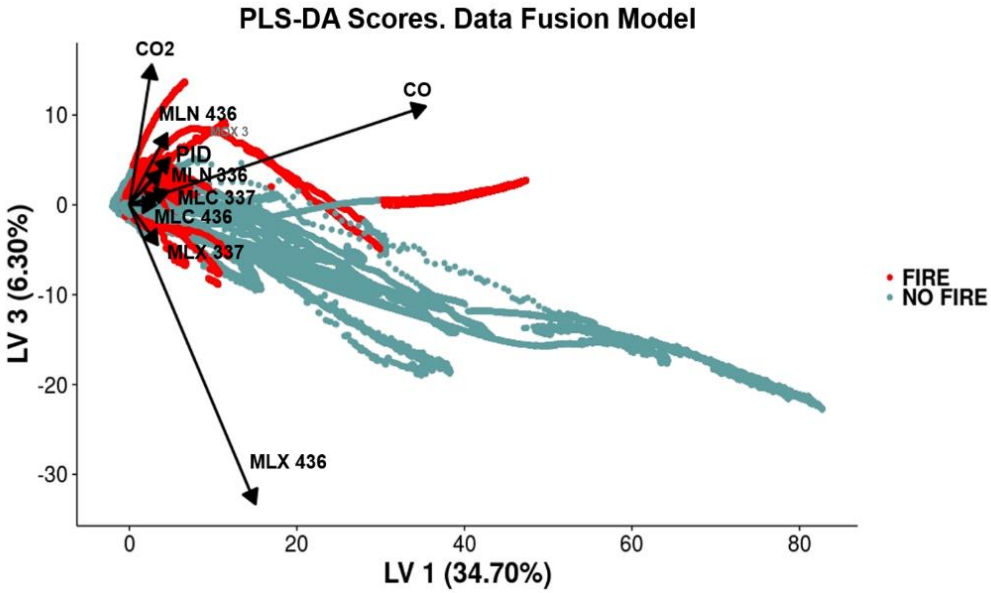

Figure 71 Biplot on the PLS-DA scores of the Data Fusion Model

7.2.2.5 Comparison

Figure 72 illustrates the performance of the models and facilitates the comparison of the different models using the following figures of merit; Classification Rate; Total of experiments correctly classified, Sensitivity (True Positive Fires Rate), Specificity (True Positive Nuisances Rate) and Area under the ROC Curve.

Several differences could be inferred from Figure 72. The Fire Room Model built only with the large-scale dataset showed a high number of false alarms, being an unreliable fire Alarm. However, most of the fires presented in the training set are classified correctly. The low robustness of the model to reject nuisances is consequence of the few numbers of fire and nuisance experiments contained in the *large scale dataset 1.*

On the other hand, the model trained with small scale datasets improves the ability to reject nuisances from 32% to 88%. However, the performance to predict fire decreases from 82% to 60%. The reduced ability to predict fires can be attributed to the fact that some of the fires are not present in the training set (PVC and Electronics) and that the standard fires used in training are an scaled down inspiration of the experiments described in the norms.

The different figures of merit confirm that the Data Fusion Model that is trained with the combination of the small-scale and large-scale datasets improves the ability of the model to classify fires from nuisances. This model presented only 3 false alarms and only one fire is misclassified. The resulting model is also capable to predict fires and reject nuisances acquired almost one year after —in the case of small scale datasets— and four months later than the measurement campaign in large scale 1 was acquired. The Data Fusion Model is then, a reliable and robust fire alarm.

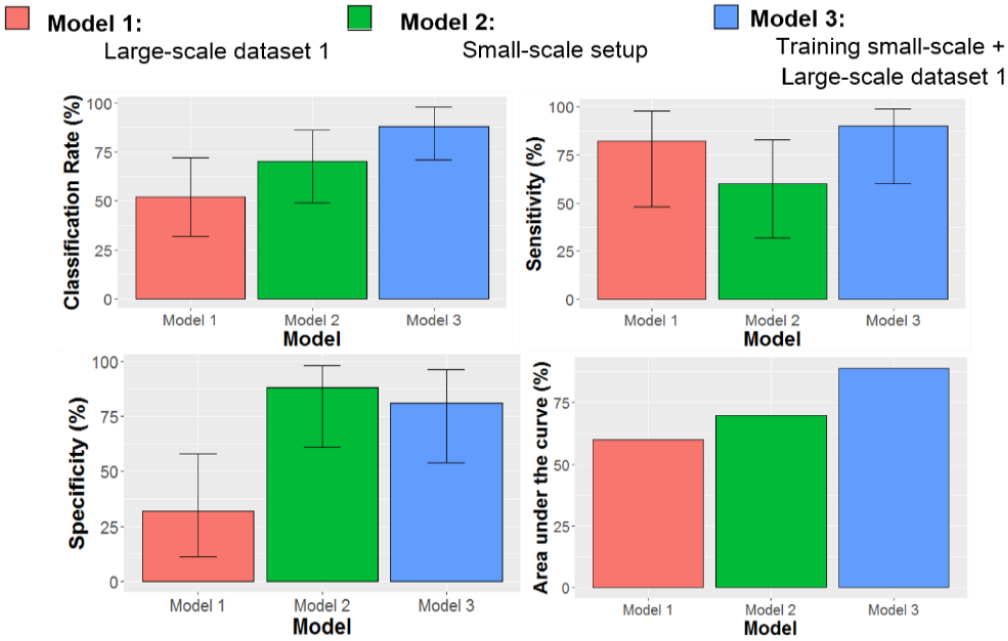

Figure 72 Figures of merit (classification rate, sensitivity, specificity and AUC) of the Fire Room, Small Scale and Data Fusion Model.

7.3 Conclusions

The calibration of fire alarms in standard fire rooms is time consuming leading to small number of calibration conditions and resulting in prediction models with a poor discrimination power. In this way, datasets acquired at small scale setups could help to increase the number of experiments for calibration. Datasets acquired at small setups are faster and with reduced experimentation costs compared with standard fire rooms.

One of the principal disadvantages to using data acquired from small scale setups is that the sensor signals from these setups are different from the sensor signals acquired at fire rooms. For this reason, the models built with small scale setups data are not easily transferable to predict data acquired from large scale setups.

The methodology proposed to compensate experimental costs consists of building calibration models trained with the combination of datasets acquired at large scale and small scale setups.

PLS-DA models were built to classify different fire scenarios and discriminate non-fire scenarios that may produce false alarms. Models that only used large-scale datasets in the calibration set, produced a huge amount of false alarms.

Nevertheless, results confirm that the model trained with the combination of the small-scale and large-scale datasets is capable of rejecting most of the nuisances achieving 81% of specificity. Also, the model shows good ability to detect fires, since only one fire was classified as nuisance. Another important improvement of the Data Fusion Models is the capability to predict fires and reject nuisances acquired more than 4 months later.

Chapter 8: Reduction of Calibration Cost Using Batches of the Same Sensor Array

Among the different gas sensing technologies, metal oxide (MOX) sensors are a popular choice due to the ease of use, fast response, high sensitivity, miniaturization options and low-cost[89], [90]. However, the calibration of MOX sensors faces two significant limitations due to the high correlation among features, sensor drift, scattering at different concentrations, and lack of reproducibility, among others [91], [92]. First, calibration models only keep their predictive performance in the same conditions in which they were built. Thus, the utility of the model is compromised by the change of environmental or sampling conditions and the aging of the sensor. In consequence, calibration models require many calibration conditions to incorporate cross-sensitivities to the model. Second, inherent sensor variability requires specific calibration models for each system, even for replicas of gas sensor arrays with the same design and sensor types. Hence, the sensor variability and the constrained conditions of the calibration models hinder the generalization capability of the models. As a result, calibration is a costly and time-consuming process for MOX sensor arrays.

Calibration costs might be reduced with methods that limit the number of calibration conditions [93]. Data pre-processing strategies are widely used to reject some effects caused by changes in concentration, sampling, or environmental conditions. After pre-processing step, the number of calibration conditions that may be presented to the calibration models to obtain accurate predictions can be reduced [94]. Besides, data pre-processing avoids the inclusion of non-relevant variance, resulting in simpler and more general models (parsimonious models). Gutierrez-Osuna et al. explored different data pre-processing methodologies for odor discrimination. The figure of merit used was the classification rate of a k-NN in a Fisher linear discriminant subspace. Their results confirmed the benefit of data preprocessing in pattern recognition methodologies for gas sensors [95]. Other strategies to make calibration models more robust are based on orthogonal projection filters. Artursson et al. proposed Component Correction [96], Padilla et al. explored Orthogonal Signal Correction [92], and Zityadinov et al. proposed Common Principal Component Analysis [97]. For the above-mentioned approaches, the resulting calibration models were more robust.

Over the years, different methodologies have also been proposed to reduce the number of calibration conditions. For example, Shmilovici et al. used Support Vector Regression to choose the best calibration points (support vectors) for the quantitative prediction of mixtures of three gases with a 12-MOX sensor array [98]. The performance of active control sampling has also been explored, aiming at the optimization of the order to present calibration conditions (gas class and concentration) to ensure, on the fly, the most relevant condition during the whole calibration sample acquisition [99].

Moreover, similarly to standardization techniques applied in spectroscopy [100]–[102], calibration transfer strategies have been explored to extend calibration models to replicas of a sensing instrument in order to reduce calibration costs. Briefly, calibration transfer strategies are based on building a calibration model with a complete set of calibration samples using a master (reference) instrument. Then, a smaller set of samples (transfer samples) is acquired with a slave instrument to determine a function that maps the responses of the slave and the master systems. This mapping of the response spaces is then used to transfer the calibration model between replicas.

The mentioned calibration transfer strategies successfully reduce calibration (and recalibration) costs of system replicas. The ratio between the number of calibration samples and the number of transfer samples determines the savings in the calibration process. This analysis is sometimes overlooked in the literature, and different strategies make use of very different ratios, ranging from 5% to 60%. Nevertheless, calibration costs of MOX sensor arrays are still identified as a major burden towards large-scale deployment of such systems [103], [104].

Specifically, we propose a calibration methodology for arrays of MOX gas sensors that takes advantage of the inherent sensor variability and, therefore, the obtained calibration model can be extended directly to other replicas of the array without the acquisition of new (transfer) samples. This has been achieved by building a general calibration model with different copies of a sensor array and searching a set of sensors that favors the simplicity of this general calibration model. We tested our methodology in the task of discrimination between six gases presented at three concentration levels over a background of synthetic air at three humidity levels. Different calibration strategies were compared to ascertain whether general models trained with several arrays provided similar predictive performances than models trained specifically for individual arrays.

8.1 Dataset

Five replicas (units) of a 24-sensor array were assembled to generate a thorough dataset to test different calibration strategies. Each sensor array included three different types of MOX gas sensors, and each array included eight units of the three types of sensors. The eight elements of the same type within an array operated at different temperatures for a total of 24 sensors per array.

The sensors were provided by ams AG [143] and are the same used in prototype 1: MLC ,MLK , MLX and MLN.

The sensors of the same type, within the same array, operated at eight different temperatures, namely, 245, 275, 303, 313, 330, 340, 356 and 381°C. The sensor heater was adjusted via a constant power board (Analog Devices; Part No.: Eval-AD5380SDZ) to ensure a constant temperature. We will refer to each combination of sensor type and operating temperature as a feature. Therefore, every sensor array provides patterns of 24 features (i.e., input space of 24 dimensions).

The sensor arrays were placed in a measurement chamber (volume = 286.9 cm^3) and exposed to different gas conditions, while sensor responses were acquired at a sampling frequency of 1Hz. A set of mass flow controllers (MFC) was used to control the composition of the sample gas, the humidity level, and the total flow through the chamber. Specifically, we used three MFCs (EL-FLOW Series provided by Bronkhorst) to control the mixture of synthetic dry air (range 0-200 sccm), humidified air (0-200 sccm), and the gas under test (0-100 sccm). The flows of three MFCs were adjusted to generate the desired concentration levels under the defined humidity level, while keeping the total flow constant. During the measurements, laboratory temperature was also regulated. Moreover, in order to verify the experimental conditions (set-points), temperature and humidity were continuously measured using an SHT11 sensor (accuracy of ±0.4ºC and ±3%RH) provided by Sensirion (Switzerland).

The experimental protocol consisted in exposing the sensor arrays to synthetic air at a defined humidity level for 90 minutes. This first (cleaning) stage was used to purge the measurement chamber from the previous

measurement and recover sensor baselines. Next, a gas sample was introduced to the measurement chamber for 30 minutes (measurement cycle). The air flow was kept constant at 196 ml/min for all the duration of the experiment (cleaning and measurement stages). The humidity level only was changed after the experiment was completed.

For each measurement and sensor, we extracted the sensor conductance 28 minutes after the gas was presented (gas response), and 2 minutes before the sample was introduced (baseline levels). Figure 73 (top) shows the signals of MLK sensors operating at four different temperatures when exposed to CO. Figure 73 (bottom) presents the corresponding set-points for CO and humidity levels. Black and green points overlapping the set points represent the time at which the sensor signals were acquired for the construction of our dataset.

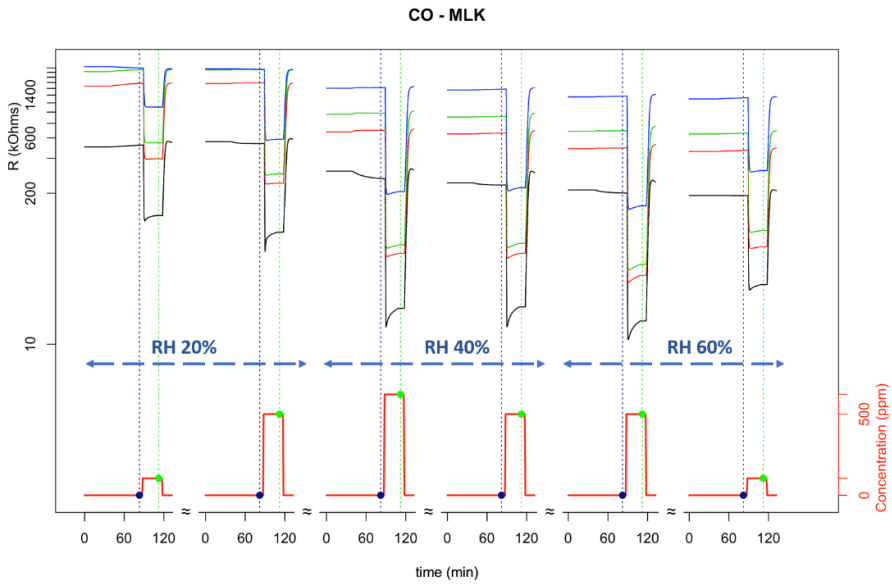

Figure 73 Sensor responses to CO presentation under different humidity levels. Acquired signals for four MLK sensors (top panel), and CO and humidity set-points (bottom panel). Sensor conductivity changes according to the presented conditions. Blue (baseline) and green (measurement cycle) dots represent sampling points for the construction of the dataset.

Six different gases were presented to the sensor arrays: *acetaldehyde*, *methane*, *ethanol*, *propane, nitrogen dioxide*, and *carbon monoxide*. Each gas was presented at three concentrations and three humidity levels. **Table 1**

details the set-points for the gas concentration and humidity levels for each of the presented gases.

Hence, in total, we considered 48 different gas conditions (six gases at eight humidity and gas concentration combinations). In order to consider a balanced dataset among all the gas conditions and the blank samples (background air), we randomly selected 8 of the background measurements (baseline measurements). From now on, for simplicity, we call *air* to the class *background air*, although it contains three humidity levels. All in all, our dataset, includes 56 (gas and air) conditions, which were evaluated once for each of the five copies of the sensor array.

8.2 Evaluation of calibration methods

In order to evaluate the performance of different calibration methods, and based on the dataset described previously, we built predictive models for the discrimination of the six gases regardless of concentration and humidity levels.

The performance of an individually calibrated sensor array was taken as reference. The performance of this individual calibration model was evaluated when applied to different replicas of the sensor array, in order to estimate the impact of sensor tolerances on the accuracy of the predictive model. As an alternative, we proposed to build a general calibration model that incorporates a number of replicas of the sensor array. We validated the model with test samples from different copies of the sensor array. Due to the characteristics of the used dataset, general calibration models were calibrated with up to four replicas and validated with the rest, but this can be changed in the general case.

Hence, we explored the prediction ability of calibration models in three different scenarios.

- Scenario 1. An individual calibration model is obtained with data from one sensor array, and it is tested with data from the same sensor array. This constitutes the reference condition for our analysis.
- Scenario 2. An individual calibration model is obtained with data from one sensor array, and it is tested with data from different sensor

arrays. This case aims at evaluating whether a direct transfer of the calibration models is feasible or not.

- Scenario 3. A general calibration model is obtained with multiple copies of the sensor array, and it is applied to a different sensor array. This model makes use of all the data captured with the units included in calibration. This scenario explores whether the model is able to extract the common behavior among a group of sensor arrays and, thereby it rejects sensor tolerances. Moreover, two other methodologies were explored to compare the performance of the general model with other training data. We also built a calibration model with the averaged response of different calibration units. Finally, we built calibration models with data from different sensing units, but keeping constant the total number of calibration measurements.

All the calibration models were built and evaluated for all the possible combinations of training/test data partitioning.

Classification models were based on a multiclass (all classes vs. all classes) Partial Least Squares - Discriminant Analysis (PLS-DA) [35], followed by k-Nearest Neighbours (k-NN) in the latent variable (LV) subspace. The optimization of the number of latent variables (LV) and neighbors (k) was performed considering the ranges LV = [1, 24] and k = [1, 19]. The combination of hyperparameters that provided maximum classification rate in internal cross-validation was used to build the final model with all the calibration samples. Then, the performance of the models was estimated with the corresponding test dataset

The size of training and test sets for each of the considered scenarios is as follows:

- Scenario 1. One measurement of each volatile and one air measurement were randomly selected as the test set, whereas the rest of the measurements constituted the training set. The model parameters were selected after internal cross-validation using Leave One Out (LOO). The process was repeated eight times until all the measurements were used for model testing (external validation). This methodology allowed to evaluate the performance of the calibration models when the models were built and tested with data from the same replica. The same process was applied to the five sensor array

replicas. Therefore, classification accuracy was evaluated with a total of 280 measurements (40 measurements per class).

- Scenario 2. All measurements from one sensor array (56) were included in the training set, and the measurements from the rest of sensor arrays constituted the test set. This procedure was repeated such that all sensor arrays were used once for model training or calibration.
- Scenarios 3. All the measurements from four sensor array replicas (224) were used to train the models, and the measurements acquired with the remaining sensor array (56) composed the test set. The process was repeated such that all the sensor arrays were used once for testing the calibration models.

All the four scenarios were evaluated in terms of classification rate using a generalization of the area under the ROC curve (AUC) for multiclass classification problems proposed by Hand and Till [148]. To test whether the results were obtained by chance, all the models were trained with permuted labels 1000 times (permutation test). The null hypothesis is that the relationship between the data and the labels cannot be learned by the classifier during training. To reject the null hypothesis we accepted a risk of 0.05.

8.3 Results and discussion

This work aims at developing calibration models that reject sensor variability and can be extended to new replicas with no need of transfer samples. To meet this goal, general calibration models were built with samples from five sensor array replicas and were scrutinized in their ability to predict samples acquired with a sensor array not present in the training set. The performance of these general calibration models was compared with that of individual models (calibrated with only one sensor array). In addition, a small subset of features was selected to construct general models that are parsimonious and more robust.

A Principal Component Analysis (PCA) provided an exploratory analysis of the captured dataset (see Figure 74). Projected data appears in regions for different gas classes, with some overlap among them. Different sensor

responses, due to the different presented gas conditions, dominate the inherent sensor variability in this PCA projection. Although Figure 74 provides a simple and yet informative visualization of the dataset in a 2-dimension space, in general, calibration models will make use of a higher number of dimensions.

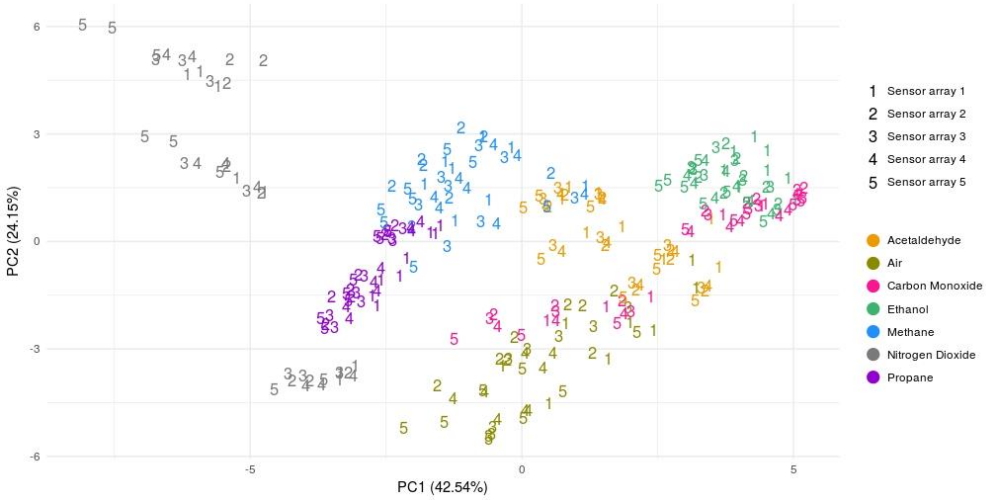

Figure 74 PCA scores of the different sensor array samples. Numbers correspond to the sensor array and color codes the gas (class).

8.3.1 Individual calibration models

Models consisting of PLS-DA followed by k-NN were built using data acquired with one sensor array. Then, the discrimination ability of the models was evaluated with data acquired with the same sensor array using data not presented in calibration (scenario 1) and using data captured with other copies of the sensor array (scenario 2).

Figure 75a and Figure 75b show the confusion matrices for scenario 1 and scenario 2, respectively. The built calibration models were able to perfectly predict the class of new samples if they were acquired with the same sensor array (100% classification rate). However, individual models substantially decreased their predictive ability for new samples measured with other replicas of the sensor array. In scenario 2, even though all the obtained models predicted propane, nitrogen dioxide and methane without

error, only 62.5% of the CO samples were correctly classified. The rest of CO samples were misclassified as background air (40 samples), ethanol (16 samples) or acetaldehyde (4 samples). Air samples acquired during the baseline cycle were wrongly predicted as CO the 25% of the times. In addition, one of the models misclassified one acetaldehyde sample as CO giving a total of 41 false positives and 60 false negatives for the task of CO detection. The overall classification rate (CR) was 91%. We run a Fisher's exact test (two-tailed) [37] to assess the significance of the observed differences between the CR obtained for the model tested with the same sensor array, and the CR obtained for the model tested with different sensor arrays. The null hypothesis that establishes that both distributions are the same was rejected (p-value<0.0001).

Thus, our results confirmed that individual models were local to the sensor array employed for calibration. To a certain extent, individual models were able to predict gas samples from other replicas, but generally failed in one of the most relevant discrimination tasks: CO detection [150]. For this gas, individual models were not able to extrapolate to data acquired with other arrays. The local behavior of models trained with one single array is well-known due to the already mentioned variability among sensors.

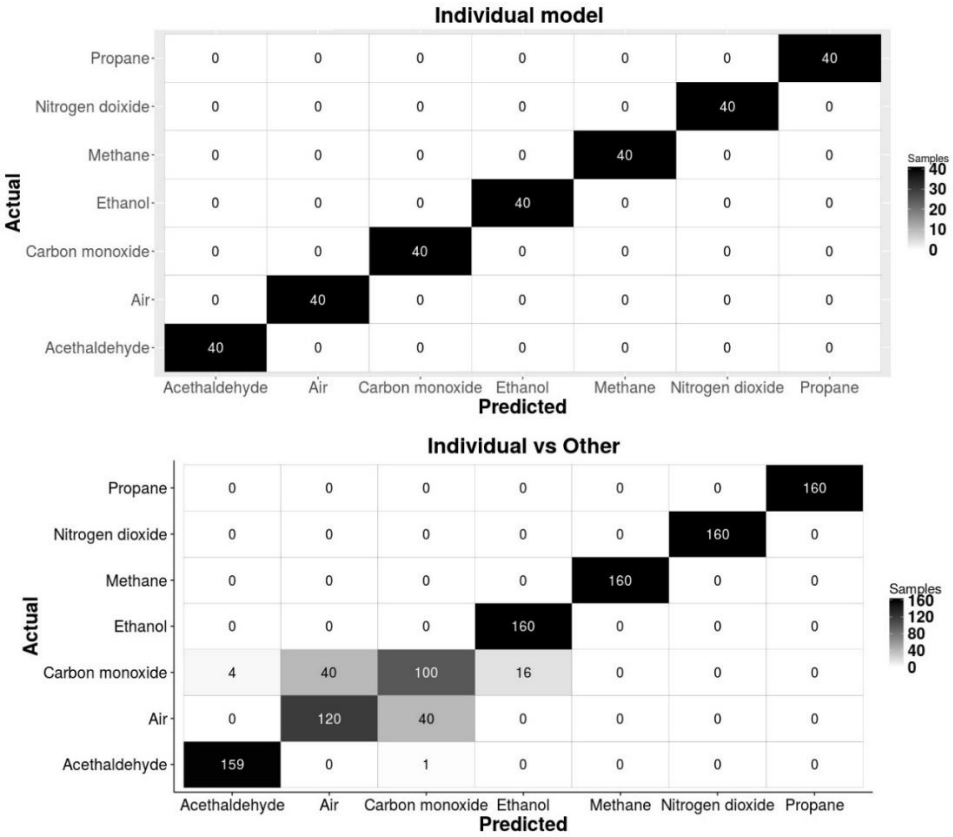

Figure 75 Confusion matrix obtained when the model is tested with data acquired with the same sensor array present in calibration (top, scenario 1) and when it is tested with data acquired with different copies of the array (bottom, scenario 2). The classification accuracy decreases if the calibration model did not include data from the sensor array used for training.

8.3.2 General calibration models

General calibration models were built using data captured with four replicas of the sensor arrays, and they were then evaluated with the remaining replica. **Error! Reference source not found.** shows the confusion matrix after all the iterations and sensor combinations were performed. Interestingly, results show that the models can be extended with high accuracy to new replicas, even though no measurements from the new sensor array were included in calibration. General models achieved a classification ratio of 99% of the test samples. From the 280 test samples, the model only confused two air samples with CO. We also performed Fisher's exact tests to evaluate the significance of the different CRs. The null hypothesis that the distribution of the general calibration model and the distribution of the individual calibration

models (tested with data from the same array) are the same cannot be rejected (p-value=0.5). The hypothesis that the general model is the same than the individual model tested with data from new arrays was rejected (p-value<0.0001). Hence, although the slightly lower CR, statistically, the distribution of the CR obtained with the general model (scenario 3) cannot be considered different to the distribution of the predictions when a calibration model is built and tested with the same unit (scenario 1).

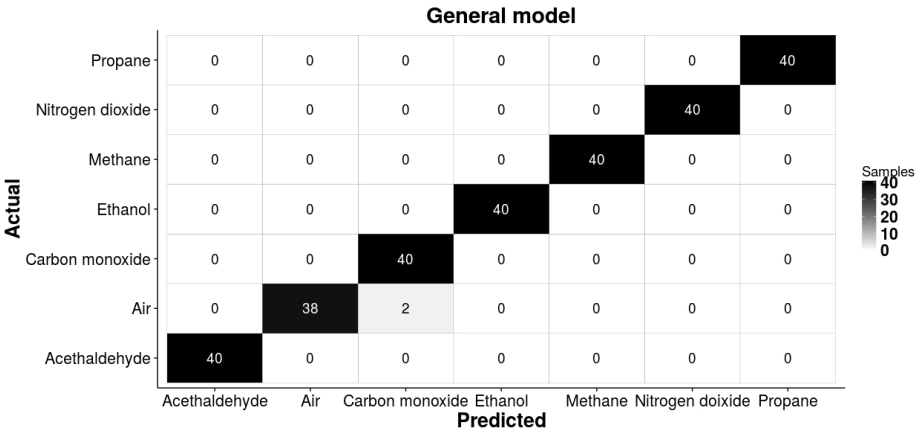

Figure 76 Average of confusion matrices of the general calibration models. Models were trained with samples of four different arrays and evaluated with samples of a different array. The performance of the general model is similar to the performance of individual calibration models when were trained and tested with samples of the same array.

Figure 77 shows the PLS-DA score plot for a general calibration model. This representation highlights the presence of different clusters that correspond to the distinct gases. In general, test samples of every gas fall close to those of the calibration set in the PLS-DA subspace, thereby suggesting a good generalization of the model.

The inclusion of the sensor array variability to the general calibration model improved the ability of the model to predict the class of samples acquired with new sensor arrays. The model is able to extract the redundant information of the sensor arrays, reducing thereby the individual sources of noise. In order to ascertain to what extent sensor variability needs to be included in the calibration process, we evaluated the performance of a new model that uses averaged sensor signals.

Specifically, we compared the performance of our calibration method that incorporates, directly, all the variability of the sensor signals, with a methodology that averages the response of four calibration units. The calibration models obtained with the averaged responses were tested with data acquired with the sensor array not included in calibration (a unit was set aside for model evaluation, and we repeated the process until all the units were used for test). Classification rate (97.5%) was higher than the one observed for individual models applied to other sensor arrays replicas (91%), but did not reach high classification rate obtained with the general models that carry all inherent sensor variability (99%). Similarly than for the global model, air samples were misclassified as CO. However, for the model built upon averaged signals, air samples were also misclassified as methane, and CO samples were wrongly classified as air and propane.

Actually, the average of the signals still carries information that is beneficial to reduce individual sources of noise [148]. Therefore, one expects the averaged model to perform better than the direct transfer of an individual calibration model. Hence, that for efficient rejection of the sensor variability, the calibration model needs to rely on a training dataset that includes measurements that are representative of the sensor variability, which is not the case in the case of averaged sensor responses across units. Additionally, averaging the sensor signals still requires the use of four sensor units, so we do not have any savings in terms of test effort. Results confirm that the averaged-signal model does not reach the classification rates obtained by the global calibration model, confirming thereby the benefits of including all sensor diversity to the calibration dataset. In this sense, the variance corresponding to the intrinsic sensor variability was better rejected with the calibration model trained with the original signals.

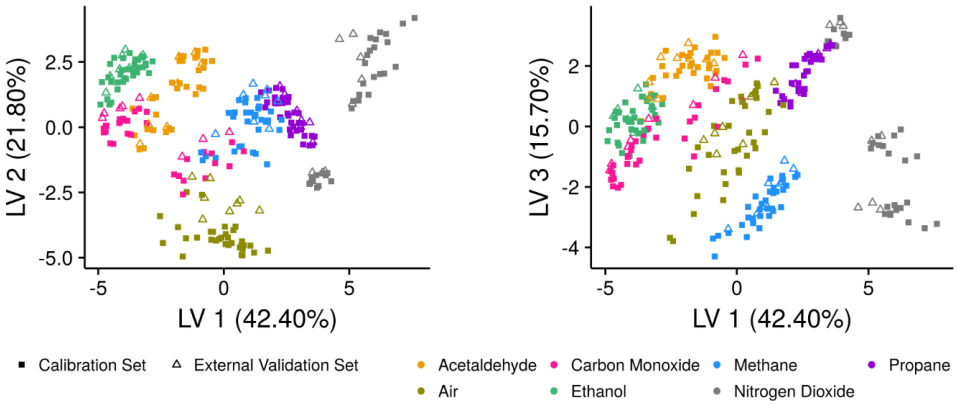

Figure 77 PLS-DA score plots for the general calibration model. Color indicates the gas type and marker type indicates calibration/test point. (left) LV 1 vs LV 2, (right) LV 1 vs LV 3. Calibration and test points appear in the same regions, confirming thereby a generalization of the models.

The superior performance of the general calibration models with respect to the individual models, when applied to new sensing units, may come from i) the higher data variability in the calibration dataset due to the inclusion of different replicates, and ii) the larger size of the calibration dataset. In order to investigate further these two effects, we built calibration models with data from different sensing units, but keeping constant the total number of calibration measurements. Figure 78 shows the model performance, in terms of classification rate, as calibration data from increasing number of units is used. Two strategies are shown in the mentioned figure: i) considering all available samples of the used arrays (each new unit adds 56 calibration measurements to the model), and ii) keeping constant the total number (56) of calibration samples. Results show that diversity from different sensor arrays is favorable for building general calibration models, although when all the available data is used, the performance of the calibration model increases more rapidly. Nevertheless, in practical calibration scenarios, one may expose the sensor arrays to the calibration conditions simultaneously. In this case, it is recommendable to use all data at hand. From Figure 78 one can observe that adding a second array to the calibration model increases significantly the prediction ability of the model, and the performance reaches a plateau when three sensor arrays are used. Hence, one can conclude that, for the considered classification task, three copies of the sensor array would suffice to build general calibration models that can be extended successfully to new arrays. However, more complex tasks or systems with different sensing elements may require a different number of units in calibration to provide reliable general models.

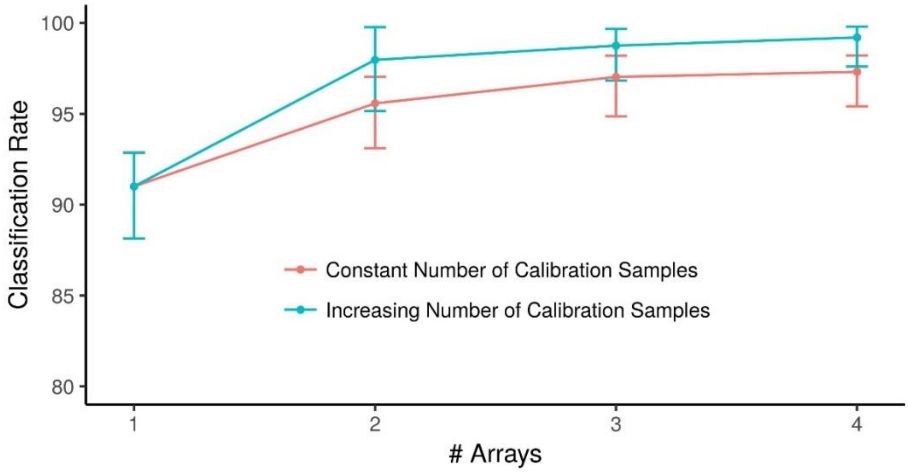

Figure 78 Performance of the models when evaluated with test samples from units not used in calibration, for different number of sensor arrays used in calibration. Keeping the number (56) of calibration samples constant (red), and using all the data available (56 per sensor array) for the units used in calibration (blue).

8.3.2.1 Area Under the ROC Curve (AUC)

In order to compare further the performance of each model, we computed a generalization of the AUC for multiclass classification to estimate the robustness of the different models. Figure 79 shows the distribution of AUC values for scenarios 2, 3, and 4. The averages of the AUC obtained for general calibration models with and without feature selection are 99%. On the other hand, the performance of individual calibration models evaluated with new samples drops to 97%, compared to 100% for the scenario in which the model was tested with samples from the same sensor array. In addition, results of permutation tests point out the statistical significance of the results. With a 95% of confidence, all the models rejected the null hypothesis that the obtained AUC values could come from a model trained with random labels (i.e., random distribution).

The obtained AUC values confirm that general calibration models show higher prediction ability to classify samples acquired with new sensor arrays than models built with one sensor array. Moreover, general calibration models with only four features are also able to successfully predict samples from new

arrays. This indicates that the selected features are informative and resulted in a parsimonious model to improve the robustness of the calibration.

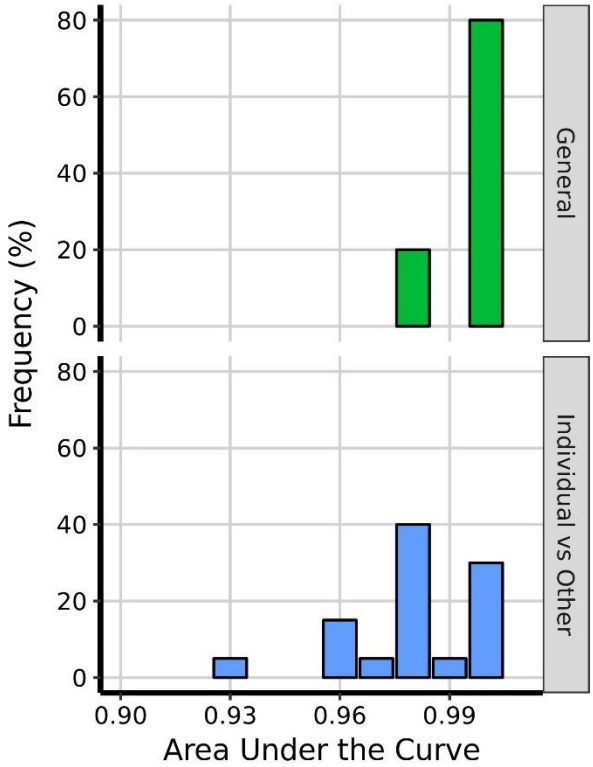

Figure 79 Relative frequency of the area under the curve (AUC) computed for each model. General models are more accurate than individual models for the prediction of new samples from arrays not presented in training. The histograms present the relative frequency for all the possible combinations of arrays.

8.3.2.2 3.6 Model complexity

The complexity of the models was studied in terms of the number of latent variables, LV, and the number of neighbors, k, that were selected during model training. **Figure 12** shows the frequency of selection of optimum LV and k values for individual and general models. For both types of models, optimum k ranges from 1 to 3, whereas the optimum number of LV tends to be larger in individual models (LV = [5,7]) than in general models (LV = [3,5]). Higher number of LV means that individual models are more complex. This possibly

indicates that the models are capturing better the particular behavior of the calibrated sensor array, but this information is specific for this sensor array and it becomes a misrepresentation of the general sensor behavior. Figure 80 also shows that general models with feature selection perform better when trained with fewer LV. This is a direct consequence of the previous dimensionality reduction. Hence, GA helps in reducing the complexity of the model.

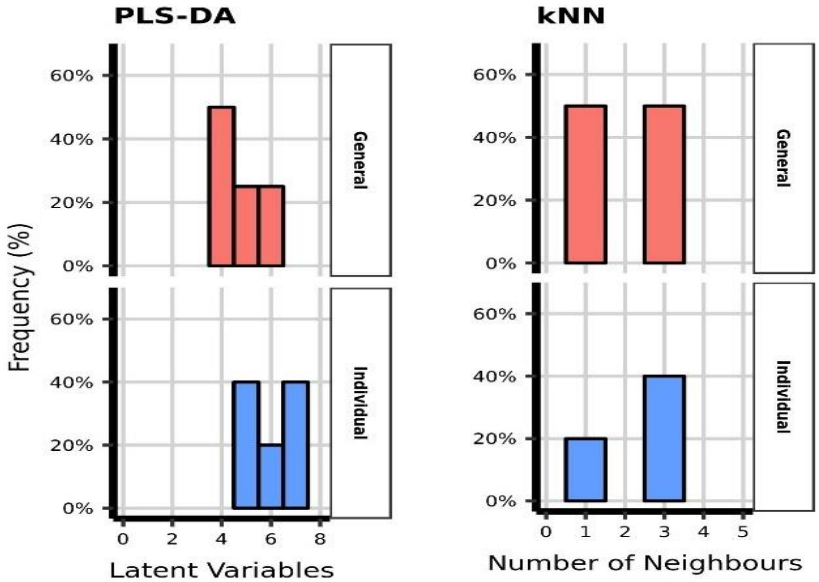

Figure 80 Relative frequency of the number of latent variables and nearest neighbors used to build general and individual models. General models use fewer latent variables than individual models, providing an easier interpretation and a better generalization of the model.

8.4 Conclusions

As expected, the best results are obtained when sensor arrays are calibrated individually, this approach is not feasible in mass-production applications due to high costs. Previous approaches to obtain robust models and reduce costs are mainly based on calibration transfer. However, these strategies still require the acquisition of calibration samples for every new system and, ultimately, they rely on calibration models built upon individual

sensor systems. Herein, we showed that general -or global- calibration models can be obtained if several replicas of the sensor array are included in the calibration process. The obtained calibration models were able to reject the intrinsic system variability: for the proposed classification task, the prediction ability of the models only decreased marginally with respect to specific calibration models. Hence, the variability present in the training set allowed building robust models that could be extended to new replicas without any further calibration, resulting in calibration models that are replica independent. Those general calibration models also reduce the calibration costs.

We also showed that general calibration models tend to be simpler (fewer number of LV) than individual calibration models, especially after selecting a subset of informative features or sensors. Individual models are trained for the particular array of sensors, and higher dimensions of the model account for the specific response of the set of sensors. This information captured at higher dimensions results in better system performance, but the same information misleads the calibration model when it is used for other arrays. Higher dimensions can be understood as a more detailed calibration model for one array, but at the same time, it could be considered as an overfitted model when used for other arrays.

Chapter 9: Conclusions

During this Ph.D. thesis, fire detectors based on multi-gas sensor arrays and sensor fusion algorithms were developed. In this section the general conclusions about fire detection using gas sensors are detailed below:

- Multi-gas sensor arrays in combination with pattern recognition techniques are capable of providing reliable fire alarms while rejecting most nuisance scenarios. The resulting fire detector is capable of providing a solid fire detection.
- Fire detectors based on gas sensor arrays can detect gaseous fire emissions in an early stage of the fire (before visible smoke). In consequence, fire detectors based on chemical sensors are faster than conventional detectors based on light scattering or ionization.
- Both early fires and nuisances release multiple gases and volatiles. Gas emission-based fire detection algorithms require the discrimination of multivariate emission fingerprints. Only with the combination of diverse gas sensor technologies optimal fingerprints can be generated. In the developed prototypes, MOX sensors are important for the early fire detection due to the fast response to different gas emissions and the rejection of nuisances. CH_4 sensor in prototype 2 and CO sensor in both prototypes contribute to the sensitivity to fire emissions and the absence of CO_2 is key to reject nuisance emissions.
- Using post-processing windows, fire detectors are capable to avoid false alarms in all the considered nuisance scenarios. However, this post-processing step increases the response time of the gas sensor-based detectors.
- The Multi-gas sensors arrays developed using commercial sensors and PLS-DA algorithms in this thesis are capable to provide fire alarms in those fires that do not produce smoke (as standard fire TF6) or when the produced smoke is white. Usually, conventional fire detectors cannot produce a fire alarm under those circumstances (absence of smoke production or white smoke). Therefore, fire detectors based on gas sensors and PLS-DA algorithms are more sensitive than conventional smoke detectors in those cases.

- In the used datasets, SVM-based fire detection algorithms are faster than PLS-DA algorithms but produced more false alarms.
- Classification models based on Partial Least Squares Discriminant Analysis (PLS-DA) and Support Vector Machines (SVM) are capable of providing fire alarms in most of the fire scenarios. In fires featuring rapid combustion, specifically TF3 and TF6, the time windows required in SVM algorithms decrease the sensitivity to those fires.
- In both prototypes, PLS-DA algorithms present the same performance in terms of true positive (100%) and true negative rates (97%). Both sensor arrays misclassify one repetition of the window cleaning experiment.
- SVM algorithms trained with measurements from prototype 2 present a high number of false-positive rates. H_2 and CH_4 sensors from prototype 2 have high cross-sensitivities to nuisance volatiles.
- From the different behavior of both prototypes, we infer that the presence of a larger diversity of MOX sensors is a positive factor to reduce false positives.
- The behavior of the CH_4 sensor in prototype 2 indicates a very early emission of hydrocarbons in fires. When detected, these emissions allow a faster detection of fires.
- Results show that the combination of the tests in a standard fire room and in small-scale setups enriches the calibration datasets and leads to better detector performance.
- Small-scale setups allow shorter tests increasing the number of calibration conditions. However, sensor responses differ from those obtained in standard fire room conditions.
- PLS-DA models that only used large-scale datasets in the calibration set showed poor specificity. Nevertheless, results indicated that the model trained with the combination of the small-scale and large - scale datasets is capable of rejecting all the nuisances and detecting most of the fire experiments.
- The presented methodology for the generation of global models avoids the development of a specific calibration model for each sensor array and the implementation of the calibration transfer technique. As a result, calibration costs can be reduced in a scenario of mass production, facilitating thereby mass deployment of gas sensor arrays.

- Results showed that global calibration or prediction models can be obtained if several replicas of the same sensor array are included in the calibration set.
- Resulting global models (trained with several replicates of the same sensor array) achieved similar performance than models trained and tested with measurements from one sensor array.

Further work is needed to keep sensitivity to fires at higher levels when false alarm immunity is increased. A higher number of nuisance experiments is needed to improve the robustness of the system. Additionally, a study of the multi-gas sensor array aging is needed to ensure the optimal performance of the fire detector through time. Also, the study and comparison of models trained with dynamic features are recommended to counteract sensor drift effects.

Chapter 10: References

1. National Research Council. *Fire and Smoke: Understanding the Hazards*; National Academies Press: Washington, DC, USA, 1986; ISBN 0309568609.
2. Reimann, P.; Schütze, A. Fire detection in coal mines based on semiconductor gas sensors. *Sens. Rev.* 2012, *32*, 47–58, doi:10.1108/02602281211197143.
3. Kohl, D.; Kelleter, J.; Petig, H. Detection of Fires by Gas Sensors. *Sens. Update* 2001, *9*, 161–223.
4. Derbel, F. Performance improvement of fire detectors by means of gas sensors and neural networks. *Fire Saf. J.* 2004, *39*, 383–398, doi:10.1016/j.firesaf.2004.03.001.
5. Gann, R.G.; Bryner, N.P. Chapter 2 Combustion Products and Their Effects on Life Safety. In *Fire Protection Handbook*; National Fire Protection Association: Quincy, MA, USA, 2008; Volume 1, pp. 11–34.
6. Chagger, R.; Smith, D. *The Causes of False Fire Alarms in Buildings*; Briefing Paper; BRE Global Ltd.: Watford, UK, 2014.
7. Podrzaj, P.; Hashimoto, H. Intelligent Space as a Fire Detection System. In Proceedings of the IEEE International Conference on Systems, Man, and Cybernetics, Taipei, Taiwan, 8–11 October 2006; pp. 2240–2244.
8. Ishii, H.; Takashi, O.; Yamauchi, Y.; Ohtani, S. An Algorithm for Improving the Reliability of Detection with Processing of Multiple Sensors Signal. *Fire Saf. J.* 1991, *17*, 469–484.
9. Kanoun, O.; Trankler, H.-R. Sensor Technology Advances and Future Trends. *IEEE Trans. Instrum. Meas.* 2004, *53*, 1497–1501, doi:10.1109/TIM.2004.834613.
10. *ASTM Standard Terminology of Fire Standards*; ASTM: West Conshohocken, PA, USA, 2004.
11. Fleming, J.M. Photoelectric and Ionization Detectors: A Review of the Literature. *Retrieved May* 2006, *12*, 2010.
12. Fabian, T.Z.; Gandhi, P.D. *Smoke Characterization Project—Technical Report*; Underwriters Laboratories: Northbrook, IL, USA, 2007.
13. Keller, A.; Rüegg, M.; Forster, M.; Loepfe, M.; Pleisch, R.; Nebiker, P.; Burtscher, H. Open photoacoustic sensor as smoke detector. *Sens. Actuators B Chem.* 2005, *104*, 1–7, doi:10.1016/j.snb.2004.03.013.
14. Meacham, B.J. The Use of Artificial Intelligence Techniques for Signal Discrimination in Fire Detection Systems. *J. Fire Prot. Eng.* 1994, *6*, 125–136.
15. Liu, Z.; Kim, A. Review of Recent Developments in Fire Detection Technologies. *J. Fire Prot. Eng.* 2003, *13*, 129–151, doi:10.1177/104239158900100101.
16. Stec, A.A. Fire toxicity—The elephant in the room? *Fire Saf. J.* 2017, *91*, 79–90.
17. Pitts, W.M. The global equivalence ratio concept and the formation mechanisms of carbon monoxide in enclosure fires. *Prog. Energy Combust. Sci.* 1995, *21*, 197–237, doi:10.1016/0360-1285(95)00004-2.
18. Supplement, E.; Poisoning, C.; Coalition, T. *Cyanide and Carbon Monoxide: The Toxic Twins of Smoke Inhalation*; Cyanide Poisoning Treatment Coalition: Indianapolis, IN, USA, 2009; Volume 2, ISBN 8885175554.
19. Paul, K.T.; Hull, T.R.; Lebek, K.; Stec, A.A. Fire smoke toxicity: The effect of nitrogen oxides. *Fire Saf. J.* 2008, *43*, 243–251.

20. Kallonen, R.; von Wright, A.; Tikkanen, L.; Kaustia, K. The Toxicity of Fire Effluents from Textiles and Upholstery Materials. *J. Fire Sci.* 1985, *3*, 145–160, doi:10.1177/073490418500300302.
21. Pauluhn, J. A Retrospective Analysis of Predicted and Observed Smoke Lethal Toxic Potency Values. *J. Fire Sci.* 1993, *11*, 109–130, doi:10.1177/073490419301100201.
22. Jafari, A.J.; Donaldson, J.D. Determination of HCl and VOC emission from thermal degradation of PVC in the absence and presence of copper, copper(II) oxide and copper(II) chloride. *J. Chem.* 2009, *6*, 685–692, doi:10.1155/2009/753835.
23. Hertzberg, T.; Blomqvist, P.; Dalene, M.; Skarping, G. *Particles and Isocyanates from Fires*; SP Swedish National Testing and Research Institute: Borås, Sweden, 2003; ISBN 9178489350.
24. Paabo, M.; Levin, B.C. A literature review of the chemical nature and toxicity of the decomposition products of polyethylenes. *Fire Mater.* 1987, *11*, 55–70, doi:10.1002/fam.810110203.
25. Coburn, R.F.; Forster, R.E.; Kane, P.B. Considerations of the physiological variables that determine the blood carboxyhemoglobin concentration in man. *J. Clin. Investig.* 1965, *44*, 1899–1910, doi:10.1172/JCI105296.
26. Smith, S.R.; Steinberg, S.; Gaydos, J.C. Errors in Derivations of the Coburn-Forster-Kane Equation for Predicting Carboxyhemoglobin. *Am. Ind. Hyg. Assoc. J.* 1996, *57*, 621–625, doi:10.1080/15428119691014675.
27. Tikuisis, P.; Madill, H.D.D.; Gill, B.J.J.; Lewis, W.F.F.; Cox, K.M.M.; Kane, D.M.M. A Critical Analysis of the Use of the CFK Equation in Predicting COHb Formation. *Am. Ind. Hyg. Assoc. J.* 1987, *48*, 208–213, doi:10.1080/15298668791384643.
28. Tyuma, I.; Ueda, Y.; Imaizumi, H.K. Prediction of the carbonmonoxyhemoglobin levels during and after carbon monoxide exposures in various animal species. *Jpn. J. Physiol.* 1981, *31*, 131–143.
29. Duker, J. Modeling carbon monoxide uptake during work. *Am. Ind. Hyg. Assoc. J.* 1981, *42*, 361–364, doi:10.1080/15298668191419884.
30. *ISO 13571:2007—Life-Threatening Components of Fire—Guidelines for the Estimation of Time Available for Escape Using Fire Data*; International Organization for Standardization: Geneva, Switzerland, 2007.
31. Stewart, R.D.; Peterson, J.E.; Fisher, T.N.; Hosko, M.J.; Baretta, E.D.; Dodd, H.C.; Herrmann, A.A. Experimental Human Exposure to High Concentrations of Carbon Monoxide. *Arch. Environ. Health Int. J.* 1973, *26*, 1–7, doi:10.1080/00039896.1973.10666210.
32. Purser, D.A. Toxicity Assessment of Combustion Products. In *SFPE Handbook of Fire Protection Engineering*; Society of Fire Protection Engineers: Boston, MA, USA, 1988; pp. 200–245.
33. Hartzell, G.E.; Switzer, W.G. On the Toxicities of Atmospheres Containing Both CO and CO_2. *J. Fire Sci.* 1985, *3*, 307–309, doi:10.1177/073490418500300501.
34. Hartzell, G.E. Overview of combustion toxicology. *Toxicology* 1996, *115*, 7–23, doi:10.1016/S0300-483X(96)03492-0.
35. Prien, T.; Traber, D.L. Toxic smoke compounds and inhalation injury—A review. *Burns* 1988, *14*, 451–460, doi:10.1016/S0305-4179(88)80005-6.
36. International Organization for Standardization (ISO). *ISO 13344:2015—Estimation of the lethal Toxic Potency of Fire Effluents*; International Organization for Standardization: Geneva, Switzerland, 2015.

37. Hartzell, G.E.; Grand, A.F.; Switzer, W.G. Modeling of Toxicological Effects of Fire Gases: VI. Further Studies on the Toxicity of Smoke Containing Hydrogen Chloride. *J. Fire Sci.* 1987, *5*, 368–391, doi:10.1177/073490418700500602.
38. Hartzell, G.E.; Switzer, W.G.; Priest, D.N. Modeling of Toxicological Effects of Fire Gases: V. Mathematical Modeling of Intoxication of Rats by Combined Carbon Monoxide and Hydrogen Cyanide Atmospheres. *J. Fire Sci.* 1985, *3*, 330–342, doi:10.1177/073490418500300504.
39. Purser, D. Interactions among carbon monoxide, hydrogen cyanide, low oxygen hypoxia, carbon dioxide and inhaled irritant gases. In *Carbon Monoxide Toxicity*; Penney, D.G., Ed.; CRC Press: Boca Raton, FL, USA, 2000; pp. 157–191.
40. Purser, D.A. The Development of Toxic Hazard in Fires from Polyurethane Foams and the Effects of Fire Retardants. In *Flame Retardants*; Plastic and Rubber Institute and British Plastic Federation, Ed.; Elsevier Applied Science: London, UK, 1990; pp. 206–221.
41. Purser, D.A.; McAllister, J.L. Assessment of hazards to occupants from smoke, toxic gases, and heat. In *SFPE Handbook of Fire Protection Engineering*; Springer: Berlin, Germany, 2016; pp. 2308–2428.
42. Sesseng, C.; Reitan, N.K.; Fjær, S. Mapping of gas concentrations, effect of dead-air space and effect of alternative detection technology in smouldering fires. *SPFR Rep. A* 2016, *16*, 20053, doi:10.13140/RG.2.1.1100.3282.
43. Siemens Switzerland. *Fire Safety Guide*; Siemens: Zug, Switzerland, 2012.
44. Pfister, G. Multisensor/Multicriteria Fire Detection: A New Trend Rapidly Becomes State of the Art. *Fire Technol.* 1997, *33*, 115–139, doi:10.1023/A:1015343000494.
45. International Organization for Standardization (ISO). *ISO 7240: Fire Detection and Alarm Systems*; ISO: Geneva, Switzerland, 2004.
46. *NFPA NFPA-72: National Fire Alarm Signaling Code*; National Fire Protection Association: Quincy, MA, USA, 2013.
47. Underwritters Laboratories. Available online: http://www.ul.com/global/eng/pages/aboutul/whatwedo/ (accessed on 13 December 2013).
48. *Underwritters Laboratories UL217-Standard for Single and Multiple Station Smoke Alarms*; Underwritters Laboratories: Northbrook, IL, USA, 2016.
49. *UL268—Smoke Detectors for Fire Alarm Systems*; UL: Northbrook, IL, USA, 2009.
50. *Underwritters Laboratories UL2034: Standard for Single and Multiple Station Carbon Monoxide Alarms*; UL: Northbrook, IL, USA, 2017.
51. *CENELEC EN 50291: Electrical Apparatus for the Detection of Carbon Monoxide in Domestic Premiss*; European Committee for Electrotechnical Standardization: Brussels, Belgium, 2010.
52. Thomas, G. *A Study on the Performance of Current Smoke Alarms to the New Fire and Nuisance Tests Prescribed in ANSI/UL 217-2015*; NIST: Gaithersburg, MD, USA, 2016.
53. *Loss Prevention Standard Testing Procedures for the LPCB Approval and Listing of Carbon Monoxide/Heat Multisensor Fire Detectors Using Electrochemical Cells*; BRE Global Ltd.: Watford, UK, 2014.
54. Procedures, T.; Resistant, B.; Components, B.; Enclosures, S. *Loss Prevention Standard*; BRE Global Ltd.: Watford, UK, 2010.
55. Fine, G.F.; Cavanagh, L.M.; Afonja, A.; Binions, R. Metal oxide semi-conductor gas sensors in environmental monitoring. *Sensors* 2010, *10*, 5469–5502.

56. Galstyan, V.; Comini, E.; Faglia, G.; Sberveglieri, G. TiO_2 nanotubes: Recent advances in synthesis and gas sensing properties. *Sensors* 2013, *13*, 14813–14838, doi:10.3390/s131114813.
57. Bertocci, F.; Fort, A.; Vignoli, V.; Mugnaini, M.; Berni, R. Optimization of perovskite gas sensor performance: Characterization, measurement and experimental design. *Sensors* 2017, *17*, 1352, doi:10.3390/s17061352.
58. Xiong, L.; Compton, R.G. Amperometric gas detection: A review. *Int. J. Electrochem. Sci.* 2014, *9*, 7152–7181.
59. Stetter, J.R.; Li, J. Amperometric gas sensors—A review. *Chem. Rev.* 2008, *108*, 352–366, doi:10.1021/cr0681039.
60. McAvoy, T.; Milke, J.; Tekin, A.K. Using multivariate statistical methods to detect fires. *Fire Technol.* 1996, *32*, 6–24.
61. Milke, J.; Mcavoy, T. Analysis of Fire and Non-fire Signatures For Discriminating Fire Detection. *Fire Saf. Sci.* 1997, *5*, 819–828, doi:10.3801/IAFSS.FSS.5-819.
62. Hagen, B.C.; Milke, J.A. Use of gaseous fire signatures as a mean to detect fires. *Fire Saf. J.* 2000, *34*, 55–67, doi:10.1016/S0379-7112(99)00046-6.
63. Milke, J.A. Using multiple sensors for disciminating fire detection. In Proceedings of the Fire Suppression and Detection Research Application Symposium, Research and Practice: Bridging the Gap, Orlando, FL, USA, 24–26 February 1999; pp. 150–164.
64. Cestari, L.A.; Worrell, C.; Milke, J.A. Advanced fire detection algorithms using data from the home smoke detector project. *Fire Saf. J.* 2005, *40*, 1–28, doi:10.1016/j.firesaf.2004.07.004.
65. Chen, S.J.; Hovde, D.C.; Peterson, K.A.; Marshall, A.W. Fire detection using smoke and gas sensors. *Fire Saf. J.* 2007, *42*, 507–515, doi:10.1016/j.firesaf.2007.01.006.
66. Chen, S.-J. Fire Alarm Algorithm Using Smoke and Gas Sensors. U.S. Patent 7,142,105, 28 November 2006.
67. Gottuk, D.T.; Peatross, M.J.; Roby, R.J.; Beyler, C.L. Advanced fire detection using multi-signature alarm algorithms. *Fire Saf. J.* 2002, *37*, 381–394, doi:10.1016/S0379-7112(01)00057-1.
68. Dreiseitl, S.; Ohno-Machado, L. Logistic regression and artificial neural network classification models: A methodology review. *J. Biomed. Inform.* 2002, *35*, 352–359, doi:10.1016/S1532-0464(03)00034-0.
69. Milke, J.A. Monitoring Multiple Aspects of Fire Signatures for Discriminating Fire Detection. *Fire Technol.* 1999, *35*, 195–209.
70. Okayama, Y. A Primitive Study of a Fire Detection Method Controlled by Artificial Neural Net. *Fire Saf. J.* 1991, *17*, 535–553.
71. Okayama, Y.; Sasaki, T. Design of Neural Net to Detect Early Stage of Fire and Evaluation by Using Real Sensors' Data. *Fire Saf. Sci.* 1994, *4*, 751–759.
72. Milke, J.A.; Mcavoy, T.J. Analysis of Signature Patterns for Discriminating Fire Detection with Multiple Sensors. *Fire Technol.* 1995, *31*, 120–136, doi:10.1007/BF01040709.
73. Okayama, Y. Approach to Detection of Fires in Their Very Early Stage by Odor Sensors and Neural Net. *Fire Saf. Sci.* 1991, *3*, 955–964.
74. Rose-Pehrsson, S.L.; Shaffer, R.E.; Hart, S.J.; Williams, F.W.; Gottuk, D.T.; Strehlen, B.D.; Hill, S.A. Multi-criteria fire detection systems using a probabilistic neural network. *Sens. Actuators B Chem.* 2000, *69*, 325–335, doi:10.1016/S0925-4005(00)00481-0.
75. Rose-Pehrsson, S.L.; Hart, S.J.; Street, T.T.; Tatem, P.A.; Williams, F.; Hammond, M.H.; Gottuk, D.T.; Wright, M.T.; Wong, J.T. Real-Time Probabilistic Neural Network Performance

and Optimization for Fire Detection and Nuisance Alarm Rejection. In Proceedings of the 12th International Conference on Automatic Fire Detection, Gaithersburg, MD, USA, 25–28 March 2001.

76. Conrad, T.; Reimann, P.; Schutze, A. A hierarchical strategy for under-ground early fire detection based on a T-cycled semiconductor gas sensor. In Proceedings of the IEEE Sensors, Atlanta, GA, USA, 28–31 October 2007; pp. 1221–1224, doi:10.1109/ICSENS.2007.4388629.
77. Schutze, A.; Reimann, P. Sensor Arrays, Virtual Multisensors, Data Fusion, and Gas Sensor Data Evaluation. In *Gas Sensing Fundamentals*; Springer: Berlin, Germany, 2013; Volume 48, pp. 67–107, ISBN 978-3-540-33918-2.
78. Bukowski, R.W.; Bright, R.G. *Some Problems Noted in the Use of Taguchi Semiconductor Gas Sensors as Residential Fire/Smoke Detectors*; NIST: Gaithersburg, MD, USA, 1974.
79. Pfister, G. Detection of smoke gases by solid state sensors—A focus on research activities. *Fire Saf. J.* 1983, *6*, 165–174, doi:10.1016/0379-7112(83)90067-X.
80. Oyabu, T. An algorithm for evaluating disasters by fuzzy reasoning. *Sens. Actuators B Chem.* 1993, *10*, 143–148, doi:10.1016/0925-4005(93)80038-D.
81. Müller, H.C.; Fisher, A. A Robust Fire Detection Algorithiii for Temperature and Optical Smoke Density using Fuzzy Logic. In Proceedings of the International Carnahan Conference on Security Technology, Surrey, UK, 18–20 October 1995; pp. 197–204.
82. Mobin, I.; Islam, N.; Hasan, R. An Intelligent Fire Detection and Mitigation System Safe from Fire (SFF). *Int. J. Comput. Appl.* 2016, *133*, 1–7.
83. Ni, M.; Stetter, J.R.; Buttner, W.J. Orthogonal gas sensor arrays with intelligent algorithms for early warning of electrical fires. *Sens. Actuators B Chem.* 2008, *130*, 889–899, doi:10.1016/j.snb.2007.10.070.
84. Sawada, A.; Higashino, T.; Oyabu, T.; Takei, Y.; Nanto, H.; Toko, K. Gas sensor characteristics for smoldering fire caused by a cigarette smoke. *Sens. Actuators B Chem.* 2008, *130*, 88–93, doi:10.1016/j.snb.2007.07.083.
85. Krüger, S.; Despinasse, M.C.; Raspe, T.; Nörthemann, K.; Moritz, W. Early fire detection: Are hydrogen sensors able to detect pyrolysis of house hold materials? *Fire Saf. J.* 2017, *91*, 1059–1067, doi:10.1016/j.firesaf.2017.04.035.
86. Adib, M.; Eckstein, R.; Hernandez-Sosa, G.; Sommer, M.; Lemmer, U. SnO_2 Nanowire Based Aerosol Jet Printed Electronic Nose as Fire Detector. *IEEE Sens. J.* 2017, *1748*, 2–8, doi:10.1109/JSEN.2017.2777178.
87. Lee, K.; Shim, Y.S.; Song, Y.G.; Han, S.D.; Lee, Y.S.; Kang, C.Y. Highly sensitive sensors based on metal-oxide nanocolumns for fire detection. *Sensors* 2017, *17*, 303, doi:10.3390/s17020303.
88. Courbat, J.; Pascu, M.; Gutmacher, D.; Briand, D.; Wöllenstein, J.; Hoefer, U.; Severin, K.; De Rooij, N.F. A colorimetric CO sensor for fire detection. *Procedia Eng.* 2011, *25*, 1329–1332, doi:10.1016/j.proeng.2011.12.328.
89. Potyrailo, R. A. Multivariable Sensors for Ubiquitous Monitoring of Gases in the Era of Internet of Things and Industrial Internet. 2016, doi:10.1021/acs.chemrev.6b00187.
90. Fine, G. F.; Cavanagh, L. M.; Afonja, A.; Binions, R. Metal oxide semi-conductor gas sensors in environmental monitoring. Sensors 2010, 10, 5469–5502.
91. Gao, H.; Jia, H.; Bierer, B.; Wöllenstein, J.; Lu, Y.; Palzer, S. Scalable gas sensors fabrication to integrate metal oxide nanoparticles with well-defined shape and size. Sensors Actuators B Chem. 2017, 249, 639–646, doi:https://doi.org/10.1016/j.snb.2017.04.031.
92. Padilla, M.; Perera, A.; Montoliu, I.; Chaudry, A.; Persaud, K.; Marco, S. Drift compensation of gas sensor array data by Orthogonal Signal Correction. Chemom. Intell. Lab. Syst. 2010,

100, 28–35, doi:10.1016/j.chemolab.2009.10.002.
93. Marco, S.; Gutierrez-Galvez, A. Signal and data processing for machine olfaction and chemical sensing: A review. IEEE Sens. J. 2012, 12, 3189–3214, doi:10.1109/JSEN.2012.2192920.
94. Monereo, O.; Prades, J. D.; Cirera, A. Self-heating effects in large arrangements of randomly oriented carbon nanofibers: Application to gas sensors. Sensors Actuators, B Chem. 2015, 211, 489–497, doi:10.1016/j.snb.2015.01.095.
95. Herrero-Carrón, F.; Yáñez, D. J.; Rodríguez, F. D. B.; Varona, P. An active, inverse temperature modulation strategy for single sensor odorant classification. Sensors Actuators, B Chem. 2015, 206, 555–563, doi:10.1016/j.snb.2014.09.085.
96. Drobek, M.; Kim, J. H.; Bechelany, M.; Vallicari, C.; Julbe, A.; Kim, S. S. MOF-Based Membrane Encapsulated ZnO Nanowires for Enhanced Gas Sensor Selectivity. ACS Appl. Mater. Interfaces 2016, 8, 8323–8328, doi:10.1021/acsami.5b12062.
97. Korotcenkov, G.; Cho, B. K. Metal oxide composites in conductometric gas sensors: Achievements and challenges. Sensors Actuators, B Chem. 2017, 244, 182–210.
98. Krivetskiy, V.; Malkov, I.; Garshev, A.; Mordvinova, N.; Lebedev, O. I.; Dolenko, S.; Efitorov, A.; Grigoriev, T.; Rumyantseva, M.; Gaskov, A. Chemically modified nanocrystalline SnO2-based materials for nitrogen-containing gases detection using gas sensor array. J. Alloys Compd. 2017, 691, 514–523, doi:10.1016/j.jallcom.2016.08.275.
99. Krivetskiy, V.; Efitorov, A.; Arkhipenko, A.; Vladimirova, S.; Rumyantseva, M.; Dolenko, S.; Gaskov, A. Selective detection of individual gases and CO/H2mixture at low concentrations in air by single semiconductor metal oxide sensors working in dynamic temperature mode. Sensors Actuators, B Chem. 2018, 254, 502–513, doi:10.1016/j.snb.2017.07.100.
100. Eranna, G.; Joshi, B. C.; Runthala, D. P.; Gupta, R. P. Oxide Materials for Development of Integrated Gas Sensors—A Comprehensive Review. Crit. Rev. Solid State Mater. Sci. 2004, 29, 111–188, doi:10.1080/10408430490888977.
101. Lee, A. P.; Reedy, B. J. Temperature modulation in semiconductor gas sensing. Sensors Actuators, B Chem. 1999, 60, 35–42, doi:10.1016/S0925-4005(99)00241-5.
102. Ortega, A.; Marco, S.; Perera, A.; Šundic, T.; Pardo, A.; Samitier, J. An intelligent detector based on temperature modulation of a gas sensor with a digital signal processor. Sensors Actuators B Chem. 2001, 78, 32–39, doi:10.1016/S0925-4005(01)00788-2.
103. Zampolli, S.; Elmi, I.; Cozzani, E.; Cardinali, G. C.; Scorzoni, A.; Cicioni, M.; Marco, S.; Palacio, F.; Gómez-Cama, J. M.; Sayhan, I.; Becker, T. Ultra-low-power components for an RFID Tag with physical and chemical sensors. Microsyst. Technol. 2008, 14, 581–588, doi:10.1007/s00542-007-0444-8.
104. Sayhan, I.; Helwig, A.; Becker, T.; Müller, G.; Elmi, I.; Zampolli, S.; Padilla, M. Discontinuously Operated Metal Oxide Gas Sensors for Flexible Tag Microlab Applications. 2008, 8, 176–181.
105. Simon, I.; Bârsan, N.; Bauer, M.; Weimar, U. Micromachined metal oxide gas sensors: Opportunities to improve sensor performance. Sensors Actuators, B Chem. 2001, 73, 1–26, doi:10.1016/S0925-4005(00)00639-0.
106. Marco, S. The need for external validation in machine olfaction: Emphasis on health-related applications Chemosensors and Chemoreception. Anal. Bioanal. Chem. 2014, 406, 3941–3956, doi:10.1007/s00216-014-7807-7.
107. Rodriguez-Lujan, I.; Fonollosa, J.; Vergara, A.; Homer, M.; Huerta, R. On the calibration of sensor arrays for pattern recognition using the minimal number of experiments. Chemom. Intell. Lab. Syst. 2014, 130, 123–134.
108. Gardner, J. W.; Bartlett, P. N. Pattern recognition in odour sensing. In Sensors and sensory systems for an electronic nose; Springer, 1992; pp. 161–179.
109. Gutierrez-Osuna, R.; Nagle, H. T. A method for evaluating data-preprocessing techniques for odour classification with an array of gas sensors. IEEE Trans. Syst. Man. Cybern. B. Cybern. 1999, 29, 626–632.
110. Artursson, T.; Eklöv, T.; Lundström, I.; Mårtensson, P.; Sjöström, M.; Holmberg, M. Drift correction for gas sensors using multivariate methods. J. Chemom. 2000, 14, 711–723.
111. Ziyatdinov, A.; Marco, S.; Chaudry, A.; Persaud, K.; Caminal, P.; Perera, A. Sensors and

Actuators B : Chemical Drift compensation of gas sensor array data by common principal component analysis. Sensors Actuators B. Chem. 2010, 146, 460–465, doi:10.1016/j.snb.2009.11.034.
112. Perera, A.; Sundic, T.; Pardo, A.; Gutierrez-Osuna, R.; Marco, S. A portable electronic nose based on embedded PC technology and GNU/Linux: hardware, software and applications. IEEE Sens. J. 2002, 2, 235–246, doi:10.1109/JSEN.2002.800683.
113. Pardo, M.; Kwong, L. G.; Sberveglieri, G.; Brubaker, K.; Schneider, J. F.; Penrose, W. R.; Stetter, J. R. Data analysis for a hybrid sensor array. Sensors Actuators B. Chem. 2005, 106, 136–143, doi:10.1016/j.snb.2004.05.045.
114. Pardo, A.; Marco, S.; Calaza, C.; Ortega, A.; Perera, A.; Šundic, T.; Samitier, J. Methods for sensors selection in pattern recognition. Proc. Inst. Phys. Publ. 2001, 83–88.
115. Vergara, A.; Llobet, E. Sensor Selection and Chemo-Sensory Optimization: Toward an Adaptable Chemo-Sensory System. Front. Neuroeng. 2012, 4, 19, doi:10.3389/fneng.2011.00019.
116. Raman, B.; Meier, D. C.; Evju, J. K.; Semancik, S. Designing and optimizing microsensor arrays for recognizing chemical hazards in complex environments☆. Sensors Actuators B Chem. 2009, 137, 617–629, doi:10.1016/j.snb.2008.11.053.
117. Raman, B.; Douglas C., M.; Semancik, S. A Statistical Approach to Materials Evaluation and Selection for Chemical Sensor Arrays. In In Computational Methods for Sensor Material Selection; Springer, New York, NY, 2009; pp. 221–244.
118. Shmilovici, A.; Bakir, G. Finding the best calibration points for a gas sensor array with support vector regression. In Intelligent Systems, 2nd International IEEE Conference; 2004; pp. 174–177.
119. Walczak, B.; Bouveresse, E.; Massart, D. L. Standardization of near-infrared spectra in the wavelet domain. Chemom. Intell. Lab. Syst. 1997, 36, 41–51, doi:10.1016/S0169-7439(96)00075-5.
120. Bouveresse, E.; Massart, D. L. Improvement of the piecewise direct standardisation procedure for the transfer of NIR spectra for multivariate calibration. Chemom. Intell. Lab. Syst. 1996, 32, 201–213, doi:10.1016/0169-7439(95)00074-7.
121. Milanez, K. D. T. M.; Araújo Nóbrega, T. C.; Silva Nascimento, D.; Galvão, R. K. H.; Pontes, M. J. C. Selection of robust variables for transfer of classification models employing the successive projections algorithm. Anal. Chim. Acta 2017, 984, 76–85, doi:10.1016/j.aca.2017.07.037.
122. Balaban, M. O.; Korel, F.; Odabasi, A. Z.; Folkes, G. Transportability of data between electronic noses : mathematical methods. 2000, 71.
123. Zhang, L.; Tian, F. C.; Peng, X. W.; Yin, X. A rapid discreteness correction scheme for reproducibility enhancement among a batch of MOS gas sensors. Sensors Actuators, A Phys. 2014, 205, 170–176, doi:10.1016/j.sna.2013.11.015.
124. Zhang, L.; Tian, F.; Kadri, C.; Xiao, B.; Li, H.; Pan, L.; Zhou, H. Sensors and Actuators B : Chemical On-line sensor calibration transfer among electronic nose instruments for monitoring volatile organic chemicals in indoor air quality. Sensors Actuators B. Chem. 2011, 160, 899–909, doi:10.1016/j.snb.2011.08.079.
125. Fernandez, L.; Guney, S.; Gutierrez-Galvez, A.; Marco, S. Calibration transfer in temperature modulated gas sensor arrays. Sensors Actuators, B Chem. 2016, 231, 276–284, doi:10.1016/j.snb.2016.02.131.
126. Fonollosa, J.; Fernández, L.; Gutiérrez-Gálvez, A.; Huerta, R.; Marco, S. Calibration transfer and drift counteraction in chemical sensor arrays using Direct Standardization. Sensors Actuators, B Chem. 2016, 236, doi:10.1016/j.snb.2016.05.089.
127. Zuppa, M.; Distante, C.; Siciliano, P.; Persaud, K. C. Drift counteraction with multiple self-organising maps for an electronic nose. Sensors Actuators, B Chem. 2004, 98, 305–317, doi:10.1016/j.snb.2003.10.029.
128. Vergara, A.; Vembu, S.; Ayhan, T.; Ryan, M. a.; Homer, M. L.; Huerta, R. Chemical gas sensor drift compensation using classifier ensembles. Sensors Actuators B Chem. 2012, 166–167, 320–329, doi:10.1016/j.snb.2012.01.074.
129. Yan, K.; Zhang, D.; Xu, Y. Correcting Instrumental Variation and Time-Varying Drift Using

Parallel and Serial Multitask Learning. IEEE Trans. Instrum. Meas. 2017, 66, 2306–2316, doi:10.1109/TIM.2017.2707898.
130. Zhang, L.; Liu, Y.; He, Z.; Liu, J.; Deng, P.; Zhou, X. Sensors and Actuators B : Chemical Anti-drift in E-nose : A subspace projection approach with drift reduction. Sensors Actuators B. Chem. 2017, 253, 407–417, doi:10.1016/j.snb.2017.06.156.
131. Zhang, L.; Zhang, D. Domain Adaptation Extreme Learning Machines for Drift Compensation in E-Nose Systems. IEEE Trans. Instrum. Meas. 2015, 64, 1790–1801, doi:10.1109/TIM.2014.2367775.
132. Tomic, O.; Eklöv, T.; Kvaal, K.; Haugen, J. E. Recalibration of a gas-sensor array system related to sensor replacement. Anal. Chim. Acta 2004, 512, 199–206, doi:10.1016/j.aca.2004.03.001.
133. Boeker, P. On "Electronic Nose" methodology. Sensors Actuators, B Chem. 2014, 204, 2–17, doi:10.1016/j.snb.2014.07.087.
134. Tsujita, W.; Yoshino, A.; Ishida, H.; Moriizumi, T. Gas sensor network for air-pollution monitoring. Sensors Actuators, B Chem. 2005, 110, 304–311, doi:10.1016/j.snb.2005.02.008.
135. De Vito, S.; Di Palma, P.; Ambrosino, C.; Massera, E.; Burrasca, G.; Miglietta, M. L.; Di Francia, G. Wireless sensor networks for distributed chemical sensing: Addressing power consumption limits with on-board intelligence. IEEE Sens. J. 2011, 11, 947–955, doi:10.1109/JSEN.2010.2077277.
136. Mead, M. I.; Popoola, O. a M.; Stewart, G. B.; Landshoff, P.; Calleja, M.; Hayes, M.; Baldovi, J. J.; McLeod, M. W.; Hodgson, T. F.; Dicks, J.; Lewis, a.; Cohen, J.; Baron, R.; Saffell, J. R.; Jones, R. L. The use of electrochemical sensors for monitoring urban air quality in low-cost, high-density networks. Atmos. Environ. 2013, 70, 186–203, doi:10.1016/j.atmosenv.2012.11.060.
137. Piedrahita, R.; Xiang, Y.; Masson, N.; Ortega, J.; Collier, A.; Jiang, Y.; Li, K.; Dick, R. P.; Lv, Q.; Hannigan, M.; Shang, L. The next generation of low-cost personal air quality sensors for quantitative exposure monitoring. Atmos. Meas. Tech. 2014, 7, 3325–3336, doi:10.5194/amt-7-3325-2014.
138. Moltchanov, S.; Levy, I.; Etzion, Y.; Lerner, U.; Broday, D. M.; Fishbain, B. On the feasibility of measuring urban air pollution by wireless distributed sensor networks. Sci. Total Environ. 2015, 502, 537–547, doi:10.1016/j.scitotenv.2014.09.059.
139. Fishbain, B.; Moreno-Centeno, E. Self Calibrated Wireless Distributed Environmental Sensory Networks. Sci. Rep. 2016, 6, doi:10.1038/srep24382.
140. Fonollosa, J.; Vergara, A.; Huerta, R. Algorithmic mitigation of sensor failure: Is sensor replacement really necessary? Sensors Actuators, B Chem. 2013, 183, 211–221.
141. Martinelli, E.; Magna, G.; Vergara, A.; Di Natale, C. Cooperative classifiers for reconfigurable sensor arrays. Sensors Actuators, B Chem. 2014, 199, 83–92, doi:10.1016/j.snb.2014.03.070.
142. ams AG.
143. Fonollosa, J.; Fernandez, L.; Huerta, R.; Gutierrez-Galvez, A.; Marco, S. Temperature optimization of metal oxide sensor arrays using Mutual Information. Sensors Actuators, B Chem. 2013, 187, 331–339.
144. Kneer, J.; Wöllenstein, J.; Palzer, S. Manipulating the gas-surface interaction between copper(II) oxide and mono-nitrogen oxides using temperature. Sensors Actuators, B Chem. 2016, 229, 57–62, doi:10.1016/j.snb.2016.01.104.
145. Ballabio, D.; Consonni, V. Classification tools in chemistry. Part 1: linear models. PLS-DA. Anal. Methods 2013, 5, 3790–3798, doi:10.1039/c3ay40582f.
146. Mevik, B.-H.; Wehrens, R. The pls Package: Principal Component and Partial Least. J. Stat. Softw. 2007, 18.
147. Scrucca, L. GA : A Package for Genetic Algorithms in R. J. Stat. Softw. 2013, 53, 1–37.
148. Hand, D. J.; Till, R. J. A Simple Generalisation of the Area Under the ROC Curve for Multiple Class Classification Problems. Mach. Learn. 2001, 45, 171–186, doi:10.1023/A:1010920819831.
149. Agresti, A. A Survey of Exact Inference for Contingency Tables. Stat. Sci. 1992, 7, 131–153,

doi:10.1214/ss/1177011454.
150. Rose, J. J.; Wang, L.; Xu, Q.; Mctiernan, C. F.; Shiva, S.; Tejero, J.; Gladwin, M. T. Carbon Monoxide Poisoning : Pathogenesis , Management , and Future Directions of Therapy. 2017, 195, 596–606, doi:10.1164/rccm.201606-1275CI.
151. Pearce, T. C.; Sánchez-Montañés, M. A. Chemical Sensor Array Optimization: Geometric and Information Theoretic Approaches. In Handbook of Machine Olfaction: Electronic Nose Technology; 2004; pp. 347–375 ISBN 9783527601592.
152. minimx GmbH [http://www.minimax-viking.com/de/]
153. Delta Electronics. Instruction manual for smoke measuring equipment. MIC type EC912; 2007.
154. Delta Electronics - madebydelta.com
155. Delta Electronics. Instruction manual for smoke measuring equipment. MIREX type EC911; 2004.
156. Gasmet. Instruction and operating manual for the Gasmet DX4000 and Gasmet DX4015 models; 2015, version E1.14.
157. Safety Systems Technology. NOVA-5000 Model S250 Ionization Smoke Detector; 2012.
158. Babrauskas, W. Research on Electrical Fires: The State of the Art. Fire Safety Science; 2008; pp 3-18. doi:10.3801/IAFSS.FSS.9-3
159. Ming, N. Orthogonal gas sensor arrays with intelligent algorithms for early warning of electrical fires. Sensors and Actuators B: Chemical; 2008; Volume 130, Issue 2, pp 889-899. doi:10.1016/j.snb.2007.10.070.
160. Bukowski, R.W. Fire Technol; 1985; pp 21: 252. doi:10.1007/BF01103583.
161. Shu, W. A Sauter mean diameter sensor for fire smoke detection; Sensors and Actuators B: Chemical; 2019; Volume 281, pp 920-932. doi:10.1016/j.snb.2018.11.021.
162. Kodur, V. "Fire hazard in buildings: review, assessment and strategies for improving fire safety"; PSU Research Review; 2019;doi:10.1108/PRR-12-2018-0033.
163. Chen, Y. Combustion properties of pure and fire-retarded cellulose; Combustion and Flame; 1990; Volume 84, Issues 1–2, pp 121-140; doi:10.1016/0010-2180(91)90042-A.
164. Jackson, M. Gas sensing for fire detection: Measurements of CO, CO2, H2, O2, and smoke density in European standard fire tests; Fire Safety Journal; 1994; Volume 22, Issue 2, pp 181-205; doi:10.1016/0379-7112(94)90072-8.
165. Docquier, N. Combustion control and sensors: a review, Progress in Energy and Combustion Science; 2002; Volume 28, Issue 2, pp 107-150, doi:10.1016/S0360-1285(01)00009-0.
166. Fonollosa, J. Chemical Sensor Systems and Associated Algorithms for Fire Detection: A Review; sensors; 2018; 18(2), 553; doi:10.3390/s18020553.
167. Dey, A. Semiconductor metal oxide gas sensors: A review; Materials Science and Engineering: B; 2018 ;Volume 229,pp 206-217,doi: 10.1016/j.mseb.2017.12.036.
168. Listyorini, T. A prototype fire detection implemented using the Internet of Things and fuzzy logic; World Transactions on Engineering and Technology Education; 2018; Vol.16.
169. Golatkar; Fire Detection ; SSRN; 2018; doi:10.2139/ssrn.3274790.
170. Andrew, A. Early Stage Fire Source Classification in Building using Artificial Intelligence; IEEE Conference on Systems, Process and Control (ICSPC); 2018; doi: 10.1109/SPC.2018.8704155
171. Texas Instrument. LM117, LM317-N Wide Temperature Three-Pin Adjustable Regulator Datasheet; 2015
172. Oller, S. aves: Acquisition, Visualization and Exploration Software; pypi.org/project/aves.
173. Xing, Y. Real-Time Thermal Modulation of High Bandwidth MOX Gas Sensors for Mobile Robot Applications. Sensors; 2019; doi: 10.3390/s19051180.
174. Mitchell, H. Multi-Sensor Data Fusion, 2007, Springer.
175. Park, S. Sensor self-diagnosis using a modified impedance model for active sensing-based structural health monitoring. Structural Health Monitoring ;2009: 71-82.
176. Alphasense; IRC-A1 Carbon Dioxide, Infrared Sensor ,Pyroelectric Detector, Datasheet.
177. Texas Instrument; LMP91000 Sensor AFE System: Configurable AFE Potentiostat for Low-Power ChemicalSensing Applications., Aplication Note.
178. Alphasense; PID-A12 Photo Ionisation Detector, Datasheet.

179. LEE, Kwangjae, et al. Highly sensitive sensors based on metal-oxide nanocolumns for fire detection. Sensors, 2017, vol. 17, no 2, p. 303. doi: 10.3390/s17020303
180. Imec; https://www.imec-int.com/en/home
181. Oudenhoven, J. Electrochemical detection of ammonia using a thin ionic liquid film as the electrolyte. Procedia engineering, 2015, vol. 120, p. 983-986. doi:10.1016/j.proeng.2015.08.636.
182. Torra, V. A review of the construction of hierarchical fuzzy systems. International journal of intelligent systems, 2002, vol. 17, no 5, p. 531-543. doi:10.1002/int.10036
183. Chen, G. When and when not to use fuzzy logic in industrial control. En Conference Record of the 1993 IEEE Industry Applications Conference Twenty-Eighth IAS Annual Meeting. IEEE, 1993. p. 2035-2040. doi: 10.1109/IAS.1993.299142
184. Cochocki, A. Neural networks for optimization and signal processing. John Wiley & Sons, Inc., 1993.
185. BARKER, Matthew; RAYENS, William. Partial least squares for discrimination. Journal of Chemometrics: A Journal of the Chemometrics Society, 2003, vol. 17, no 3, p. 166-173. doi:10.1002/cem.785
186. WANG, L.; ZHANG, Z.; DESIGN, C. Xu RF Circuit. Theory and applications. Support Vector Machines, Springer-Verlag, Berlin Heidelber, 2005.
187. Mehmood, T. A review of variable selection methods in partial least squares regression. Chemometrics and Intelligent Laboratory Systems, 2012, vol. 118, p. 62-69. doi:10.1016/j.chemolab.2012.07.010

Appendix A: Confusion Matrices PLS-DA and SVM Algorithms for Fire Detection

Table 14 Percentage of the experiments correctly classified in function of the time window using a prediction model based on PLS-DA

	Classification Rate							
Experiment	1s		15s		30s		60s	
	Prototype 1	Prototype 2	Prototype 1	Prototype 2	Prototype 1	Prototype 2	Prototype 1	Prototype 2
TF2	100 %	100 %	100 %	100 %	100 %	100 %	100 %	100 %
TF3	100 %	100%	100 %	66%	100 %	66%	100 %	33%
Cable Fire	100 %	100 %	100 %	100 %	100 %	100 %	100 %	100 %
TF6	100 %	100 %	100 %	0%	0%	0%	0%	0%
Electrical Fire	100%	100%	100%	100%	66%	100%	66%	100%
PVC	100%	100%	100%	100%	100%	100%	100%	100%
Window Cleaning	100%	100%	100%	100%	100%	100%	100%	100%
Gasoline	66%	100%	66%	100%	100%	100%	100%	100%
Air Freshener	100%	100%	100%	100%	100%	100%	100%	100%
Ethanol	33%	66%	66%	66%	100%	66%	100%	100%
Turpentine	100%	100%	100%	100%	100%	100%	100%	100%
Boiling Water	100%	0%	100%	100%	100%	100%	100%	100%

Table 15 Percentage of the experiments correctly classified in function of the time window using a prediction model based on SVM

	Classification Rate							
Experiment	1s		15s		30s		60s	
	Prototype 1	Prototype 2	Prototype 1	Prototype 2	Prototype 1	Prototype 2	Prototype 1	Prototype 2
TF2	66 %	100 %	66%	100 %	33 %	100 %	33 %	100 %
TF3	100 %	66%	66 %	66%	66 %	66%	66 %	66%
Cable Fire	100 %	100 %	100 %	100 %	100 %	100 %	100 %	100 %
TF6	100 %	0 %	100 %	0%	100%	0%	100%	0%
Electrical Fire	66%	100%	66%	100%	66%	100%	66%	100%
PVC	100%	100%	100%	100%	100%	100%	100%	100%
Window Cleaning	100%	100%	100%	100%	100%	100%	100%	100%
Gasoline	100%	100%	100%	100%	100%	100%	100%	100%
Air Freshener	100%	33%	100%	33%	100%	100%	100%	100%
Ethanol	66%	33%	66%	33%	100%	33%	100%	100%
Turpentine	66%	100%	66%	100%	66%	100%	66%	100%
Boiling Water	100%	0%	100%	100%	100%	100%	100%	100%

Appendix B: Resumen en Castellano

Actualmente el principio de funcionamiento de los detectores de incendios comerciales está basado en la detección de humo o de partículas [1]. Sin embargo, para algunos tipos de combustión o fuego, los detectores de incendios convencionales tienden a producir alarmas de incendio en estados muy avanzados o bien, no producen alarma de incendio[2]. Estas tardías alarmas pueden poner en peligro la vida de las personas dentro de los edificios ya que una gran cantidad de gases tóxicos son liberados durante el incendio[2].

Es por ello que la búsqueda por tecnologías de detección de incendios más rápidas y confiables sigue siendo un tema de estudio. Los sensores de gas son un buen candidato para producir alarmas de incendio más rápidas que los detectores convencionales [3.4]. Sin embargo, el uso de un solo sensor de gas para la detección temprana de incendios produce un alto ratio de falsas alarmas [8]. Es por ello que se están explorando detectores de incendio que incorporan diversas tecnologías (tipos de sensores). Una de las soluciones más ampliamente usadas es aquella que incorporan detectores de humo convencionales y sensores electroquímicos de monóxido de carbono [9].

Se han realizado diferentes estudios relacionado con la viabilidad del uso de sensores químicos para la detección de incendios. Sin embargo, no existen en la actualidad detectores de incendios basados exclusivamente en sensores de gas. Esto se debe a los problemas habituales de los sensores químicos. La principal desventaja del uso de sensores químicos en la detección de incendios son las sensibilidades cruzadas ya que pueden producir falsas alarmas [6]. Para desarrollar detectores de incendio confiables basados –exclusivamente- en sensores químicos se precisa usar técnicas de reconocimiento de patrones y procesado de señal para poder discriminar de manera correcta todas aquellas señales producidas por gases o volátiles no provenientes de un incendio [7].

Trabajos de investigación previos demuestran que es posible detectar incendios usando la combinación de sensores químicos y reconocimiento de patrones [8]. Pero el desarrollo de un instrumento basado exclusivamente en sensores de gas sigue siendo un problema abierto.

OBJETIVOS

Esta tesis doctoral tiene dos objetivos principales. El primer objetivo es desarrollar una alarma inteligente y robusta para una detección temprana y confiable de incendios. Esta disertación presenta nuevos enfoques que resuelven problemas importantes de los sensores químicos en la detección de incendios.

El desarrollo exitoso de un detector de incendios basado en sensores de gas (objetivo 1) depende de la realización de una serie de objetivos en tres campos diferentes***; Diseño de del instrumento, generación de datos y desarrollo y validación de algoritmos de detección de incendios.***

El segundo objetivo se centra en la reducción de costos para la calibración del instrumento. De esta manera se presentan dos metodologías.

La ***primera metodología*** permite la reducción de los costos de calibración. Dicha metodología se basa en el uso de la fusión de datos de mediciones adquiridas en una habitación de incendios estándar y en una cámara a pequeña escala. La ***segunda metodología*** permite construir modelos de predicción reduciendo los costos de calibración individual (y, en consecuencia, los costos de producción en masa) utilizando copias de una misma matriz de sensores.

PROTOCOLO EXPERIMENTAL

Habitación Estándar de Fuegos

Las habitaciones estándar permiten el control de las condiciones ambientales y aseguran la correcta ejecución de los experimentos de fuegos e interferencias. La sala de incendios estándar usada para desarrollar nuestros los experimentos está dentro de las facilidades de la empresa Minimax (Bad Oldesloe, Alemania). La habitación cuenta con un área experimental y un área de control. El área experimental tiene una dimensión de 10m x 6m x 4m (LxWxH). Todos los experimentos de incendio se realizaron en el centro del área experimental. Los sistemas de medida se colocan en el techo de la zona de experimentos. El techo cuenta con 3 soportes circulares de 6 metros de diámetro que permiten la instalación de los sistemas y aseguran la exposición de humo y partículas liberadas durante los experimentos. El centro de las circunferencias coincide con el centro del techo. La Figure 81 muestra la distribución general de la cámara de fuegos.

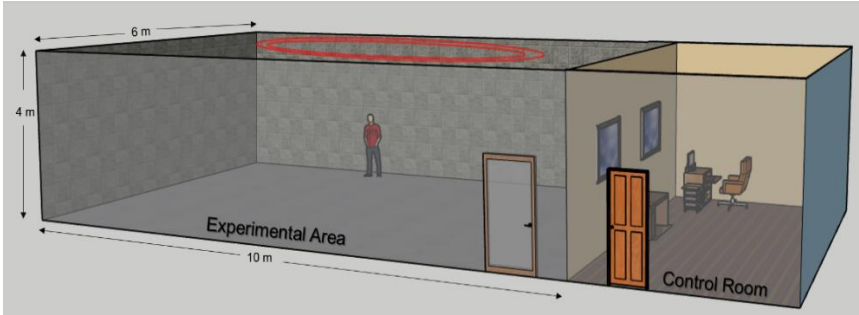

Figure 81. Distribucion de la sala de fuegos en donde fueron ejecutados los experimentos de fuegos e interferencias. La facilidad localizada en Minimax cuenta con un area experimental y un area de control.

Por otro lado, la producción de humo durante los experimentos se ha medido tanto con una cámara de ionización (MIC) como con un medidor de extinción de infrarrojos (MIREX), ambos localizados en el techo de la habitación de fuegos. Instalado también en el techo de la habitación de fuegos se encuentra un tubo que permite la absorción de humo y gases para los sistemas aspirados.

Cámara de Fuegos a Pequeña Escala.

La campaña de medidas en la cámara de fuegos se realizó en una pequeña cámara situada en el laboratorio del grupo ISP situado en la Universidad de Barcelona. La cámara de fuegos tiene por dimensiones 55x55x90 cm (LxWxH) con un volumen total de 272 litros. La cámara se colocó dentro de una campana extractora para facilitar la evacuación de humo. La matriz de sensores se instaló en el techo de la cámara. Todos los experimentos escalados fueron realizados en la parte baja de la cámara mientras los sensores adquirían señales de manera constante. La Figure 82 muestra el esquema y distribución de la cámara de fuegos.

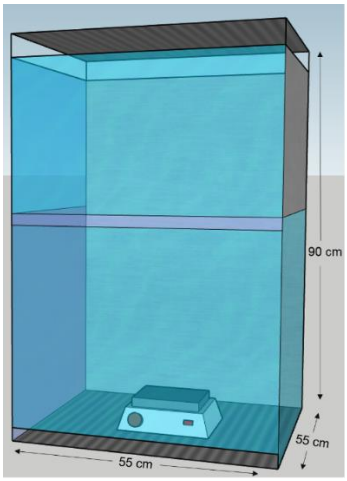

Figure 82. Dimensiones de la cámara de fuegos en donde los experimentos a pequeña escala fueron ejecutados.

Protocolo Experimental en la Habitación de Fuegos.

Se realizaron 2 tipos de experimentos: Experimentos e fuegos y Experimentos de interferencias. Los experimentos de fuego realizados son dos experimentos estándar: TF2 (4 piezas de madera de haya) y TF3 (tiras de algodón de 10cm) y 2 experimentos de fuego no estándar: Cables (10 piezas de cable de 1 cm de diámetro) Electrónicos (Placa PCB montada). Los experimentos de fuego son inducidos a partir del incremento de temperatura de un plato calefactor (hotplate). El calefactor puede alcanzar una temperatura de 600°C. El experimento estándar TF3, se inicializa de manera diferente. El estándar establece que se debe encender los bordes de los listones y luego extinguir la flama soplando. El inicio del experimento comienza cuando las mechas de algodón están incandescentes. En el caso de estos experimentos, se utilizó una antorcha de alcohol metilado.

Los escenarios de interferencia que están en forma líquida (gasolina, aguarrás, vinagre y etanol) se colocaron dentro de un contenedor de 200 x 200 x 50. Y el contenedor se situó en el centro del suelo del área experimental (en la misma posición que los experimentos de fuego). El material se deja evaporando por 15 minutos antes de retirarlo. El experimento de aromatizante fue implementado mediante

un atomizador. El atomizador ha sido presionando 10 veces dentro de la habitación estándar. Por último, el experimento de limpieza de ventanas se realizó limpiando con el producto de limpieza las dos ventanas que dividen el área experimental del área de control.

Protocolo Experimental en la Cámara de Fuegos.

Los experimentos en la cámara de fuegos fueron ejecutados en 4 fases. En la primera fase los sensores adquieren medidas de la cámara vacía (sin material dentro), esta fase corresponde a la línea de base de las señales.

En la segunda fase el material se introduce en la cámara de fuegos. Esta segunda etapa corresponde al inicio de los escenarios de interferencia (etanol, aromatizante, limpiador de suelos y vinagre) ya que los volátiles de estas comienzan a liberarse. Para los experimentos en donde es necesario un incremento de temperatura (todos los fuegos, blanco y agua hirviendo), el material es introducido en esta segunda etapa sin calentarlo.

En la tercera etapa el calentamiento o ignición del material comienza. Los materiales son calentados hasta 280 ºC en una placa calefactora. El experimento continúa hasta que la alarma de uno de 2 detectores comerciales colocados dentro de la cámara ha saltado. Si después de 15 minutos la alarma comercial no ha saltado, el experimento finalizará y el material se retira de la cámara.

Bases de Datos.

En total se han adquirido 3 bases de datos diferentes, dos en la sala estándar y una en la pequeña cámara de fuegos. Cada base de datos fue adquirida en una campaña de medidas distinta. Las identificaremos como *Fire Room 1* y *Fire Room 2* a las dos campañas realizadas en la sala de fuegos estándar y *Chamber* a la base de datos adquirida en la pequeña cámara de fuegos.

Fire Room 1 contiene 18 experimentos; 6 tipos de fuegos lentos y 6 tipos de interferencias.

Fire Room 2 contiene 40 experimentos; 5 tipos de fuegos lentos, 6 tipos de interferencia y adicionalmente se ejecutaron 2 fuegos de tipo flama pero que no producen humo o partículas, ***TF4*** (Etanol), ***TF6*** (Poliuretano) y 1 fuego no estándar; ***Bengalas***.

Small-Scale contiene 34 experimentos; 4 tipos de fuegos lentos y 6 tipos de interferencias.

Cada campaña tiene una duración de 4 días y los experimentos, tanto en la habitación estándar como en la cámara de fuegos, se ejecutaron en orden aleatorio. La Figure 16 detalla todos los experimentos de fuegos e interferencias que han sido incluidos en cada base de datos con su respectivo número de repeticiones. Los nombres usados son los que aparecen en los archivos.

Table 16 Experimentos y sus repeticiones realizados en cada campaña de medidas

Nombre del Experimento	Material	FIRE ROOM 1 (Repeticiones)	FIRE ROOM 2 (Repeticiones)	Small-scale (Repeticiones)
Blank	Plato Calefactor	0	0	2
Air freshener	Aromatizante	2	3	4
Ethanol	Etanol	2	3	4
Boiling water	Agua Hirviendo	0	0	4
Cleaning Product	Limpiador de pisos	0	0	3
Vinegar	Vinagre	1	1	3
Turpentine	Aguarras	1	3	0
Gasoline	Gasolina	1	3	0
Window Cleaner	Limpiador de ventanas	1	3	0
TF2	Madera de pino	2	2	3
TF2 bis	Madera de haya	0	0	4
TF3	Mechas de Algodon	1	3	3
Electrical fire	Tablillas Electronicas	2	2	0
Cable fire	Cables	2	2	4
PVC	PVC	2	2	0
PET	PET	2	0	0
TF4	Etanol	0	2	0
TF6	Poliuretano	0	2	0
Sparkles	Bengala	0	1	0

PROTOTIPOS PARA LA DETECCION DE INCENDIOS

Matriz de Sensores Usando Sensores Comerciales.

La matriz de sensores químicos empleada para adquirir las bases de datos se ha diseñado combinando diversos tipos de sensores comerciales e incluyendo toda la circuitería necesaria para el acondicionamiento y adquisición de la señal. La selección de los sensores se ha hecho conforme a aquellos que son especialmente sensibles a gases liberados en situaciones de fuego. El instrumento contiene específicamente:

- *1 sensor electroquímico de monóxido de carbono (EC-CO) — CO-BF4 de Alphasense*
- *1 detector fotoionizante (PID) para detección de compuestos orgánicos volátiles — PID-A1 de Alphasense*
- *8 sensores de oxido metálico (MOX); 4 tipos diferentes, cada uno operado a dos temperaturas — MLK a 337°, MLK a 436°, MLC a 337°, MLC a 436°, MLX a 337°, MLX a 436°, MLN a 337°, MLN a 436°. Todos los sensores son de AMS.*
- *1 sensor infrarrojo no dispersivo (NDIR-CO_2) de dióxido de carbono — NDIR-A1 de Alphsense.*

El sistema emplea un Arduino DUE para la adquisición de las señales con una frecuencia de muestreo de 10 muestras por segundo. El Arduino manda los valores adquiridos a una computadora de escritorio que almacena y permite la visualización de los valores en tiempo real.

Prototipo Safesens.

Otra matriz de sensores de múltiples tecnologías se desarrolló en el marco del proyecto europeo SAFESENS. El instrumento integra sensores de gas de diversas compañías. El prototipo consiste en dos PCB separados. En la PCB inferior hay un microcontrolador que adquiere y envía las señales registradas por los sensores. El PCB superior es para alojar los sensores.

El prototipo 2 incluye cuatro sensores MOX de ams, un sensor de humedad/temperatura de ams, una celda electroquímica de metano proporcionada por IMEC y también un sensor Bosch de H2-FET (Figura 10).

Adicionalmente al prototipo 2 y como parte del mismo sistema, se conectaron 2 sistemas estándar y se adquirieron mediciones durante todas las campañas de medición en la habitación de fuegos estándar. Los sistemas corresponden a un sensor NDIR de CO2 de BOSCH y un detector de CO basado en espectroscopía láser de NEO. Todas las lecturas de los sensores se convierten en formato JSON y se envían al servidor SAFESENS.

ALGORITMOS PARA LA DETECCION DE INCENDIOS

Metodología.

Procesamiento de señales y extracción de características

Previo a la construcción de los modelos de detección de incendios, se consideró necesario preprocesar las señales. La visualización de la señal de las señales del prototipo 1 confirmó la necesidad de filtrar las señales del sensor de CO (sensor electroquímico de Alphasense) y el sensor PID (de Alphasense) debido a un nivel significativo de ruido. Para ello, se empleó un filtro de mediana de 0.7 y 0.5 segundos.

Además, el sensor óptico NDIR-CO2 (de Alphasense) proporciona una señal de referencia que compensa las variaciones en la señal activa debido a cambios en las condiciones ambientales. Las señales se corrigieron de la siguiente manera:

Equation (5)

$$\mathrm{NDIR\ (t)} = \frac{(\mathrm{(Activo\ (t)\ -Activo\ (t0))})}{(\mathrm{Referencia\ (t)})}$$

En el caso del prototipo 2, las señales del sensor CH4 (de IMEC), H2 (de Bosch) se filtraron utilizando un filtro de ventana de 3 y 7 segundos respectivamente. La extracción de características se realizó después de transformar los valores de voltaje capturados de los sensores MOX de ambos (prototipo 1 y prototipo 2) en conductancia. Además, para el prototipo 1 para cada sensor, la extracción de características se realizó cortando las señales en segmentos de 1 segundo. La característica seleccionada fue el promedio obtenido de las 10 medidas en cada segmento.

Etiquetado

Las etiquetas a los experimentos se han colocado muestra a muestra. La etiqueta es cero "0" cuando el evento es no fuego, este es el caso de los experimentos de interferencia y de la primera etapa de los experimentos de fuego. En los experimentos de fuego la etiqueta cambia a uno "1" cuando los sensores comienzan a reaccionar a la liberación de volátiles debido al calentamiento o ignición de material. Es decir, las etiquetas de un experimento será 0 para todas las situaciones de no fuego y será 1 para las situaciones de fuego. La muestra en la izquierda las señales adquiridas durante un experimento de fuego tipo TF3 (mechas de algodón) y la etiqueta colocada para el mismo. Nótese que la etiqueta comienza en 0 para la situación de no fuego y cambia a 1 en el momento en el que alguno de los sensores comienza a reaccionar. En el lado derecho de la Figure 83 se muestran las señales adquiridas durante el experimento de interferencia de limpieza de ventanas, en este experimento la etiqueta continua en 0 durante todo el evento ya que no existe estado de fuego.

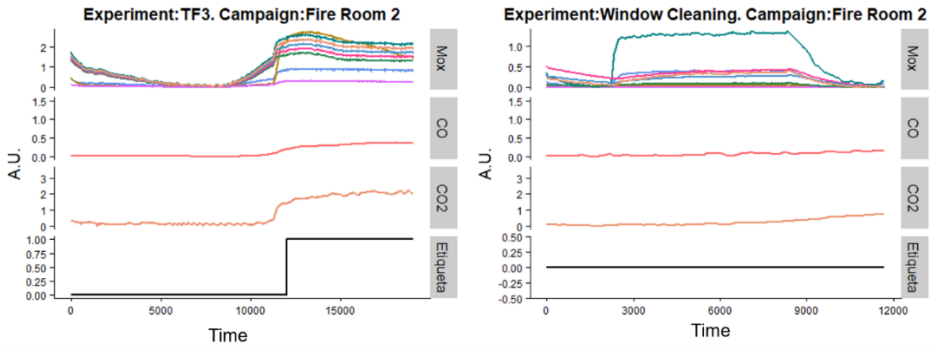

Figure 83 Señales y etiquetas del experimento TF3 y limpieza de ventanas.

Modelo de Predicción

Con el fin de construir algoritmos de predicción de incendios robustos, los modelos fueron entrenados con experimentos tanto de fuego como de interferencias. Específicamente, los modelos se basaron en el análisis discriminante de mínimos cuadrados parciales (PLS-DA) y las máquinas de vectores de soporte (SVM).

Los modelos se entrenaron usando los datos tomados en la campaña de medidas en la habitación de incendios de febrero de 2017. El conjunto de datos incluye 26 experimentos (13 incendios y 13 molestias). El orden de los modelos de predicción (número de variables latentes y costo y gamma) se seleccionó mediante validación cruzada interna. Para realizar la validación interna el conjunto de entrenamiento se dividió en 2 conjuntos; Entrenamiento interno (10 incendios y 10 experimentos de interferencias) y Validación interna (6 incendios y 6 interferencias). El orden de los modelos se seleccionó en función de la máxima precisión de las ratios de clasificación. El procedimiento se repitió hasta que todos los experimentos estuvieron al menos una vez en el conjunto de validación.

La validación externa se utilizó para evaluar el rendimiento del modelo de predicción. El conjunto de datos que se utilizó como conjunto de validación fue el adquirido durante la campaña de medidas de junio de 2017 (en la habitación de fuegos). La Figure 84 muestra la metodología completa para construir los modelos.

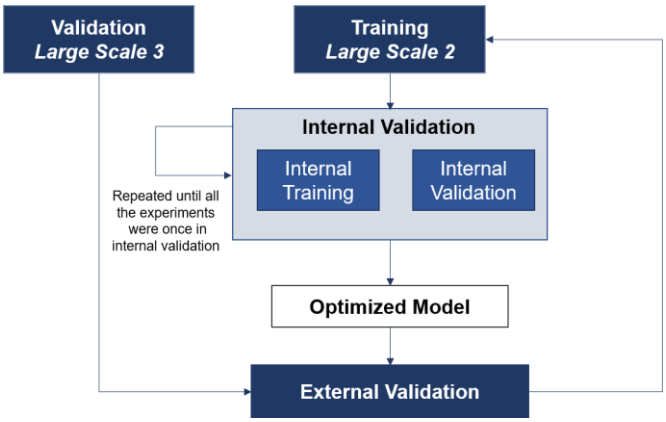

Figure 84 Metodologia para la construccion de los modelos de prediccion de incendios.

Post-procesado de datos

Para evitar un alto número de falsas alarmas, implementamos tres ventanas de tiempo de post-procesamiento diferentes; 1, 15, 30, 60 segundos. El modelo de clasificación debe emitir "alarma de incendio" durante al menos t segundos, donde t es el mayor de la ventana de post-procesamiento.

Resultados.

Se han construido modelos de predicción basados en algoritmos SVM y PLS-DA. Se han construido un modelo SVM y un modelo PLS-DA para cada uno de los prototipos (prototipo 1 y prototipo 2) presentados en esa tesis. Los algoritmos de predicción se construyeron son el fin de predecir diferentes escenarios de incendio y discriminar posibles interferencias que pueden producir falsas alarmas. Para aumentar la confiabilidad de la predicción, se implementaron ventanas de tiempo.

Después de la validación interna para el ***modelo PLS-DA 1***, la ventana de tiempo optimizada es de 60 segundos y para el modelo ***PLS-DA 2*** seleccionamos una ventana de tiempo de 30 segundos. En el caso del ***modelo SVM 1*** y ***modelo SVM 2***, las ventanas de tiempo seleccionadas son 30 segundos para ambos.

La Figure 85 muestra el rendimiento de los 4 modelos diferentes y el detector comercial en un espacio ROC. Según la figura, los detectores de incendios basados en PLS-DA son la mejor opción, para la detección de este tipo de incendios y el rechazo de esas molestias particulares. Además, el algoritmo proporciona una interpretación más simple de los resultados.

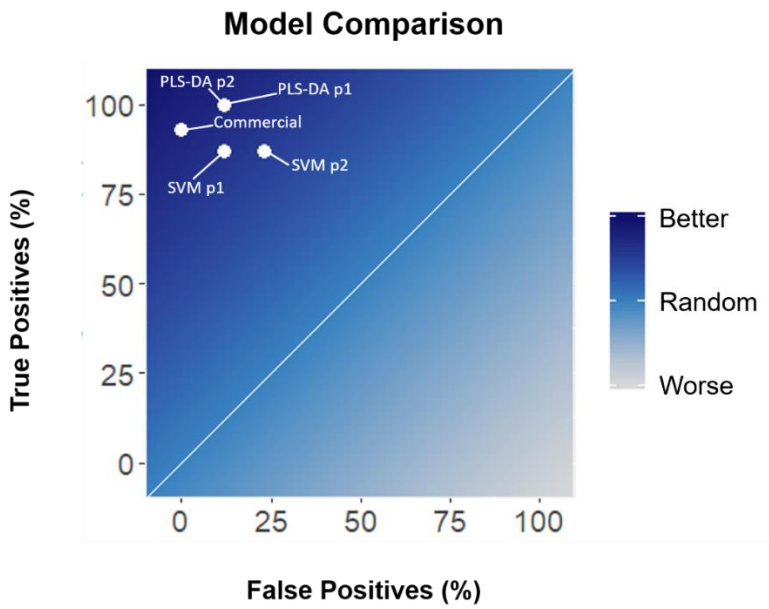

Figure 85 Comparacion de los distintos modelos en funcion de los falsos positivos y falsos negativos presentados por cada uno.

Los resultados obtenidos de los algoritmos de los detectores de incendios pueden considerarse satisfactorios, mostrando un mejor rendimiento que el estado del arte y con un amplio margen de mejora.

La detección de incendios en la primera etapa temprana de un incendio es posible incluso sin la presencia de humo visible. Para este propósito, se desarrolló y probó un conjunto heterogéneo de sensores de gas en una sala de incendios que cumplía con los estándares en el campo de la prevención de incendios.

Debido al limitado conjunto de datos disponibles para entrenar a los modelos, se produjeron varias falsas alarmas. Sin embargo, la implementación de ventanas de tiempo de post-procesamiento se ocupó de ese problema y proporcionó una predicción de incendios más confiable.

De los dos algoritmos diferentes: los modelos basados en PLS-DA son más robustos, sin falsos negativos en el prototipo 1 y un pequeño número de falsas alarmas. El modelo PLS-DA logra el 88% y el 100% de los rechazos molestos en el prototipo 1 y el prototipo 2, respectivamente. Por otro lado, los modelos SVM muestran una detección de fuego muy rápida en los experimentos realizados, pero con una interpretación más compleja de los resultados y los costos computacionales durante el desarrollo. Además, SVM clasifica erróneamente algunos incendios en ambos prototipos. Esto podría provocar una alarma de incendio poco confiable. Sin embargo, el rendimiento de ambos algoritmos aún debe explorarse en un conjunto de datos más grande para reducir la tasa de falsas alarmas y reducir los tiempos de alarma de incendio.

REDUCCIÓN DE COSTOS DE CALIBRACIÓN USANDO ESCENARIOS EXPERIMENTALES A PEQUEÑA ESCALA

Los detectores de incendios utilizados para detectar incendios en edificios o industrias deben probarse de acuerdo con las normas de incendios EN54. Todos los experimentos para evaluar el rendimiento de los detectores de incendios deben realizarse en salas dedicadas (salas de incendios). Sin embargo, la disponibilidad de salas de bomberos es limitada y costosa. Además, un experimento estándar en la sala de incendios puede tomar alrededor de 1 hora.

Los modelos de calibración robustos incluyen una gran cantidad de experimentos de fuego y molestias. Los sistemas de sensores de gas entrenados con una cantidad limitada de muestras dan como resultado algoritmos menos generales y robustos. Para construir algoritmos útiles de detección de incendios es necesario realizar campañas de medición con una duración de varios meses y horas. Esto resulta en costosas campañas de experimentos.

De esta manera, nuestra hipótesis es que los algoritmos de predicción podrían mejorarse utilizando conjuntos de datos adquiridos en una cámara de experimentos a pequeña escala.

Para probar esta hipótesis, construimos tres modelos diferentes. El ***modelo 1***, fue entrenado utilizando datos experimentos realizados en la habitación de fuego estándar, ***el modelo 2***, utiliza datos de experimentos realizados en una pequeña cámara y finalmente ***el modelo 3***, usó la combinación del conjunto de datos de los experimentos realizado en la habitación estándar de incendios y el conjunto de datos de experimentos realizados en la pequeña cámara. Todos los datos se adquirieron utilizando el prototipo 1.

Los modelos de calibración están basados en PLSDA. Para poder comparar el rendimiento de los diferentes modelos de predicción, el conjunto de validación corresponde en todos los casos datos adquiridos en adquirido en la sala de bomberos estándar en febrero de 2017 Hay varios meses entre las adquisiciones de los diferentes conjuntos de datos. ***El modelo 1*** fue entrenado con datos adquiridos en febrero de 2017 y ***el modelo 2*** fue entrenado usando datos de la cámara pequeña en marzo de 2016. ***El modelo 3*** se entrenó con datos de febrero de 2017 y datos adquiridos en la pequeña sala en marzo 2016. En consecuencia, los algoritmos de fusión de datos no solo combinan datos de diferentes escenarios, sino que también incluyen información sobre diferentes fechas.

Los resultados confirman que ***el modelo 3*** es capaz de rechazar la mayoría de las molestias logrando el 81% de especificidad. Además, el modelo muestra una buena capacidad para detectar incendios, ya que solo un incendio se clasificó como molesto. Otra mejora importante de los modelos de fusión de datos es la capacidad de predecir incendios y rechazar molestias adquiridas más de 4 meses después. La Figure 86 resume el desempeño de los 3 modelos.

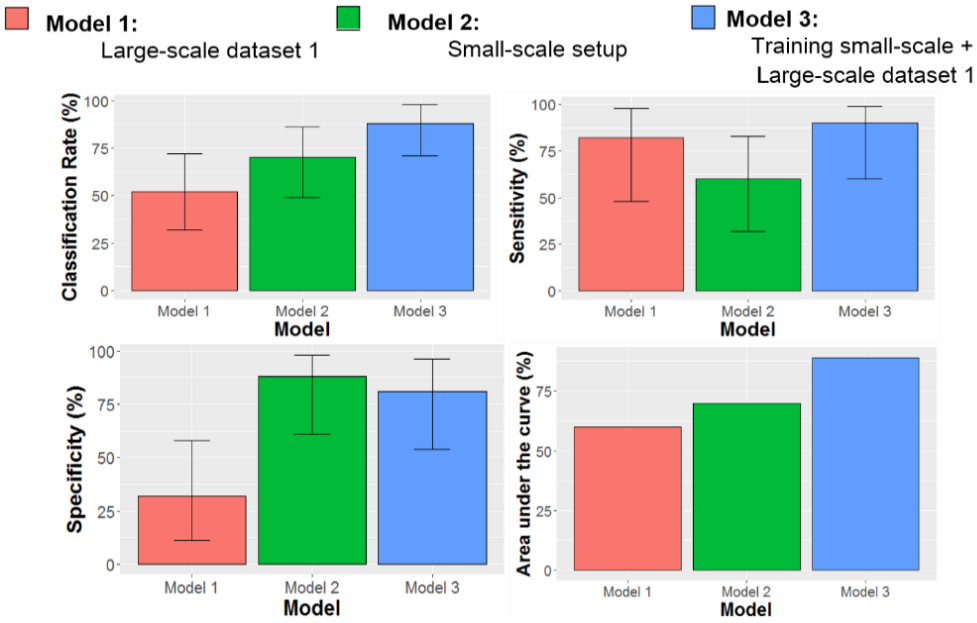

Figure 86 Area bajo la curva, especificidad, sensibilidad y ratio de clasificacion de los diferentes modelos. Modelo 1 esta construido con datos de la habitacion de incendios, modelo 2 esta construido con datos de la peque;a camara y modelo 3 esta construido usando la fusion entre ambos escenarios.

REDUCCIÓN DE COSTOS DE CALIBRACIÓN USANDO RÉPLICAS DE UNA MATRIZ DE SENSORES.

Los costos de calibración para las réplicas de una matriz de sensores son considerables y ya que se requiere una calibración individual debido a la variabilidad del sensor, lo que limita la producción en masa.

Para reducir costos de calibración, presentamos una metodología que rechaza la variabilidad del sensor y proporciona modelos de calibración general (universal) para réplicas de una matriz de sensores que evitan la calibración individual. Nuestro método ha sido validado utilizando datos de cinco réplicas de una matriz de sensores que contiene sensores tipo MOX. Las matrices de sensores se colocaron (secuencialmente) en una cámara de medición de 287 ml mientras las condiciones de gas se cambiaron y se adquirieron las conductancias del sensor.

Las matrices de sensores MOX estaban compuestos por AS-MLK, AS-MLC, AS-MLX, todo proporcionado por ams. Los sensores dentro de cada tipo fueron operados a ocho diferentes temperaturas (de 245ºC a 381ºC). Las

matrices fueron expuestas a monóxido de carbono, acetaldehído, metano, etanol, dióxido de nitrógeno y propano.

Los modelos están basados en Parial Least Squares Discriminant Análisis (PLS-DA). Las matrices de sensores contienen 24 características diferentes. Entiéndase por característica la combinación de tipo de sensor y temperatura. Para cada tipo de sensor (3) seleccionamos un elemento a cada temperatura (8).

El modelo fue entrenado considerando cuatro matrices de sensores y fue probado con la matriz de sensores restante. Para optimizar el orden de los modelos se realizó validación interna usando la metodología “one leave out” dejando siempre una matriz de sensores fuera. El modelo general obtuvo una tasa de clasificación del 86%, con una sensibilidad del 94% y una especificidad del 85%. Además, el área bajo el ROC fue de 0.90. Después de una prueba de permutación de las etiquetas, un Se obtuvo el valor p = 0,007. La Figure 87 muestra matriz de confusión del modelo de calibración general.

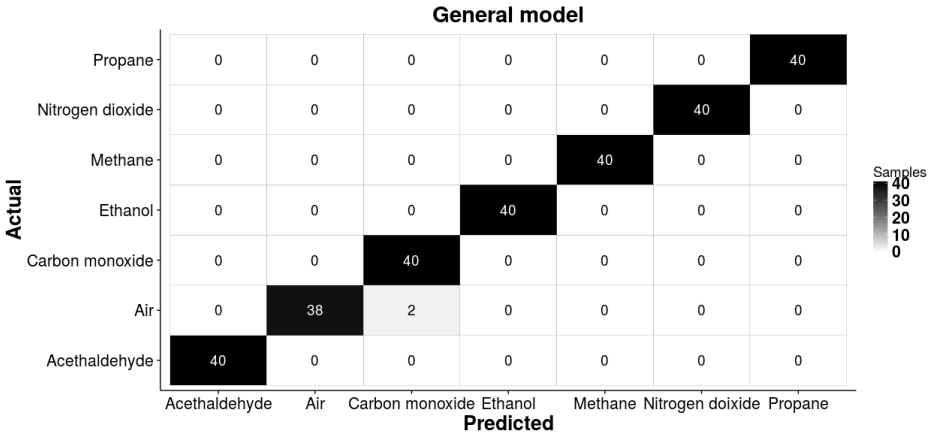

Figure 87 Matriz de confusion del modelo general construido usando diferentes lotes de una misma matriz de confusion.

Mostramos que los modelos entrenados con varias matrices de sensores también proporcionan un alto ratio de clasificación cuando se aplican a nuevas réplicas de la matriz de sensores. El modelo de calibración debe entrenarse con varias réplicas de una misma matriz de sensores, de esta manera el modelo puede rechazar la variabilidad del sensor. Además, la metodología puede reducir los costos de entrenamiento y calibración de las matrices de sensores facilitando la producción masiva de las matrices de sensores.

CONCLUSIONES

Las matrices de sensores de gas en combinación con técnicas de reconocimiento de patrones son capaces de proporcionar alarmas de incendio confiables mientras rechazan la mayoría de los escenarios molestos

- Al utilizar ventanas de tiempo para filtrar la salida del algoritmo de predicción, los detectores de incendios pueden rechazar todos los escenarios molestos. Sin embargo, el tiempo de respuesta incrementa.
- En ambos prototipos, los algoritmos PLS-DA presentan el mismo rendimiento en términos de tasas verdaderamente positivas (100%) y verdaderas negativas (97%).
- Los resultados muestran que la combinación de las pruebas en una sala de incendios estándar y en la cámara de experimentos a pequeña escala enriquece los conjuntos de datos de calibración y conduce a un mejor rendimiento del detector.
- Los modelos de calibración entrenados con réplicas de una misma matriz de sensores mostraron que se pueden obtener modelos globales de calibración. Los modelos globales resultantes son capaces de clasificar más del 90% de las muestras pertenecientes a nuevas matrices de sensores.